Naval Research Laboratory
Washington, DC 20375-5000

NRL Memorandum Report 6886

Post-Flashover Fires in Simulated Shipboard Compartments: PHASE I — Small Scale Studies

J. T. LEONARD, C. R. FULPER, R. L. DARWIN,* G. G. BACK,**
J. L. SCHEFFEY,** R. L. WILLARD,** P. J. DiNENNO,** J. S. STEEL,**
R. J. OUELLETTE,** AND C. L. BEYLER**

Navy Technology Center for Safety and Survivability
Chemistry Division

**Naval Sea Systems Command*
Washington, DC

***Hughes Associated, Inc.,*
Wheaton, Maryland

September 3, 1991

REPORT DOCUMENTATION PAGE

Form Approved
OMB No 0704-0188

1. AGENCY USE ONLY (Leave blank)	2. REPORT DATE	3. REPORT TYPE AND DATES COVERED
	1991 September 3	Interim

4. TITLE AND SUBTITLE

Post-Flashover Fires in Simulated Shipboard Compartments:
PHASE I — Small Scale Studies

5. FUNDING NUMBERS

PE — 63514N
S1565-SL
J.O.# — 61-2961-0-1

6. AUTHOR(S)

J. T. Leonard, C. R. Fulper, R. L. Darwin,* G. G. Back,** J. L. Scheffey,** R. L. Willard,** P. J. DiNenno,** J. S. Steel,** R. J. Ouellette,** and C. L. Beyler**

7. PERFORMING ORGANIZATION NAME(S) AND ADDRESS(ES)

Naval Research Laboratory
Washington, DC 20375-5000

8. PERFORMING ORGANIZATION REPORT NUMBER

NRL Memorandum
Report 6886

9. SPONSORING/MONITORING AGENCY NAME(S) AND ADDRESS(ES)

Naval Sea Systems Command
Washington, DC 20362-5101

10. SPONSORING/MONITORING AGENCY REPORT NUMBER

11. SUPPLEMENTARY NOTES

*Naval Sea Systems Command, Washington, DC 20375-5000.
**Hughes Associated, Inc., Wheaton, Maryland 20902

12a. DISTRIBUTION/AVAILABILITY STATEMENT

Approved for public release; distribution unlimited.

12b. DISTRIBUTION CODE

13. ABSTRACT *(Maximum 200 words)*

Following the missile attack on the USS STARK in the Persian Gulf, the Internal Ship Conflagration Control Program was initiated to assess the impact of a fire resulting from burning missile propellant in a shipboard compartment. To support this program it was necessary to "design" a test fire which would simulate the post-flashover fire conditions in a shipboard compartment following a propellant burn. Initially, the problems were bounded using small scale testing in simulated shipboard compartments, and then further defined on the Navy full scale fire research and test ship, th ex-USS SHADWELL.

A total of sixty fires were conducted in a simulated shipboard compartment to develop a design fire for full scale testing. the design fire was developed to approximate a "worst case" post-flashover compartment fire. The design fire can produce average compartment temperatures of over 1000° C (1832° F) a'most instantly. During this analysis, estimates on the likelihood and times for fire spread were also developed.

14. SUBJECT TERMS			15. NUMBER OF PAGES
Compartment fires, Post-flashover, STARK	Flame spread Design fire		169
			16. PRICE CODE

17. SECURITY CLASSIFICATION OF REPORT	18. SECURITY CLASSIFICATION OF THIS PAGE	19. SECURITY CLASSIFICATION OF ABSTRACT	20. LIMITATION OF ABSTRACT
	UNCLASSIFIED	UNCLASSIFIED	UL

NSN 7540-01-280-5500

Standard Form 298 (Rev 2-89)
Prescribed by ANSI Std 239-18
298-102

CONTENTS

CONTENTS (Continued)

FIGURES

FIGURES (Continued)

TABLES

POST-FLASHOVER FIRES IN SIMULATED SHIPBOARD COMPARTMENTS: PHASE I — SMALL SCALE STUDIES

1.0 INTRODUCTION

1.1 Background

The Internal Ship Conflagration Control (ISCC) program was initiated to address issues raised by the missile-induced fire on the USS STARK [1]. The overall objectives of the program were to develop guidance to the Fleet on the control of horizontal and vertical fire spread and to develop concepts and criteria for new ship design. Ultimately, SHIPALTS and procurement specs will be prepared.

1.2 General Approach

The approach to the project was to divide the "fire curve" of a missile induced conflagration into two discreet elements: the missile propellent burning phase and the resulting compartment fire. The basic hypothesis was that the high intensity/short duration missile fuel fire almost immediately ignites all materials within the compartment, driving the compartment to flashover. As the propellent burns out, there is a transition to a steady-state, post-flashover fire supported by the combustible contents of the ship, primarily cables and various Class A materials. The temperature of the involved space and the duration of the fire are then dependent on the amount, configuration, and the physical properties of the combustibles within the compartment and on the availability of air for combustion.

While separate work continues on characterizing the missile fuel threat [2, 3], this report focuses on characterizing the fire spread resulting from post-flashover compartment fires, Internal Ship Conflagration. By basing this study on natural ventilation fires which produce maximum compartment temperatures, fire spread characteristics may be quantified for a "worst case" fire. Different threats, in terms of thermal impact and duration, were also quantified to develop a range of fire spread characteristics.

This report covers the initial tests that were conducted at the Chesapeake Bay Detachment (CBD) Fire Test Facility of

Manuscript approved June 24, 1991.

the Naval Research Laboratory (NRL). This phase includes a series of tests covering a range of ventilation and fuel configurations were conducted to determine their effect on compartment fire temperatures and heat fluxes. From this series, a "design" or worst case fire was developed to serve as a test protocol for large scale testing to be performed on the Navy Full Scale Fire Research and Test Ship, the ex-USS SHADWELL. The information from the Shadwell tests will be published separately. Later, the design fires will be used to characterize the threat of a post-flashover fire and to evaluate active and passive fire protection measures.

2.0 OBJECTIVES

The objectives of the first test series at CBD were to:

1. Bound and quantify the conditions required to achieve maximum compartment fire temperatures under natural ventilation conditions;

2. Gather baseline data on the effects of vent and fuel surface area on compartment fire temperatures;

3. Based on the above knowledge, develop design fires for characterization of post-flashover fire threats, which then can be used on the ex-USS SHADWELL for larger scale testing;

4. Develop preliminary estimates of vertical and horizontal fire spread rates along with human/material tolerance limits based on heat transfer characteristics to adjacent compartments;

5. Develop an overall lessons learned list to give preliminary guidance to the Fleet and aid in better understanding the tests to be conducted on the ex-USS SHADWELL; and

6. Begin preparations for future tests of active and passive fire protection/extinguishment systems.

3.0 THEORY

3.1 Fire Growth Curve

The term "compartment fire" is used to describe a fire confined to a room or similar enclosure. Compartment fire behavior can be illustrated by the average gas temperatures in the compartment as shown in Figure 1. Following the ignition of combustibles in a compartment, the fire, while

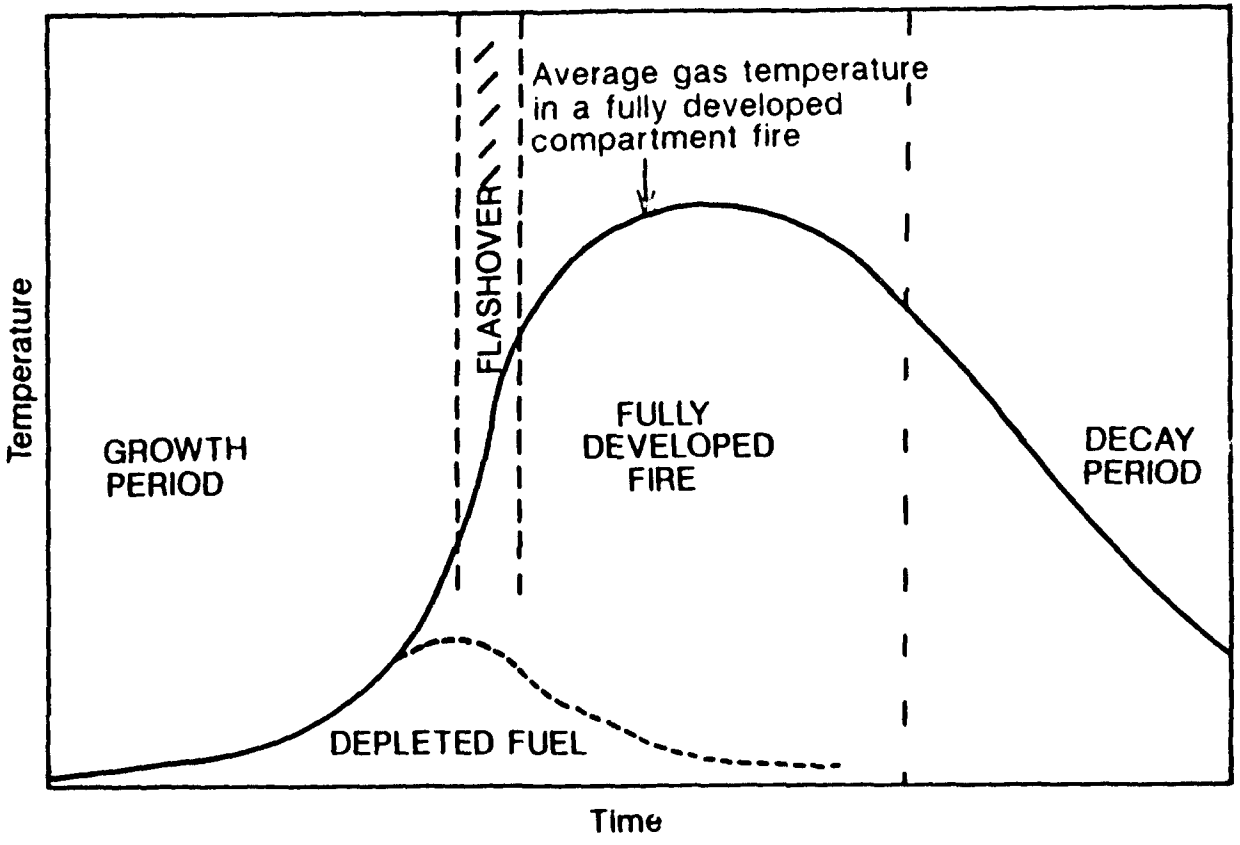

Fig. 1 - Fire growth curve

still small, will behave as it would in the open air. If conditions exist such that the fire can spread either over the initial item first ignited or to adjacent objects and adequate ventilation exists, the fire may reach a point where enclosure effects begin to occur. The enclosure acts to confine the heat and re-radiate it back to the fuel, thus increasing the burning rate. The compartment temperature and the fuel burning rate continue to increase until a transition period known as flashover occurs. It is during this transition period that the fire spreads from the localized region, where ignition first occurred, to all combustible surfaces within the compartment. Commonly accepted thermal characteristics for compartments approaching flashover are a total heat flux to the floor 20 kW/m^2 (1.8 BTU/ft^2 sec) and an upper layer temperature exceeding 500°C (932°F) [4]. These values are sufficient to promote piloted ignition and rapid flame spread over most combustible materials. After the transition through flashover, the fire is said to have reached a post-flashover stage. During this fully developed stage, the rate of heat release reaches a maximum, and the threat to neighboring compartments is greatest. It is this stage of the fire that is most severe and is further investigated throughout this report. As depletion of the combustibles continues, a decay period is reached in which the severity of the fire decreases.

In summary, the growth of a compartment fire can be divided into three stages as follows.

1. Pre-Flashover - growth stage where the average temperature is low and the fire is localized to the vicinity of its origin. For a propellant-induced fire, this stage is very short, i.e., less than two minutes.

2. Post-Flashover - fully developed stage where all combustible items in the compartment are involved and the threat to adjacent compartments is greatest.

3. Decay - stage where the severity of the fire decreases substantially as the combustibles are consumed.

3.2 Burning Regimes

There are two regimes by which burning may be characterized: ventilation controlled and fuel controlled. The conventional interpretation of a ventilation controlled fire states that in a range of ventilation opening sizes, the rate of burning of the fuel is controlled by the rate at which air can flow into the compartment. Above this range of

ventilation sizes, the rate of burning becomes independent of the size of the opening and is driven instead by the amount, configuration, and burning characteristics of the fuel. This range of opening sizes is referred to as the fuel controlled regime.

A ventilation controlled fire is produced when the volatilization and burning rates of combustibles exceed the value required to consume all the oxygen available in the compartment. The excess super heated fuel vapor leaves the compartment and burns in the outside air resulting in a large fire plume protruding from the compartment. Visual observations would lead one to believe a ventilation controlled fire produces the most severe fire conditions. However, the excess volatiles act as a heat sink and actually remove heat thus lowering the temperatures inside the compartment.

If the ventilation opening is increased, a condition will be reached where the rate of burning of the fuel becomes independent of the size of the opening and is determined instead by the surface area and burning characteristics of the fuel. This regime is referred to as fuel controlled. The air flow into the compartment is more than ample to consume the fuel. The excess air does however have the effect of cooling the compartment making the fuel controlled regime the least severe of the three burning regimes. In this regime, the fire has sufficient air and remains totally contained in the enclosure with only products of combustion flowing out of the ventilation opening.

In the transition phase between the ventilation controlled and fuel controlled regimes lies a narrow range where stoichiometric burning occurs. Stoichiometric conditions depend on the relation between the rate of pyrolysis of the fuel and the compartment air inflow rate. Stoichiometric burning is reached when the amount of fuel being vaporized is precisely the amount needed to consume all the oxygen entering the compartment during the combustion process. The maximum amount of energy is released in the compartment during this combustion process. The heat sinks of excess fuel or air are absent, resulting in the highest compartment temperatures for a given ventilation opening.

In actuality, stoichiometric burning is difficult to achieve. This is due to the inability to efficiently mix the "perfect" ratios of air and fuel. What we refer to as stoichiometric burning is an optimization of air/fuel ratios required to achieve maximum temperatures.

3.3 Fully Developed Fire Behavior

After flashover has occurred, the exposed surfaces of all combustible items in the compartment will be burning and the rate of heat release may reach a steady state value. The burning rate will remain steady until the rate of generation of flammable volatiles begins to decrease as a result of fuel consumption. It is during this stage where the threat of fire spread to adjacent compartments, and the likelihood of failure of structural members is the greatest. It was the objective of this evaluation to quantify the thermal threat to the compartment of origin and to adjacent compartments during this steady state region.

A major experimental program to improve the understanding of the behavior of fully developed compartment fires was conducted by Thomas and Heselden [5]. Fire research laboratories from eight countries collaborated in this work which was carried out under the auspices of the Counseil Internationale du Batiment (CIB). Over 400 experiments in small scale compartments were conducted. The experiments consisted of varying the compartment size and shape, ventilation size and location (height) and the fire load (wood cribs). It was concluded from these tests that the maximum temperature for their compartment fire scenario is attained in the range of opening factors from 8-15 $m^{-\frac{1}{2}}$, (Fig. 2), where

$$\text{opening factor} = A_T/(A_W H^{\frac{1}{2}}) \qquad (1)$$

A_T = total surface area of the compartment minus the floor and vent areas (m^2)

A_W = vent area (m^2)

H = height to the top of the vent (m)

The temperature drop observed for opening factor less than 8 $m^{-\frac{1}{2}}$ was the result of an insufficient compartment volume required to house the amount of fuel (wood) necessary to produce maximum temperatures. Other conclusions and data from the CIB program have been incorporated in the development of fire models relating to fire resistance requirements and in the understanding of the behavior of flames protruding from the ventilation openings.

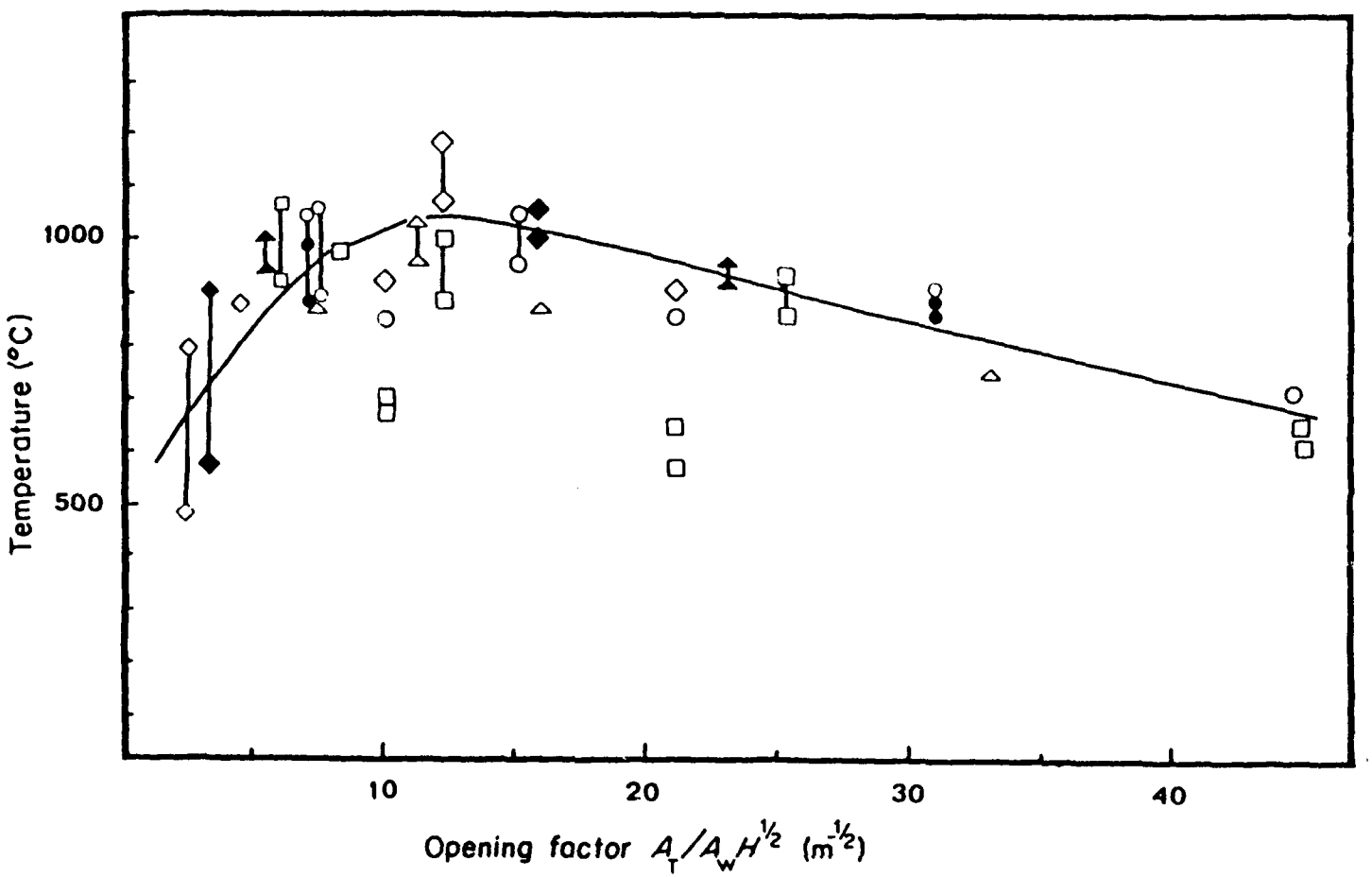

Fig. 2 - Thomas curve (avg. comp. temp. vs. opening factor) data from the CIB Program [ref.5]

3.3.1 Energy Balance Analysis

The maximum compartment temperature that occurs during the fully developed fire stage is a function of the energy being released and the energy being lost. This is illustrated by the energy/heat balance equation (2).

$$\dot{q}_c = \dot{q}_l + \dot{q}_r + \dot{q}_w \qquad (2)$$

where

$\dot{q}_c$ = rate of heat release due to combustion

$\dot{q}_l$ = rate of heat loss due to replacement of hot gases by cold

$\dot{q}_r$ = rate of heat loss by radiation through the openings

$\dot{q}_w$ = rate of heat loss through the walls, ceiling and floor

Equation 2 illustrates that the energy released in the compartment is dissipated or lost by three mechanisms each a function of the gas temperature in the compartment. These three mechanisms are convective losses due to the outflow of hot gases, radiation losses out the vent opening and conductive losses through the compartment boundaries. By assuming the fire is ventilation controlled, the compartment average gas temperatures can be estimated. In the ventilation controlled regime, the heat release rate ($\dot{q}_c$) can be approximated from the vent flow rate and the heat of combustion of air (3.0 MJ/kg).

3.3.2 Numerical Methods

Several mathematical models for estimating the time/temperature history of potential compartment fires have been developed [4, 6, 7, 8]. The applicability of these models to shipboard compartments is questionable. These methods were developed and tested based on thermally thick construction materials (i.e., gypsum) and may not be applicable to steel enclosures. Although these post-flashover compartment models may not be suitable for use in predicting steel compartment fire temperatures, they served as a good "first guess" at the conditions produced during this test series.

3.4 Fire Resistance

The conventional definition of "fire-resistance" is the ability of a structural member or boundary (wall) of a building to continue to perform its function as a barrier or structural component during the course of a fire. Fire will spread horizontally and vertically by two methods: (1) flame penetration through a boundary due to burn-through, collapse or melting of the element; and (2) ignition in adjacent compartments due to heat transfer through compartment boundaries. Due to the high structural integrity of steel, the focus in the present study was on fire spread through unbreached boundaries due to the heat transfer through the walls and ceiling.

4.0 APPROACH

The approach chosen to evaluate post-flashover fire conditions centers around the development of a "design fire" which will produce the most severe fire conditions (highest temperatures) in a simulated shipboard compartment. This approach included

* design and construction of a mock-up which could withstand multiple high intensity fires while still approximating "typical" shipboard conditions;

* conducting scoping tests to select a fuel type and configuration (i.e., pool, spray);

* evaluating fuel load/vent size relationships required to produce the highest temperatures;

* based on the above information, develop a "design" fire which is controllable and predictable. This design fire will be used on the ex-USS SHADWELL for subsequent large scale testing; and

* based on the "design fire," quantify the thermal insult to the ship and likelihood of fire spread for this worst case scenario.

In addition, several other tests were performed to duplicate the thermal conditions of the hydrocarbon fuel fires using wood cribs. The objective of these tests was to develop a Class A, fightable fire which may be used in the ex-USS SHADWELL test series.

5.0 TEST DESCRIPTION

5.1 Mock-Up Description

An intermediate scale mock-up was constructed at CBD for this evaluation. The mock-up was designed to withstand multiple high intensity fires while still simulating the thermal characteristics of a "typical" shipboard compartment. The mock-up consisted of four 2.4 x 2.4 x 2.4 m (8 x 8 x 8 ft) cubical enclosures as shown in Figs. 3 and 4. The mock-up was constructed of 0.95 cm (3/8 in.) thick steel plates. Stiffeners having "T" shape cross sections were welded vertically to the center of each wall in each compartment. The outside lower compartments each contained two 0.66 x 1.68 m (26 x 66 in.) doors (standard Navy size), one to the outside air and one to the center compartment. The upper compartment contained a door and a hatch, each opening to the outside air. The center compartment, selected as the fire compartment, had three doors, one to each of the adjacent compartments and one to the outside air. The door to the outside air was enlarged to produce a range of opening sizes. Sizes were selected to approximate openings of from one to three standard Navy doors.

5.2 Instrumentation

The instrumentation scheme was designed to measure the thermal insult to the compartments produced by the various fire scenarios. Instruments were installed to measure compartment air temperatures, temperatures of escaping gases, air temperatures in the adjacent compartments and temperatures of the interior and exterior bulkheads and decks. Thermal radiation and total heat flux were measured in each compartment. Oxygen, carbon monoxide and carbon dioxide were measured just below the lintel in the doorway of the fire compartment. The pressure differential across the opening was also measured. A load cell assembly was used to measure the fuel consumption rate (mass loss rate) in both the spray fire and wood crib tests. The instrumentation locations are shown in Figs. 5 and 6. At a minimum, the compartment temperatures and fuel consumption rate (mass burning rate) were displayed for real-time observation by the test team.

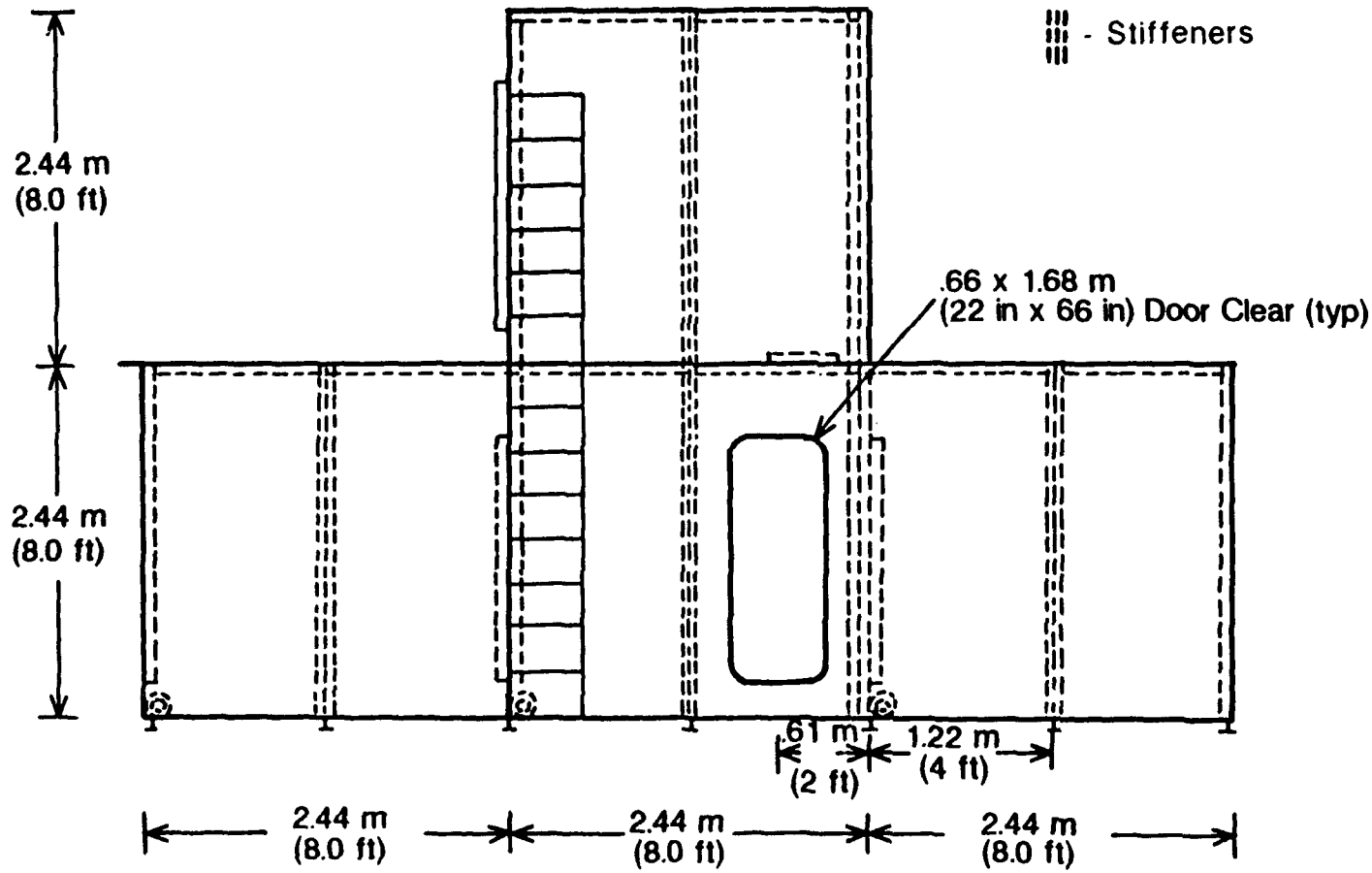

Fig. 3 - Ship compartment mock-up (elevation)

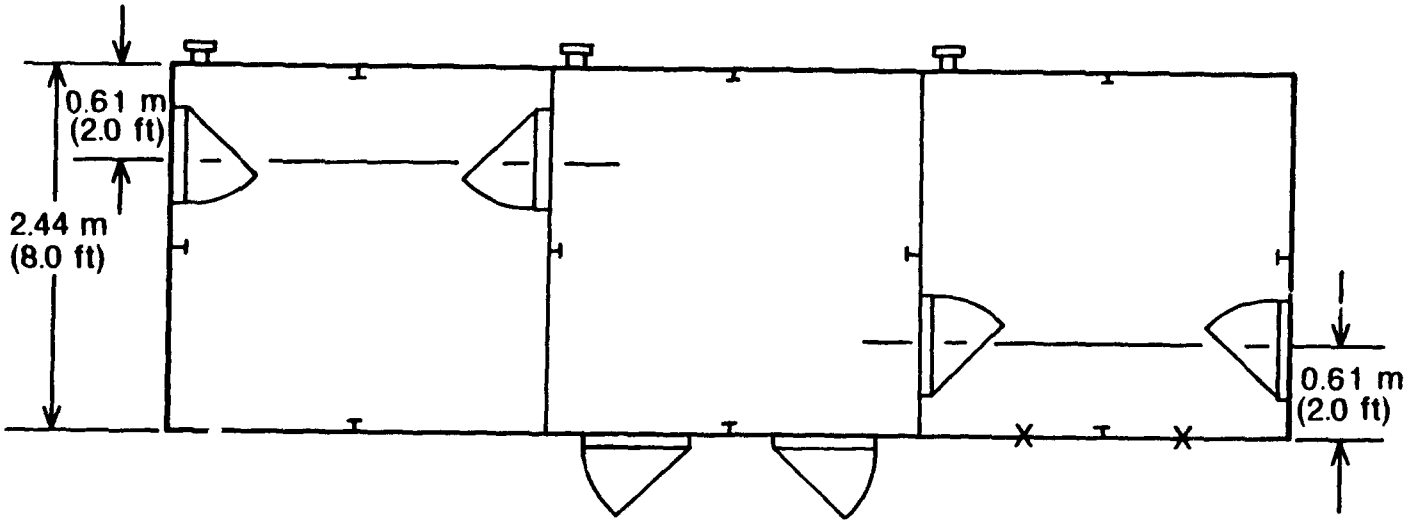

Lower compartment

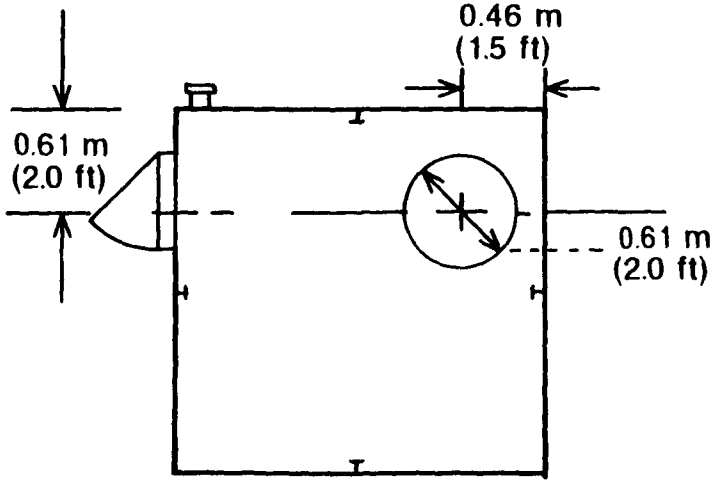

Upper compartment

Fig. 4 - Ship compartment mock-up (plan)

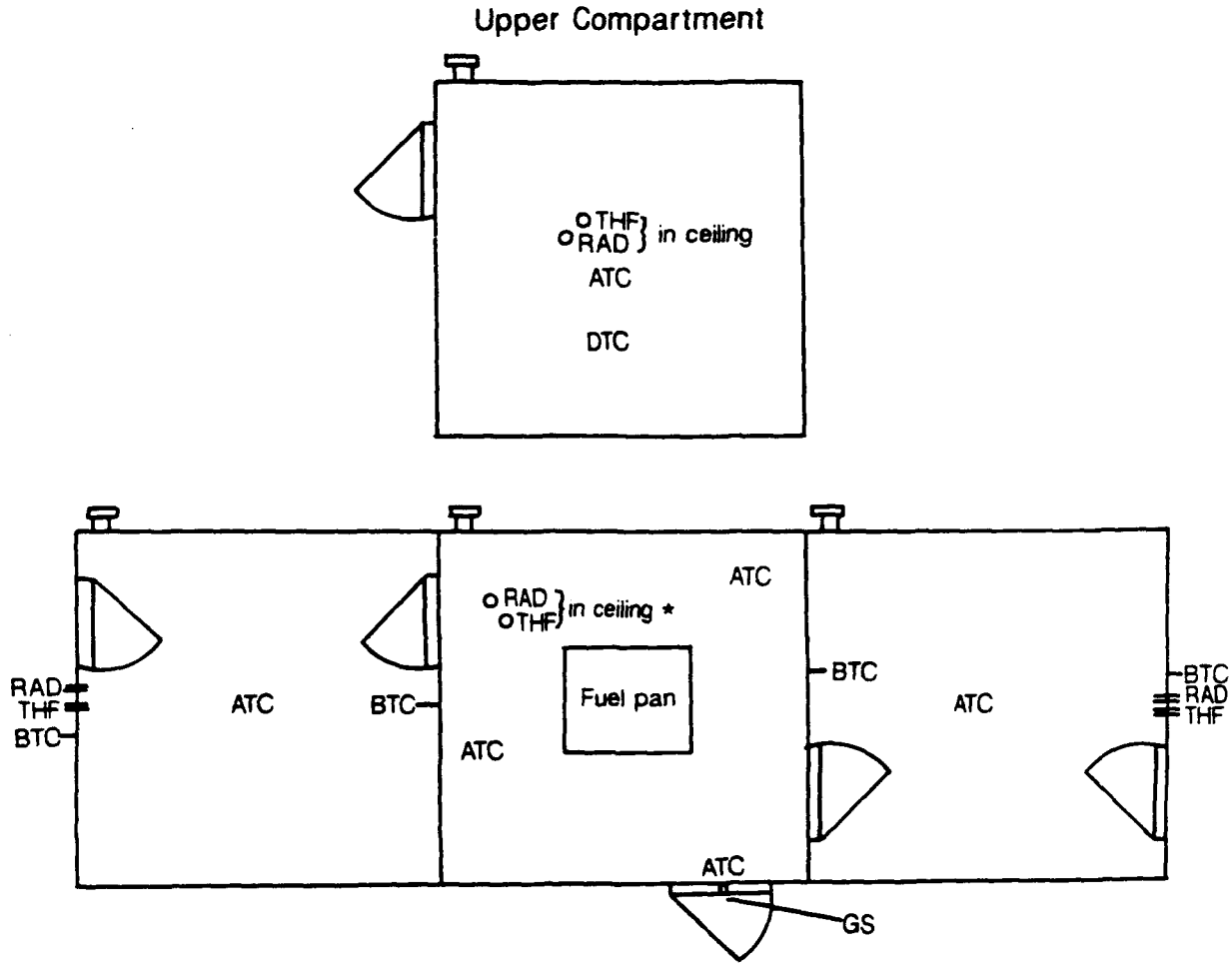

ATC - Air Thermocouples (Type K)
DTC - Deck Thermocouples (Type K)
BTC - Bulkhead Thermocouples (Type K)
GS - Gas Sampling (O_2,CO, CO_2)
RAD - Radiometers 110 kW/m^2 (10 BTU/ft^2 sec) Range
THF - Total Heat Flux Transducers
110 kW/m^2 (10 BTU/ft^2 sec) Range
*330 kW/m^2 (30 BTU/ft^2 sec) Range

Fig. 5 - Instrumentation layout (plan)

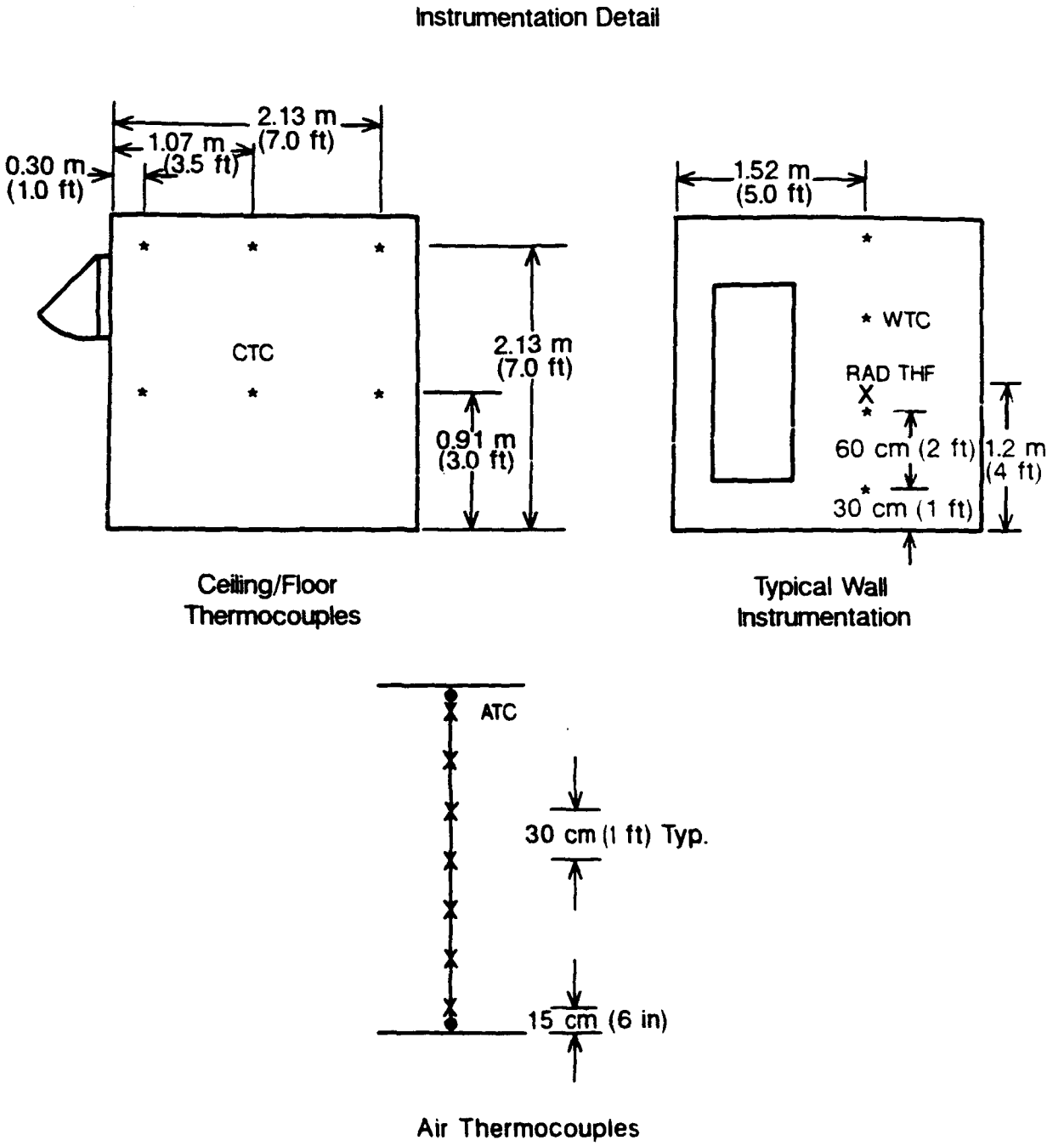

Fig. 6 - Instrumentation layout (detail)

5.2.1 Thermocouples

5.2.1.1 Air Temperature Thermocouples

Thermocouple trees were installed in all compartments to provide air temperature measurements. All thermocouples used in the test series were Type K. Inconel-sheathed thermocouples were installed in the fire compartment, while high temperature glass braided thermocouples were installed in the adjacent compartments. The locations of thermocouple trees along with exact spacing are shown in Figures 5 and 6.

5.2.1.2 Surface Temperature Thermocouples

Matrices of thermocouples installed on both exposed and unexposed surfaces of the bulkheads and decks bounding the fire compartment provided information on the energy being conducted through the steel boundaries. Inconel-sheathed thermocouples were used to measure surface temperature. These thermocouples were fastened to the boundaries by drilling a small hole and peening the end of the thermocouple to the surface. The locations of these thermocouples are shown in Figures 5 and 6.

5.2.2 Heat Flux Transducers

Total heat flux transducers and radiometers were installed in each of the four compartments as shown in Figures 5 and 6. High range (330 kW/m^2 (30 BTU/ft^2 sec)) radiometers and total heat flux transducers were installed in the ceiling of the fire compartment and medium range (110 kW/m^2 (10 BTU/ft^2 sec)) were installed in each of the adjacent compartments. From these measurements, the likelihood and time of ignition of various materials in these compartments were estimated.

5.2.3 Gas Sampling

Gas analyzers were installed to continuously measure oxygen, carbon monoxide, and carbon dioxide from a sampling line located just below the top of the ventilation opening (lintel) of the fire compartment as shown in Figures 5 and 6. This information was used to estimate the amount of oxygen consumed during the combustion process. These data also aided in the determination of the burning regime based on the composition of the hot gases exiting the compartment.

5.2.4 Load Cells

Two load cell assemblies were used to measure the fuel consumption rate (mass loss rate) during these tests. The first assembly consisted of a large scale produced by four load cells and was designed to measure the mass loss rate of the pressurized fuel storage tank during the JP-5 tests.

The second assembly was trapeze hanging mechanism constructed with two load cells designed to measure the burning rate of the wood cribs during the Class A material fire tests.

5.2.5 Pressure Transducers

One differential pressure transducer was installed in the front of the fire compartment on the centerline just above the compartment floor. The pressure transducer was used to determine the pressure differential across the ventilation opening and was used with compartment temperature data to estimate the mass flow rates in and out of the compartment.

5.2.6 Digital Scale

A digital weight scale was used to aid in the calibration of the load cell assemblies.

5.2.7 Computer

An IBM compatible computer, a DOS-8, and 7 EXP-16 cards produced by Metrabyte Corporation were used to scan the above instruments. The data were collected in ten second intervals. A commercial software package (Lab Tech Notebook) was used to drive the entire system. The data were stored in ASCII format on floppy disks to be analyzed and manipulated after the tests were concluded.

5.2.8 Video and 35 mm Still Cameras

Photographs, both still and motion, were made of each test. These records served as a means of estimating the volume of flame outside the compartment and were archived to serve as a visual record.

5.3 Scoping Tests

The primary objective of the scoping tests was to determine a fuel and fire type (i.e., pool, spray) to be used during the later test series and onboard the ex-USS SHADWELL.

The desired characteristics of this fire are

1. safe and controllable;

2. capable of producing extremely severe fire conditions quickly and consistently;

3. adjustable heat release rate; and

4. capable of burning for long durations (on the order of 1 hr).

Secondary objectives of the scoping tests are

1. develop and refine test and safety procedures;

2. institute personnel responsibilities and build familiarity and confidence with individual jobs;

3. check instrumentation, equipment, and overall scene; and

4. check air tight integrity of adjacent compartments.

The test series began with an evaluation of three fire types: JP-5 pool fires, JP-5 spray fires, and Class A materials. The JP-5 pool fires were produced using various sized pans. All the pans had approximately 10 cm (4 in.) high sides. The JP-5 spray fires consisted of a fine atomizing nozzle spraying vertically in the fire compartment. Various size and configurations of wood cribs were used as the Class A materials. Modifications and combinations of these fire types were also evaluated.

All three fire types were found to have some undesirable characteristics. The radiation from the hot layer along with the heating of the compartment caused the fuel in the pan to vaporize and burn faster as the amount of fuel in the pan decreased. The wood crib fires were unable to sustain a steady burning rate for more than 20 minutes, far less than the desired 45-60 minutes. The JP-5 spray fires altered the natural ventilation in the compartment producing inconsistent data between similar tests. The momentum of the spray and the geometry of the plume dramatically altered the location of the neutral plane. A large volume of flame protruded out the vent opening with inflow of air developing around the periphery of the plume. It was determined during these tests that the optimum fire source would combine the duration and safety aspects of a spray fire and the low momentum of a pool fire.

In an attempt to produce a fire with these characteristics, a modified spray fire system was developed. The system consisted of a fan nozzle FF series, produced by Bete Fog Nozzle Inc., spraying tangentially across the surface of a fuel pan. This fuel system (Fig. 7) and modified spray fire (Fig. 8) configuration allowed the flexibility to vary the fire size by adjusting the fuel flow, but did not alter the natural ventilation through the compartment. This design also permitted immediate shut down in case of an emergency.

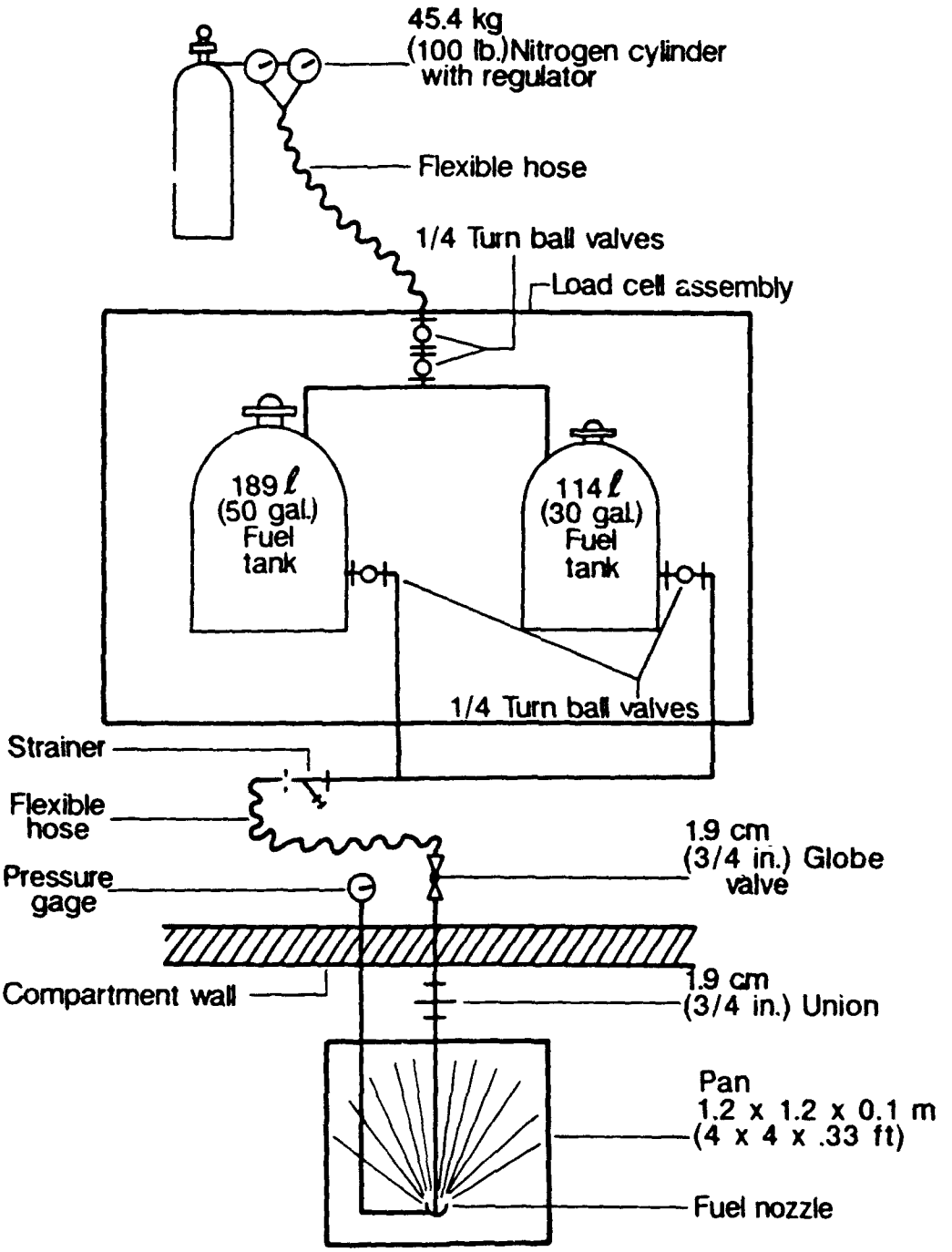

Fig. 7 - Fuel system

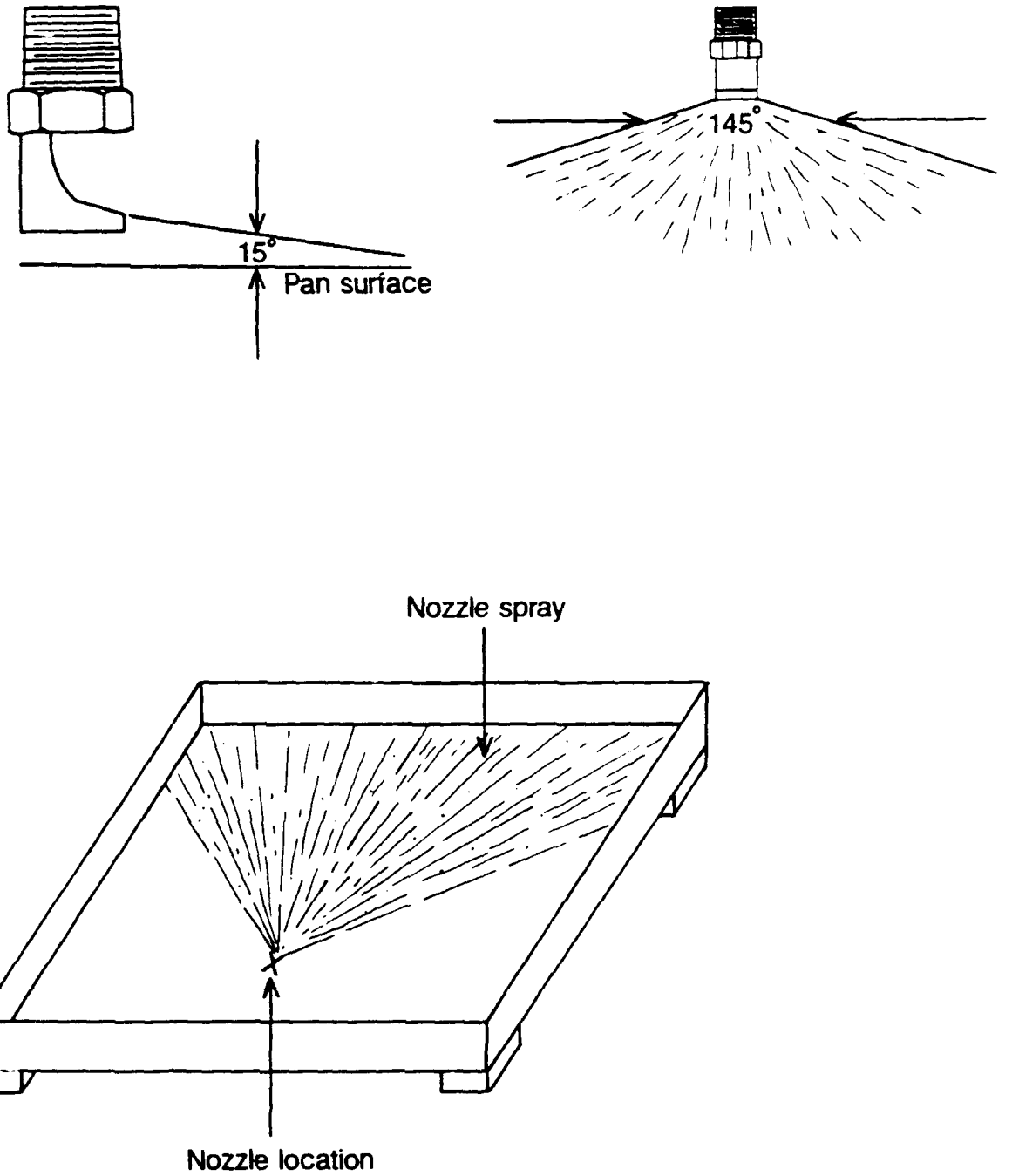

Fig. 8 - Fire type configuration

It was determined that optimum performance was achieved using an orifice sized to yield the desired flow at 138-207 kPa (20-30 psi). The nozzle was installed at the center line of a square pan just inside the front lip. The pan sides were between 5-10 cm (2-4 in) high to contain the fuel spray. The size of the pan was calculated by determining the fuel surface area required to free burn the fuel being applied to the pan [9]. It was found that better performance was obtained by applying the fuel to the pan at a lower rate (50% is a good reduced rate) for the first minute to preheat the pan and prevent accumulation of excess fuel.

5.4 Preliminary Assumptions and Calculations

Having decided on the spray pan fire, the focus was then placed on the ventilation size and corresponding fuel load required to produce the highest temperatures in the simulated shipboard compartment. It was necessary that both the fuel flow rate and ventilation size be varied in this evaluation. The vent size was held constant while varying the fuel flow rate until the highest temperature was reached. Vent sizes consisting of 1, 2 and 3 door openings were evaluated in this test series.

The lower center compartment was designed to be the fire compartment. From this configuration, data on heat transfer to adjacent and upper compartments was obtained. These data provided a better understanding of shipboard fire spread.

As shown in Figure 4, the fire compartment contained three doors each equal in size and height to a standard Navy shipboard door. The size of the opening to the outside air was enlarged during these tests. These opening sizes corresponded to a range of opening factors from 6-21 $m^{-\frac{1}{2}}$. This range was selected to encompass the 8-15 $m^{-\frac{1}{2}}$ range previously determined by CIB to produce the highest temperatures.

Before testing could begin, an estimation of the fuel flow rate required to produce the highest temperatures for each of the three ventilation sizes, was required. In theory, the highest temperature is achieved when the fuel flow rate is just sufficient to completely react with all the air entering the compartment (stoichiometric burning). Implicit in this theory is that the reaction should go to completion entirely within the fire compartment.

The first step in calculating the fuel flow rate required to approach stoichiometric burning is to determine the amount of air being drawn into the compartment. Kawagoe and Sekine [10] have determined that the maximum induced air flow into a heated compartment can be expressed simply as

$$\dot{m}_{air} \approx 0.52 \; A_w\sqrt{h} \qquad (3)$$

where

$\dot{m}_{air}$ = the maximum air flow rate, kg/s

A_w = the area of the opening, m^2

h = the height of the opening, m^2

To obtain the stoichiometric fuel release (gasification) rate, $\dot{m}_f$ (kg/s), the stoichiometric air to fuel ratio, R, such that

$$1 \text{ kg fuel} + R \text{ kg air} \rightarrow (1 + R) \text{ kg products} \qquad (4)$$

is required. The value of R is readily computable for fuels containing C, H, and O, from the chemical formula of the fuel, assuming the products to be CO_2, H_2O, and N_2. Substituting the above equations, the fuel flow rate is then calculated:

$$\dot{m}_f = \frac{0.52 \; A \sqrt{H}}{R} \qquad (5)$$

Inserting R = 14.3 for JP-5 (similar characteristics as diesel fuel) [11] and the ventilation parameters, the required fuel release rate to approach stoichiometric burning is determined. The calculated values are: one door - 3.8 lpm (1.0 gpm); two doors - 7.6 lpm (2.0 gpm); and three doors - 11.4 lpm (3.0 gpm). In order to verify the fuel flow required to produce maximum temperatures, fuel flow rates were varied from 75% to 125% of the calculated value for each ventilation opening.

5.5 Test Plan

5.5.1 Test Series #1, #2, and #3 (Spray Pan Fire)

Fuel flow rates, both above and below the calculated value, were tested to determine the flow rate which produced the highest temperatures for the one, two and three door ventilation configurations.

5.5.2 Test Series #4 (Wood Cribs, Variable Vent)

Two sizes wood cribs (Underwriters Laboratories, Inc. designations 6A, 10A) [12] were burned in each of the above ventilation configuration (one, two and three doors). The 6A wood crib produces an estimated heat release rate of 3 MW (10.2×10^6 BTU/hr) and 10A wood crib produces 6 MW (20.4×10^6 BTU/hr) [13]. These energy release rates are fairly close to stoichiometric JP-5 energy release rates in the one and three door tests, respectively. These tests were conducted to determine if Class A materials could approach the temperatures produced by the hydrocarbon fires.

6.0 RESULTS AND DISCUSSION

Only representative data will be included in this section. Complete sets of data for all tests may be found in Appendix A.

6.1 Test Series #1 - Spray Pan Fires

The first set of tests consisted of a one door fixed vent ($20.1\ m^{-\frac{1}{2}}$ opening factor) and varying fuel flow rates. The fuel flow rate required to produce maximum compartment temperatures for this ventilation condition was calculated from equation (5) to be 3.8 lpm (1 gpm). The range of 75-125 percent of the calculated fuel flow was investigated during each of the three test series. The data for this test series are summarized in Table 1.

The following definitions apply to the items listed in this and subsequent tables:

Equivalent energy release rate - theoretical energy released by the complete combustion of the fuel,

Upper layer temperature - steady state average of the top three thermocouples from the two trees in the fire compartment,

Compartment temperature - steady state average of all thermocouples in the fire compartment,

Peak upper compartment temperature - maximum air temperature in upper compartment,

Upper compartment temperature - average of all thermocouples in the upper compartment during steady state conditions,

Table 1. Summary Data Sheet for Test Series #1 - Spray Pan Fires
1 Door Tests (Opening Factor $A_T/A\sqrt{H}$ = 20.1 $m^{-\frac{1}{2}}$)

Test Number	11	12	16
JP-5 Flow Rate, lpm	2.7	3.8	4.5
(gpm)	(0.7)	(1.0)	(1.2)
Equivalent Energy Release Rate of Fuel, MW	1.6	2.2	2.7
(BTU/hr x 10^6)	(5.5)	(7.5)	(9.2)
Fire Compartment			
Upper Layer Temp., °C	725	900	700
(°F)	(1337)	(1652)	(1292)
Comp. Temp., °C	675	800	650
(°F)	(1247)	(1472)	(1202)
Peak Upper Comp. Temp., °C	325	350	250
(°F)	(617)	(662)	(482)
Upper Comp. Temp., °C	275	300	200
(°F)	(527)	(572)	(392)
Adj. Comp. Temp., °C (east)	200	250	150
(°F)	(392)	(482)	(302)
Max. Wall Temps.			
Interior, °C	650	700	600
(°F)	(1202)	(1292)	(1112)
Exterior, °C	600	675	525
(°F)	(1112)	(1247)	(977)
Max. Ceiling Temps.			
Interior, °C	--	--	650
(°F)	--	--	(1202)
Exterior, °C	--	--	575
(°F)	--	--	(1067)
O_2 Content, % vol (dry)	6	2	0
CO Content, % vol (dry)	0	1	4
CO_2 Content, % vol (dry)	8	10	9

Adjacent compartment temperature - average of all thermocouples in the adjacent (east) compartment during steady state conditions,

Maximum ceiling and wall temperatures - maximum bulkhead and deck surface temperatures,

Interior - surface in fire compartment

Exterior - surface in adjacent or upper compartment.

The upper layer temperatures along with the average compartment temperatures are plotted as a function of fuel flow rate in Fig. 9. As illustrated in this figure, the calculated value of fuel flow rate required to produce maximum compartment temperatures proved to be accurate. The upper layer temperature was observed to increase from 725°C (1337°F) at a fuel flow rate of 2.7 lpm (0.7 gpm) to a maximum temperature of 900°C (1652°F) for a fuel flow rate of 3.8 lpm (1 gpm). Increasing the fuel flow above this critical value resulted in a substantial decrease in temperature (700°C (1292°F)) at 4.5 lpm (1.2 gpm). The temperature was expected to decrease for fuel flow rates greater than the calculated value, but the temperature reduction recorded in this test series appears to be unprecedented in the literature. The average fire compartment temperatures followed the same trend and were measured to be 50-100°C (122-212°F) less than the upper layer.

Surface temperatures measured on the boundaries of the fire compartment and the air temperature measured in the surrounding compartments followed the same trend with fuel flow rate (see Table 1). Unexposed surface temperatures were measured to be 25-75°C (77-167°F) less than the exposed surfaces.

Gas concentrations measured just below the top of the ventilation opening (lintel) reflected the amount of oxygen being consumed during the combustion process. The oxygen steadily dropped with increasing fuel flow, reaching 2% at the stoichiometric flow rate and decreasing to zero for flow rates above the calculated stoichiometric value. This indicates that the combustion efficiency at the stoichiometric fuel flow rate was somewhat less than 100%. The carbon dioxide concentrations reached peak values (10% by volume) at the calculated fuel flow rate and decreased on either side of the desired rate.

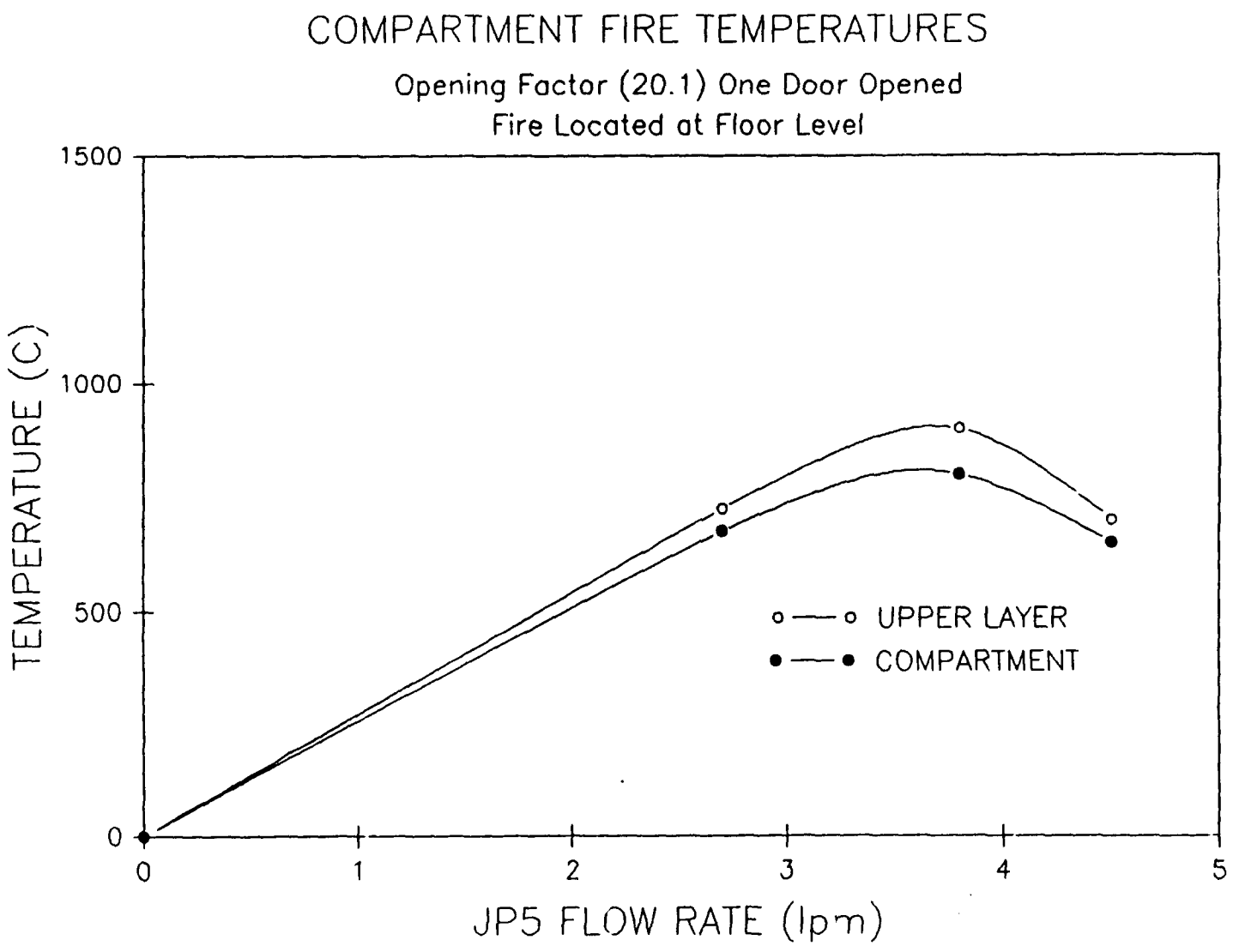

Fig. 9 - Compartment temperatures as a function of fuel flow rate for test series #1 (one door tests, 20.1 $m^{1/2}$ opening factor)

6.2 Test Series #2 - Spray Pan Fires

The second set of tests consisted of a two door fixed vent (9.6 $m^{-\frac{1}{2}}$ opening factor) and varying fuel loads. The fuel flow rate required to produce maximum compartment temperatures was calculated from equation (5) to be 7.6 lpm (2 gpm). A range covering 75-125 percent of the calculated value was analyzed during this test series. The data for this test series are summarized in Table 2.

A total of five tests were conducted with this size vent opening due to the similarity in data between tests with different flow rates. The upper layer temperatures along with average compartment temperatures are plotted as a function of fuel flow rate in Fig. 10 for these five tests. Although the temperature data follow the same trend as the preceding tests series, it should be emphasized that the measurements only varied slightly from the maximum for flow rates above and below the calculated value. The upper layer temperature was observed to gradually increase from 1030°C to 1100°C (1886-2012°F) for increased fuel flow rates from 4.5-7.6 lpm (1.2-2.0 gpm). The flow rate corresponding to 125% of the calculated value produced temperatures only 50°C (122°F) less than the maximum recorded during these tests. The high velocity of air flowing through the compartment resulted in vigorous flame movement. The total heat flux measurements recorded in the compartment became unsteady and consequently must be expressed in ranges. Total heat flux measurements were recorded to be on the order of 70-120 kW/m^2 (6.4-11.0 BTU/ft^2 s).

Exposed surface temperatures measured during these tests produced similar temperatures (800°C (1472°F) independent of fuel flow rate. Unexposed surface temperatures remained 25-75°C (77-167°F) lower than the exposed surface temperatures. No obvious trends in the surface temperature measurements were observed during these tests. The absence of trends could be attributed to variations in direct flame impingement on the bulkheads and decks bounding the fire compartment. Gas sampling followed the same trends as the previous test series showing oxygen approaching zero and increasing carbon monoxide for increasing fuel flow rates. Peak values (9% by volume) of carbon dioxide were also measured around the calculated fuel flow rate and decreased for flow rates above and below the stoichiometric value.

Table 2. Summary Data Sheet for Test Series #2 - Spray Pan Fires
2 Door Tests (Opening Factor $A_T/A\sqrt{H} = 9.6\ m^{-\frac{1}{2}}$)

Test Number	24	28	26	27	29
JP-5 Flow Rate, lpm (gpm)	4.5 (1.2)	5.7 (1.5)	6.4 (1.7)	7.6 (2.0)	9.5 (2.5)
Equivalent Energy Release Rate of Fuel, MW (BTU/hr x 10^6)	2.7 (9.2)	3.4 (11.6)	3.8 (13.0)	4.5 (15.3)	5.6 (19.1)
Fire Compartment Upper Layer Temp., °C (°F)	1030 (1886)	1075 (1967)	1075 (1967)	1100 (2012)	1050 (1922)
Comp. Temp., °C (°F)	980 (1796)	1000 (1832)	1010 (1850)	1050 (1922)	975 (1787)
Peak Upper Comp. Temp., °C (°F)	380 (716)	425 (797)	425 (797)	425 (797)	380 (716)
Upper Comp. Temp., °C (°F)	350 (662)	375 (707)	375 (707)	375 (707)	350 (707)
Adj. Comp. Temp., °C (east) (°F)	250 (482)	275 (527)	275 (527)	275 (527)	225 (437)
Max. Wall Temps. Interior, °C (°F)	840 (1544)	800 (1472)	810 (1490)	775 (1427)	725 (1337)
Exterior, °C (°F)	780 (1436)	730 (1346)	750 (1382)	700 (1292)	675 (1247)
Max. Ceiling Temps. Interior, °C (°F)	800 (1472)	850 (1562)	810 (1490)	850 (1562)	800 (1472)
Exterior, °C (°F)	740 (1364)	775 (1427)	750 (1382)	775 (1427)	725 (1337)
Max. Total Heat Flux Fire Comp. (Range), kW/m^2 (BTU/ft^2 sec)	50-100 (4-9)	70-110 (6-10)	70-110 (6-10)	70-120 (6-11)	60-110 (5-10)
Upper Comp., kW/m^2 (BTU/ft^2 sec)	16 (1.4)	19 (1.7)	18 (1.6)	19 (1.7)	17 (1.5)
Adj. Comp. (east) kW/m^2 (BTU/ft^2 sec)	13 (1.2)	8 (0.7)	11.5 (1)	7 (0.6)	6 (0.5)
O_2 Content, % vol (dry)	8	5	4	2	1
CO Content, % vol (dry)	0	0	1	2	2
CO_2 Content, % vol (dry)	7	8	9	9	7

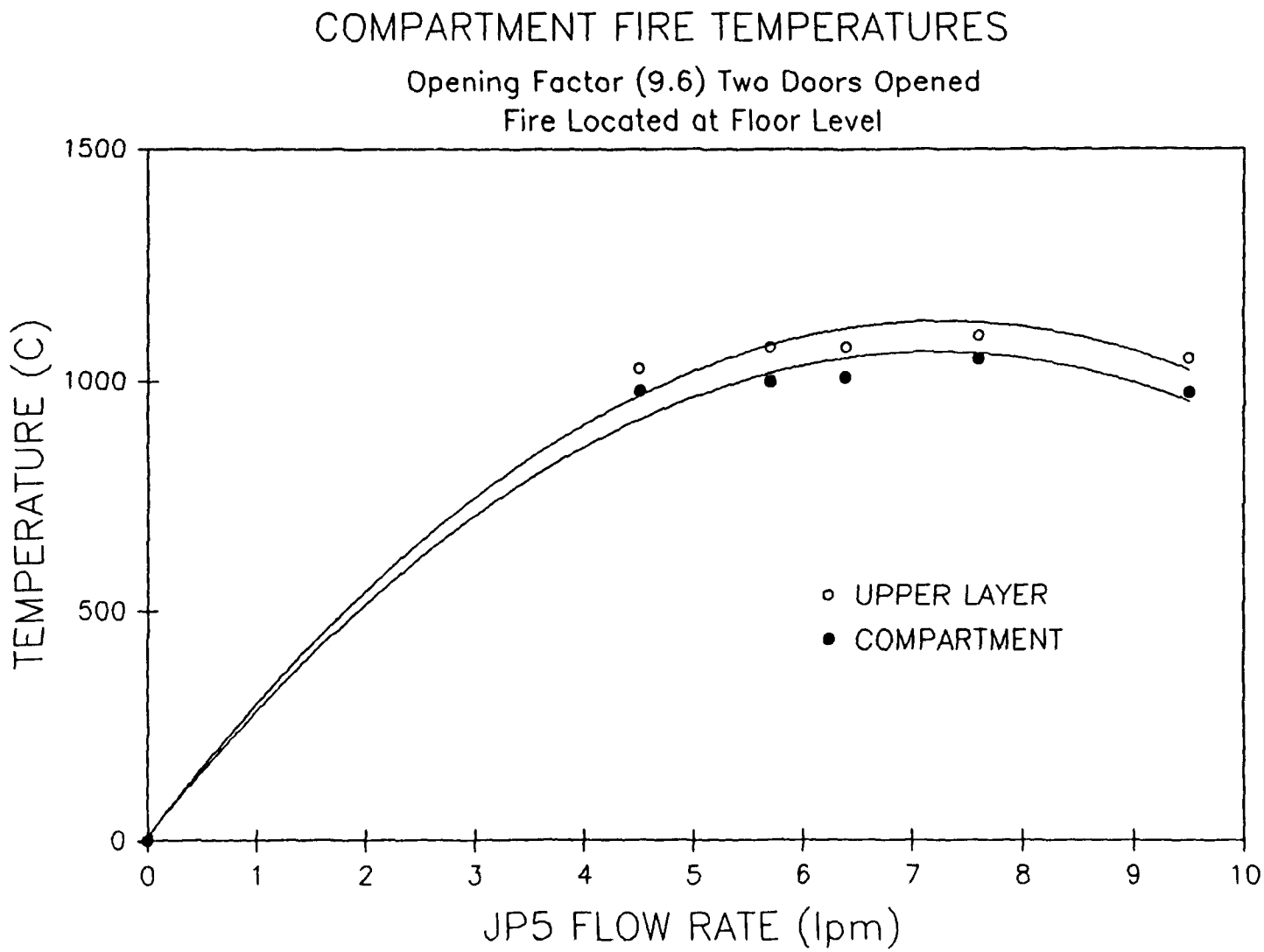

Fig. 10 - Compartment temperatures as a function of fuel flow rate for test series #2 (two door tests, 9.6 $m^{-1/2}$ opening factor)

6.3 Test Series #3 - Spray Pan Fires

The third set of tests consisted of a three door fixed vent (6.2 $m^{-\frac{1}{2}}$ opening factor) and varying fuel flow rates. The fuel flow rate required from equation (5) to produce maximum compartment temperatures was calculated to be 11.4 lpm (3 gpm). A range of flows covering 75-125 percent of the calculated value were analyzed. The data for this test series are summarized in Table 3.

The upper layer temperatures along with the average compartment temperatures are plotted as a function of fuel flow rate in Fig. 11. As illustrated in this figure, the stoichiometric fuel flow rate also produced the highest temperatures in this test series. Although following the same trends, the measurements only decreased marginally from the maximum value for varying fuel flow rates in the 40-167% range. The upper layer temperature was observed to increase from 725°C (1337°F) for 40% of the calculated value (4.5 lpm (1.2 gpm)) to a maximum value of 1100°C (2012°F) for a flow of 11.4 lpm (3.0 gpm). The higher flow rate 18.9 lpm (5 gpm) provide similar results with upper layer temperatures measured to be approximately 75°C (167°F) lower. Total heat flux measurements were observed to be on the order of 50-140 kW/m^2 (4.4-12.3 BTU/ft^2 s).

Exposed surface temperatures measured on the joining bulkheads were measured to be 725°C (1337°F) while unexposed temperatures were recorded as 675°C (1247°F). The deck separating the fire compartment and upper compartments recorded higher temperatures as expected (850°C (1562°F) exposed, 800°C (1472°F) unexposed). Air temperatures in both the upper and adjacent compartments recorded increasing temperature with increased fuel flow. This steady increase is contributed to the volume of flame protruding from the fire compartment and impinging on the outer boundaries of these compartments. The upper compartment was observed to increase from 275°C (527°F) to 475°C (887°F) for flow rates of 4.5-8.9 lpm (1.2-5 gpm). Temperatures in adjacent compartments were measured to be only marginally less. Gas analyses remained consistent with the previous test series.

Table 3. Summary Data Sheet for Test Series #3 - Spray Pan Fires
3 Door Tests (Opening Factor $A_T/A\sqrt{H}$ = 6.2 $m^{-\frac{1}{2}}$)

Test Number	49	42	43	45
JP-5 Flow Rate, lpm	4.5	7.6	11.4	18.9
(gpm)	(1.2)	(2.0)	(3.0)	(5.0)
Equivalent Energy Release Rate of Fuel, MW	2.7	4.5	6.7	11.2
(BTU/hr x 10^6)	(9.2)	(15.3)	(22.9)	(38.2)
Fire Compartment				
Upper Layer Temp., °C	725	925	1100	1075
(°F)	(1337)	(1697)	(2012)	(1967)
Comp. Temp., °C	650	875	1025	1000
(°F)	(1202)	(1607)	(1877)	(1832)
Peak Upper Comp. Temp., °C	325	450	500	510
(°F)	(617)	(842)	(932)	(950)
Upper Comp. Temp., °C	275	400	425	475
(°F)	(527)	(752)	(797)	(887)
Adj. Comp. Temp., °C (east)	275	360	410	450
(°F)	(527)	(680)	(770)	(842)
Max. Wall Temps.				
Interior, °C	575	725	725	750
(°F)	(1067)	(1337)	(1337)	(1382)
Exterior, °C	545	675	675	675
(°F)	(1013)	(1247)	(1247)	(1247)
Max. Ceiling Temps.				
Interior, °C	625	850	850	825
(°F)	(1157)	(1562)	(1562)	(1517)
Exterior, °C	575	800	800	700
(°F)	(1067)	(1472)	(1472)	(1292)
Max. Total Heat Flux				
Fire Comp. (Range), kW/m^2	50-100	80-140	90-140	70-110
(BTU/ft^2 sec)	(4.4-8.8)	(7.1-12.3)	(7.9-12.3)	(6.2-9.7)
Upper Comp., kW/m^2	3.0	7.0	6.0	10.0
(BTU/ft^2 sec)	(0.3)	(0.6)	(0.5)	(0.9)
Adj. Comp. (east), kW/m^2	2.0	3.0	3.0	4.0
(BTU/ft^2 sec)	(0.2)	(0.3)	(0.3)	(0.4)
O_2 Content, % vol (dry)	8	6	2	0
CO Content, % vol (dry)	0	0	2	3
CO_2 Content, % vol (dry)	9	9	10	10

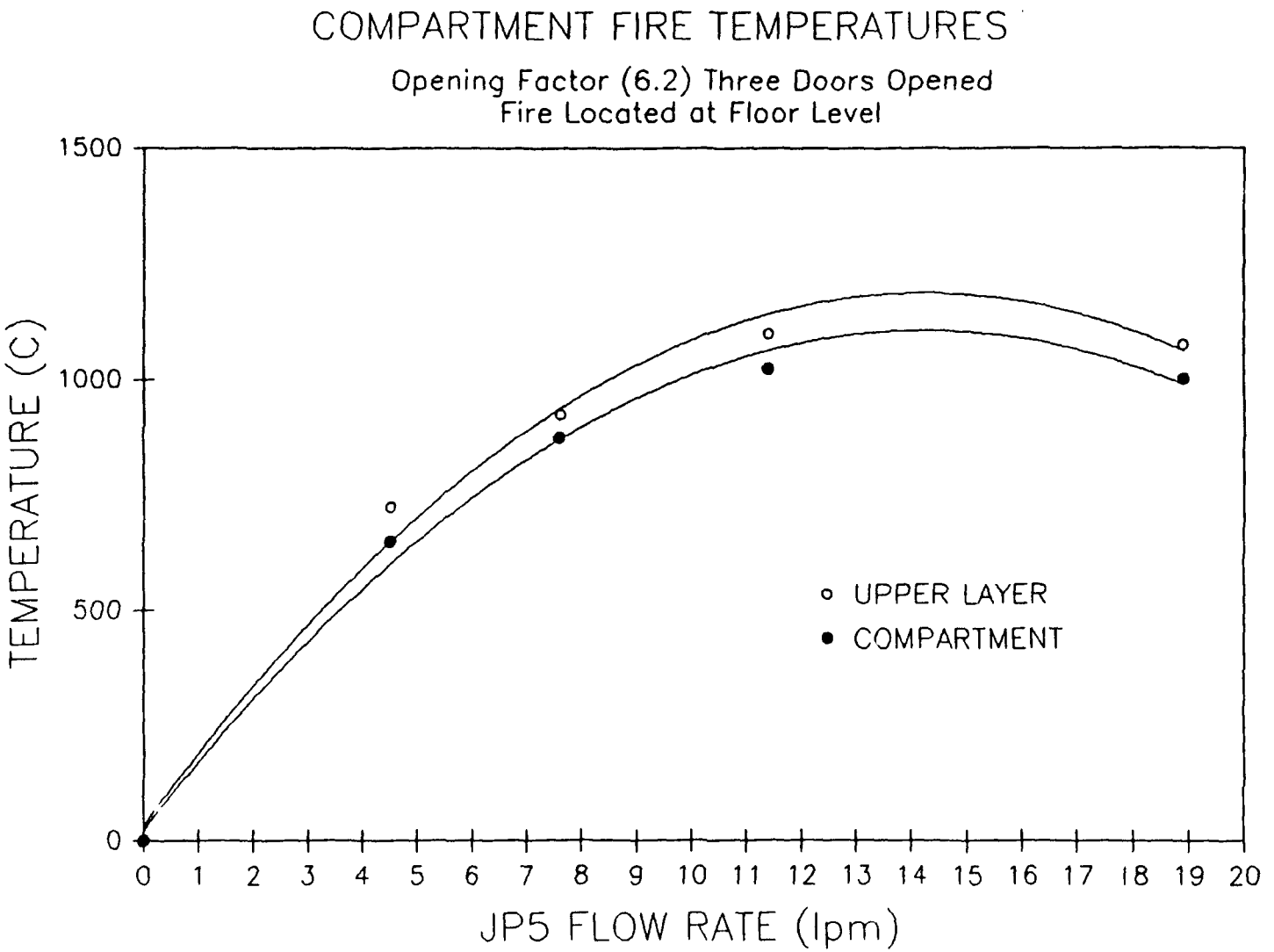

Fig. 11 - Compartment temperatures as a function of fuel flow rate for test series #3 (three door tests, 6.2 $m^{1/2}$ opening factor)

6.4 Test Series #4 - Class A Fires

A test series was also conducted to determine if equally severe fire conditions could be obtained using Class A materials. The Class A materials were selected so that during the manned test series, to be conducted on the ex-USS SHADWELL, the fire fighters would face a more representative fire than the spray pan fires of the earlier series. The data from these tests are summarized in Table 4. Two standard size wood cribs (6A & 10A) [12] were used in this test series.

The wood cribs were unable to produce the extreme temperatures observed during the JP-5 spray fires. The maximum temperatures observed were upper layer temperatures of 750°C (1382°F), and an average compartment temperature of 700°C (1292°F) as compared to the JP-5 tests where both upper layer and average compartment temperatures were over 1000°C (1832°F). The moisture content of the wood cribs varied from piece to piece and in many cases was measured to over 20% by weight. This excessively high moisture content made the actual energy release rate of the wood cribs difficult to determine. The questionable heat release rates only served to confuse the issues of the fuel load required to produce maximum temperatures.

Two other mechanisms also contributed to variations in the compartment temperature data. The first is the increase in elevation of the fuel load above the floor which serves to alter the air flow through the compartment. The interface between the inflow of cold air and outflow of hot gases is raised, reducing the airflow through the opening which in turn increases the height of the neutral plane. Also, the vertical column of flame produced by the wood crib would not fit into the compartment, resulting in the bending of the plume out the ventilation opening. The high moisture content, increased fuel elevation, and flame geometry caused the wood crib fires to be less severe than the JP-5 spray fires and consequently inappropriate for protocol testing on the ex-USS SHADWELL. It should also be noted that the volume of wood cribs required to sustain burning for the desired duration would more than fill the entire fire compartment.

Table 4. Full Scale Mock-Up Summary Data Sheet for Test Series #4 - Class A Fires

Test Number	19	18	37	38	57	58	59
Number of Doors	1 door	1 door	2 doors	2 doors	3 doors	3 doors	3 doors
Opening Factor	20.1	20.1	9.6	9.6	6.2	6.2	6.2
Crib Size & Burning Rate	6A 121 g/s	10A 190 g/s	6A 129 g/s	10A 234 g/s	6A 136 g/s	10A 227 g/s	10A 190 g/s
Equivalent Energy Release Rate of Fuel, MW (BTU/hr x 10^6)	2.4 (8.2)	3.7 (12.6)	2.5 (8.5)	4.6 (15.7)	2.7 (9.2)	4.4 (15.0)	3.7 (12.6)
Fire Compartment Upper Layer Temp., °C (°F)	625 (1157)	575 (1067)	700 (1292)	750 (1382)	725 (1337)	750 (1382)	750 (1382)
Comp. Temp., °C (°F)	550 (1022)	550 (1022)	650 (1202)	675 (1247)	650 (1202)	700 (1292)	675 (1247)
Peak Upper Comp. Temp., °C (°F)	175 (347)	200 (392)	225 (437)	225 (437)	175 (347)	250 (482)	250 (482)
Upper Comp. Temp., °C (°F)	150 (302)	175 (347)	200 (392)	200 (392)	150 (302)	200 (392)	200 (392)
Adj. Comp. Temp., °C (east) (°F)	100 (212)	125 (257)	150 (302)	175 (347)	125 (257)	175 (347)	175 (347)
Max. Wall Temps. Interior, °C (°F)	410 (770)	440 (824)	500 (932)	575 (1067)	380 (716)	500 (932)	475 (887)
Exterior, °C (°F)	380 (716)	400 (752)	475 (887)	525 (977)	350 (662)	475 (887)	450 (842)

Table 4. Summary Data Sheet for Test Series #4 - Class A Fires (Continued)

Max. Ceiling Temps.							
Interior, °C (°F)	575 (1067)	525 (977)	675 (1247)	650 (1202)	700 (1292)	475 (887)	425 (797)
Exterior, °C	500 (932)	475 (887)	600 (1112)	600 (1112)	600 (1112)	450 (842)	400 (842)
Max. Total Heat Flux							
Fire Comp. (Range), kW/m^2 (BTU/ft^2 sec)	35 (3.1)	35 (3.1)	35-50 (3.1-4.4)	45 4.0	40-60 (3.5-5.3)	65-80 (5.7-7.1)	60-70 (5.3-6.2)
Upper Comp., kW/m^2 (BTU/ft^2 sec)	3.0 (0.3)	4.0 (0.4)	2.0 (0.2)	2.0 (0.2)	2.0 (0.2)	2.0 (0.2)	2.0 (0.2)
Adj. Comp. (east), kW/m^2 (BTU/ft^2 sec)	2.0 (0.2)	3.0 (0.3)	1.0 (0.1)	1.0 (0.1)	1.0 (0.1)	1.0 (0.1)	1.0 (0.1)
O_2 Content, % vol (dry)	3.0	1.0	5.0	3.0	6.0	5.0	--
CO Content, % vol (dry)	2	--	0	2	0	1	--
CO_2 Content, % vol (dry)	8	--	8	9	9	8	--

6.5 Burning Regimes

Upper layer temperatures along with average compartment temperatures are plotted as of function of fuel flow rate for each opening factor in Figs. 9, 10, and 11. As illustrated by these figures, the calculated value of the fuel flow required to approximate stoichiometric burning and maximum temperature (peak values on these figures) proved to be accurate. The values to the left of the peak values correspond to the fuel controlled regime and the values to the right, to the ventilation controlled regime.

During these tests, the volume of flame protruding out the ventilation opening dramatically increased for the two and three door tests, independent of the burning regime. Unexpectedly, flames protruded out the vent opening even during the fuel controlled (fuel lean) scenarios which as predicted by the burning regime description should not become visible until the fire becomes ventilation controlled (fuel rich). Although the temperature and heat flux measurements remained fairly predictable with respect to fuel flow rate, the visual observations did not. The excess flame observed during these tests was the result of insufficient residence time for combustion. In other words, the compartment was too small to contain the fire plume.

In the development of the theory of the burning regimes, an assumption is made that the combustion process occurs infinitely fast, i.e., is not limited by mixing effects. In actuality, this is not always the case. Although the combustion process itself occurs very quickly, the time required to mix the fuel and air spray droplets is substantially greater. During the two and three door tests, the air flow through the compartment doubles and triples respectively. The amount of time the oxygen spends in the compartment (residence time) is dramatically shortened. If the residence time is not sufficient to allow mixing of the fuel droplets and air, the combustion process is not completed until the plume outside the compartment, resulting in increased volumes of flame protruding out the ventilation opening.

This can also be described in terms of the flame to compartment volume ratio, based on a constant volumetric heat release rate. Observations by Rasbash and by Orloff and deRis [13] suggest that the critical volumetric heat release is approximately 1200 kW/m^3 (32 BTU/ft^3 sec). When the flame/compartment volume calculated on this basis exceeds ≈ 0.2, the compartment appears to no longer behave as a "well mixed reactor." In Appendix B, C. Beyler also concludes that above the critical ratio of 0.2, the compartment no longer behaves as a well-stirred reactor, but it is better

characterized as a large open flame confined by the presence of the enclosure. This confined flame theory would also explain the volume of fire out the ventilation opening.

Although the later test series demonstrated high flame to compartment volume ratios, the one door tests met the "well-stirred reactor" criteria and are described as follows.

6.5.1 Fuel Controlled

The fuel controlled regime is the condition where the burning rate of the fuel is independent on the size of the opening and is determined instead by the surface area and burning characteristics of the fuel. The air flow into the compartment is more than ample to consume all the pyrolized fuel. Compartment temperatures in this regime were measured to be substantially lower than the other two regimes. This is due to both the cooling effect of the excess air flowing into and out of the compartment and to a lower total heat release. This is illustrated by the region to the left of the peak values on Figs. 9, 10 and 11. As shown from the Fig. 12 (1B), the combustion process takes place just behind the fuel surface and just below the ceiling producing a distinct temperature gradient in which the temperature increases with increased elevation, Fig. 12 (1A). The combustion process takes place entirely inside the compartment resulting in little or no flaming outside the door in Fig. 12 (1C). Oxygen concentrations measured just below the lintel were greater than two percent, and are indicative of the this regime. Negligible CO and increasing CO_2 readings were also observed.

6.5.2 Stoichiometric

Stoichiometric burning is achieved when the amount of fuel being vaporized is precisely the amount needed to consume all of the air entering the compartment. Under these conditions, the maximum amount of energy is being released in the compartment and the convective losses are at a minimum, producing the highest temperatures recorded for a given vent opening. Stoichiometric burning is an optimization of air/fuel ratios required to achieve maximum temperatures. These temperatures correspond to the peak values on Figs. 9, 10 and 11. The combustion zone fills most of the volume of the compartment, as shown in Fig. 12 (2B). The compartment approaches a well-stirred reactor condition illustrated by the consistency of the temperatures recorded throughout the compartment (Fig. 12 (2A)). The combustion process is brought to completion inside the compartment resulting in only "licks" of flame protruding from the ventilation opening (Fig. 12 (2C)). Gas sampling taken during this regime show

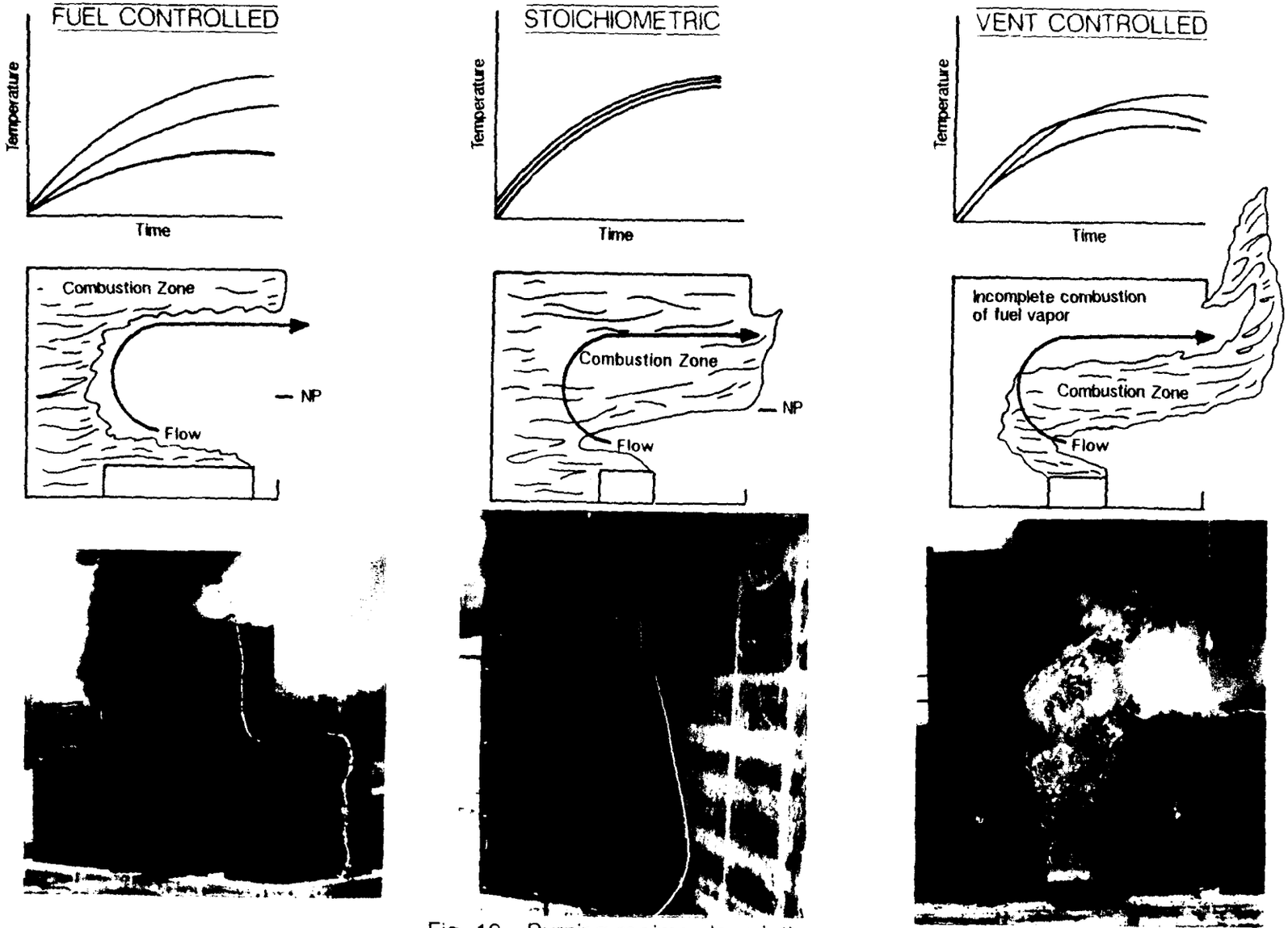

Fig. 12 - Burning regime descriptions

oxygen down to one percent, measurable amounts of CO being produced and peak valves of carbon dioxide (10%).

6.5.3 Vent Controlled

Increasing the fuel flow above that required for stoichiometric burning, drives the fire into the ventilation controlled regime. This is illustrated by the region to the right of the peak values on Figures 9, 10 and 11. This regime is achieved when the fuel vaporization rate is greater than the rate needed to consume all the available oxygen entering the compartment. The combustion zone is compressed to an area encompassing the neutral plane while the superheated unburnt or partially combusted vapors above this zone complete the burning process outside the compartment where oxygen is more readily available (Fig. 12 (3B, 3C)). The excess unburnt fuel leaving the compartment increases the convective losses out the ventilation opening, resulting in an overall lower compartment temperature. In the ventilation controlled regime, the highest temperatures measured in the compartment are recorded near the neutral plane as shown in Figure 12 (3A). Gas analysis taken during this regime show zero oxygen, increased carbon monoxide and decreasing carbon dioxide.

6.6 Fully Developed Fire Behavior

6.6.1 Temperature as a Function of Ventilation Parameters

In our attempt to approximate a "typical" shipboard compartment, many of the controlling variables, such as wall materials and ventilation parameters, have been bounded. Incorporating the existing knowledge of how to calculate fire size in order to approximate stoichiometric conditions and using the temperatures recorded during these tests, an analysis of the ventilation parameters required to produce maximum temperatures was conducted. The maximum upper layer and compartment temperatures for the three test series as a function of opening factor are show in Fig. 13. As illustrated by this figure, the optimum opening factor lies in the range of approximately 6-10 $m^{-\frac{1}{2}}$ which corresponds to our 2 & 3 door opening factors. At opening factors above 10 $m^{-\frac{1}{2}}$, conditions were only marginally less severe than worse case conditions.

As stated in the theory section of this report, CIB has conducted over 400 experiments in small compartments to determine the relation of temperature to ventilation size or opening factor. CIB concluded that the maximum temperature for their compartment fire scenario is observed in the range of opening factors of 8-15 $m^{-\frac{1}{2}}$ (see Fig. 14). For larger ventilation openings, the compartment volume was inadequate

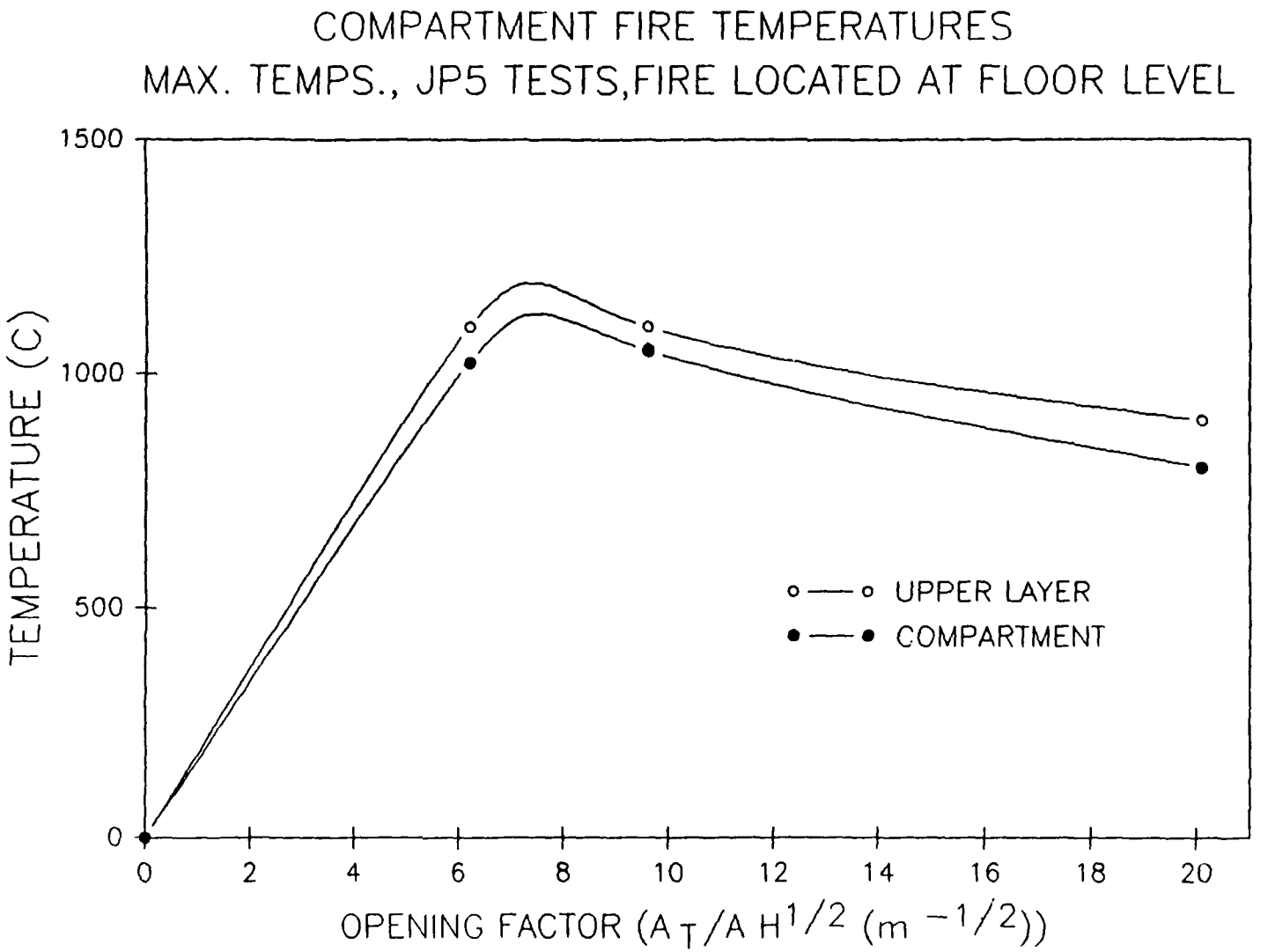

Fig. 13 - Compartment temperatures as a function of opening factor

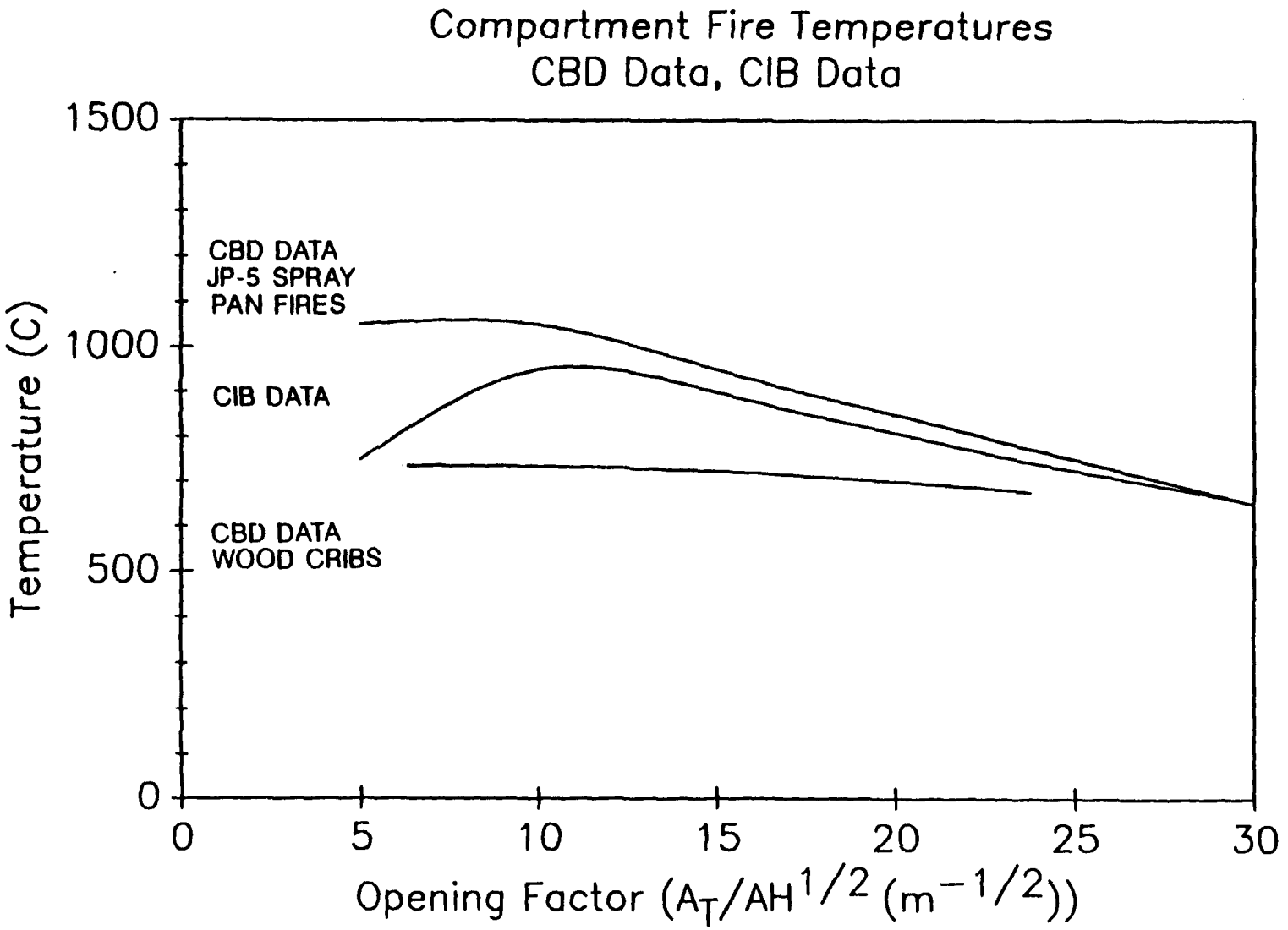

Fig. 14 - Data comparison with CIB data

to house the amount of fuel (wood) required to produce maximum temperatures. Data collected in this test series produce the same characteristic curve with maximum temperatures occurring in a range of opening factors from 6-12 $m^{-\frac{1}{2}}$. For larger ventilation openings (smaller opening factors), the temperature was observed to decrease slightly. This slight decrease may have been a function of the increased vulnerability to environmental conditions due to the larger vent openings. The temperatures recorded during these tests were surprisingly close to those recorded by CIB despite the difference in wall materials. The CIB tests were conducted in compartments made of thermally thick materials as compared to the steel enclosure used during this analysis. The thermally thick material should have resulted in higher temperatures observed in the CIB tests than those recorded during this test series. The compartments surrounding the fire compartment in this test series must have effectively insulated the fire compartment producing similar results.

6.6.2 Temperature Predictions using Numerical Methods

The concept of post-flashover compartment fires and predictions of their temperatures have long been studied and are widely accepted. A calculation method to predict post-flashover compartment fire temperatures without the use of computer codes has been developed by V. Babrauskas [4]. The drawback to this method is that it only predicts the temperature in the fire compartment as compared to computer models which produce a detailed fire history including heat balance, wall temperatures, flow velocities, and other related information. A comparative analysis between the Babrauskas method and the computer model from which it was derived (COMPF2) for compartments constructed of thermally thick materials show agreement within 3% [4]. The applicability of the Babrauskas method when applied to steel enclosures has not been determined.

The approach taken in developing the Babrauskas method was to produce the simplest calculation procedure which will, to a suitable degree of precision, duplicate the results of more detailed numerical methods. The method is based on the temperature produced by adiabatic combustion decreased by five efficiency factors, each of which can range from 0 to 1. These five factors are: burning rate stoichiometry; wall losses (steady state); wall losses (transient); opening height effects; and combustion efficiency.

When applied to our given set of parameters, this method predicted substantially lower temperatures than were recorded during this test series (see Table 5).

Table 5. Comparison of Compartment Temperatures predicted by Babrauskas' Method with CBD Test Data

Opening Factor ($m^{-\frac{1}{2}}$)	Door Equivalent	Babrauskas (°C)	Actual (°C)
20.1	1	545	800
9.6	2	741	1050
6.2	3	874	1025

An analysis of the five efficiency factors calculated for this scenario suggests that the steady state wall losses are the primary factor contributing to these low temperature predictions. The inaccuracy of these wall loses make this model inappropriate for structures having steel walls.

An analysis was also conducted by Gross and Davis of NBS [7] incorporating the computer model FIRST, modified to model thermally thin boundaries, to predict temperature, energy release rates, and heat transfer in a burning compartment as a function of compartment size, vent size, combustible loading, and compartment enclosure materials. Only two of the twenty-two runs conducted in their analysis had similar characteristics to this test series. The modified model, FIRST, was only able to correctly predict results for one test. The computer run consisted of a one door equivalent vent opening (20.1 $m^{-\frac{1}{2}}$) and an energy release rate of 2.7 MW. The upper layer temperatures were calculated to be 850°C (1562°F) and wall temperatures were estimated to be 640°C (1184°F). This compares to measurements of 700°C (1292°F) and 575°C (1064°F), respectively. The parameters incorporated in this run produced a fire which was ventilation controlled (fuel rich). In the actual test, the volume of flame outside the compartment may have contributed to the higher temperatures in the fire compartment by heating of the compartment from the outside.

An analysis of the fire compartment temperatures obtained in the test series was also conducted by Craig Beyler (Appendix B). In short, Beyler concluded that due to a high ratio of flame to compartment volume, most of these tests did not fulfill the assumption of a "well-stirred" reactor required in all post-flashover compartment fire models. The fire volume and residence time were such that incomplete mixing of the air and fuel in the compartment resulting in a significant amount of gases combusting outside the ventilation opening. Compartment fires of this type

(flame to compartment volume ratios of over 0.2) produce much higher temperatures than predicted using numerical methods.

Although not predictable using numerical methods, fires that exceed the critical flame to compartment volume ratios produce the most severe thermal insult (highest temperatures and large volumes of fire out the door) to the compartment and to the ship. For these fires, it is appropriate to predict compartment temperatures of approximately 1000°C regardless of the heat losses through the compartment boundaries. Beyler also observed these high flame volume ratios in the CIB test series would explain the consistency between the experimental CBD data and the CIB data.

6.7 Design Fire Development

Incorporating the modified spray fire developed in the scoping tests, the knowledge of burning regimes and an understanding of the energy loss mechanisms, the selection of a design fire can be made. Based on the criteria that the design fire must produce the highest temperatures in a simulated shipboard compartment, the selection of a design fire was simplified. As previously stated, the highest temperatures for a given opening occur when the fuel to air ratio approaches stoichiometric conditions. As concluded by CIB and confirmed in this evaluation, the highest temperatures obtainable for a given compartment fire occur when the ventilation opening is sized to produce an opening factor in the range of 8-15 $m^{-\frac{1}{2}}$. Only one test conducted in this evaluation meets this criterion. Test #27 listed in Table 2 consisted of the fuel flow calculated to approach stoichiometric conditions 7.6 lpm (2 gpm) with two doors opened which corresponds to an opening factor of 9.6 $^{m-\frac{1}{2}}$. Upper layer temperatures of 1100°C (2012°F) and average compartment temperatures of 1050°C (1922°F) were observed during this test. Total heat flux measurements of 50-120 kW/m^2 (4.4 - 10.6 BTU/ft^2) were also observed. It should be noted that the larger vent opening (3 doors with an opening factor of $6.2^{m-\frac{1}{2}}$) at stoichiometric conditions produced a fire of similar severity (upper layer temperatures of 1100°C (2012°F), average compartment temperatures of 1025°C (1877°F) and total heat flux measurements of 90 to 140 kW/m (8.0 - 12.4 BTU/ft^2)). The larger ventilation opening was not selected as the design fire because the increased fuel flow did not produce higher temperatures, while increasing the fuel demand. The smaller opening (1 door/ $20.1^{m-\frac{1}{2}}$ opening factor), at stoichiometry, produced significantly less severe conditions (upper layer temperatures of 900°C (1652°F) and average compartment temperatures of 800°C (1472°F)) and for this reason was not selected as the design fire.

The design fire to be used on the ex-USS SHADWELL will incorporate an opening factor of approximately 10 $m^{-\frac{1}{2}}$ determined by equation (2). The air flow into the compartment will be calculated using equation (3). From this air flow, the fuel flow rate can be determined using the stoichiometric ratio found in the Chemical Engineers' Handbook [11] for the desired fuel (14.3 for JP-5). It should be noted that the design fire was selected as the fire which produces the most severe condition in the compartment of origin. A highly ventilation controlled fire may produce a greater threat to the overall ship due to flames protruding from the fire compartment down passageways or into adjacent compartments by means of doors, hatches, or bulkhead breaches.

6.8 Fire Resistance and Severity

6.8.1 Energy Balance Analysis

An energy balance analysis conducted on the compartment illustrates that the energy of combustion is dissipated or lost by three mechanisms, each a function of the gas temperature in the compartment. These mechanisms are convective losses due to the outflow of hot gases, radiation losses out the opening(s) and conduction losses through the compartment boundaries.

An attempt to estimate the energy losses at stoichiometric burning for each of the three opening factors is shown in Tables 6 and 7. Table 6 lists the actual test data incorporated in these calculations and Table 7 shows the experimental results. Stoichiometric burning was selected for this analysis to simplify the problem. Under stoichiometric conditions, the energy being released in the compartment is directly related to the mass flow rate of air entering the compartment and the gases leaving the compartment can be assumed to be the products of complete combustion, not various percentages of unburned fuel and oxygen.

The energy of combustion may be calculated by two methods. The first is by using the heat of combustion of the fuel multiplied by the fuel flow rate recorded during these tests. The second is by estimating the air flow into the compartment by equation (3) and multiplying by the heat of combustion of air. Assuming stoichiometry, these two calculation techniques should produce approximately the same value which was the case during this evaluation. Heat losses by radiation out the opening are calculated using the Stefan-Boltzman law which is expressed by equation (6).

Table 6. Energy Balance - Background Data

Test	$\dot{m}_{air}$ (kg/s) (lb/s)	Compartment Temperature (Average) (°C) (°F)	Compartment Temperature Upper Layer (°C) (°F)	Ceiling Average Temperature (In/Out) (°C) (°F)	Upper Compartment Temperature (Average) (°C) (°F)
12	0.74 (1.63)	800 (1472)	900 (1652)	620/586 (1148/1087)	230 (446)
27	1.48 (3.26)	1050 (1922)	1100 (2012)	678/635 (1252/1175)	238 (460)
43	2.22 (4.89)	1025 (1877)	1100 (2012)	721/682 (1330/1260)	351 (664)

Test	$\dot{m}_{fuel}$ (kg/s) (lb/s)	West Wall Average Temperature (In/Out) (°C) (°F)	West Compartment Average Temperature (°C) (°F)	East Wall Average Temperature (In/Out) (°C) (°F)	East Compartment Average Temperature (°C) (°F)	Outside Walls Average Temperature (In/Out) (°C) (°F)
12	0.05 (0.11)	603/557 (1117/1035)	225 (437)	551/514 (1024/957)	190 (374)	545/500 (1013/932)
27	0.10 (0.22)	635/570 (1175/1058)	355 (671)	676/625 (1249/1157)	210 (410)	587/550 (1089/1022)
43	0.16 (0.35)	656/604 (1213/1119)	310 (590)	711/691 (1312/1276)	304 (579)	609/580 (1128/1076)

Table 7. Energy Balance Results

Test	Radiant Losses, kW (BTU/s)	Convective Losses, kW (BTU/s)	Energy Losses Through the Compartment Boundaries, kW (BTU/s)					Losses, MW (BTU/s)	Energy of Combustion
			West	East	Ceiling	Outer	Floor		
12	83 (78.7)	940 (891.1)	137 (129.9)	113 (107.1)	161 (152.6)	216 (204.8)	30 (28.4)	1.7 (1611.6)	2.2
27	384 (364.0)	2200 (2085.6)	143 (135.6)	197 (186.8)	209 (198.1)	252 (238.9)	30 (28.4)	3.4 (3223.3)	4.5
43	533 (505.3)	3295 (3123.7)	161 (152.6)	257 (243.7)	233 (220.9)	258 (244.6)	30 (28.4)	5.8 (5498.5)	6.7

$$\dot{q}_R = A_w \ \epsilon_F \ \sigma \ (Tg^4 - To^4) \qquad (6)$$

where

$\dot{q}_R$ = radiant heat losses (kW/m^2)

A_w = total area of vent openings (m^2)

ϵ_F = emissivity of the hot gases

σ = Stefan-Boltzman constant (5.67×10^{-11} $kW/m^2 \ K^4$)

Tg = temperature of the hot gases (K)

To = ambient temperature (K)

Convective heat losses out the opening are determined by equation (7), viz:

$$\dot{q}_L = \dot{m}_F \ Cp \ (T_g - T_o) \qquad (7)$$

where

$\dot{q}_L$ = convective heat losses (kW/m^2)

$\dot{m}_F$ = sum of the fuel and air mass flow rates (kg/s)

Cp = specific heat of the gases leaving the compartment (KJ/kg K)

T_g = upper layer gas temperature (K)

T_o = ambient temperature (K)

The energy lost through the compartment boundaries may be calculated three ways. After steady state conditions are reached, the energy absorbed by the boundary should equal the heat conducted through the material and equal to the energy emitted from the unexposed side of the boundary. The absorbed and emitted energies may be estimated using Stefan-Boltzman's law assuming an additional percentage for convective heat losses. The energy conducted through the boundary is a function of the temperature difference across the wall, the thickness of the wall, and the thermal conductivity of the boundary material. The calculation for the energy being radiated by the unexposed side of the

boundary used for this analysis is based on equation (6), viz:

$$\dot{q}_w = A_s \quad \epsilon\sigma \ (T_w^4 - T_c^4) \qquad (8)$$

where

$\dot{q}_w$ = heat losses through the walls (kW/m^2)

A_s = total surface area of the bulkheads and/or decks (m^2)

ϵ = emissivity of the material

σ = Stefan-Boltzman constant (5.67×10^{-11} $kW/m^2\ K^4$)

T_w = surface temperature of bulkhead or deck (K)

T_c = adjacent compartment air temperature (K)

As expected, the majority of the energy losses from the compartment are due to convective losses out the ventilation opening(s) (50-60%). These losses are the result of the superheated gases exiting the compartment. Energy losses through the boundaries account for almost (30-40%) with 10% lost through the ceiling. This is somewhat lower than the value of (20%) lost through the ceiling predicted by NBS [7] using the model, FIRST. The lower energy losses may be attributed to the insulating effects produced by the surrounding compartments. The remaining energy (less than 20%) is radiated out the ventilation opening(s). In this analysis, only 75% of the calculated energy of combustion can be accounted for. Effects of combustion efficiency, fire protruding out the ventilation openings and the assumptions made to simplify these calculations could result in such a difference.

6.8.2 Heat Transfer Through Boundaries

In order to accurately evaluate and predict fire spread from a compartment of origin to adjacent compartments, an understanding of heat transfer through compartment boundaries is warranted. Fire will spread from the compartment of origin to adjacent compartments by means of a mechanical breach or by heat conducted through the boundary. An analysis of fire spread through breached boundaries would be extensive due to the magnitude of factors which contribute to this type of fire spread. However, it may be assumed that a post-flashover fire will spread almost immediately through a

breached boundary. Fire spread through a boundary without a breach requires a more detailed analysis.

Fire spreads through boundaries without a mechanical breach by means of heat conduction through the boundary material. The quantity of heat being transferred is a function of the temperature difference across the boundary, the thickness of the boundary, and the thermal conductivity of the boundary material. For a constant energy release in the fire compartment, boundary materials with low thermal conductivities will develop a large temperature difference across the material. For common ship materials (i.e., steel, aluminum) which have high thermal conductivities, the temperature difference should be very small. This small temperature difference would result in a higher risk of fire spread through this type material.

Surface temperature measurements were taken on the bulkheads joining the adjacent compartments to the fire compartment and on the deck overhead joining the upper and fire compartments. The measured temperature difference across the boundaries was on the order of 50°C (122°F). This temperature gradient remained constant, independent of the bulkhead or deck surface temperatures as shown in Fig. 15. The temperature gradient was checked against a common finite element heat transfer program (FIRES-T3) [15]. This method predicted a temperature difference closer to 15°C (59°F). This discrepancy may be attributed to the method of attachment of the thermocouples to the steel plate. The thermocouples were attached to the steel by first drilling a small hole and then peening the thermocouple to the surface. This method may have allowed heat conduction down the thermocouple lead to the tip increasing the temperature difference measured across the boundary. Regardless, both experimental and predicted temperature gradients a high energy transmission through the boundary, which translates into a substantial threat of fire spread to adjacent compartments and justifies further investigation.

As illustrated in Tables 6 and 7, the average heat flux though a compartment boundary is on the order of 20-40 kW/m^2 (1.8 - 3.5 BTU/ft^2). In many cases, unexposed surface temperatures of bulkheads and decks exceeded 750°C (1382°F). The heat being transferred to the surrounding compartments resulted in a steady air temperature rise in the compartments throughout the duration of the test. Temperatures were measured at various elevations in the center of each of the surrounding compartments. The temperature profile in the adjacent compartment indicates the development of a 1 m (3 ft) thick hot layer below the ceiling with lower temperatures recorded near the deck. Although the temperature gradient across the compartment away from the heated bulkhead was not

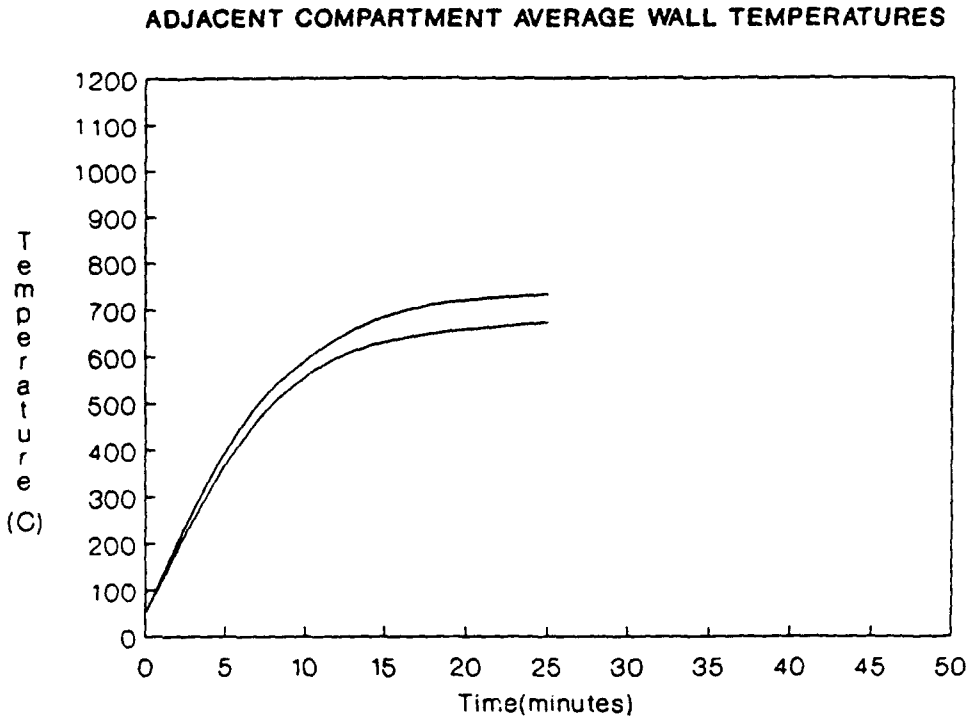

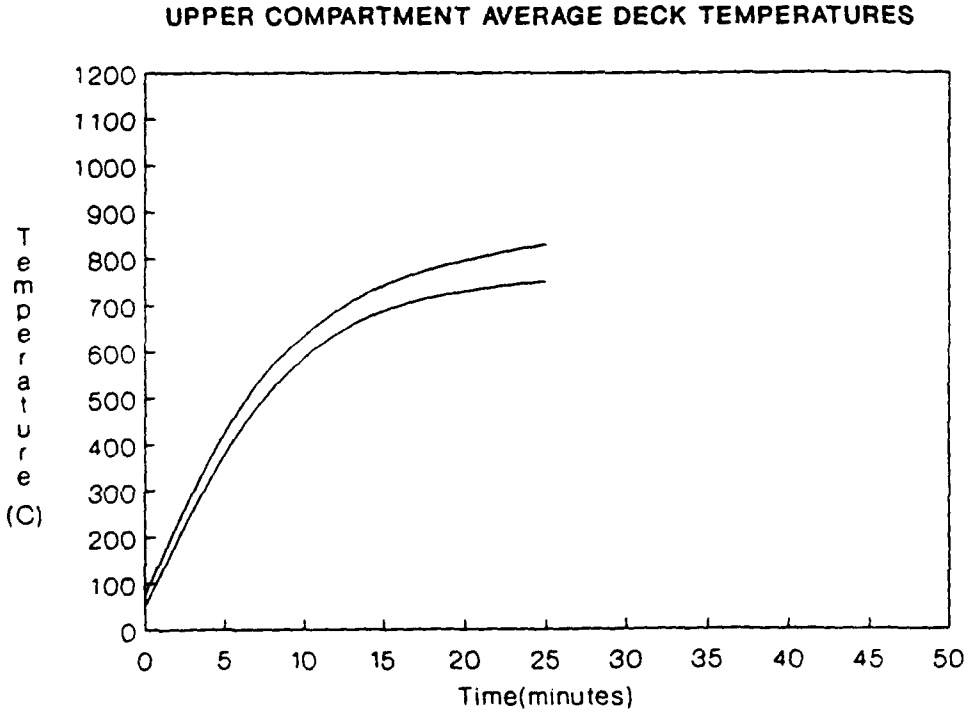

Fig. 15 - Surface temperature difference across the fire boundaries

measured, it may be presumed that the air temperatures in the adjacent compartments were higher closer to the heated boundary. Temperatures recorded in the upper compartment showed no sign of the development of a hot layer due to fairly even heating of the deck separating the two compartments. The highest temperatures were recorded closest to the floor and decreased with increased elevation. Air temperatures were recorded as high as 600°C (1112°F) at various locations in the surrounding compartments. The time and likelihood of ignition of various materials and an analysis of compartment tenability was presented in the following sections based on these measurements.

6.8.2.1 Compartment Tenability

Besides the ignition of combustibles in adjacent spaces around the fire compartment, the ability of a fire fighter(s) to man the space to either approach the fire or to prevent further fire spread is of great importance and warrants further investigation.

The analysis of compartment tenability was based on two criteria: radiant heat flux and compartment air temperature. Two widely accepted values for human tenability are an upper layer temperature of 183°C (361°F) (radiant heating) and a lower level temperature of 100°C (212°F) (immersion) [16]. The upper layer temperature corresponds to an overhead smoke layer temperature required to produce a downward radiant flux of 2.5 kW/m^2 (0.2 BTU/ft^2 sec), which has been identified as a flux level near the threshold of human tenability based on bare skin. The lower level temperatures are based on lung damage due to inhalation of hot gases. The deck or bulkhead separating the compartment in question and the fire compartment is the most significant radiant heat source. The average air temperature will be used as the lower level temperature. In the radiant heat analysis, the assumption is made that the heated surface radiates as a black body with a view factor of 1.

The human tolerance criteria are overlayed on actual temperature data recorded in the adjacent and upper compartments during the design fire (Test #27) which represents worst case conditions. The radiant heat flux criteria is overlayed on the unexposed surface temperatures of data in Figure 16 and the upper level temperature criterion is overlayed on the average air temperature recorded in the adjacent spaces in Figure 17. As shown in Figures 16 and 17, the spaces around the fire compartment rapidly become untenable. If an unprotected crewmember is present in an adjacent or upper compartment during the initial stages of the fire, he has only a few minutes before experiencing pain and burning skin and is forced to leave the compartment. A more realistic scenario is when a fire

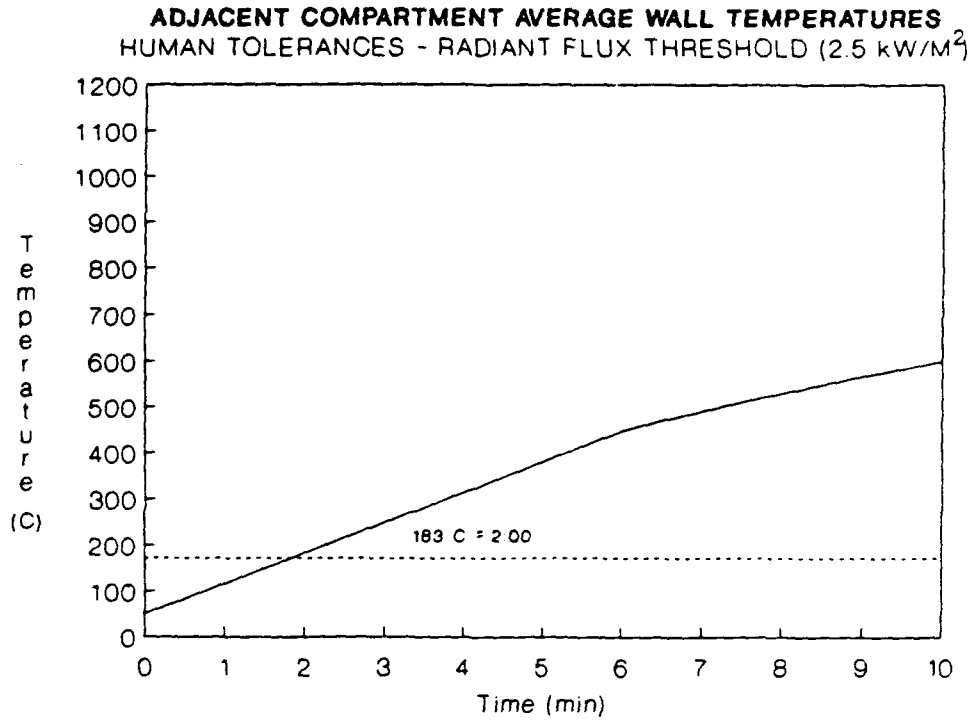

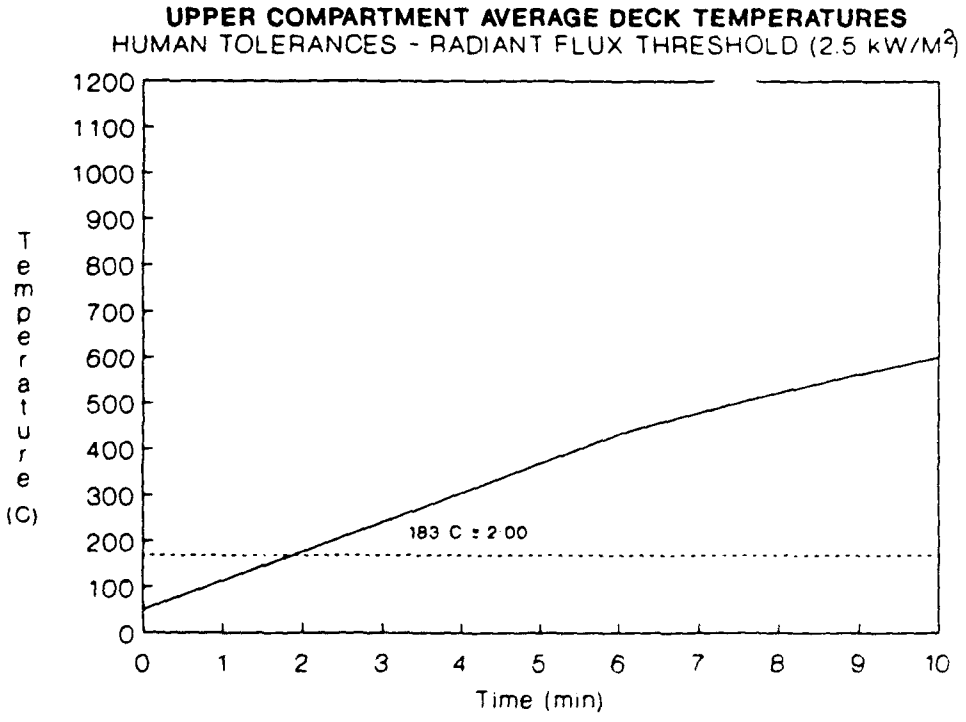

Fig. 16 - Tenability of adjacent and upper compartments (based on a radiant heat flux 2.5 kW/m^2)

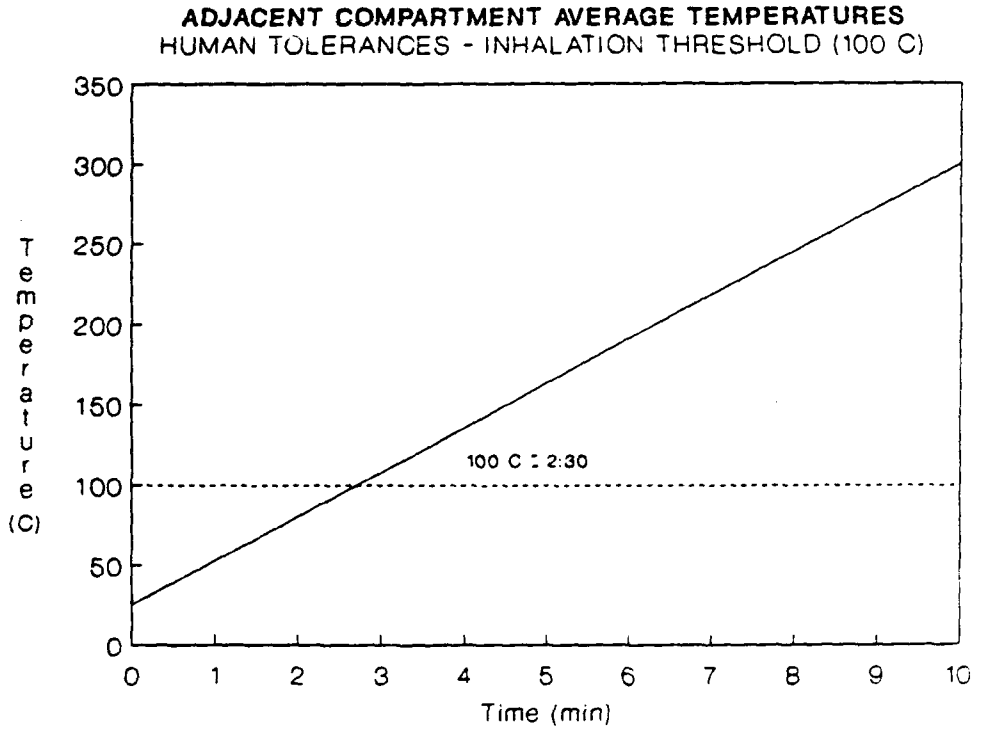

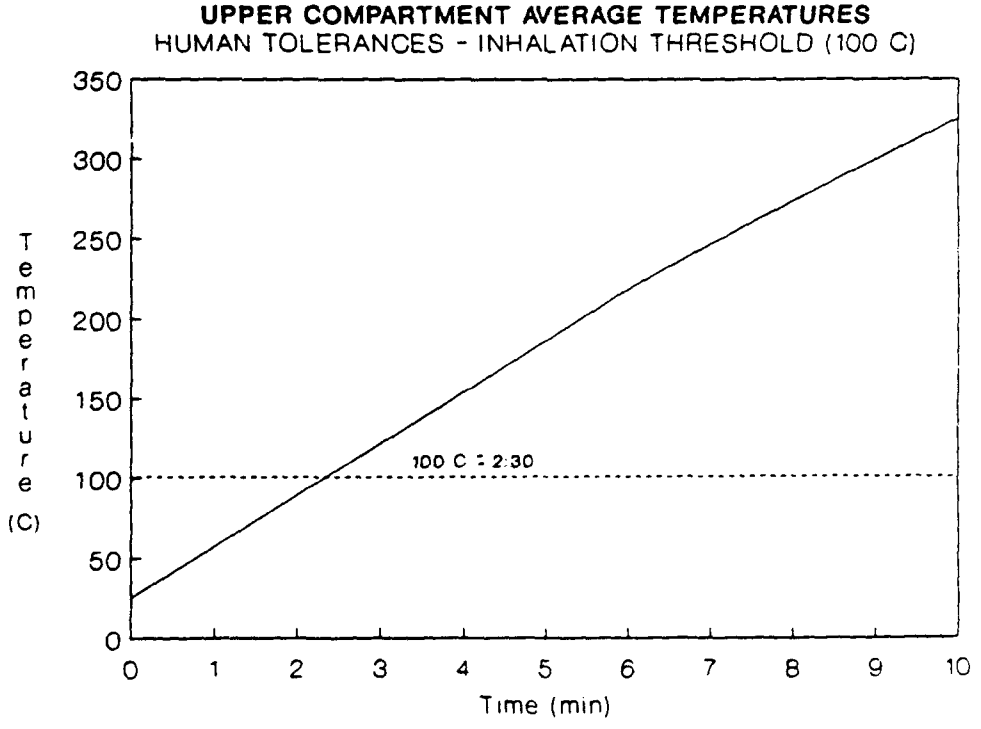

Fig. 17 - Tenability of adjacent and upper compartments (based on 100 C gas temperature)

fighter or crewmember arrives minutes after the onsite of fire. Neglecting the likelihood of spontaneous ignition of materials around the fire boundary, the compartment is already untenable and requires substantial cooling before access can be gained. If not cooled immediately, fire spread to adjacent areas is inevitable.

6.8.2.2 Fire Spread Analysis

Using the data collected during these tests, an analysis was conducted of the time and likelihood of horizontal and vertical fire spread. Although ignition of materials is a function of many variables such as the time/temperature exposure of the sample and fuel configuration, widely accepted hot gas temperatures and radiant heat flux exposures aided in the estimation of these fire spread times.

The initial analysis of fire spread was based on exposures of materials to hot gases. One of the first methods used to determine self-ignition temperatures was the Setchkin Furnace [17]. This method was later incorporated into standard tests by ASTM (ASTM D1929) [18]. The standard ignition test consists of placing a sample in the inner tube of a coaxial vertical furnace. Air is admitted at a known rate and the temperature gradually increased until the sample ignites. Typical results of this test show paper igniting at 230°C (446°F) and various cable coatings (PVC, polyethylene, and polyurethane) between 350°C-450°C (662-842°F) [19]. Although the convective air flow in the simulated ship compartments are unknown, these temperatures should be fairly representative of the conditions required to ignite these materials in actual shipboard conditions.

The previously mentioned self-ignition temperatures for paper and cabling were overlayed on the average temperature curves (Fig. 18) recorded in the adjacent spaces around the fire compartment during the design fire (Test 27). Average temperatures were used for this evaluation, so it should be noted that materials in the overhead of the adjacent compartments and lower in the upper compartment would ignite faster than predicted by this analysis. Figure 18 suggests that paper products would ignite with six to seven minutes of the development of the conflagration followed by some types of cables between twelve and fifteen minutes. Actual fire spread rates may be substantially faster or slower depending on the situation. Also, ignition of any of the combustibles in the compartment may dramatically decrease the ignition times for the other combustibles in the compartment.

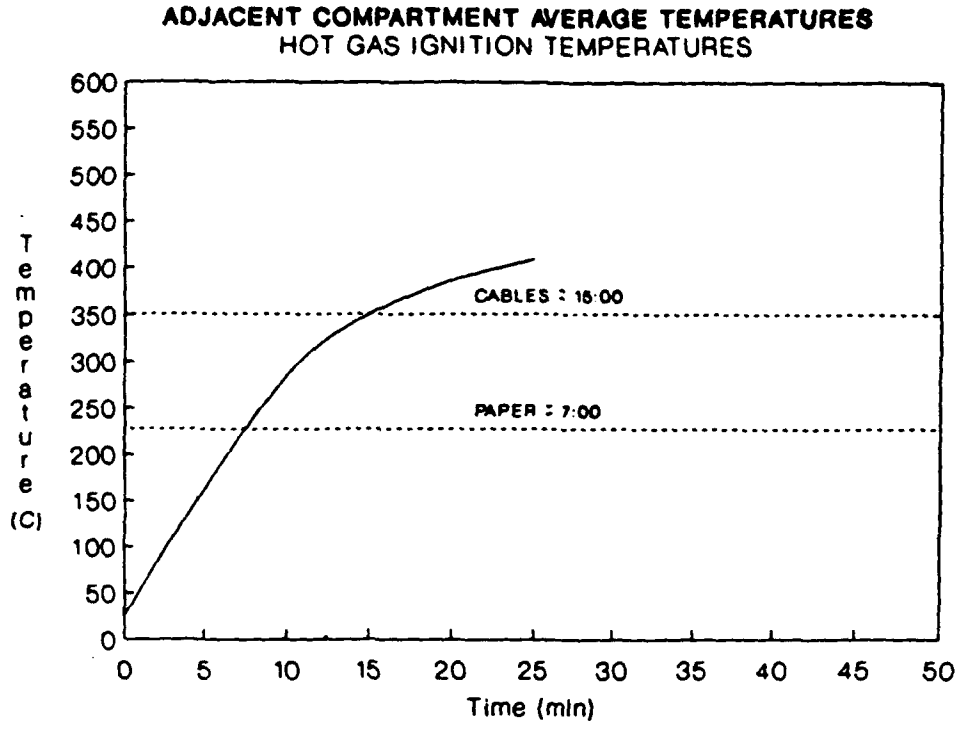

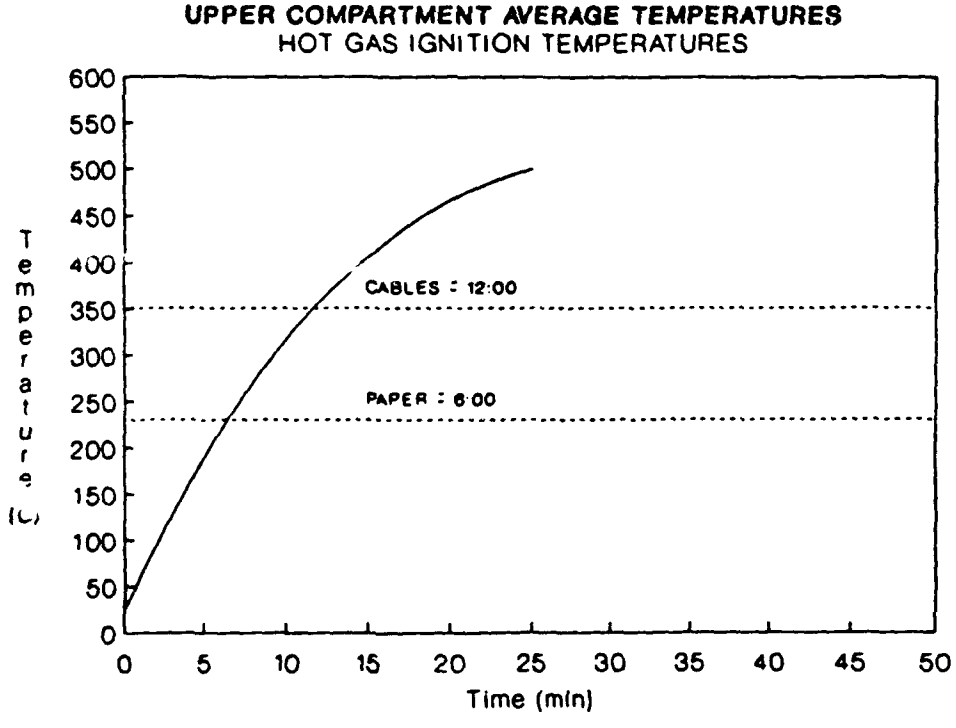

Fig. 18 - Fire spread to adjacent and upper compartments (based on compartment air temperatures)

A second analysis of fire spread was based around the criterion for flashover (500°C (932°F) upper layer temperature which corresponds to a flux to the deck of 20 kW/m^2 (1.8 BTU/ft^2 sec)). Again, the fire compartment boundary was assumed to be the most significant radiant source and was assumed to behave as a perfect black body with a view factor of 1. The ignition times of combustibles in the compartment were estimated based on an unexposed surface temperature of 500°C (932°F) measured on bulkhead or deck separating the compartment in question and the fire compartment.

The flashover ignition criterion was overlayed on the unexposed surface temperatures of the bulkheads and decks bounding the fire compartment in Figure 19. This figure, in agreement with the first analysis, suggests that fire would spread to both adjacent and upper spaces within six to seven minutes after the fire compartment reaches flashover.

Due to the high thermal conductivity of steel and aluminum, fire will spread both vertically and horizontally fairly rapidly after the onset of a post-flashover fire. The above analysis was based on fire spread through unbreached boundaries, which would produce slower fire spread rates than through a boundary with pre-existing mechanical breaches. Wall penetrations due to cable runs or boundaries damaged in combat could result in a dramatically faster fire spread. Also, it should be recognized that the material with the lowest ignition temperature will ignite first spreading fire by direct flame impingement and will increase the temperature of the compartment causing faster ignition times than previously estimated. In conclusion, fire will spread both horizontally and vertically within six to seven minutes after the fire compartment reaches the post-flashover stage if preventive measures are not taken. This is in agreement with predictions of heat transfer made by D. Gross of NBS [7] using the computer model FIRST and on timelines prepared during the damage assessments performed on the USS STARK [20].

6.9 USS STARK Fire Comparison

6.9.1 Thermal Insult to the USS STARK

The criterion initially placed on the design fire development was to produce the most severe fire possible in a "simulated" shipboard compartment. In actual shipboard conditions, it would be very unlikely that the fuel load, configuration, and ventilation opening would yield stoichiometric conditions. Research conducted by SRI International [21] shows that even the minimum energy release rate calculated for the fires at CBD substantially exceeds

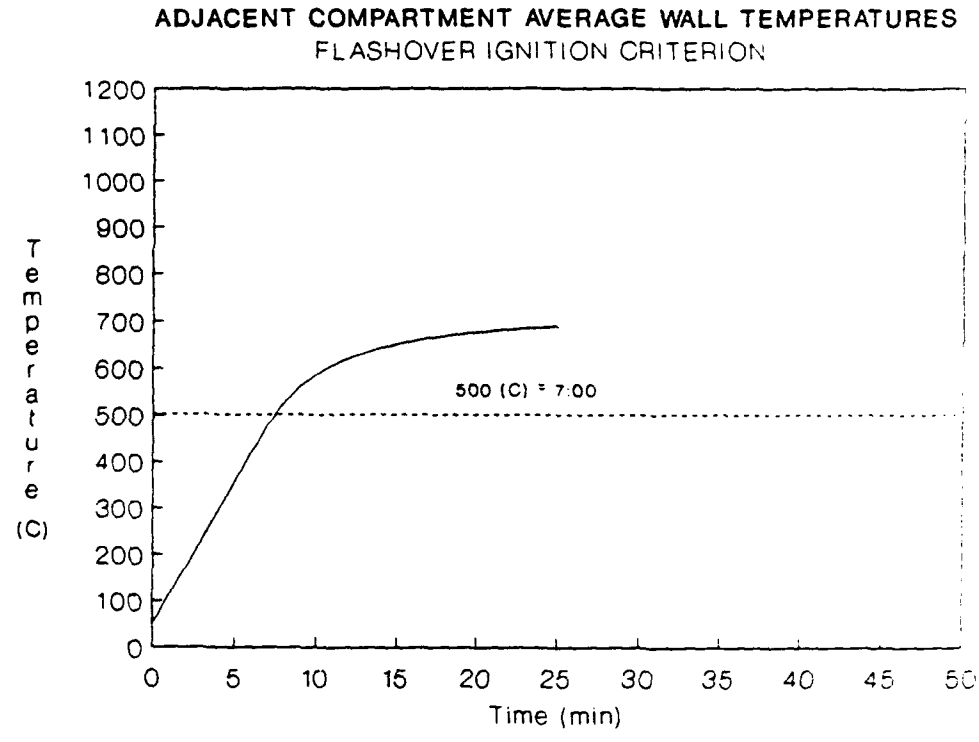

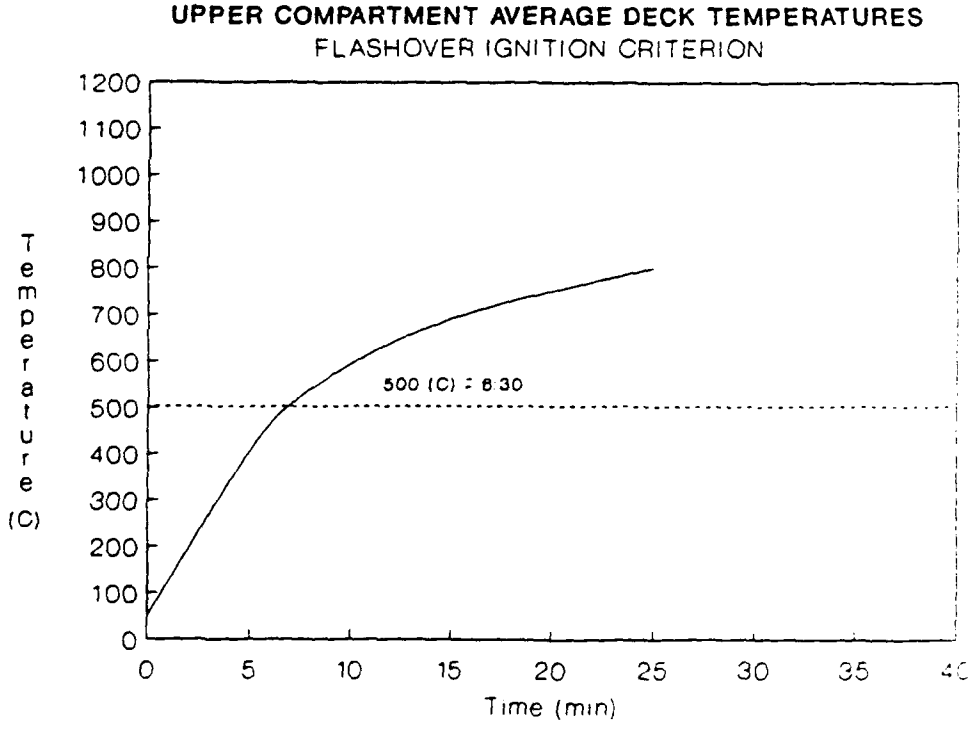

Fig. 19 - Fire spread to adjacent and upper compartments (based on bulkhead and deck surface temperatures)

the estimates for the Berthing Compartment on the USS STARK. The STARK Berthing Compartment energy release rates were based on estimations of typical berthing compartment fire loading and on fire duration estimates provided by the crew on the USS STARK. Due to the uncertainty of the conditions which occurred onboard the USS STARK, it would not be unreasonable to assume SRI estimates may deviate substantially from the actual conditions. Even allowing for these uncertainties, the design fire is still more severe than any SRI estimations. It should be noted that the "design fire" was intended to simulate a "worst case" fire scenario to be used in the development of fire fighting procedures and that any countermeasures developed to protect neighboring compartments from a fire of this severity should be more than adequate when applied to less severe conflagrations.

6.9.2 Fire Spread on the USS STARK

The sequence of events which occurred onboard the USS STARK was compiled primarily from JAG investigation reports, interviews and other available documentation [1, 20]. These events were grouped within the general time frame during which they were believed to have occurred. The time line of events estimates that fire spread from the compartment of origin in virtually all directions within five to ten minutes after the missiles impacted the ship. The majority of fire may be presumed to have spread by means of open doors, passageways, and wall penetrations due to warhead fragmentation. Although it is uncertain exactly how each of these fires spread, the time line estimations coincide with the fire spread analysis conducted in this report as shown in Fig. 18.

6.10 Miscellaneous Observations from the Simulated Shipboard Compartment

The majority of the instrumentation provided useful and accurate readings throughout this test series with the exception of the radiometers and the pressure transducer in the fire compartment. The radiometers in the fire compartment worked for only the first few minutes of each test before the sapphire window became obstructed due to carbon deposits. Even with increased air flow through the purge line, the condition continued to exist. The pressure transducer in the fire compartment also did not produce the desired results. The environmental conditions (wind speed and direction) caused the instrument to be very unstable and in turn difficult or impossible to interpret.

Throughout the test series, a set of general trends were observed. The fire compartment developed steady state

conditions almost immediately after ignition of the fuel spray. The walls and ceiling bounding the fire compartment continued to heat until approximately 25-30 minutes into the test. The air temperatures in the surrounding compartments continued to rise for 10 to 15 minutes after the fire was extinguished. This continued temperature rise is attributed to the energy being transferred from the heated surfaces bounding the fire compartment.

Surprisingly, the thermocouples in the upper compartment measured higher temperatures closer to the heated deck than were observed in the overhead. This is the result of nearly consistent heating of the deck separating the fire and upper compartments. The adjacent compartment temperatures did however show the development of a hot layer with the highest temperatures recorded in the ceiling.

Almost immediately after ignition, a hot layer was established in the fire compartment and a natural convective air flow into and out of the compartment was produced. A neutral plane developed approximately one-third the way up the vent opening. The neutral plane is the interface between the cool inflow of air and outflow of hot gases. All compartment fires of substantial magnitude (post-flashover) develop neutral planes in roughly this same location. The maximum air flow through a vent opening is achieved and remains fairly constant for flashover compartment fires and can be calculated using equation (3). This airflow coupled with a 3:1 expansion of the gases due to the increase in temperature results in the establishment of a neutral plan at this location.

From the very first test, the mock-up began to show signs of deformation. The area above the vent opening (lintel) which was exposed to heat on both the inside due to exposure to the fire and the outside due to the outflow of hot gases continually warped throughout the test series. The walls and ceiling bounding the fire compartment glowed orange red after each test. The stiffeners became hotter than the steel plates bounding the compartment due to heating on all sides of the stiffener as compared to only one side of the steel plate. The temperature difference between the stiffeners and the plates caused the stiffener to expand more than the steel plate producing various amounts of stress throughout the structure.

7.0 SUMMARY AND CONCLUSIONS

A total of sixty fires were conducted in a simulated shipboard compartment [2.4 x 2.4 x 2.4 m (8 x 8 x 8 ft)] under a variety of fuel flow rates and ventilation conditions to develop a design fire for full scale fire testing. Based on these tests, the design fire should consist of a JP-5 spray fire in which the fuel is sprayed tangentially into a steel pan of adequate size to free burn the fuel. The fire should be located at floor level in a compartment having a ventilation opening factor of approximately 10 $m^{-\frac{1}{2}}$. The fuel flow rate should be adjusted to approach stoichiometric conditions.

This fire was found to produce both upper layer and average compartment temperatures of over 1000°C (1832°F) almost instantly. Total heat fluxes of over 100 kW/m^2 (9.1 BTU/ft^2 sec) within the compartment are characteristic of this fire.

With this fire, the heat transfer to the surrounding compartments was measured to be on the order of 20-40 kW/m^2 (1.8-3.6 BTU/ft^2 sec). In many cases, unexposed surface temperatures of bulkheads and decks exceeded 750°C (1382°F) and the air temperatures at specific locations in surrounding compartments reached 600°C (1112°F). These temperatures and fluxes are more than adequate to cause combustibles in these compartments to spontaneously ignite. Based on an analysis of fire spread through uninsulated unbreached boundaries, it was concluded that ignition of combustibles located in the compartment directly above the fire may occur within as little as 2 minutes for combustibles in direct contact with the deck, and within 4½ minutes for other materials in the space. In adjacent compartments, ignition of combustibles in direct contact with bulkheads may occur in as little as 2 minutes, and within 6 minutes for other combustibles in the space. Unprotected personnel may have as little as 2 minutes before they must exit adjacent spaces because of heat. Additionally, it was concluded that fire would spread almost immediately through breaches in boundaries and down passageways especially during fires where there is insufficient air.

The above conclusions apply to fires in a simulated shipboard compartment. Somewhat lower temperatures may be found in adjacent and overhead compartments when the design fire is placed in an actual shipboard compartment due to factors such as the heat sink characteristics of the massive ship structure.

8.0 REFERENCES

1. "FFG 7 - Blue Ribbon Panel Report," Office of the Secretary of the Navy, October 15, 1987.

2. K. Farmer et al., "Quantification of the Thermal Environments Generated by Combustion of Solid Pocket Propellant in Shipboard Compartments," Naval Weapons Center TP 7178 (in publication).

3. J.T. Leonard et al., "Project HULVUL: Propellant Fires in a Shipboard Compartment," Naval Research Laboratory (in publication).

4. V. Babrauskas, "A Closed-form Approximation for Post-Flashover Compartment Fire Temperatures," Fire Safety Journal 4, 1981, pp. 63-73.

5. P.H. Thomas, and A.J.M. Heselden, "Fully Developed Fires in Single Compartments, A Cooperative Research Programme of the Conseil Internationale du Batiment," Conseil Internationale du Batiment Report No. 20, Fire Research Note No. 20, 1972.

6. J.F. Lawson, and J.G. Quintiere, "Side-Rule Estimates of Fire Growth," National Bureau of Standards, NBSIR 85-3196, Washington, D.C., June 1985.

7. D. Gross, and W. Davis, "Burning Characteristics of Combat Ship Compartments and Vertical Fire Spread," National Bureau of Standards, August 1988.

8. J.G. Quintiere, "A Simple Correlation for Predicting Temperature in a Room Fire," National Bureau of Standards, NBSIR 83-2712, Washington, D.C., June 1983.

9. V. Babrauskas, "Pool Fires: Burning Rates and Heat Fluxes," Fire Protection Handbook, Sixteenth Edition, National Fire Protection Association, Quincy, MA, 1986, Section 21, Chapter 6, pp. 39-40.

10. D. Drysdale, "The Post-Flashover Compartment Fire," in An Introduction to Fire Dynamics, John Wiley and Sons, New York, 1985, ch. 10, pp. 304-350.

11. R.H. Perry and C.H. Chilton, Chemical Engineers' Handbook, Fifth Edition, McGraw-Hill, New York, 1973, Chapter 9, pp. 16-25.

12. Underwriters Laboratories, Inc., Standard 711, "Rating and Fire Testing of Fire Extinguishers," Northbrook, IL, Third Edition, July 1982.

13. L. Orloff, and J. deRis, "Froude Modeling of Fire," Nineteenth Symposium (International) on Combustion, The Combustion Institute, Pittsburgh, PA, 1982, p. 885.

14. F.W. Williams, L.A. Jonas, R.J. Ouellette, J.R. Saams, and J.L. Scheffey, "Analysis of Quick Response Fire Fighting Equipment for Submarines - Phase I, Scoping Tests," NRL Memorandum Report 6484, June 1989.

15. R.H. Iding, Z. Nizamuddin, and B. Bresler, "A Computer Program for the Fire Response of Structures - Thermal Three - Dimensional Version, FIRES-T3," Fire Research Group Report UCB FRG 77-15, October 1977.

16. L.Y. Cooper and D.W. Stroup, "Calculating Available Safe Egress Time (ASET) - A Computer Program and User's Guide," NBSIR 82-2578, September 1982.

17. N.P. Setchkin, National Bureau of Standards Journal of Research, National Bureau of Standards, Gaithersburg, MD, 1949.

18. American Society of Testing and Materials, "ASTM D1929, Standard Test Method for Ignition Properties of Plastics," Philadelphia, PA, 1983.

19. C.F. Cullis, M.M. Hirschler, "The Combustion of Organic Polymers," International Series of Monographs on Chemistry, Clarendon Press, Oxford, 1981.

20. Naval Sea Systems Command, "Damage Assessment and Analysis, USS STARK (FFG 31)," February 1988.

21. R.S. Alger, "The STARK Conflagration: Task I - Pretest Calculations and Analysis," SRI International Report Project PYU-6129, Menlo Park, CA, July 1988, Table 2.1.

Appendix A

Test Data

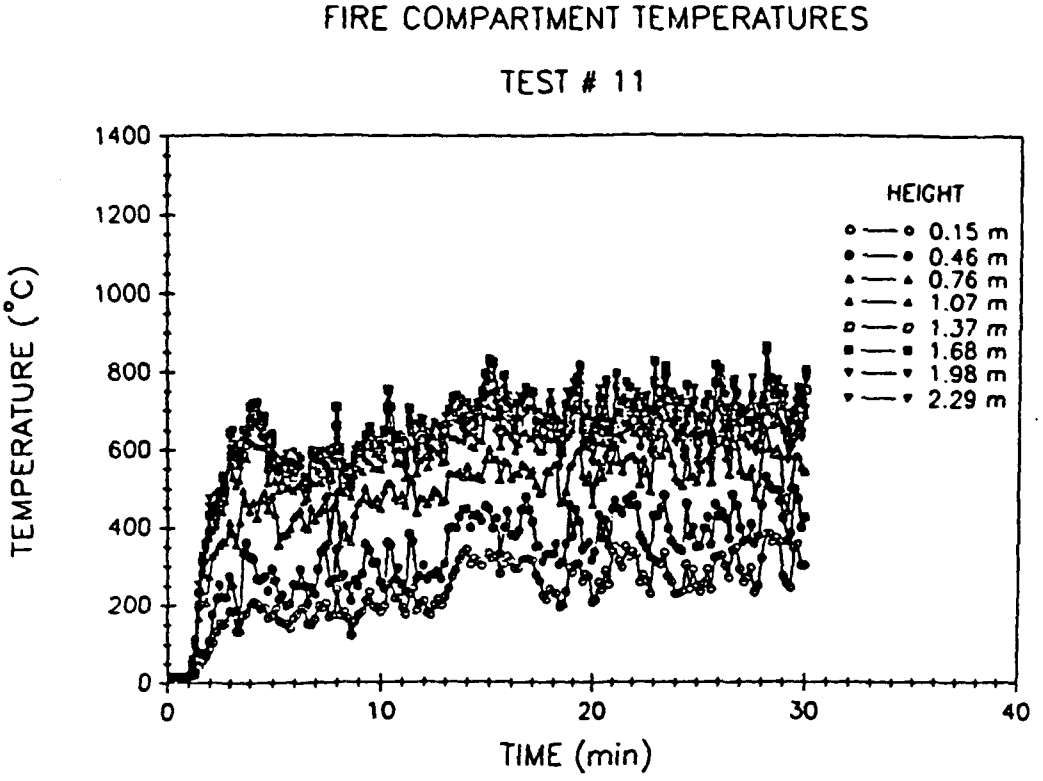

Fig. A1 – Fire comparment air temperatures

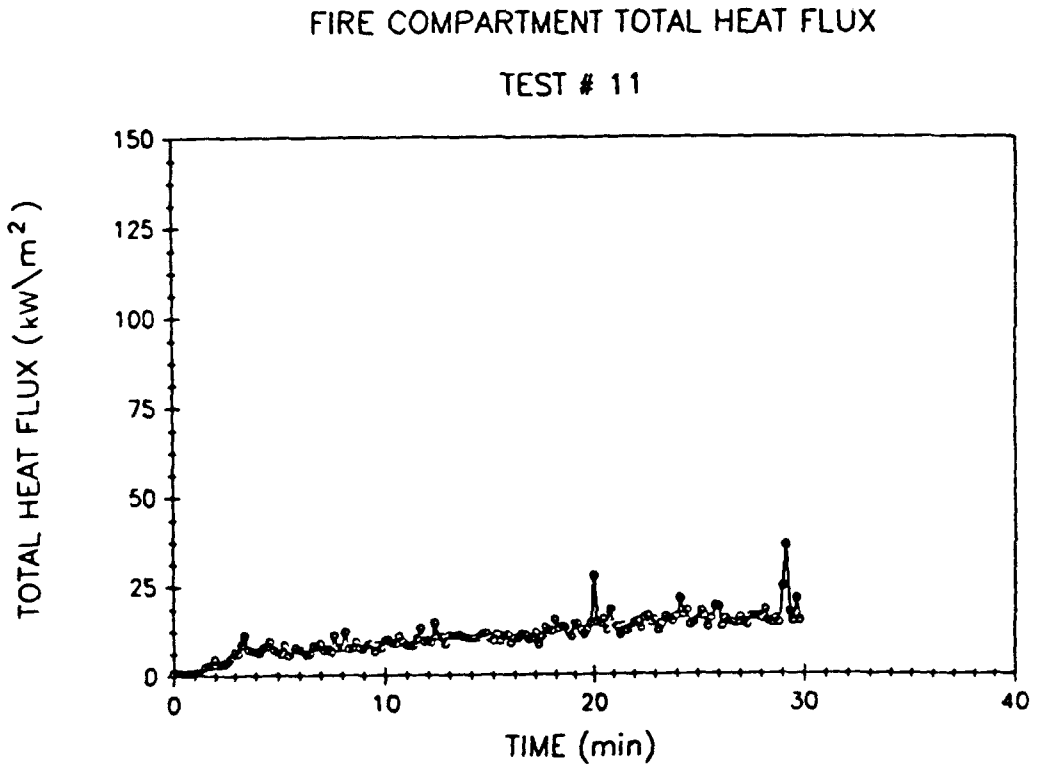

Fig. A2 – Fire compartment total heat flux

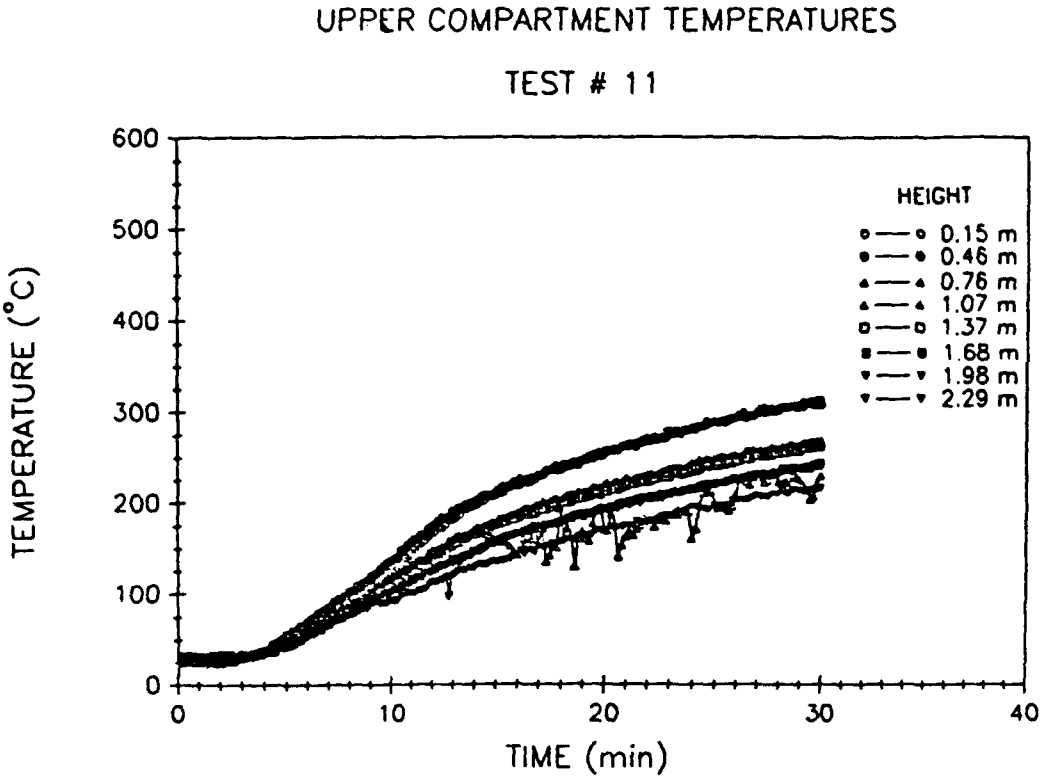

Fig. A3 – Upper compartment air temperatures

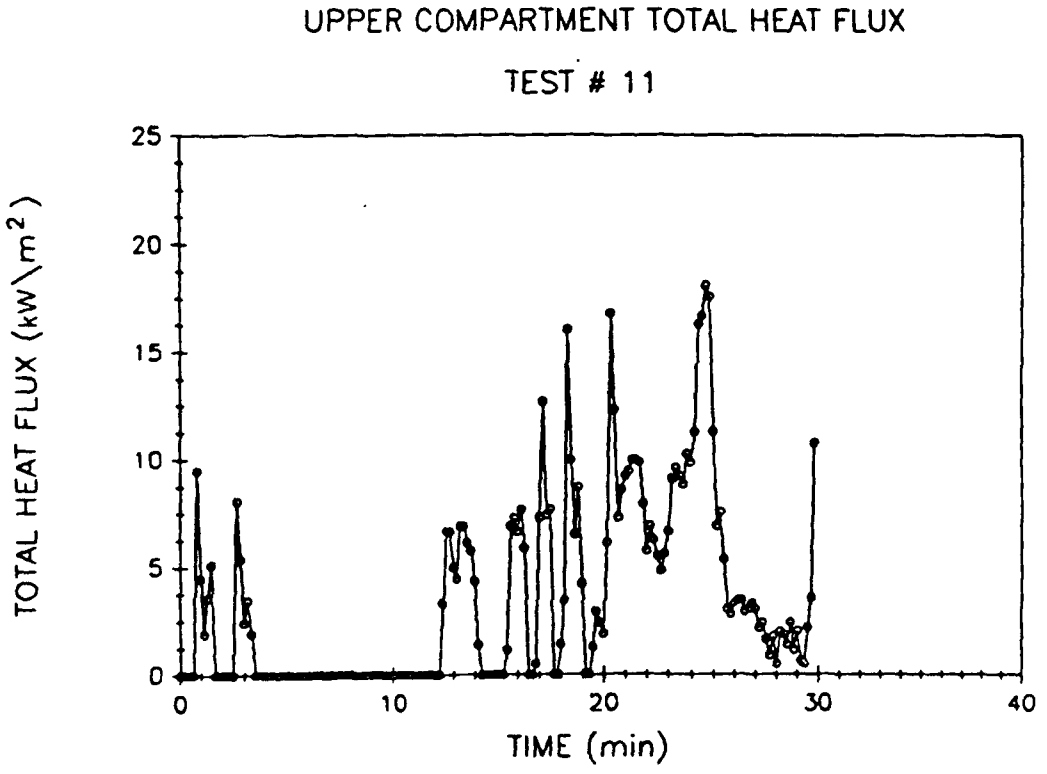

Fig. A4 – Upper compartment total heat flux

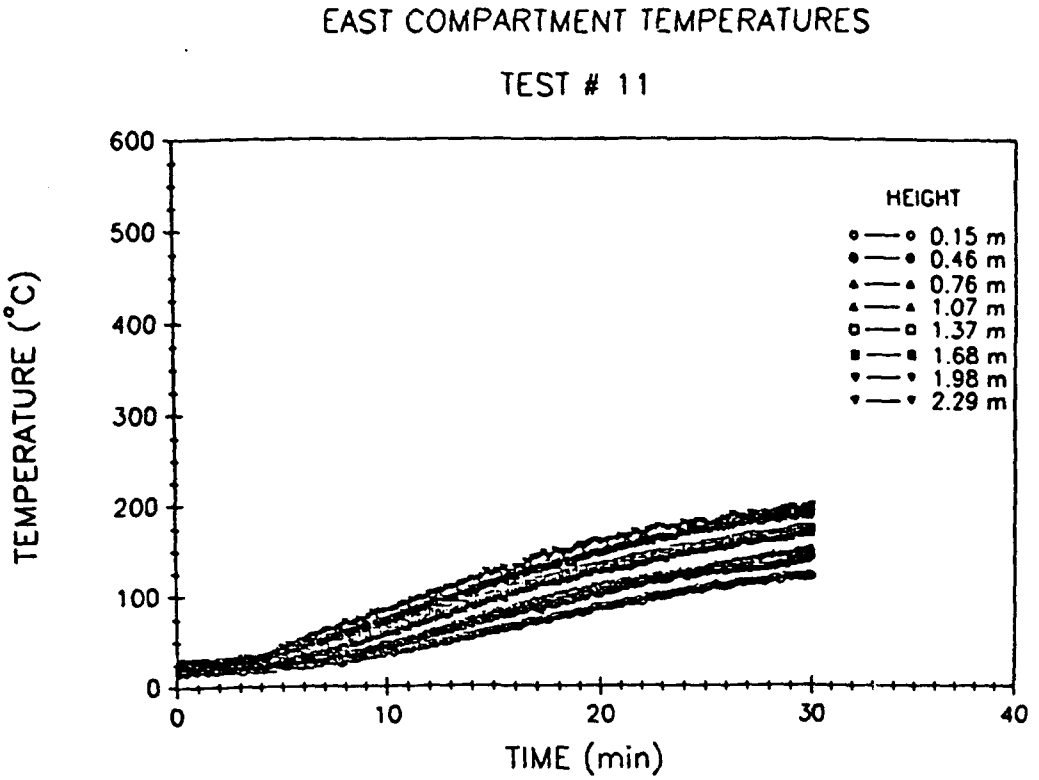

Fig. A5 – East compartment air temperatures

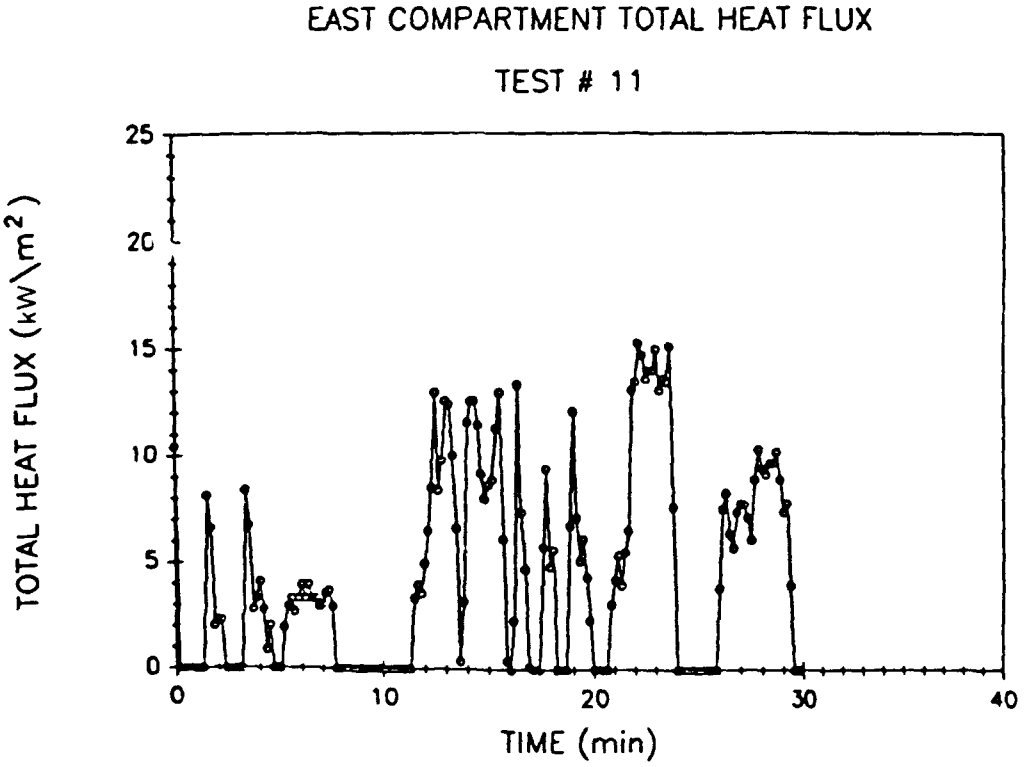

Fig. A6 – East compartment total heat flux

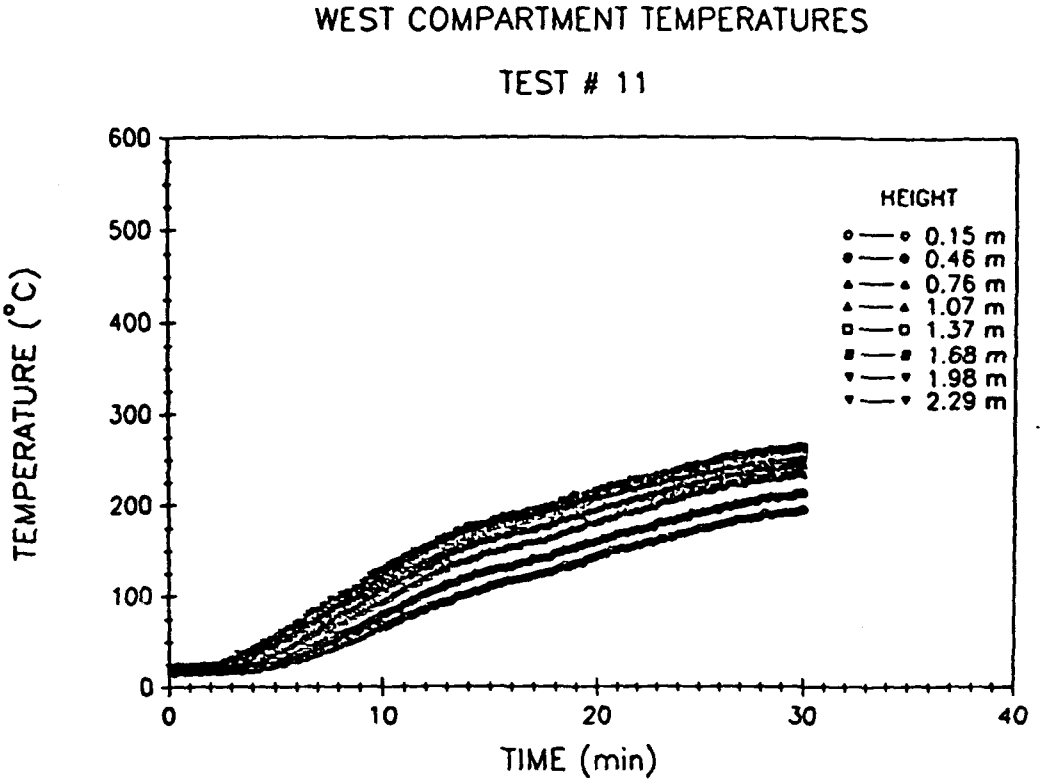

Fig. A7 – West compartment air temperatures

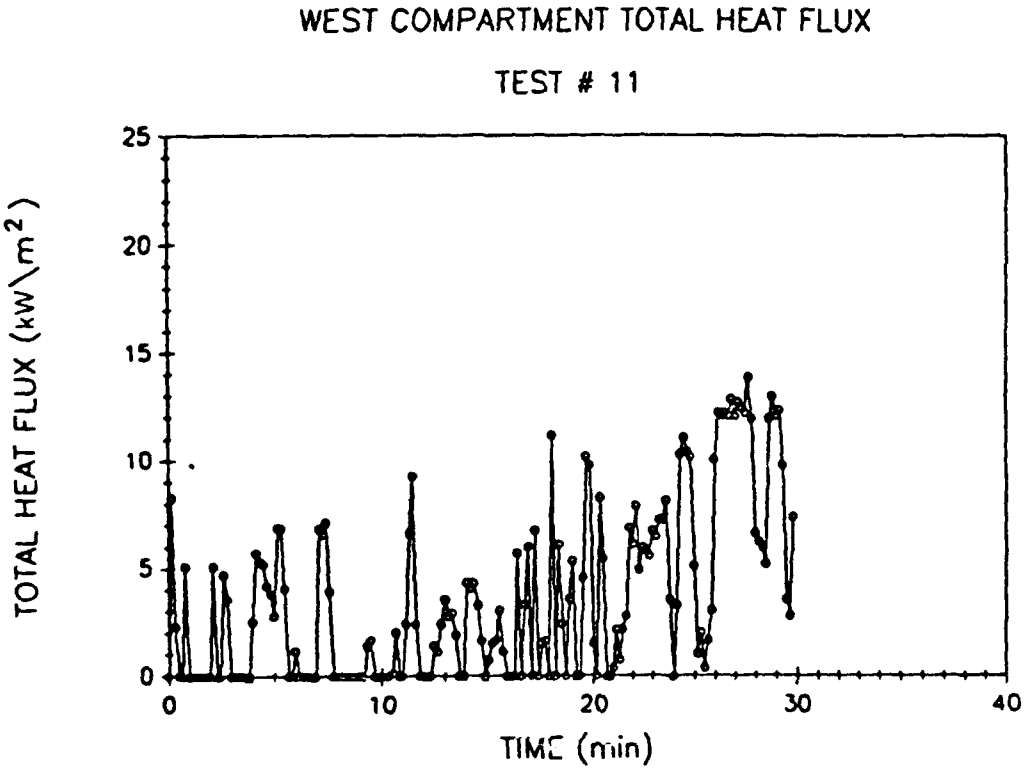

Fig. A8 – West compartment total heat flux

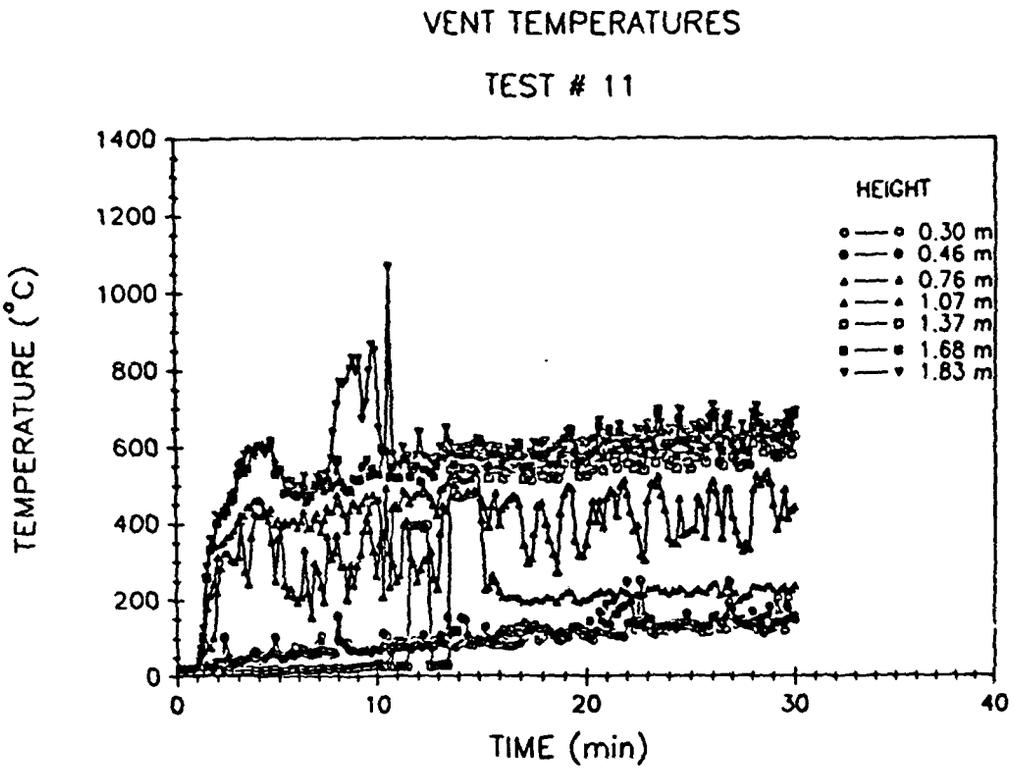

Fig. A9 – Vent air temperatures

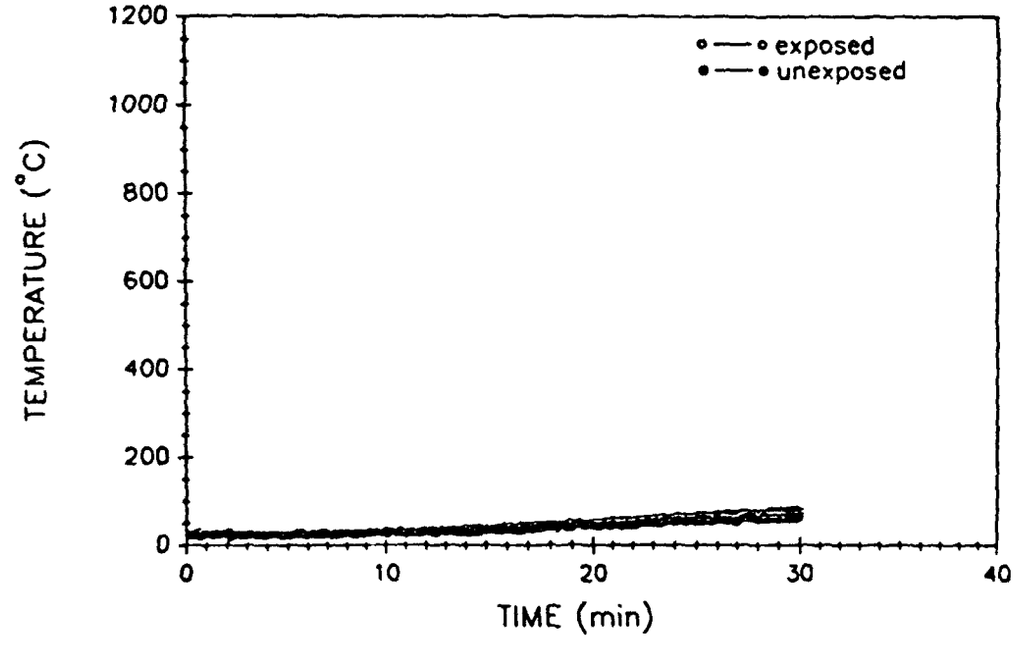

Fig. A10 – Upper deck surface temperatures

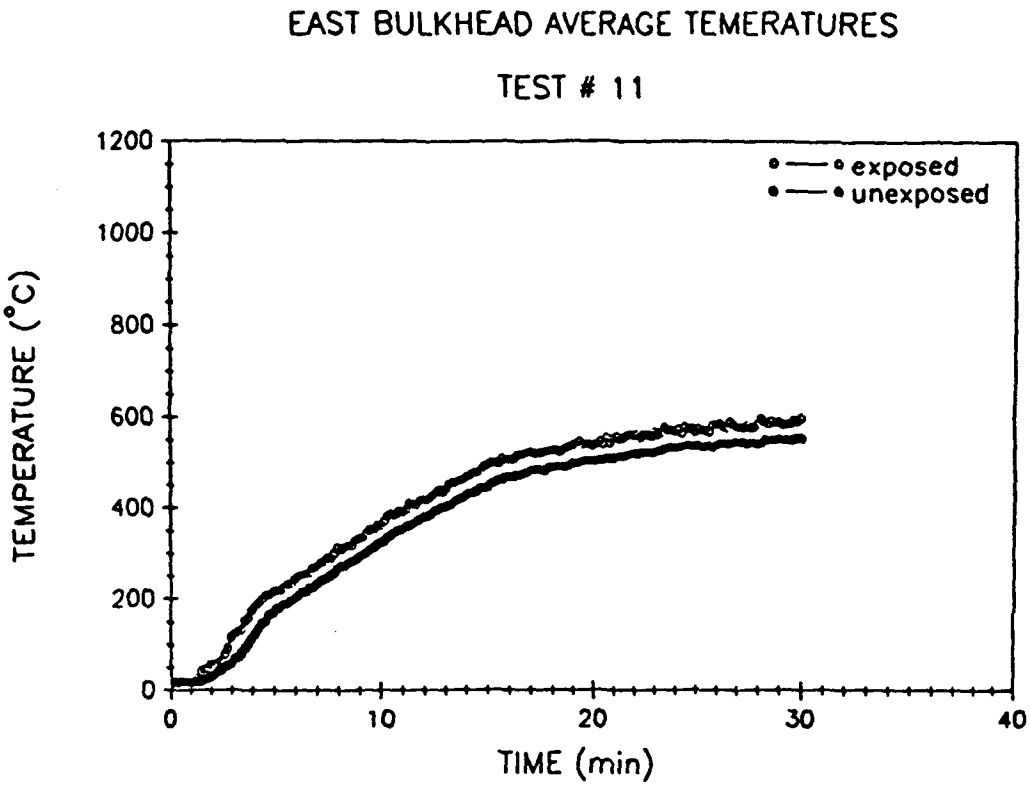

Fig. A11 – East bulkhead average surface temperatures

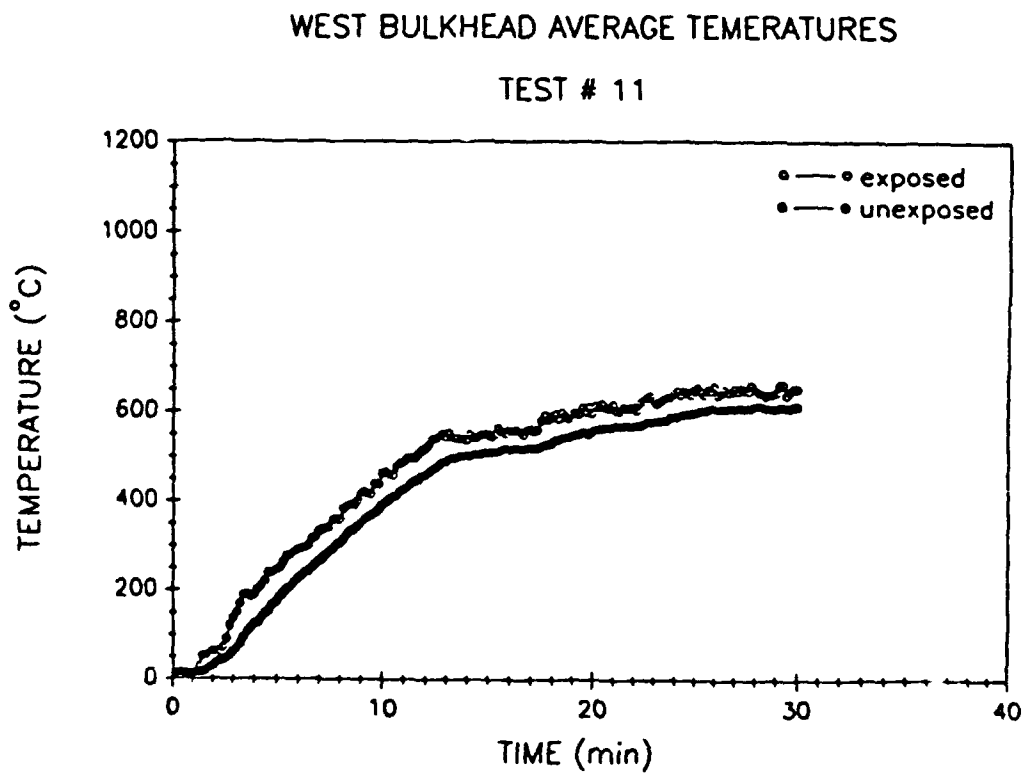

Fig. A12 – West bulkhead average surface temperatures

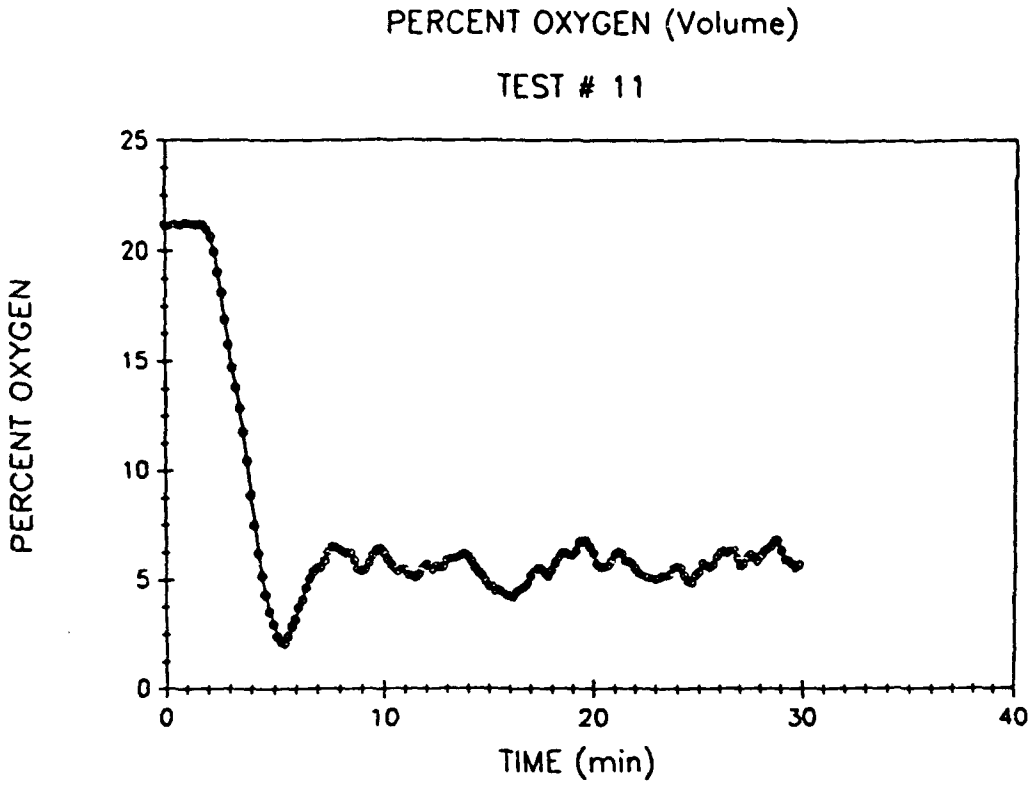

Fig. A13 – Percent oxygen (volume)

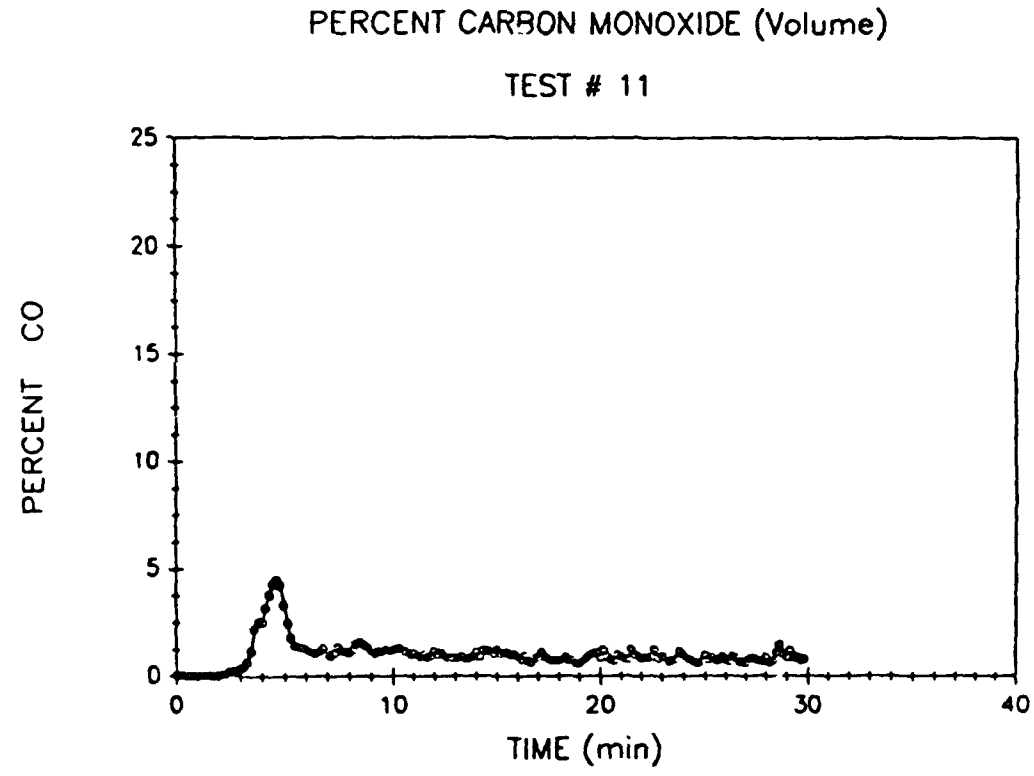

Fig. A14 – Percent carbon monoxide (volume)

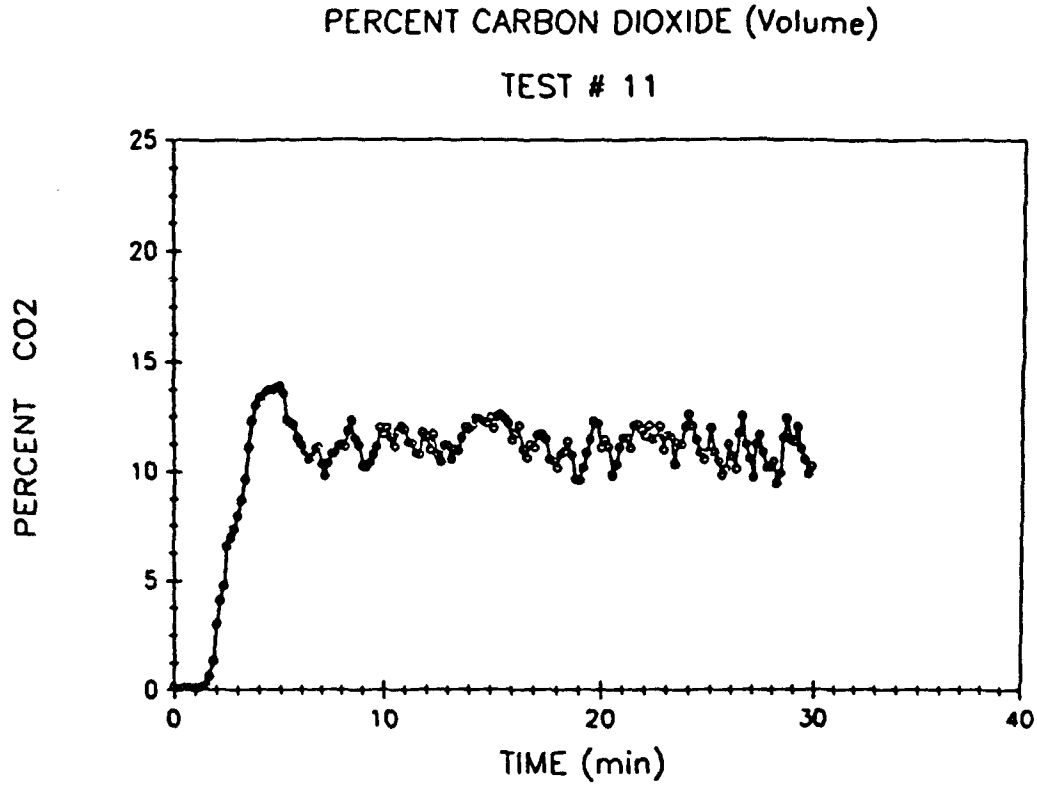

Fig. A15 – Percent carbon dioxide (volume)

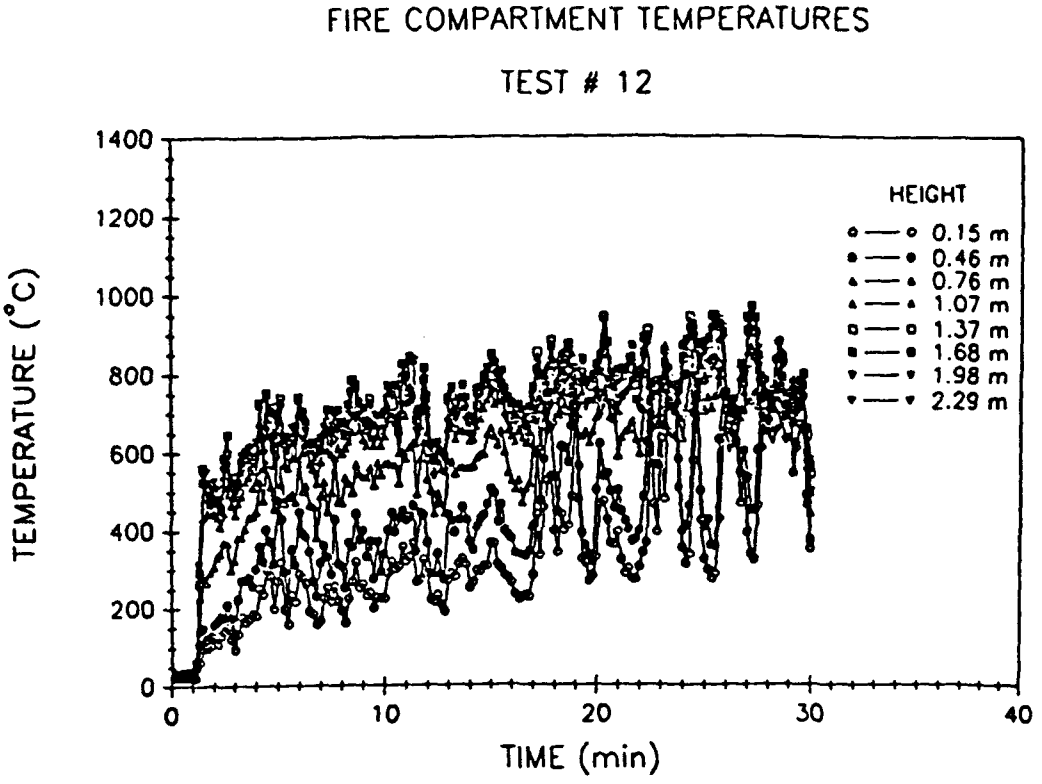

Fig. A16 – Fire comparment air temperatures

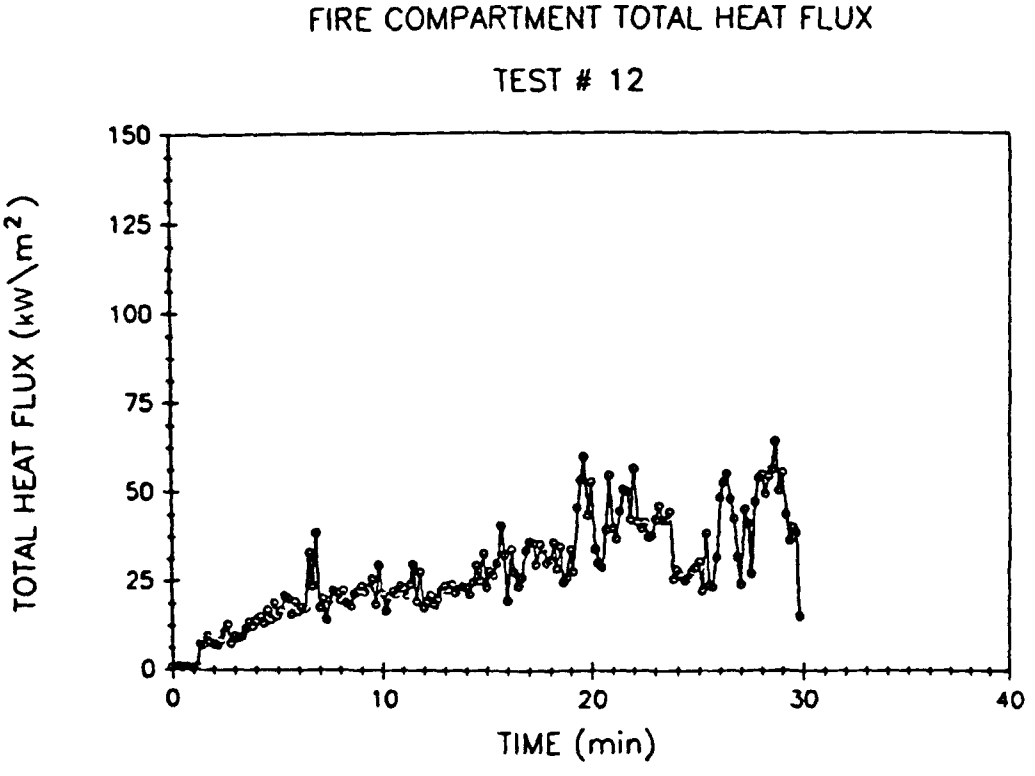

Fig. A17 – Fire compartment total heat flux

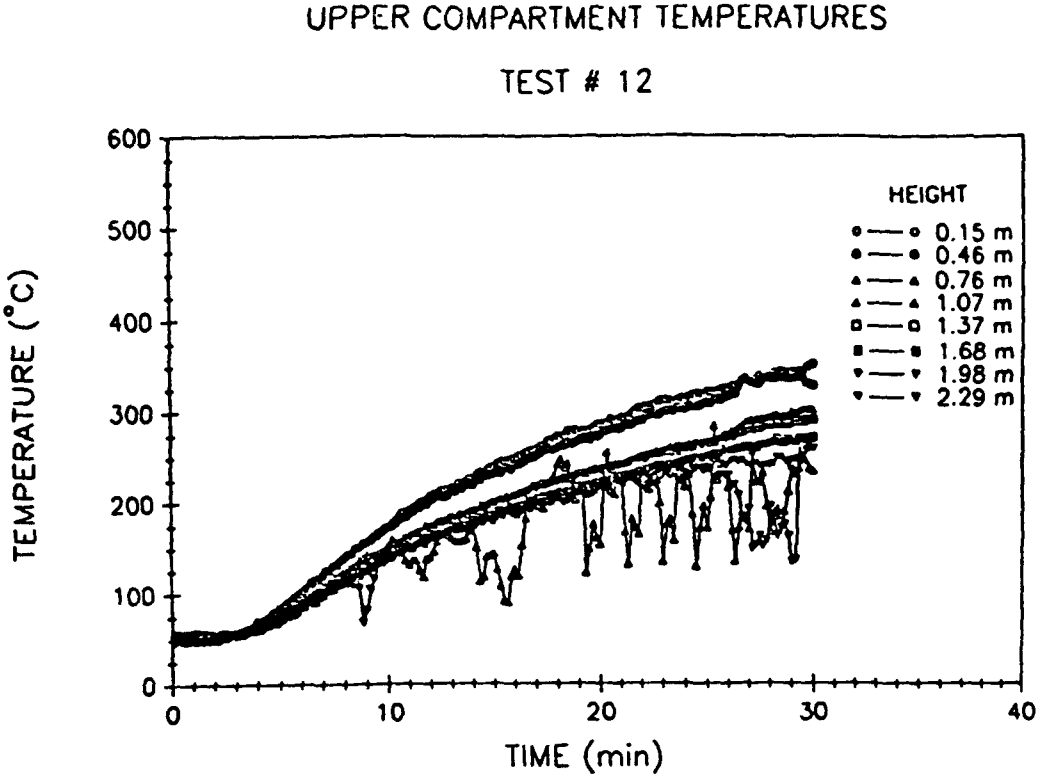

Fig. A18 – Upper compartment air temperatures

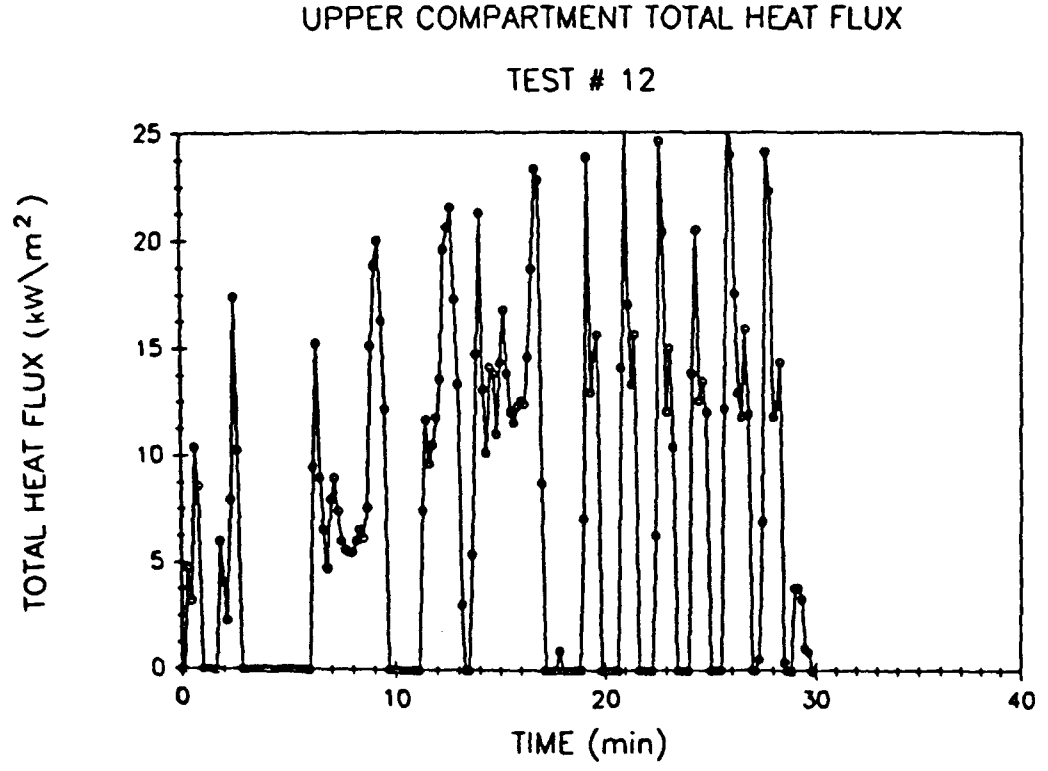

Fig. A19 – Upper compartment total heat flux

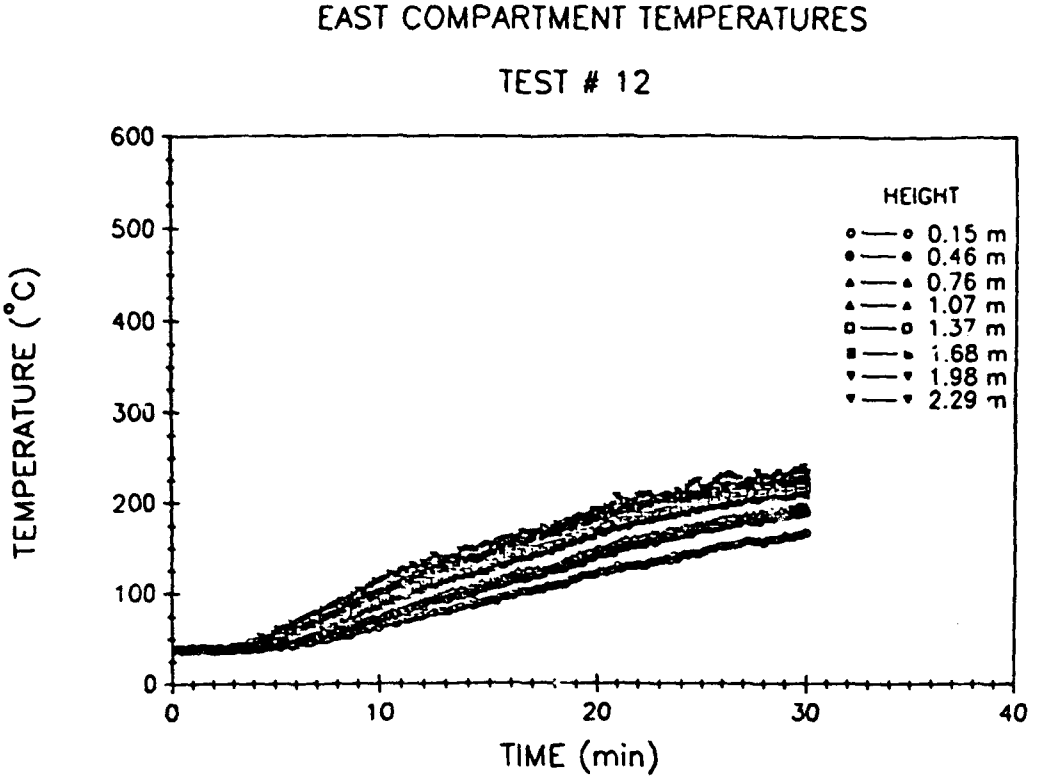

Fig. A20 – East compartment air temperatures

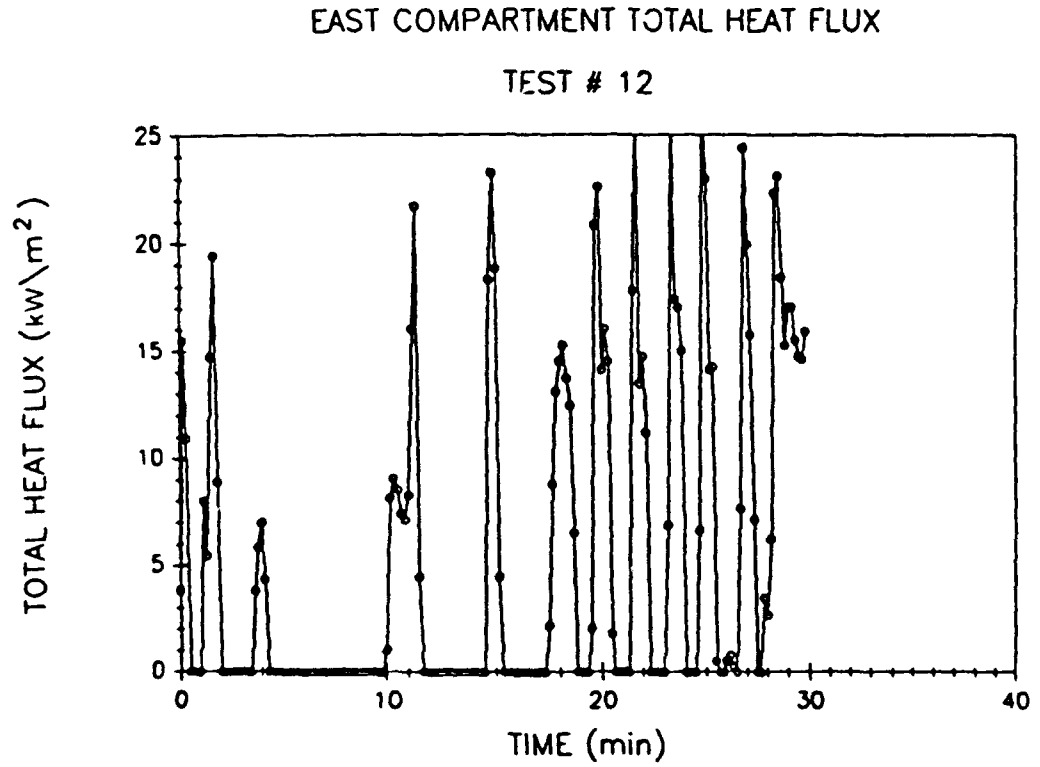

Fig. A21 – East compartment total heat flux

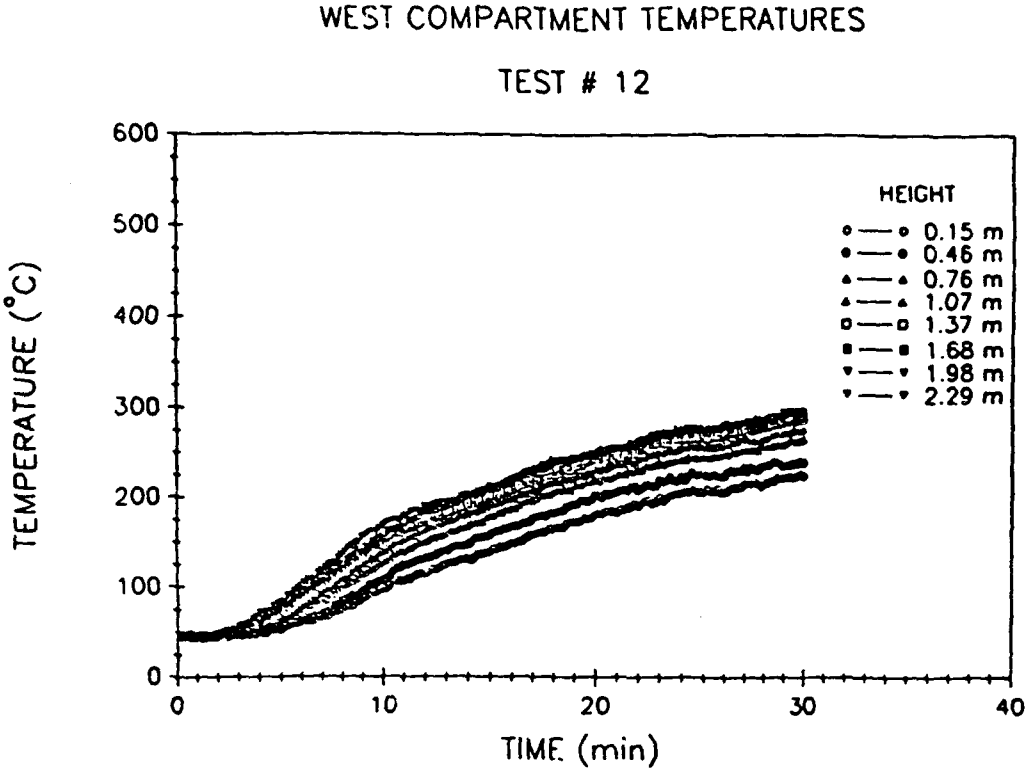

Fig. A22 – West compartment air temperatures

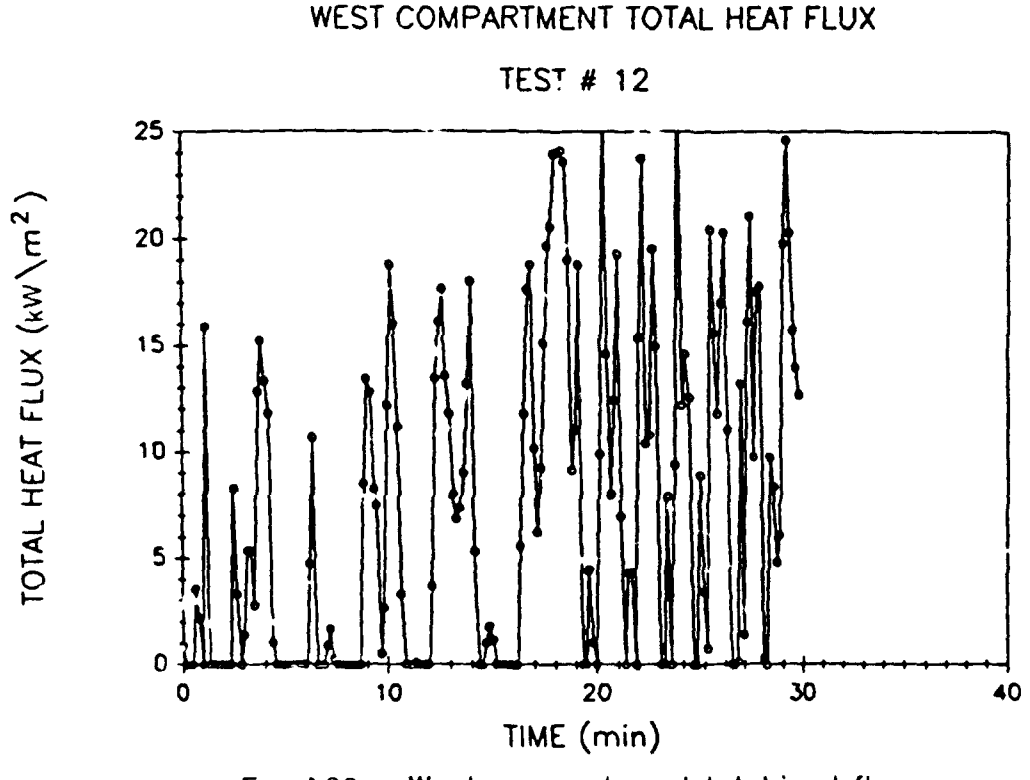

Fig. A23 – West compartment total heat flux

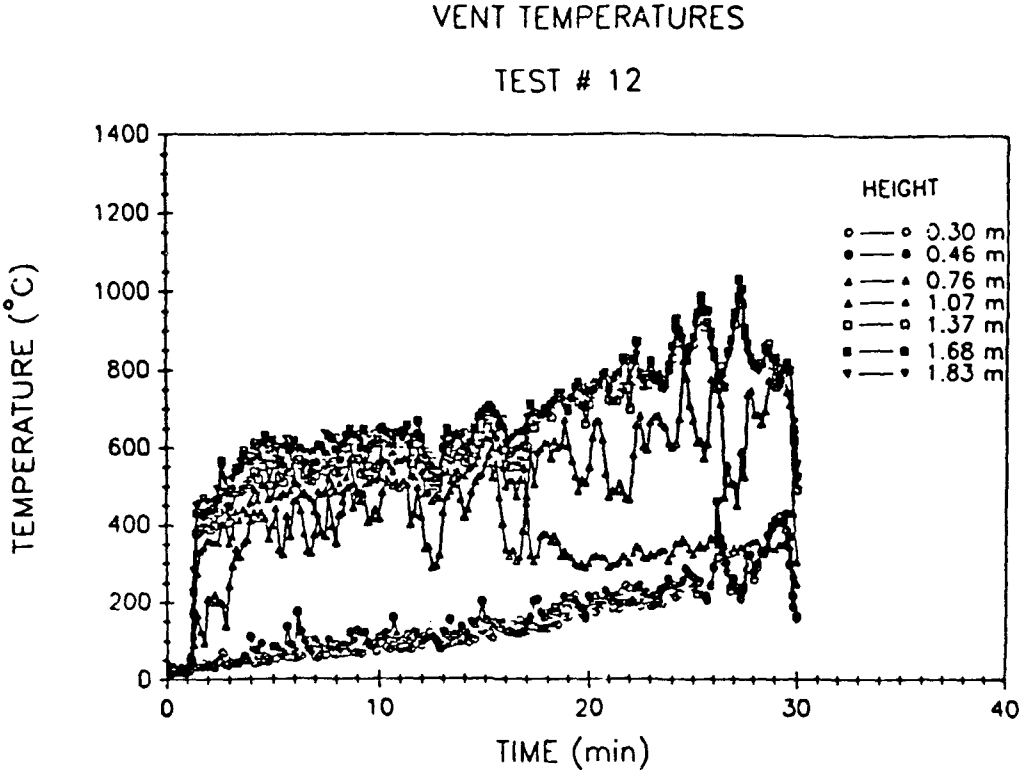

Fig A24 – Vent air temperatures

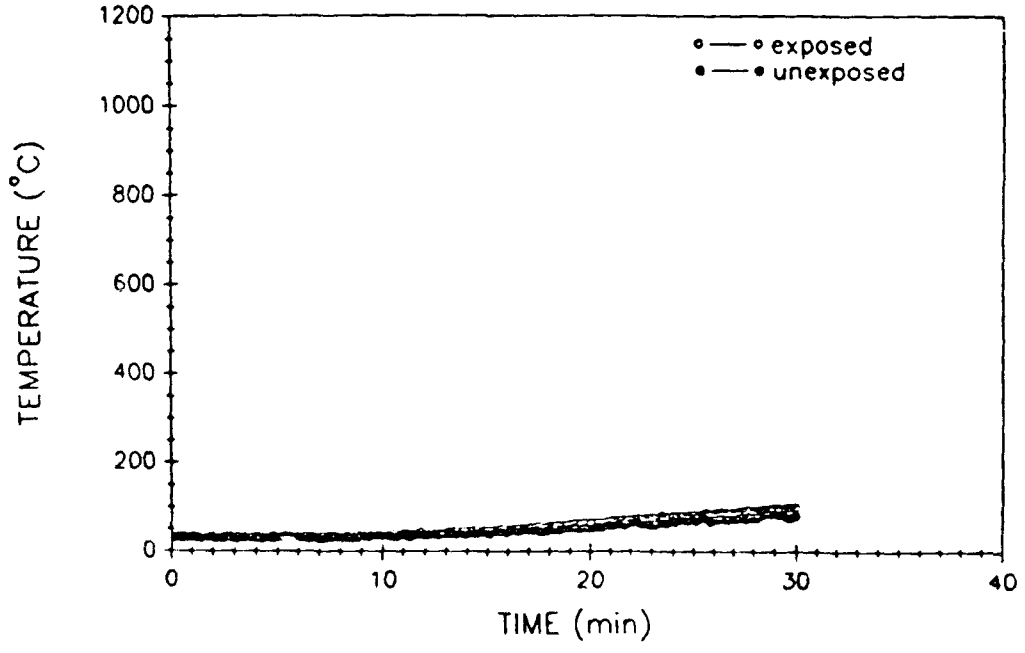

Fig A25 – Upper deck surface temperatures

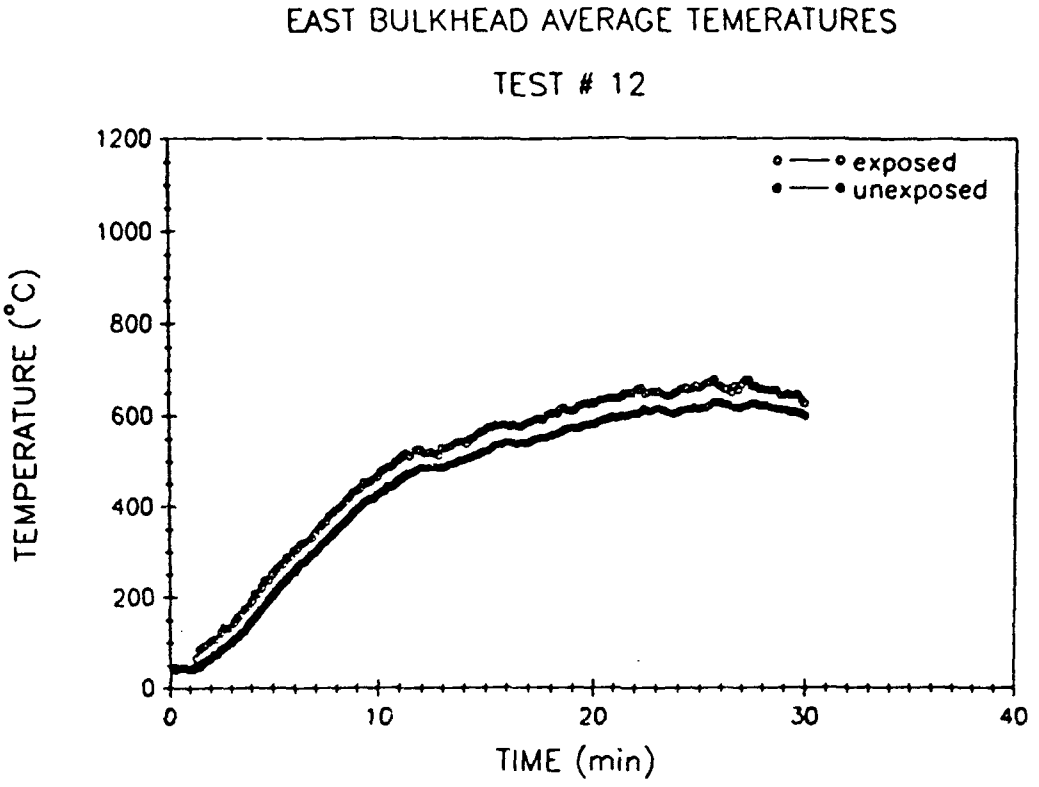

Fig. A26 – East bulkhead average surface temperatures

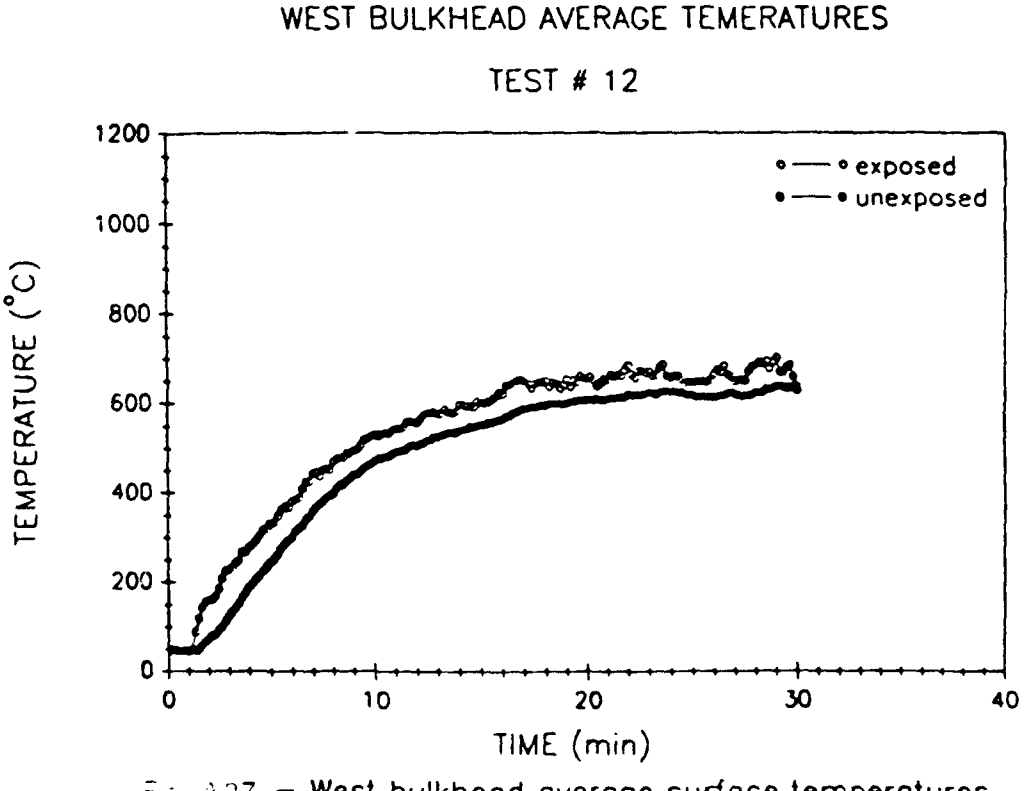

Fig. A27 – West bulkhead average surface temperatures

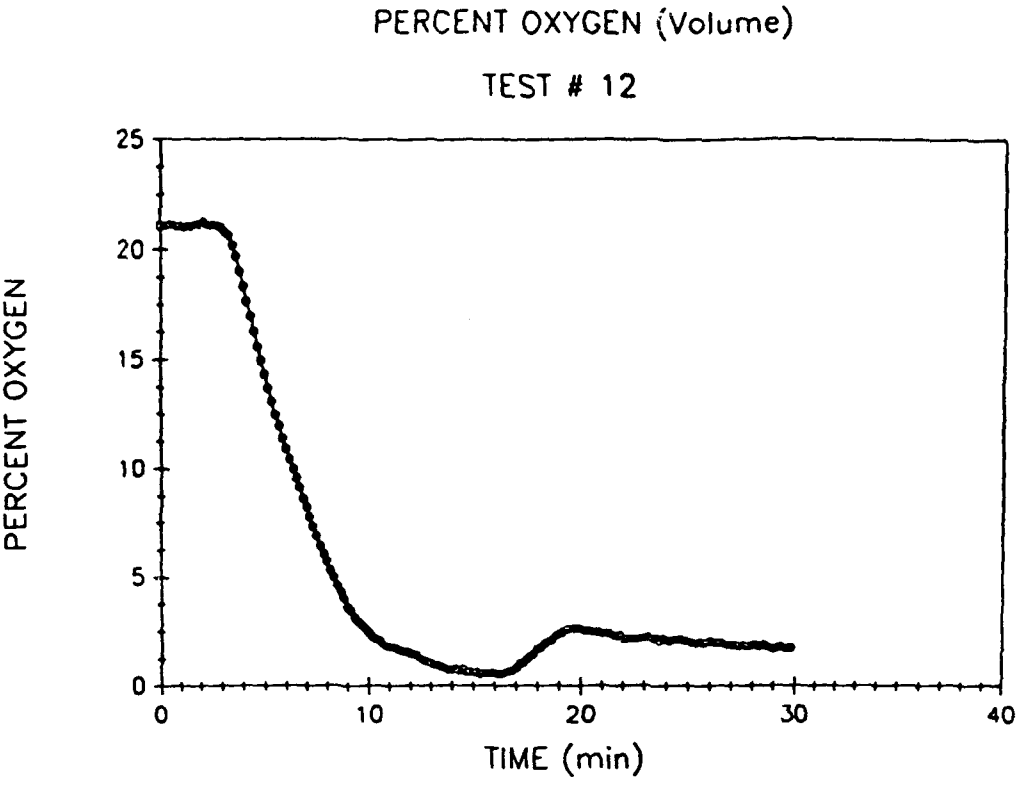

Fig. A28 – Percent oxygen (volume)

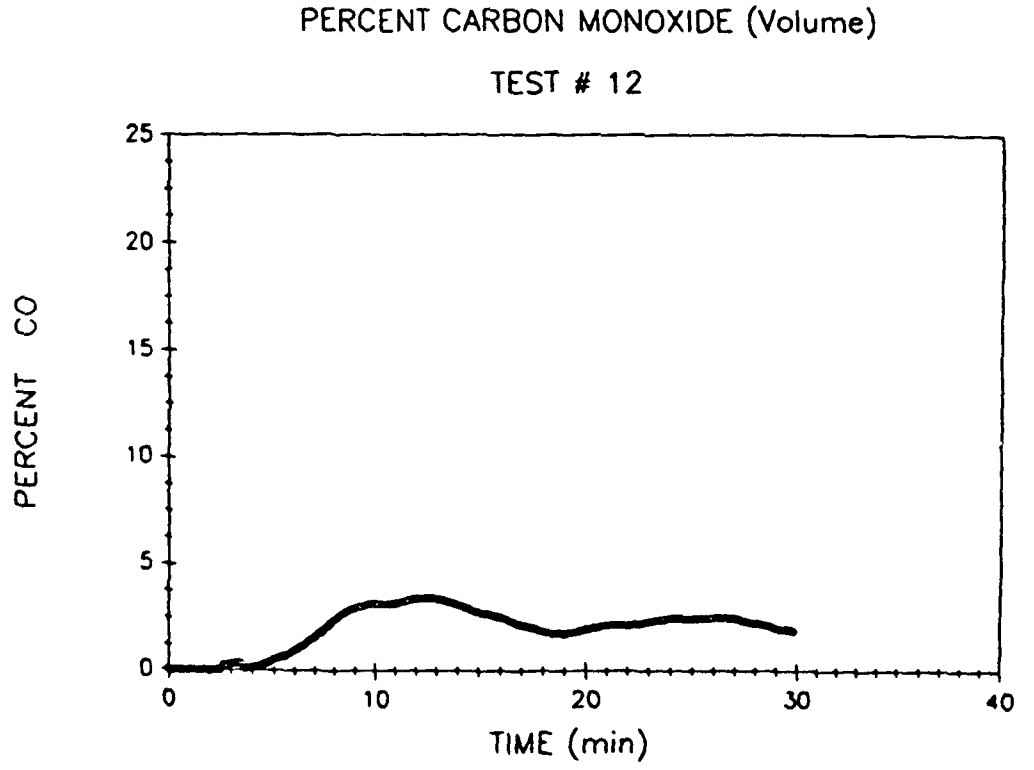

Fig. A29 – Percent carbon monoxide (volume)

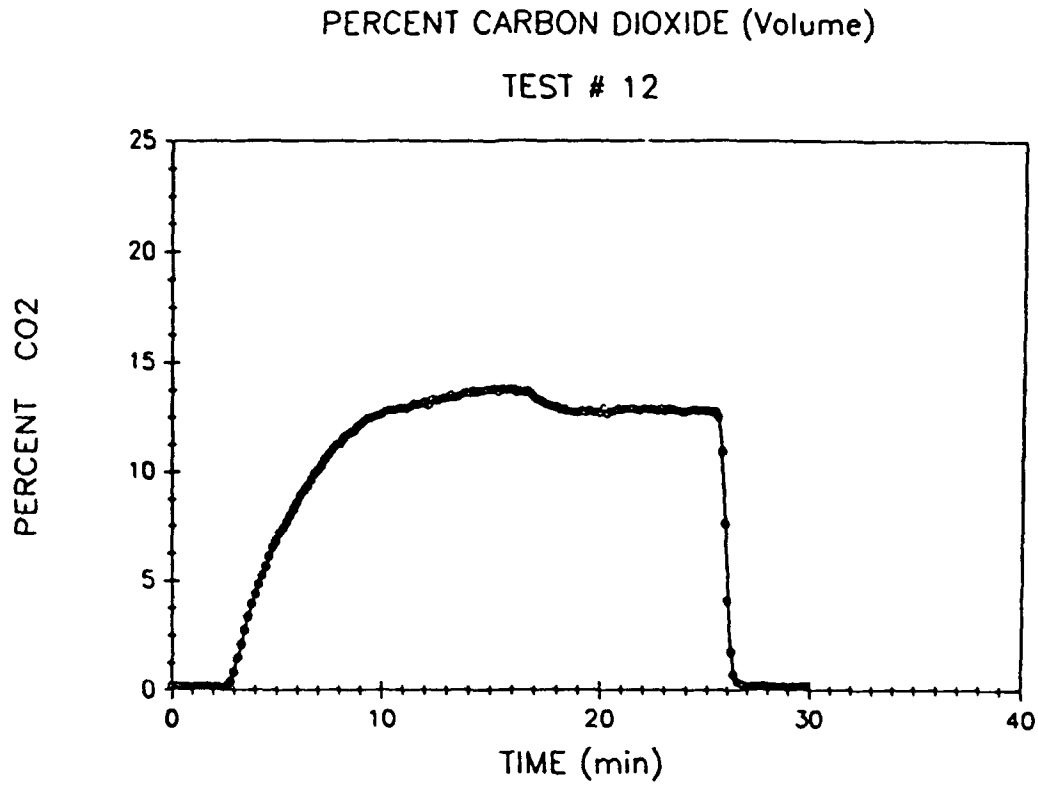

Fig. A30 – Percent carbon dioxide (volume)

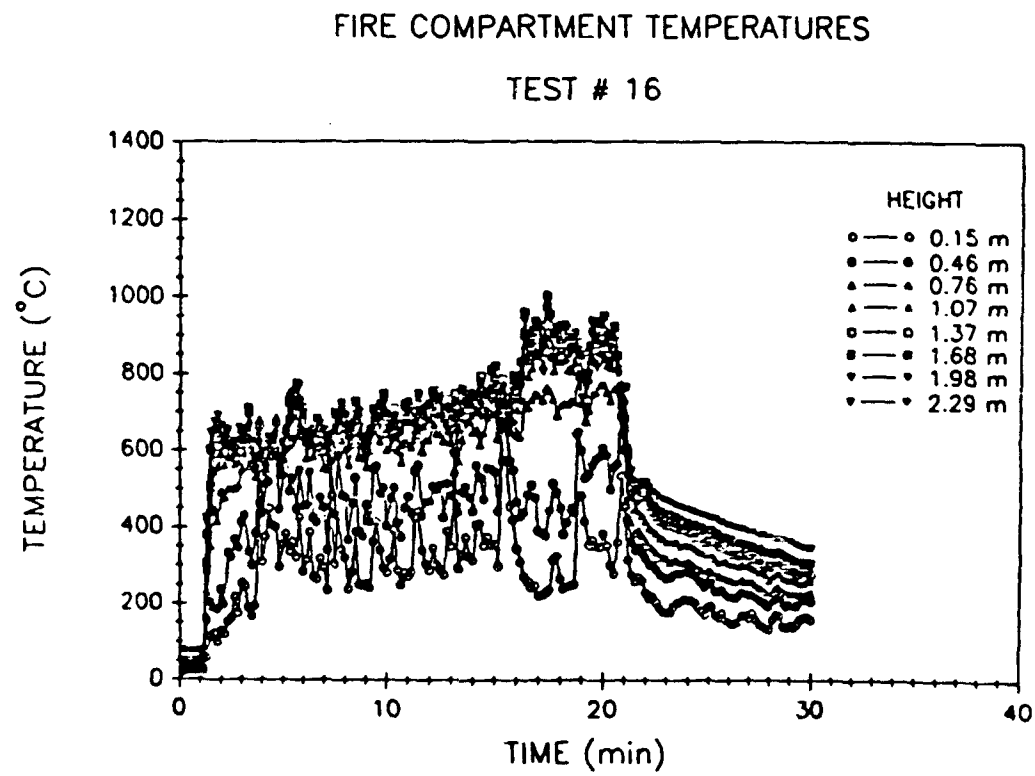

Fig. A31 – Fire comparment air temperatures

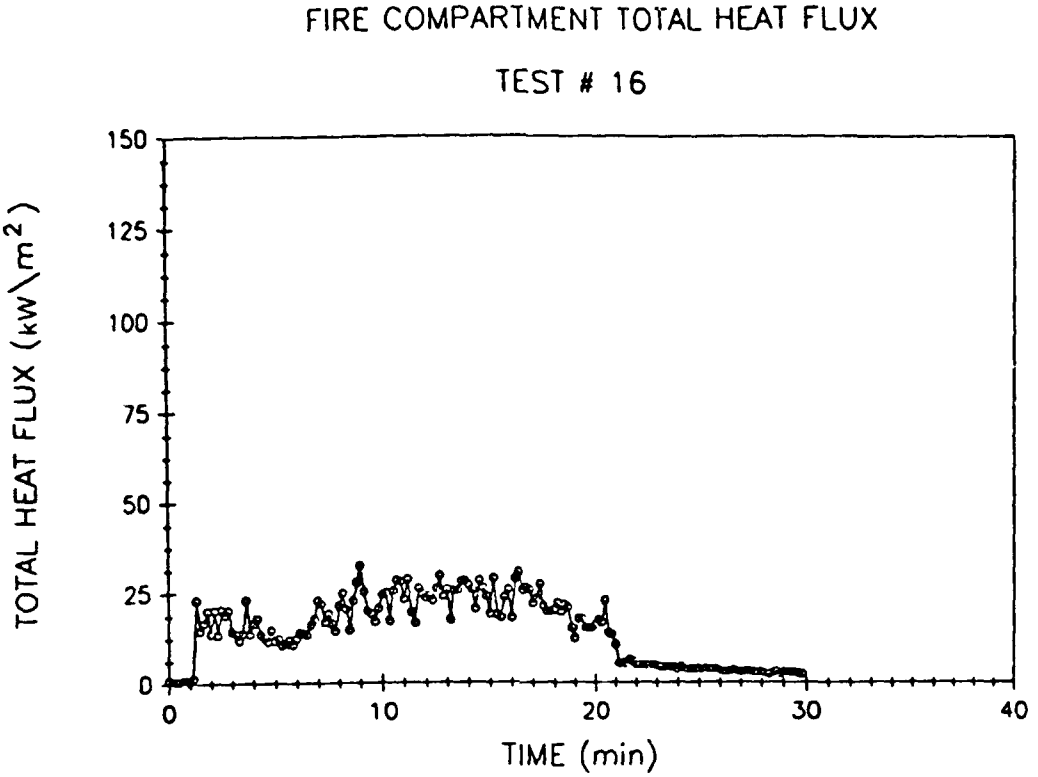

Fig. A32 – Fire compartment total heat flux

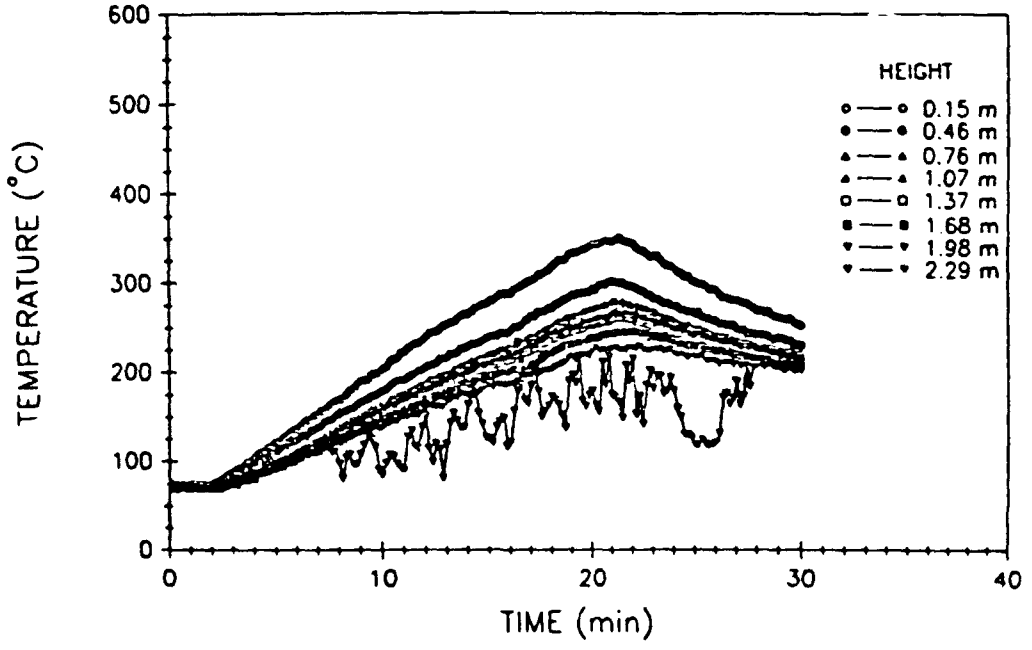

Fig. A33 – Upper compartment air temperatures

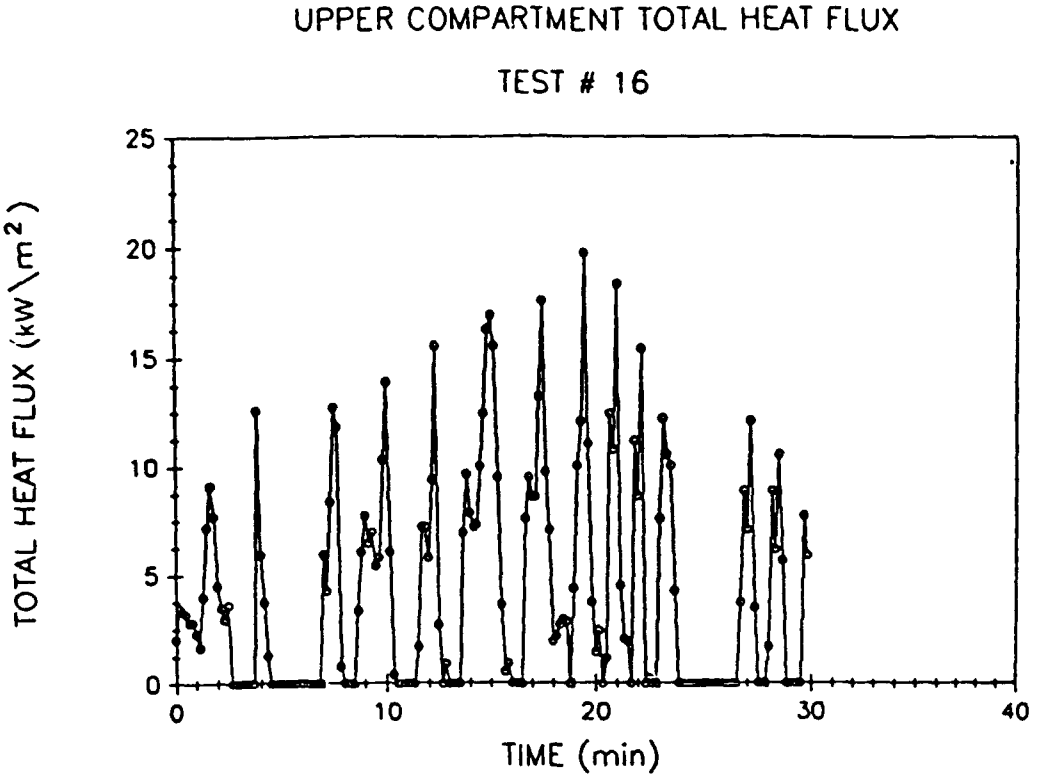

Fig. A34 – Upper compartment total heat flux

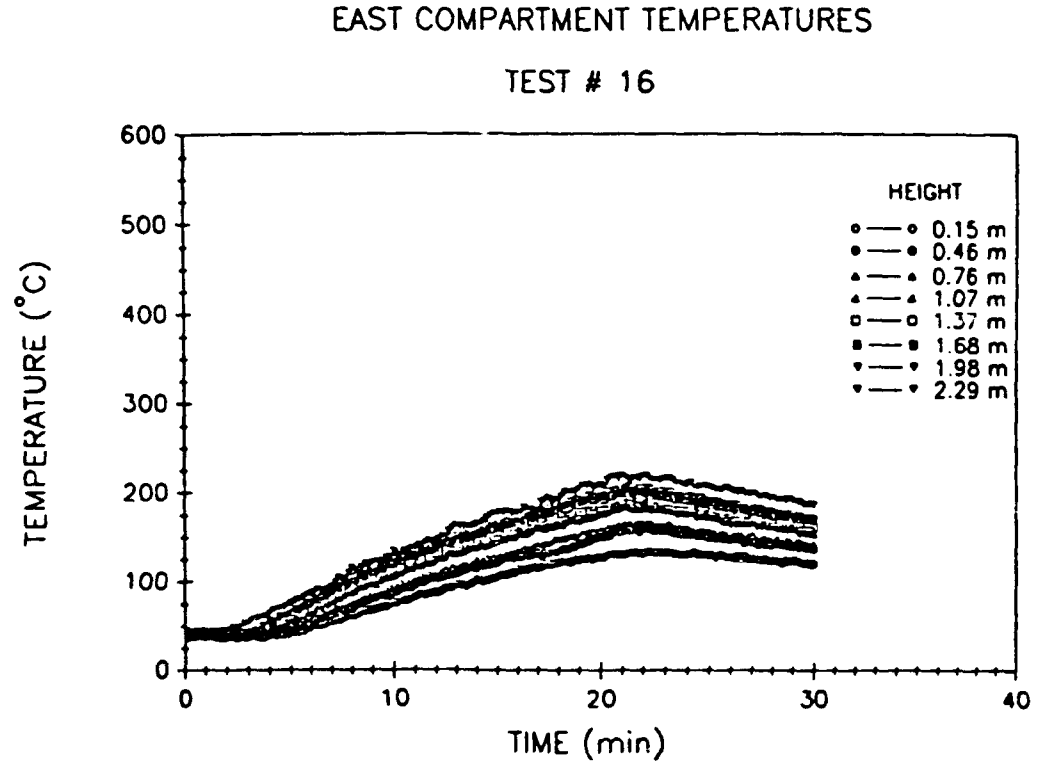

Fig. A35 – East compartment air temperatures

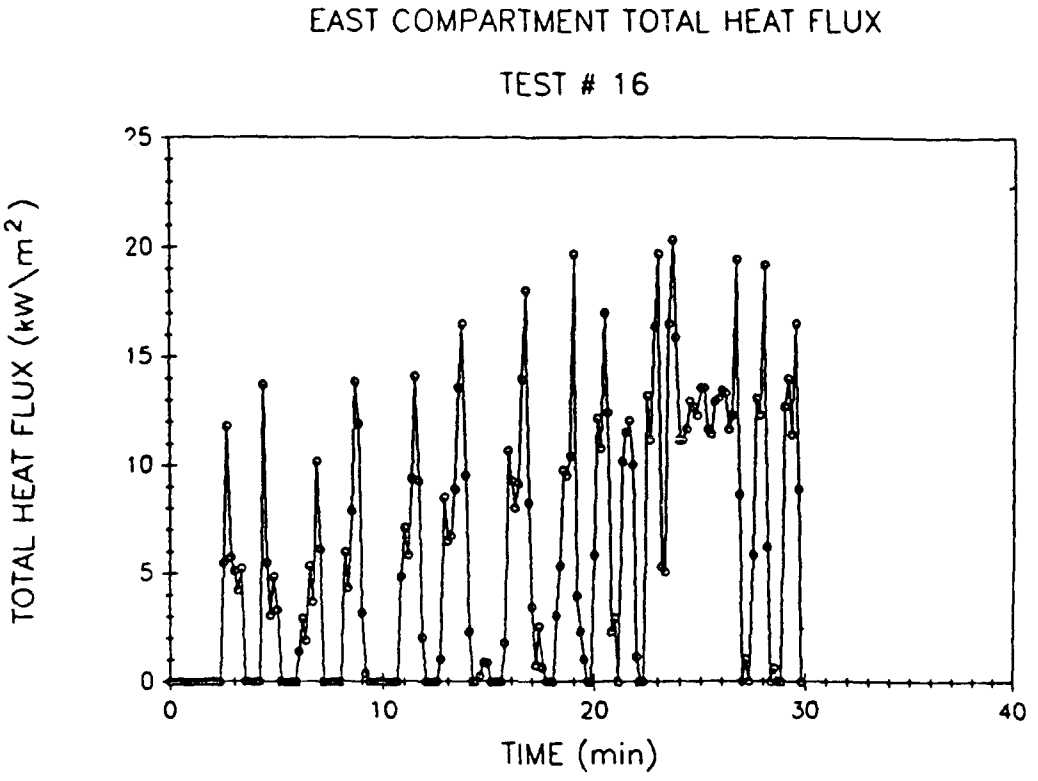

Fig. A36 – East compartment total heat flux

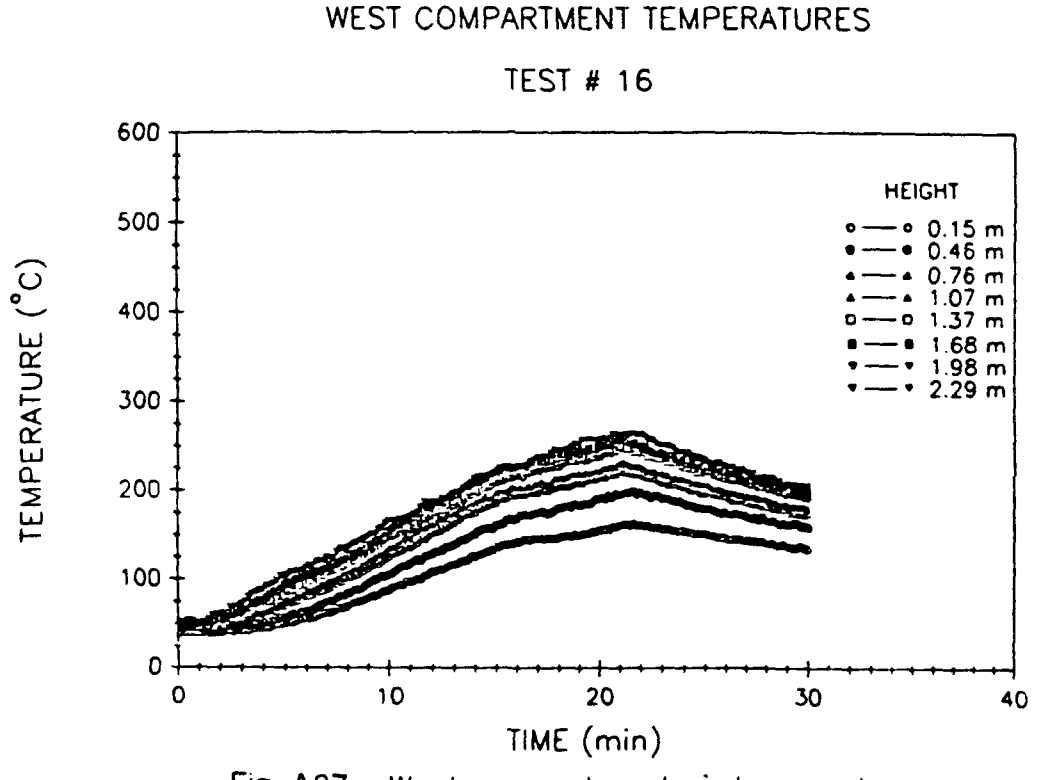

Fig. A37 – West compartment air temperatures

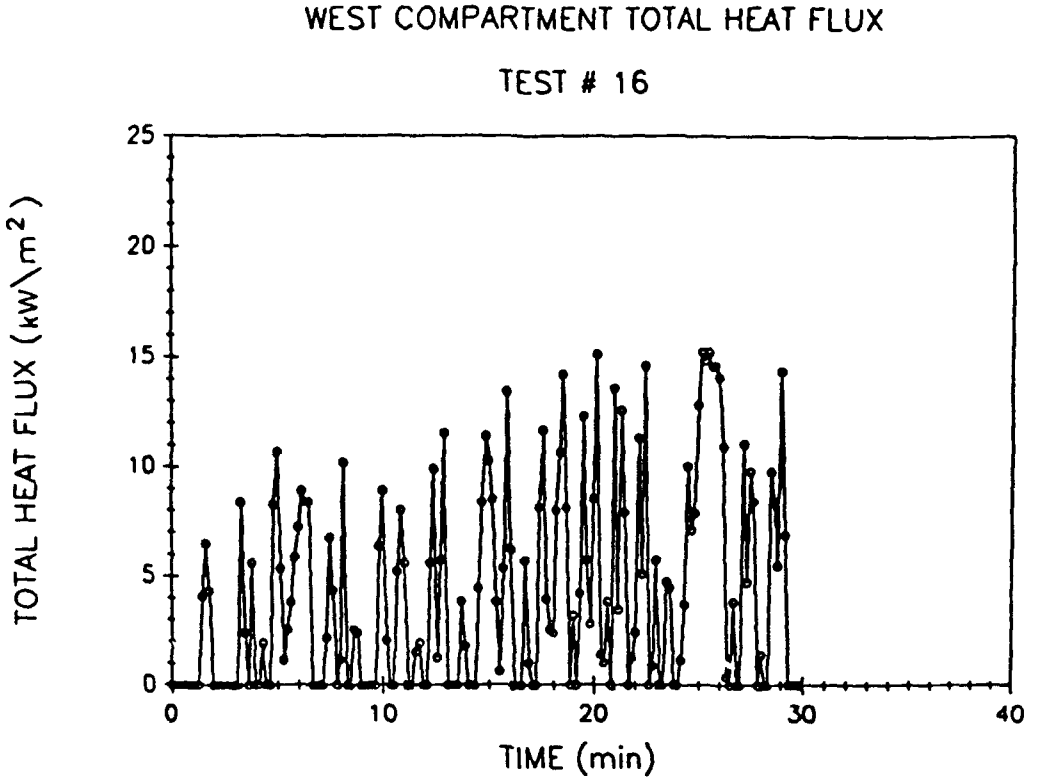

Fig. A38 – West compartment total heat flux

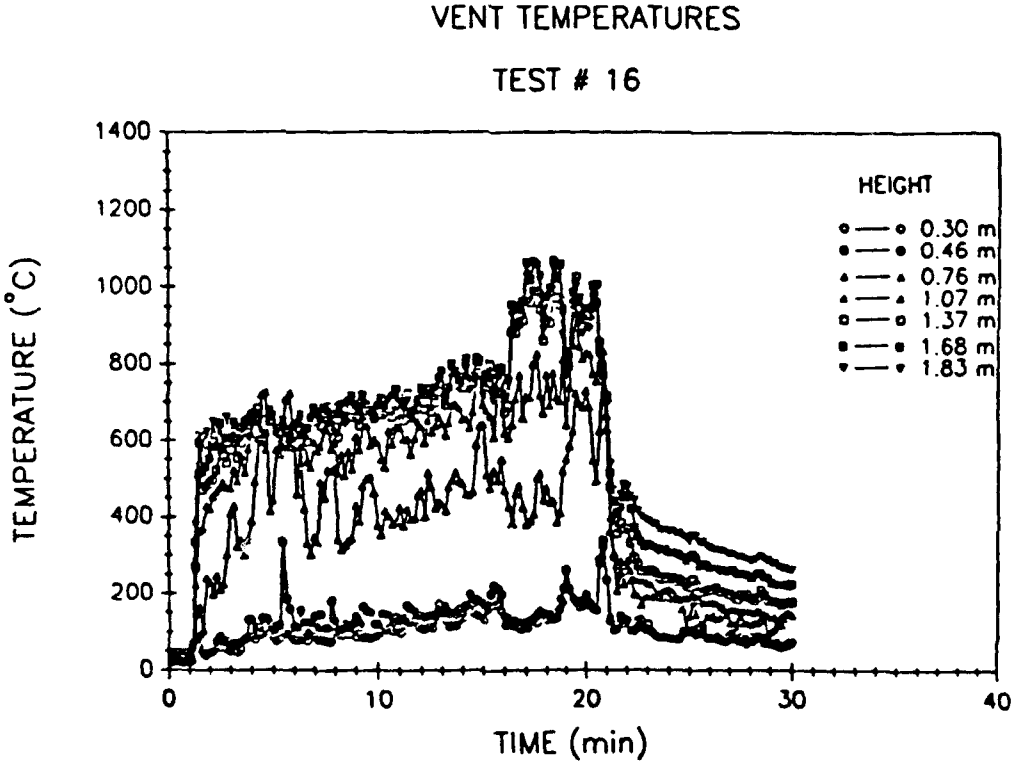

Fig. A39 – Vent air temperatures

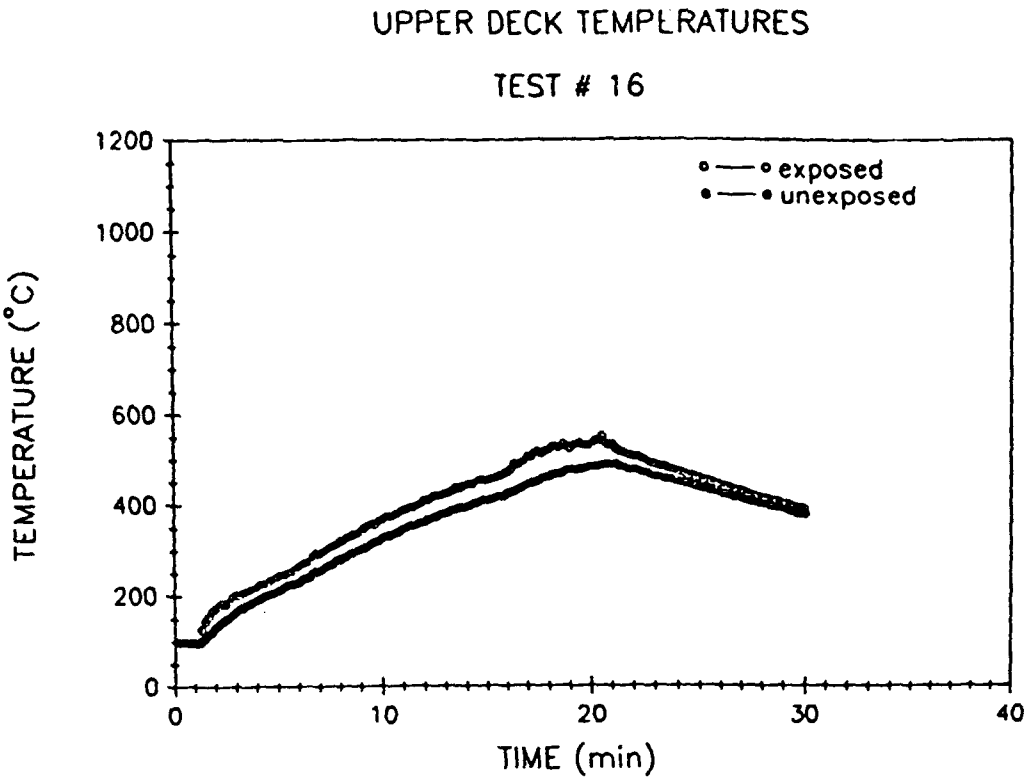

Fig. A40 – Upper deck surface temperatures

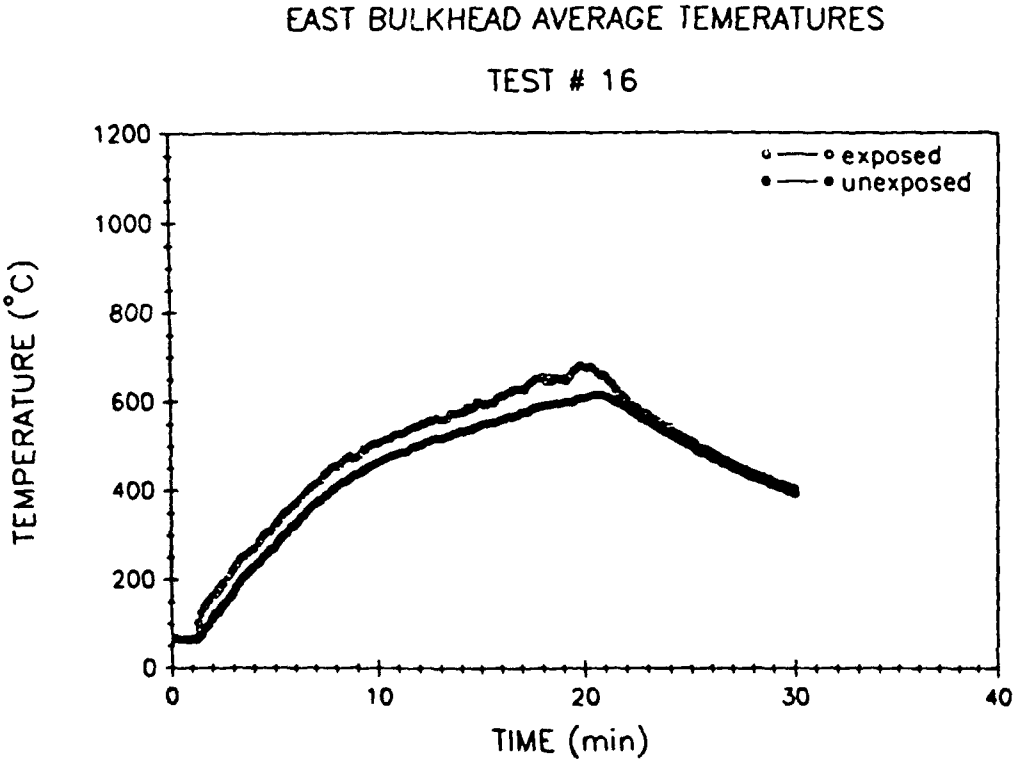

Fig. A41 – East bulkhead average surface temperatures

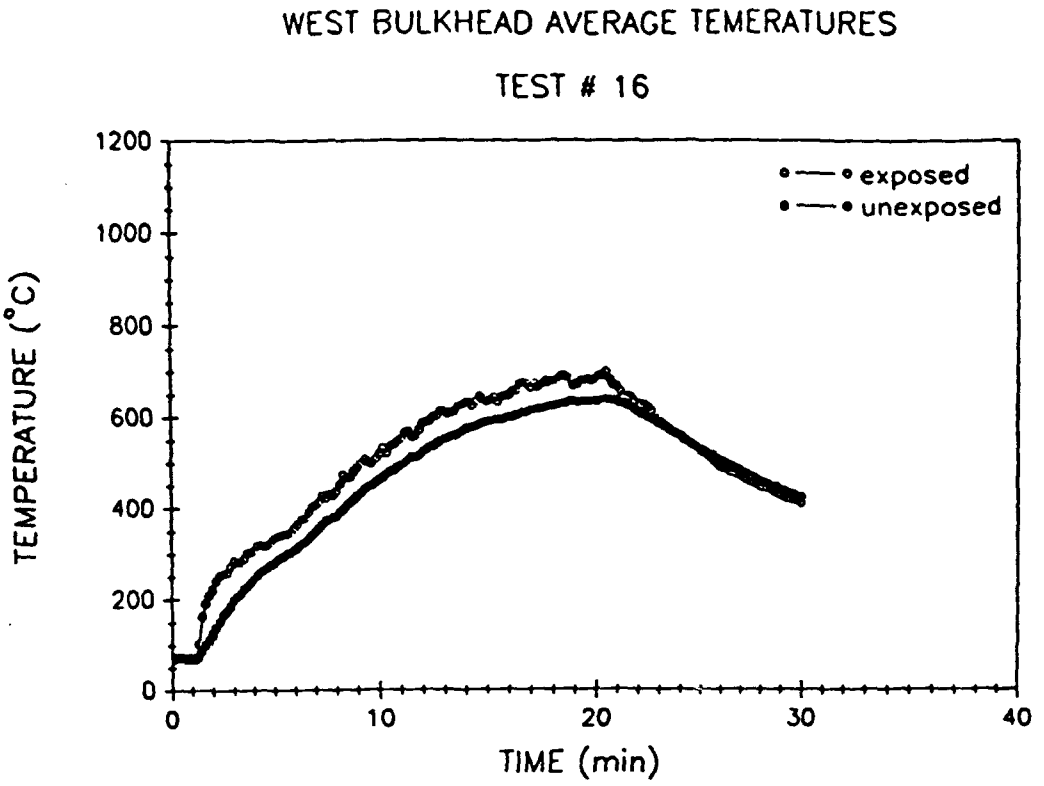

Fig. A42 – West bulkhead average surface temperatures

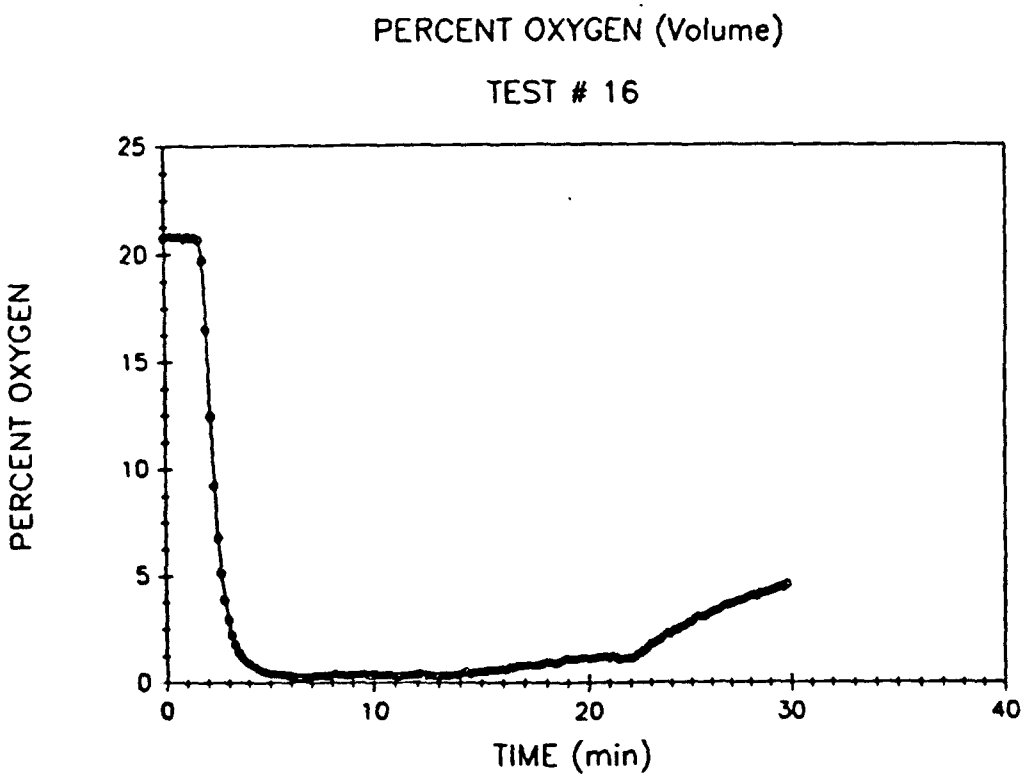

Fig. A43 – Percent oxygen (volume)

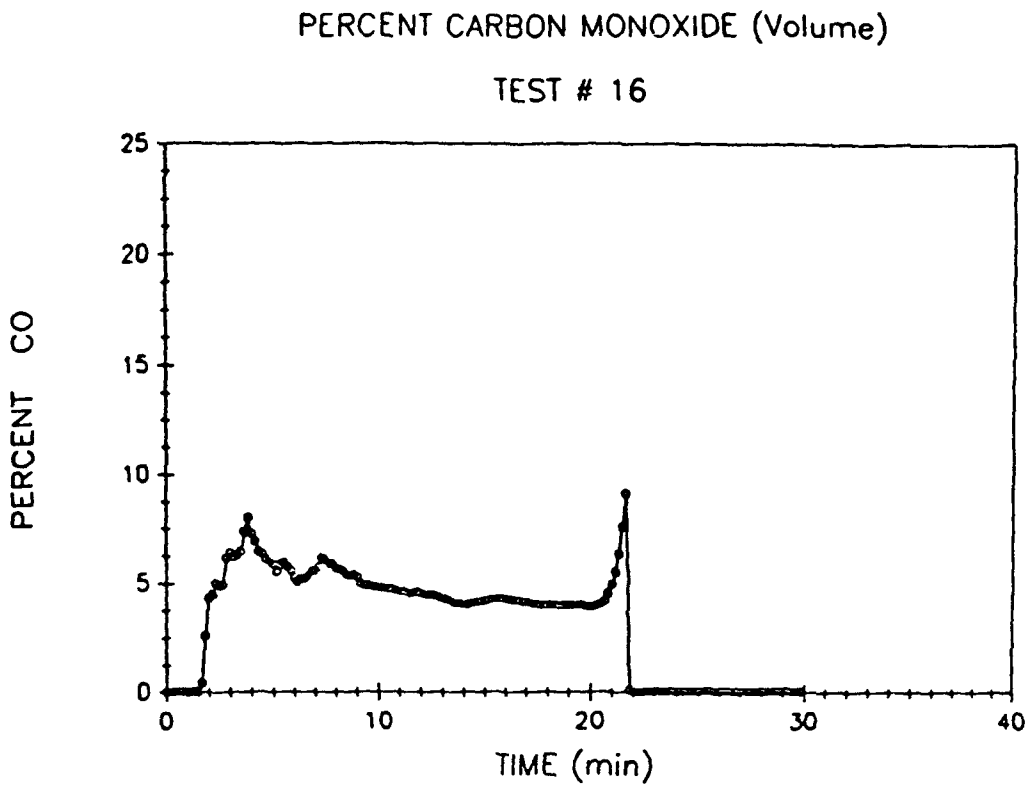

Fig. A44 – Percent carbon monoxide (volume)

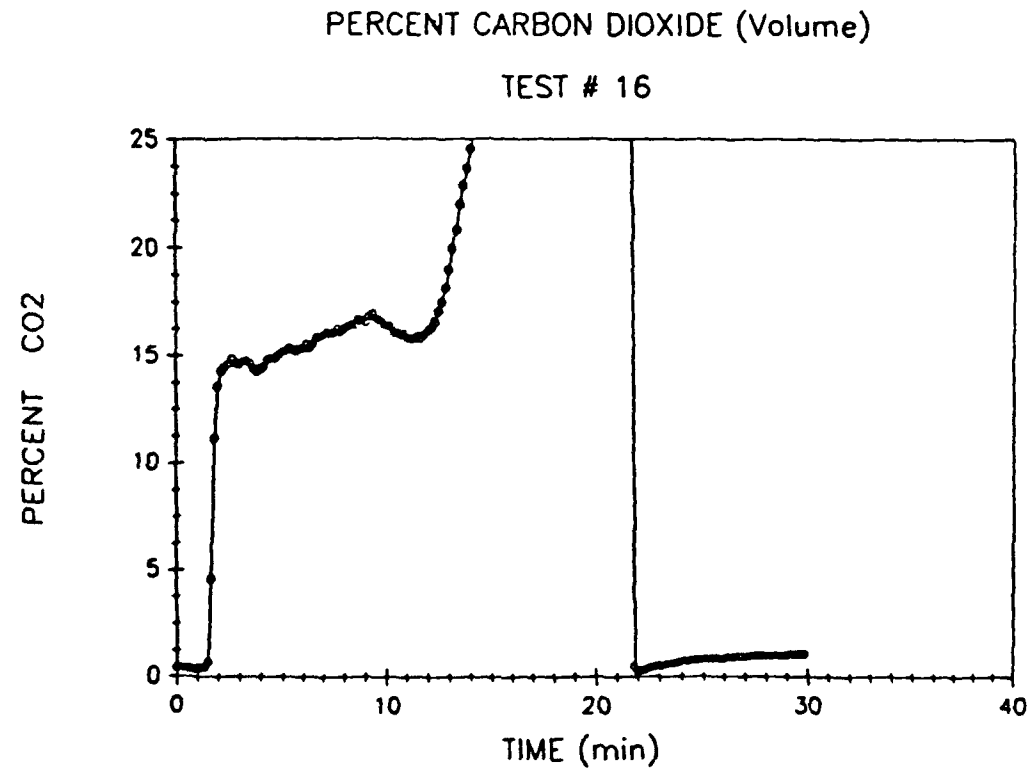

Fig. A45 – Percent carbon dioxide (volume)

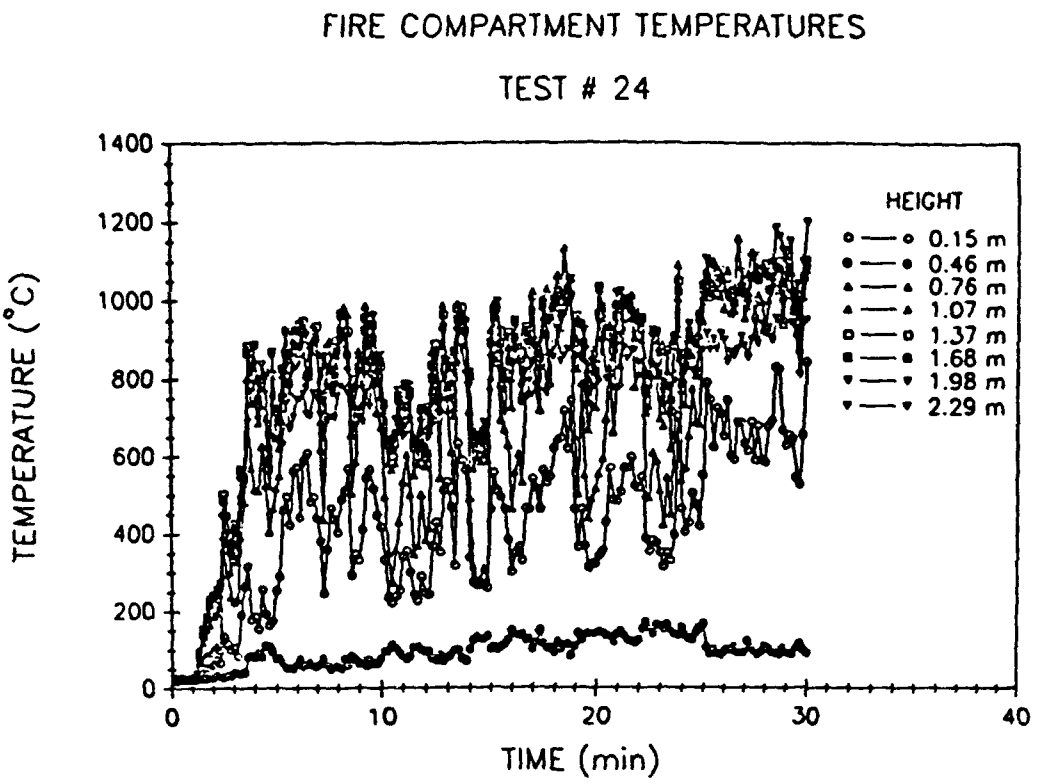

Fig. A46 – Fire comparment air temperatures

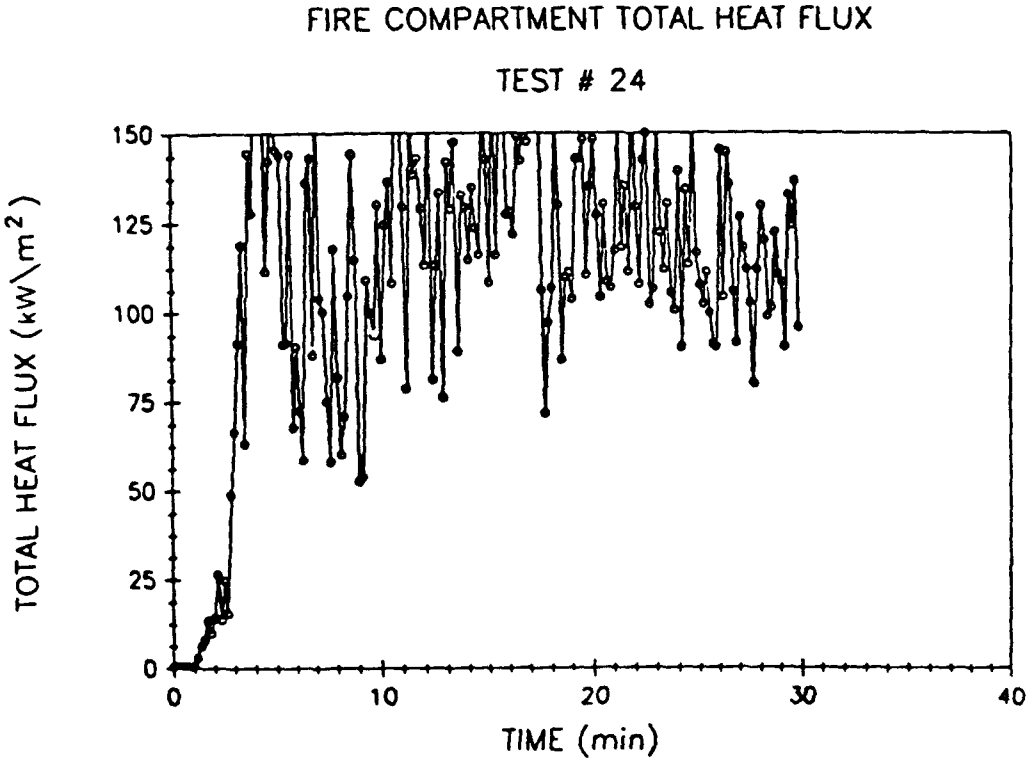

Fig. A47 – Fire compartment total heat flux

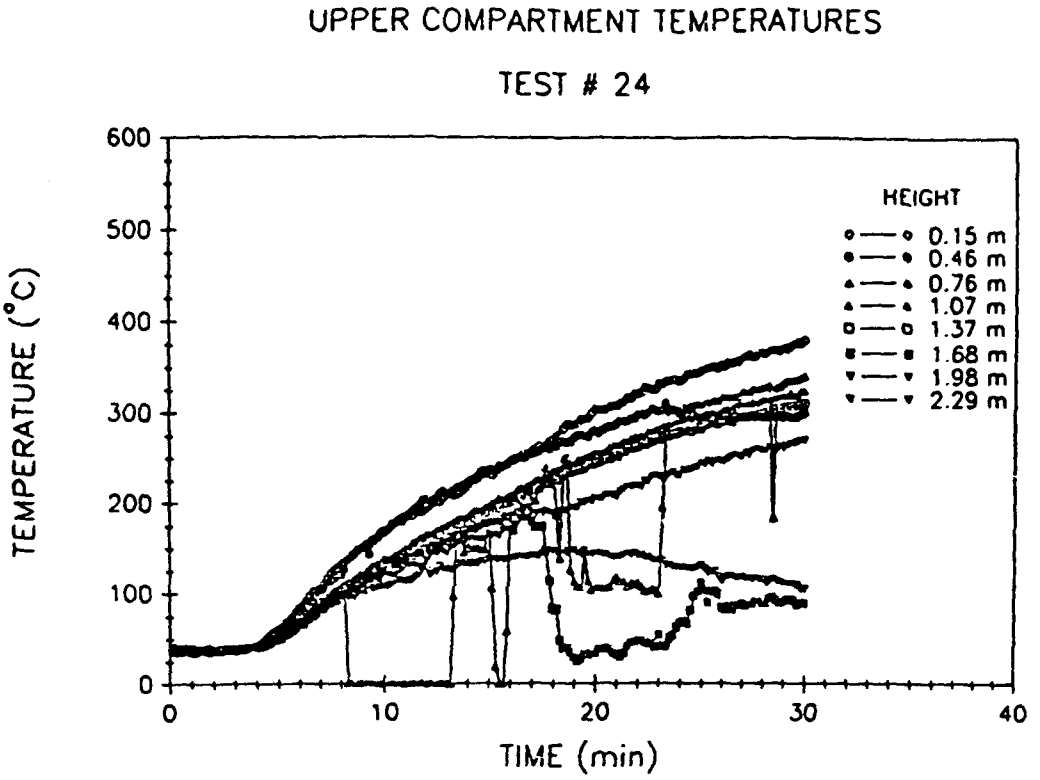

Fig. A48 – Upper compartment air temperatures

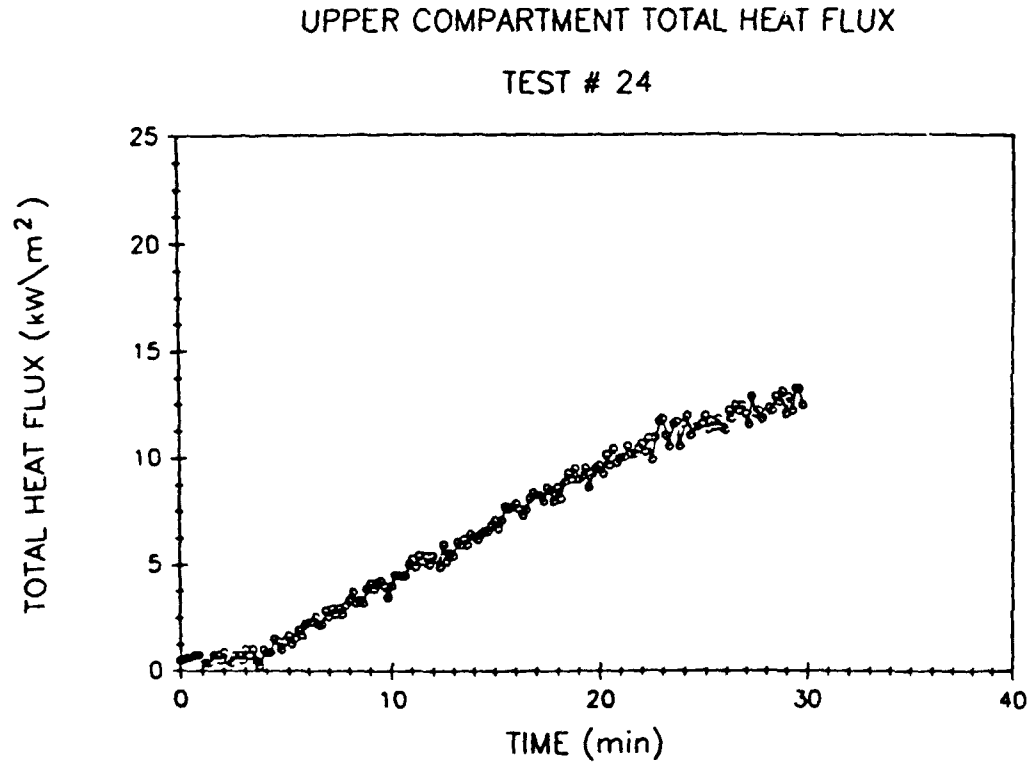

Fig. A49 – Upper compartment total heat flux

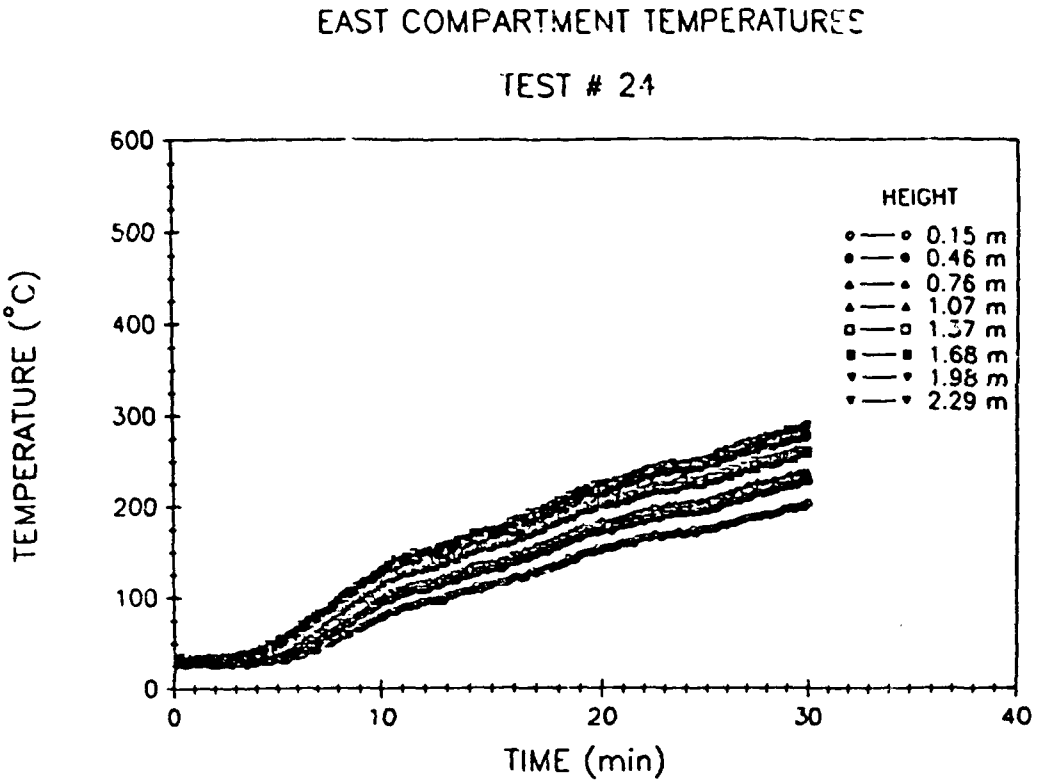

Fig. A50 – East compartment air temperatures

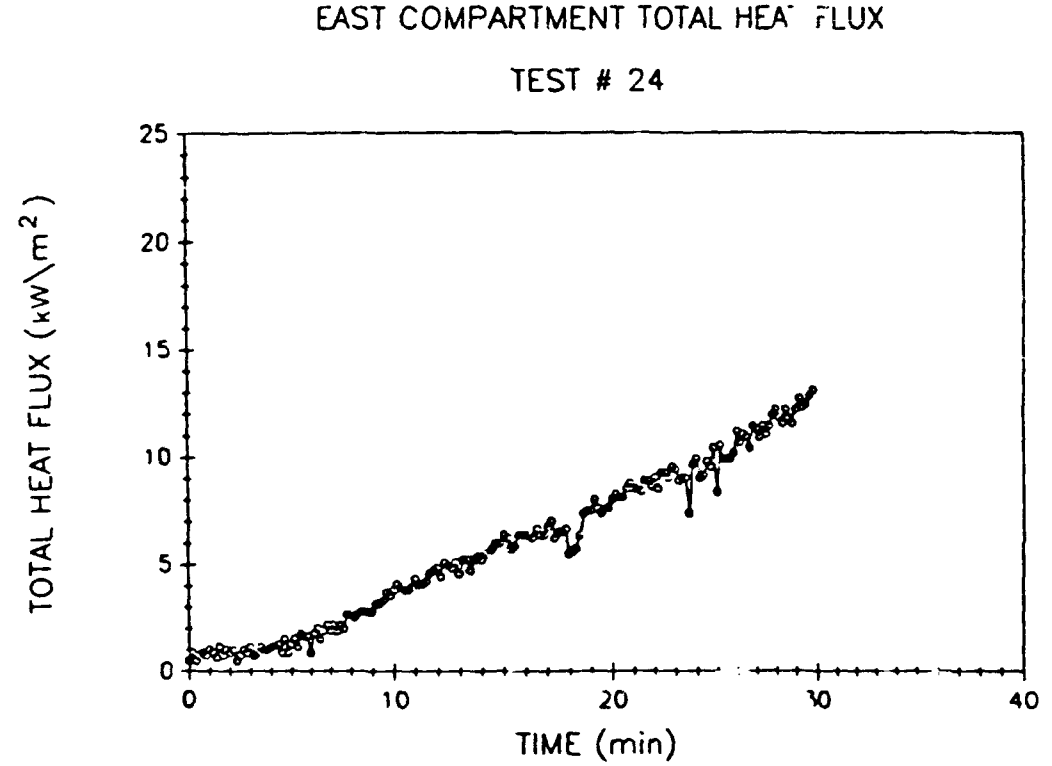

Fig. A51 – East compartment total heat flux

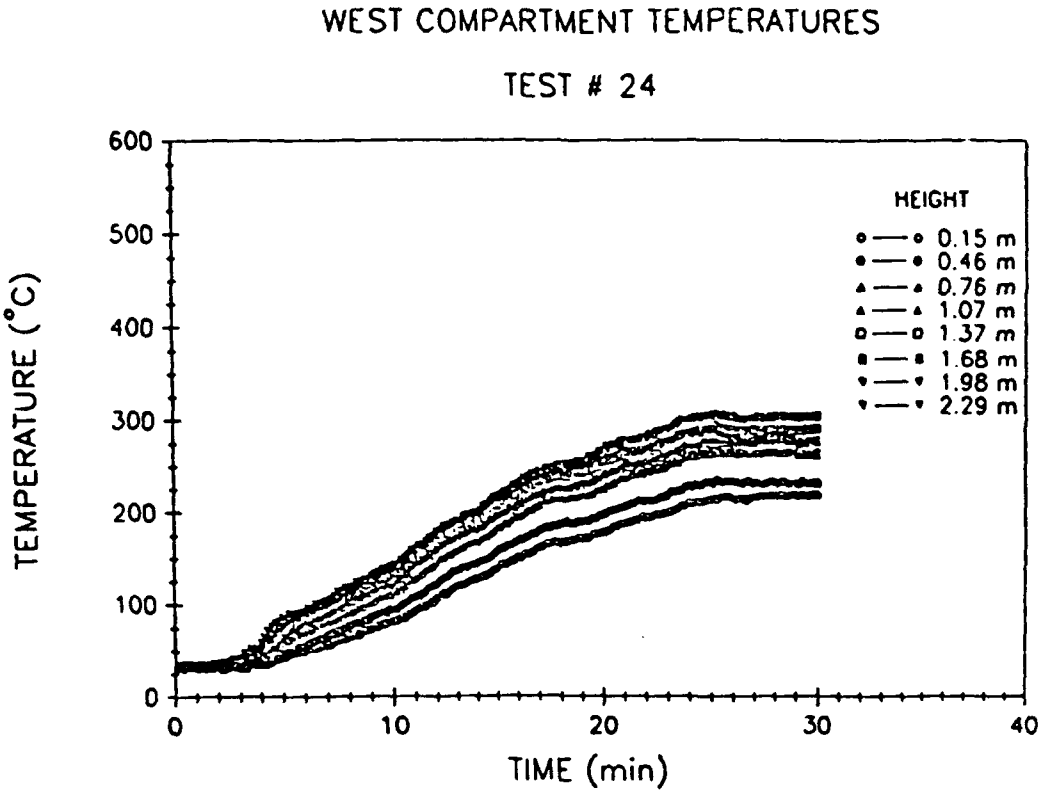

Fig. A52 – West compartment air temperatures

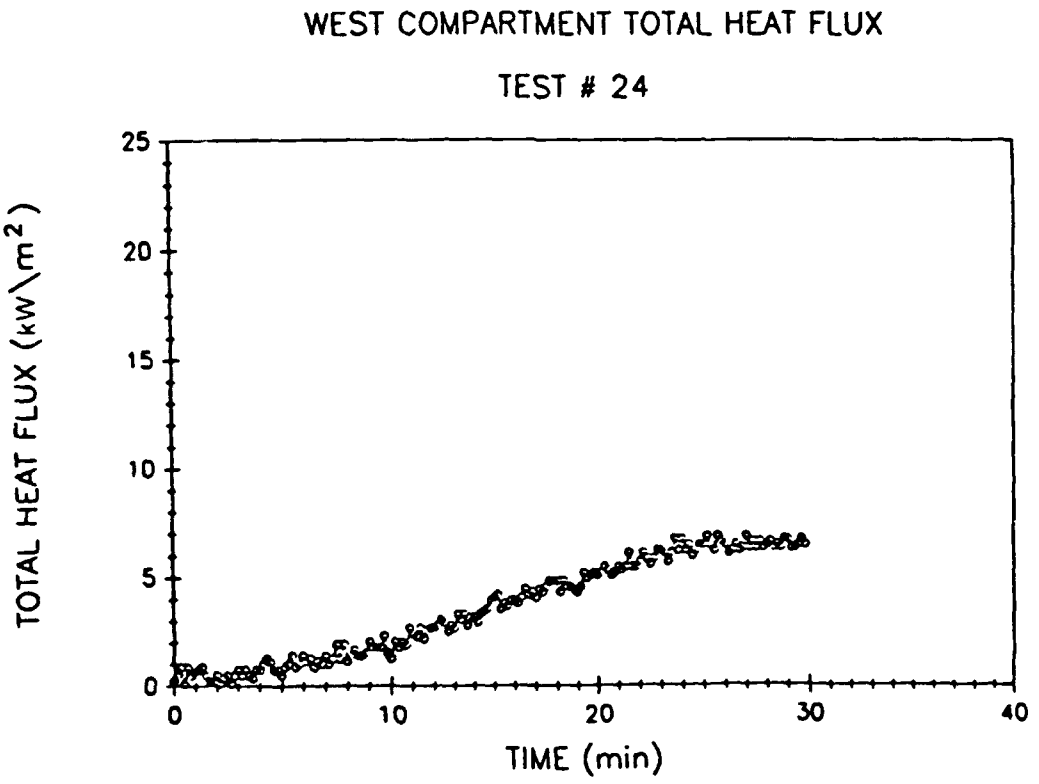

Fig. A53 – West compartment total heat flux

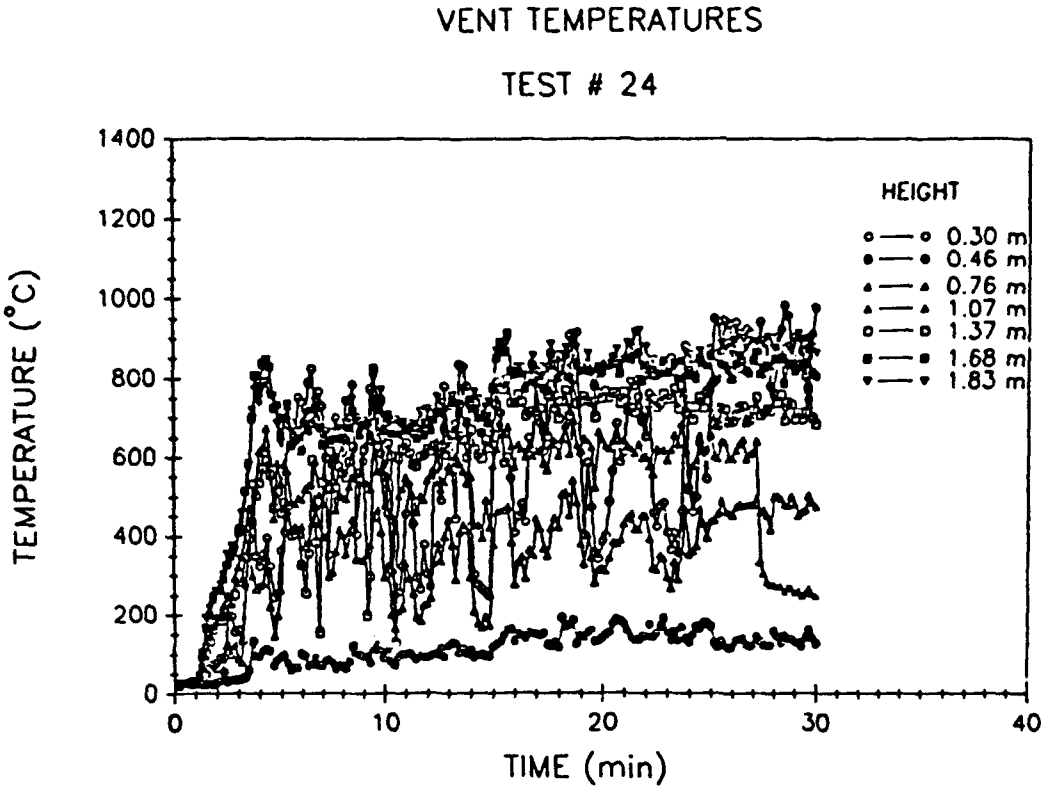

Fig. A54 – Vent air temperatures

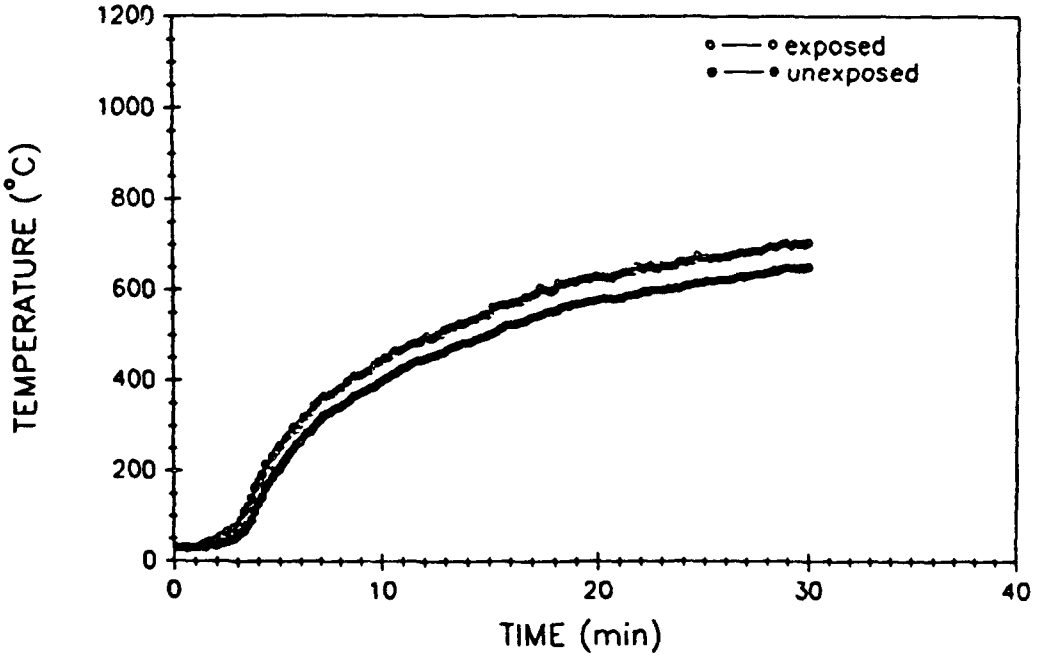

Fig. A55 – Upper deck surface temperatures

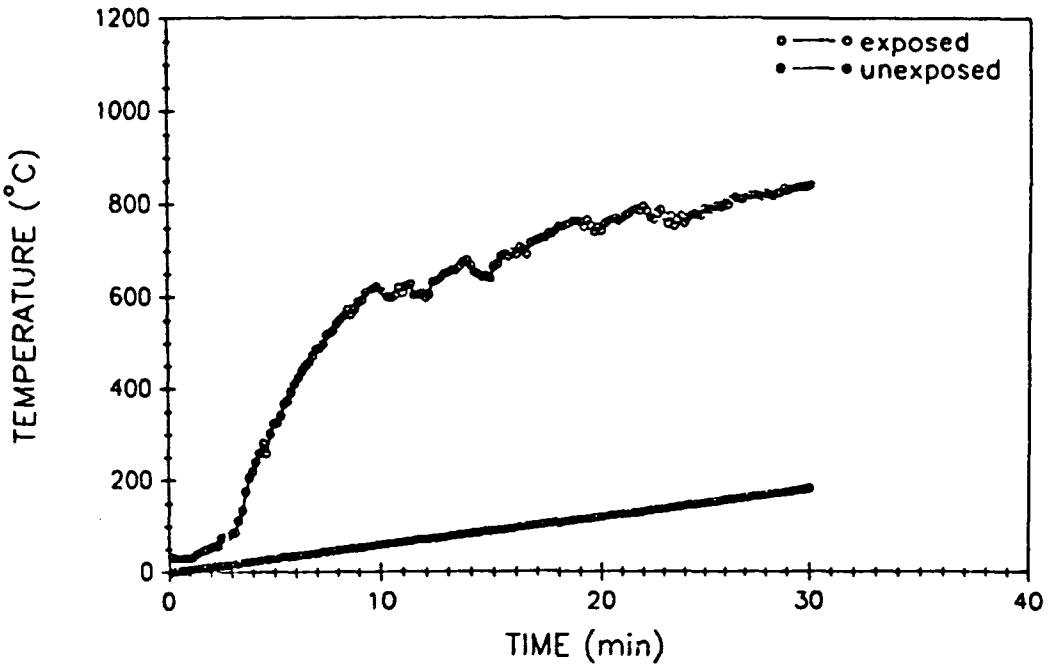

Fig. A56 – East bulkhead average surface temperatures

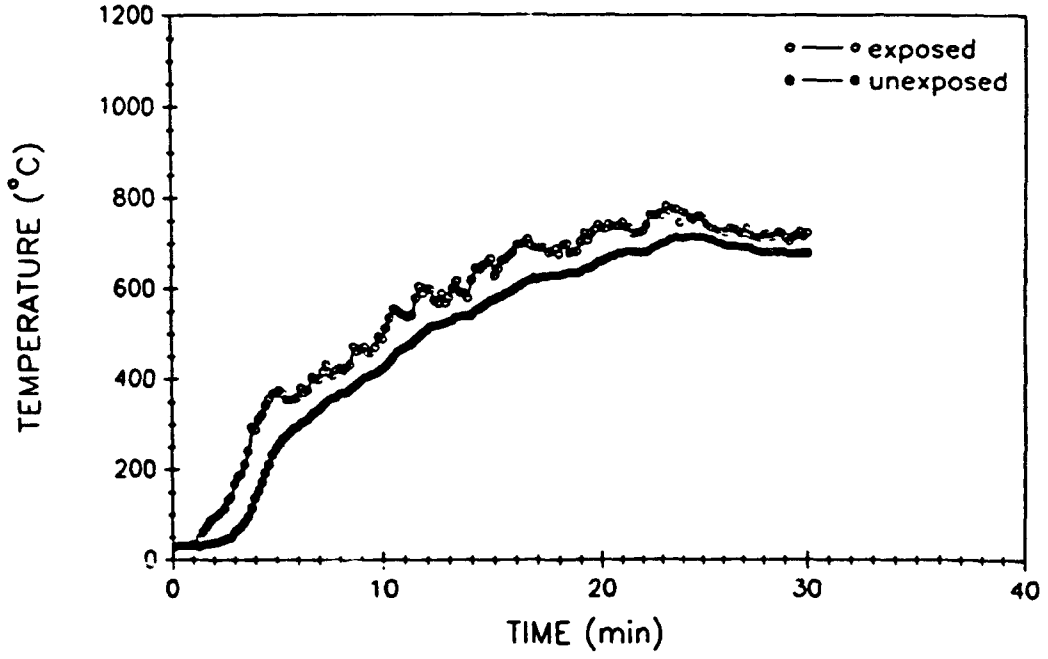

Fig. A57 – West bulkhead average surface temperatures

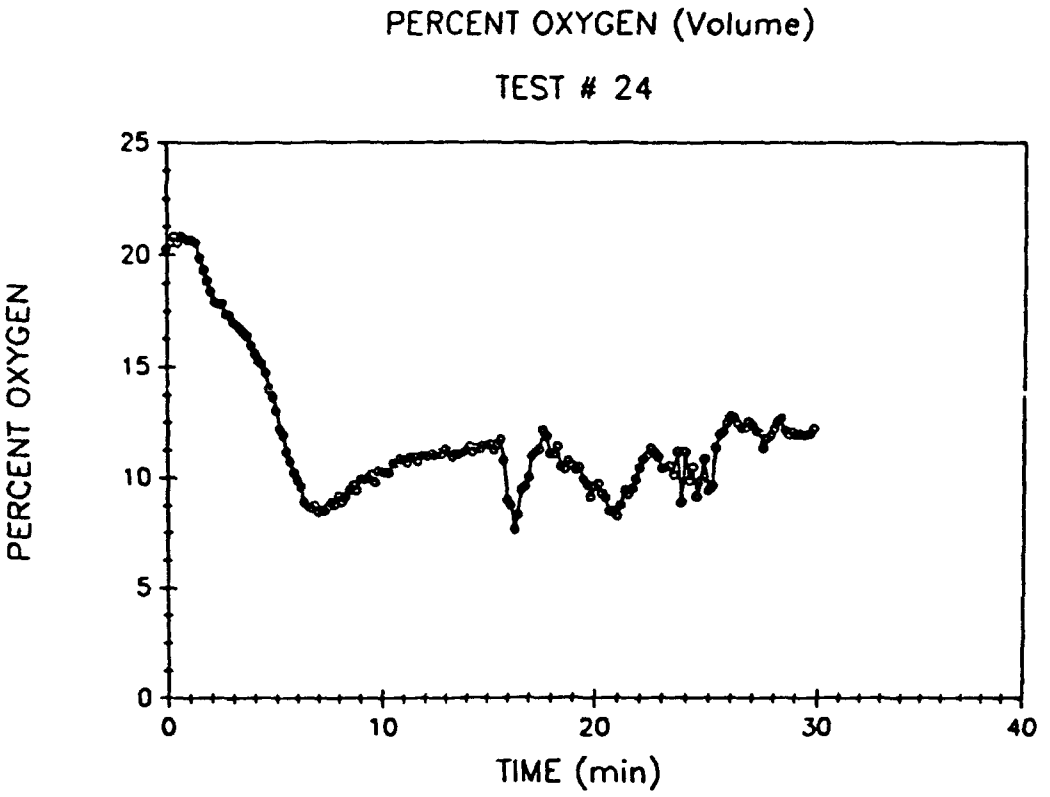

Fig. A58 – Percent oxygen (volume)

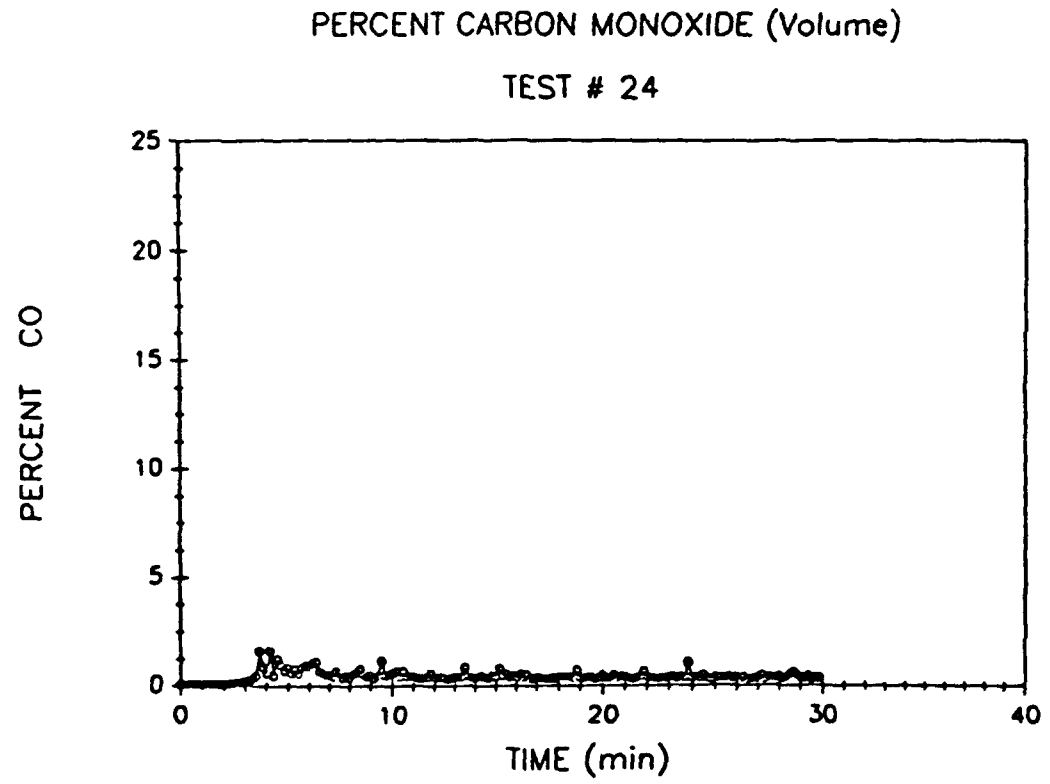

Fig. A59 – Percent carbon monoxide (volume)

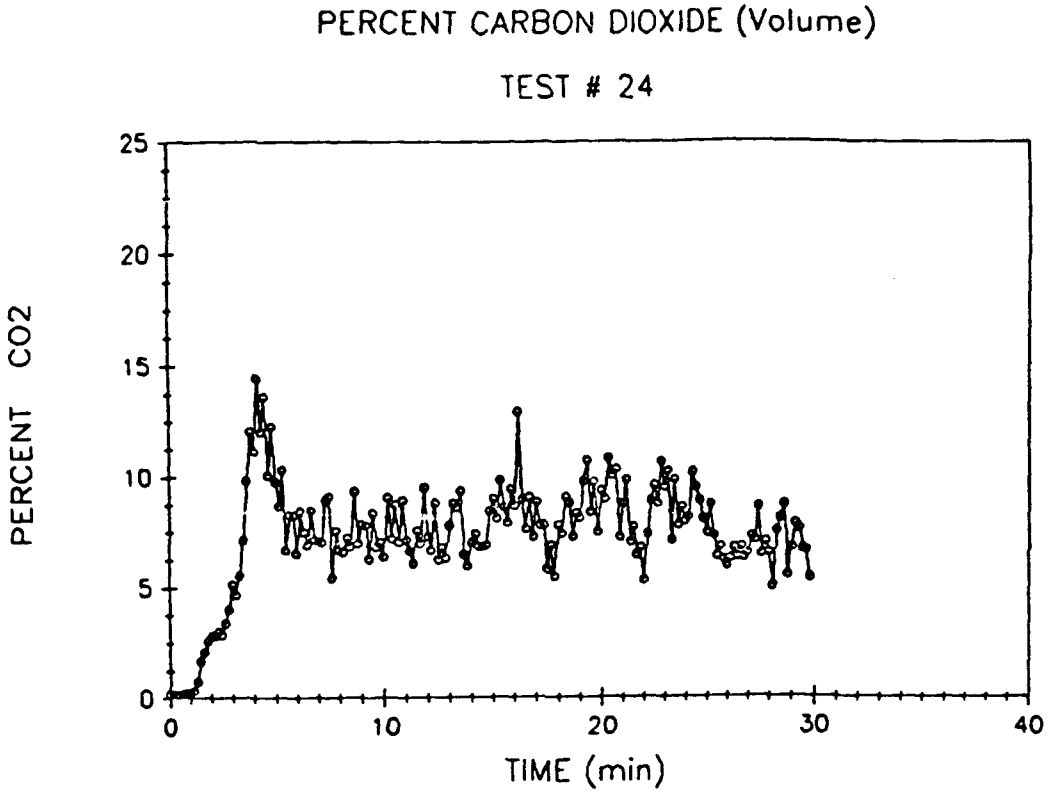

Fig. A60 – Percent carbon dioxide (volume)

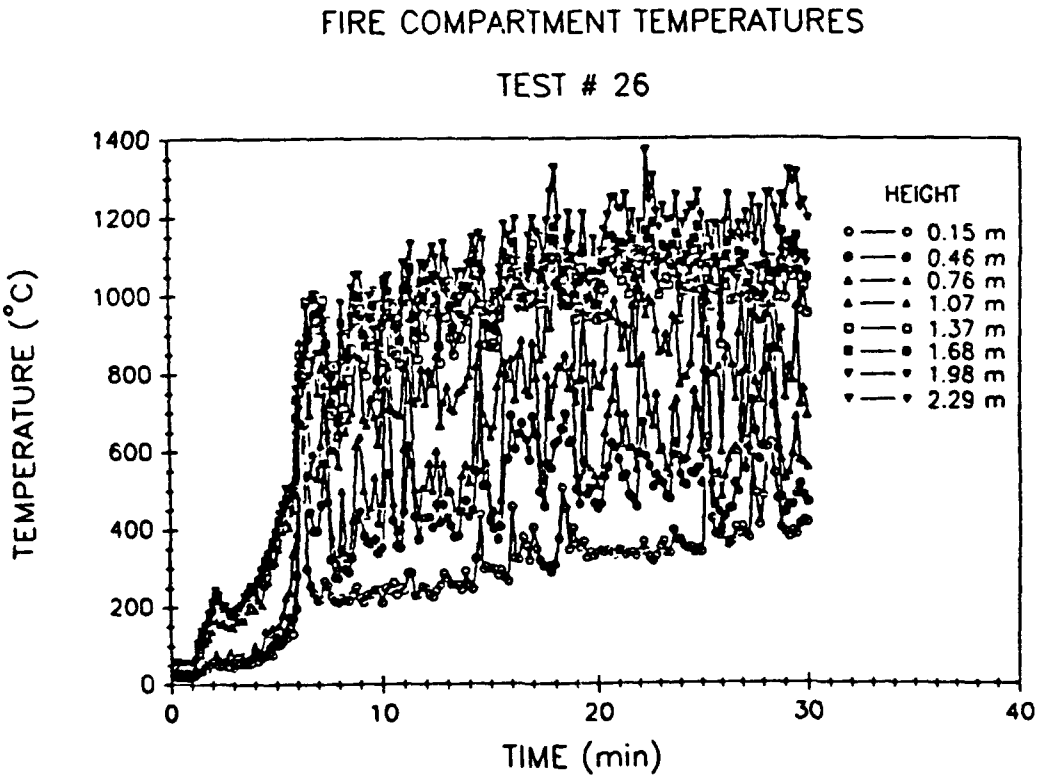

Fig. A61 – Fire comparment air temperatures

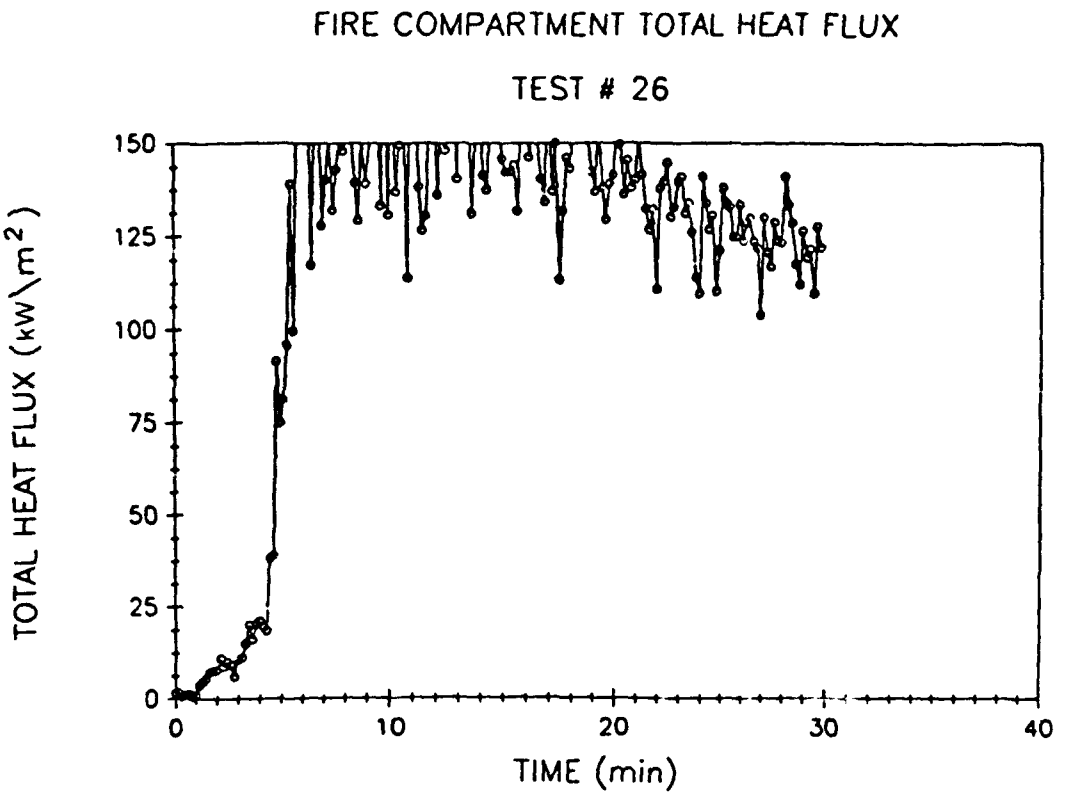

Fig. A62 – Fire compartment total heat flux

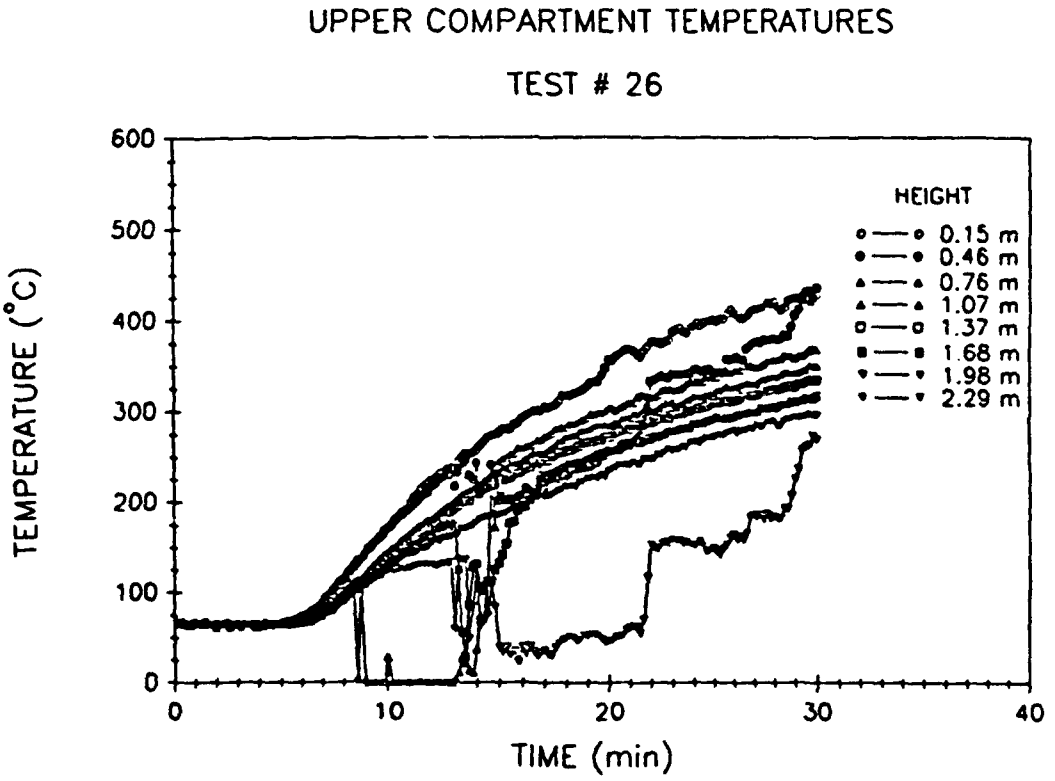

Fig. A63 – Upper compartment air temperatures

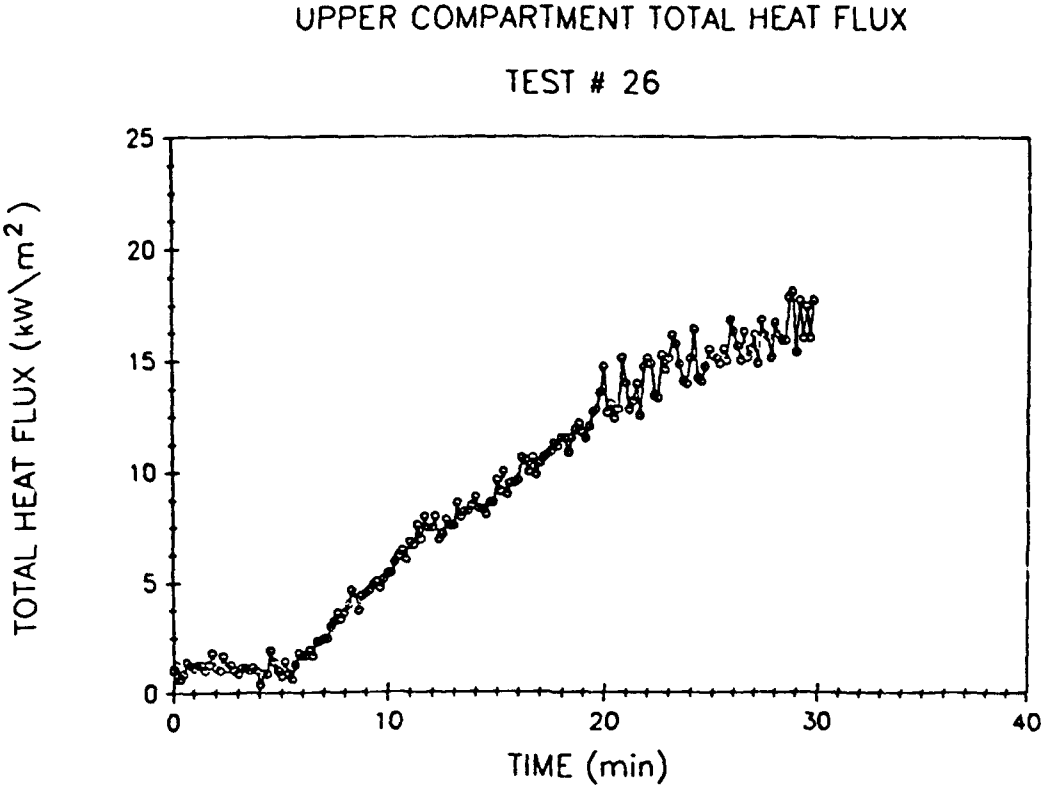

Fig. A64 – Upper compartment total heat flux

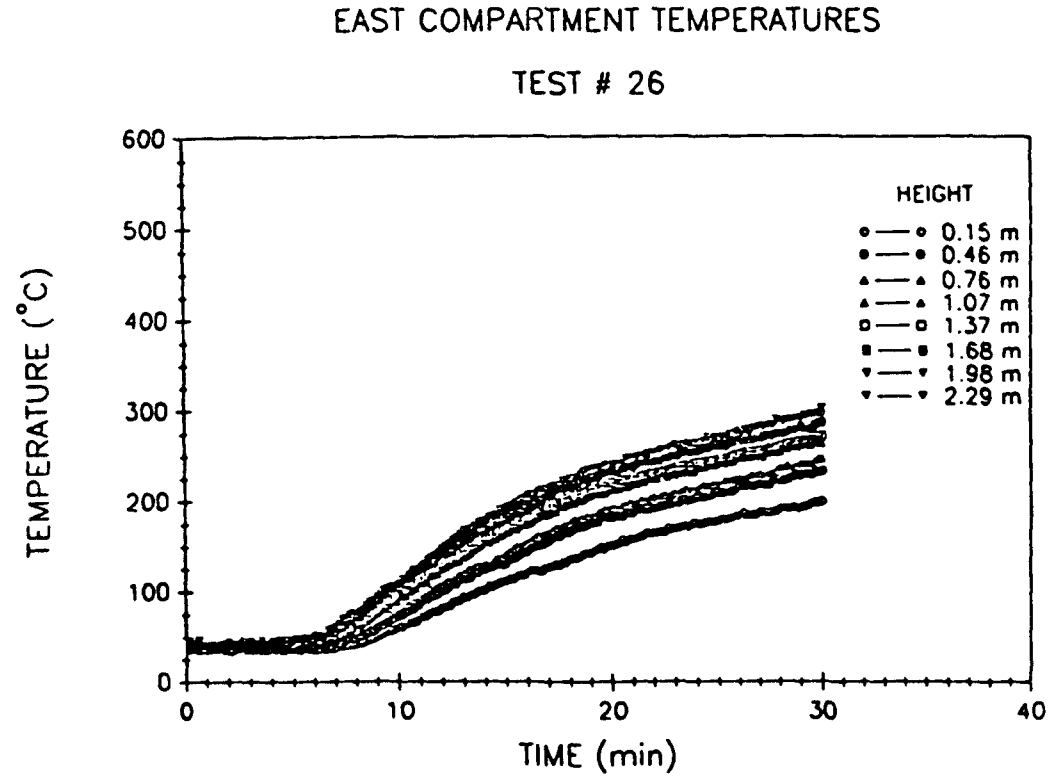

Fig. A65 – East compartment air temperatures

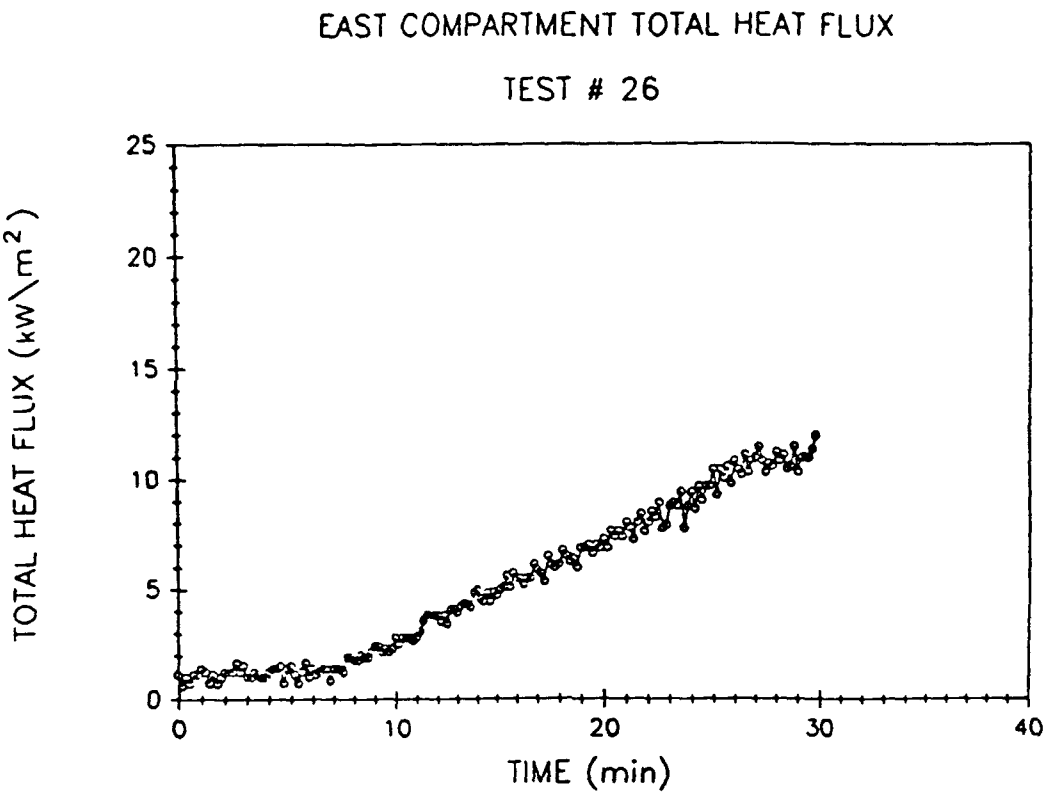

Fig. A66 – East compartment total heat flux

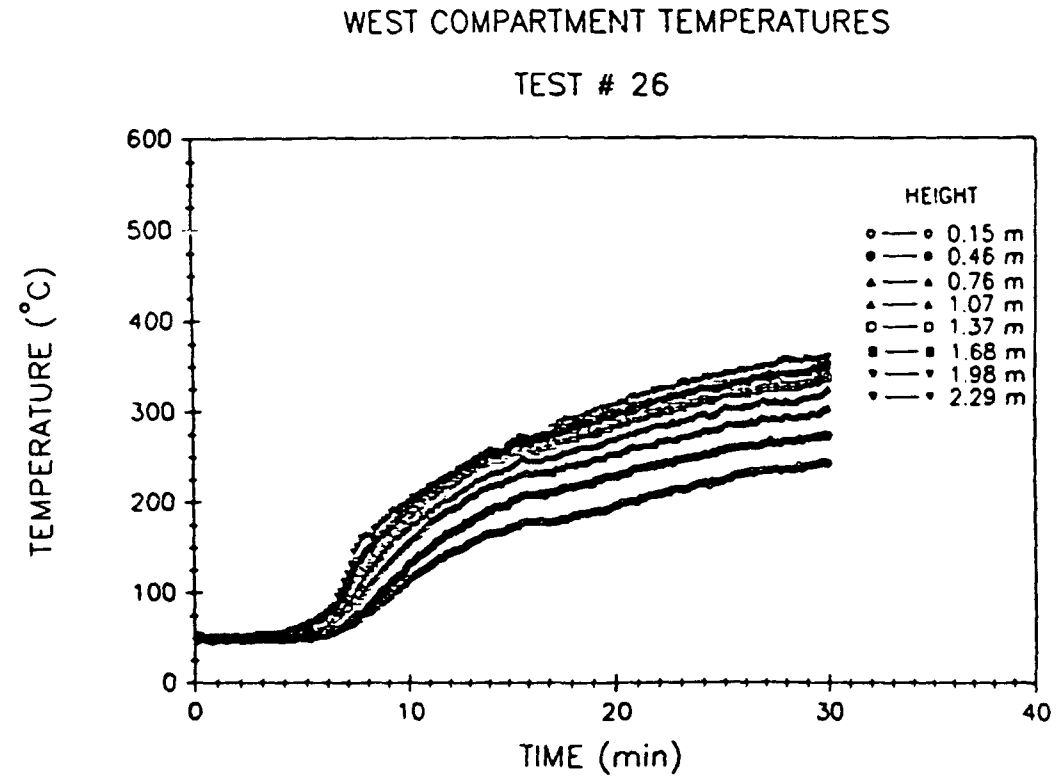

Fig. A67 – West compartment air temperatures

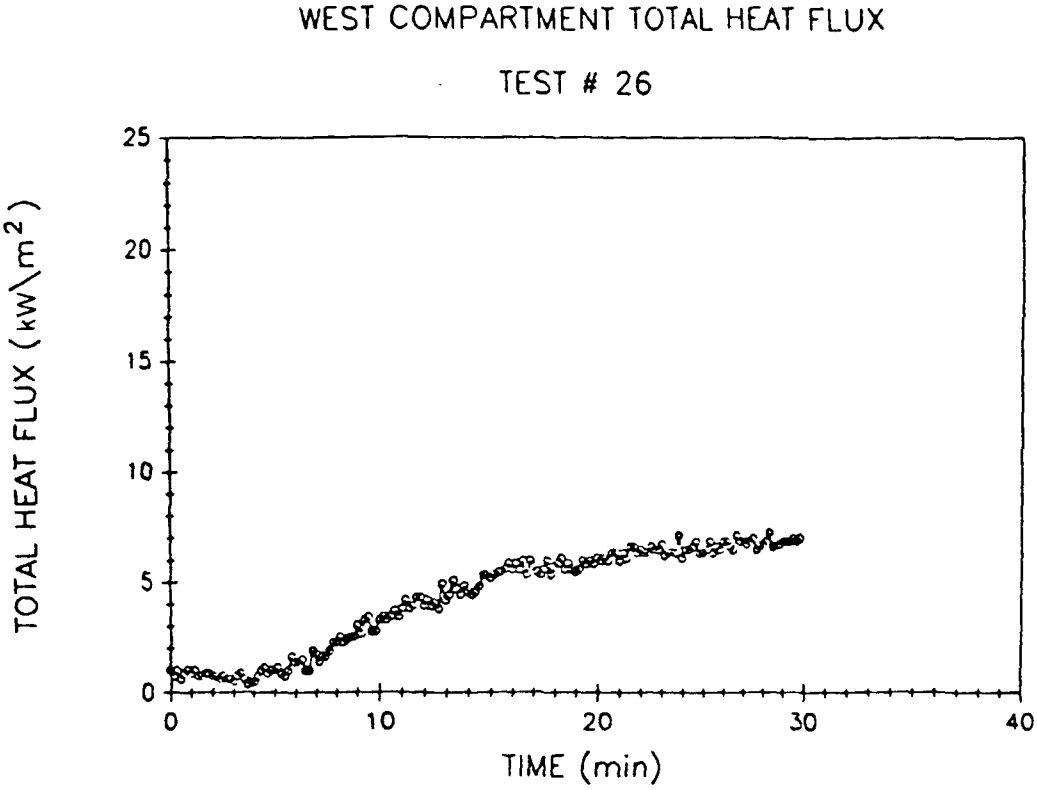

Fig. A68 – West compartment total heat flux

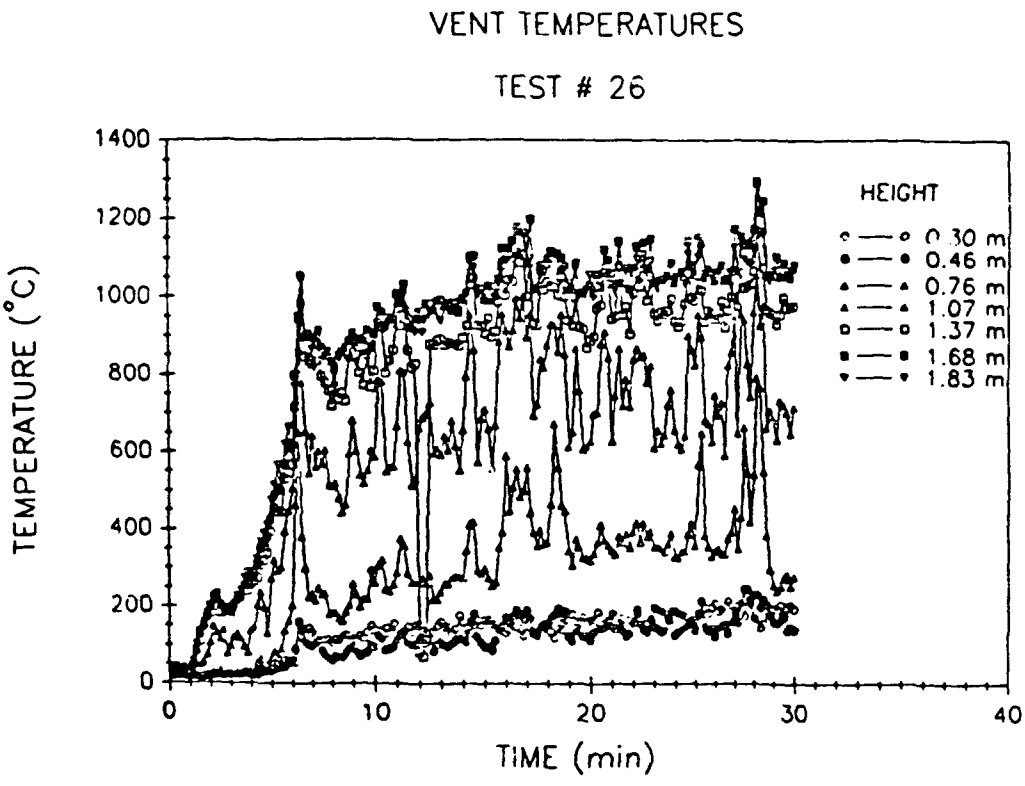

Fig. A69 – Vent air temperatures

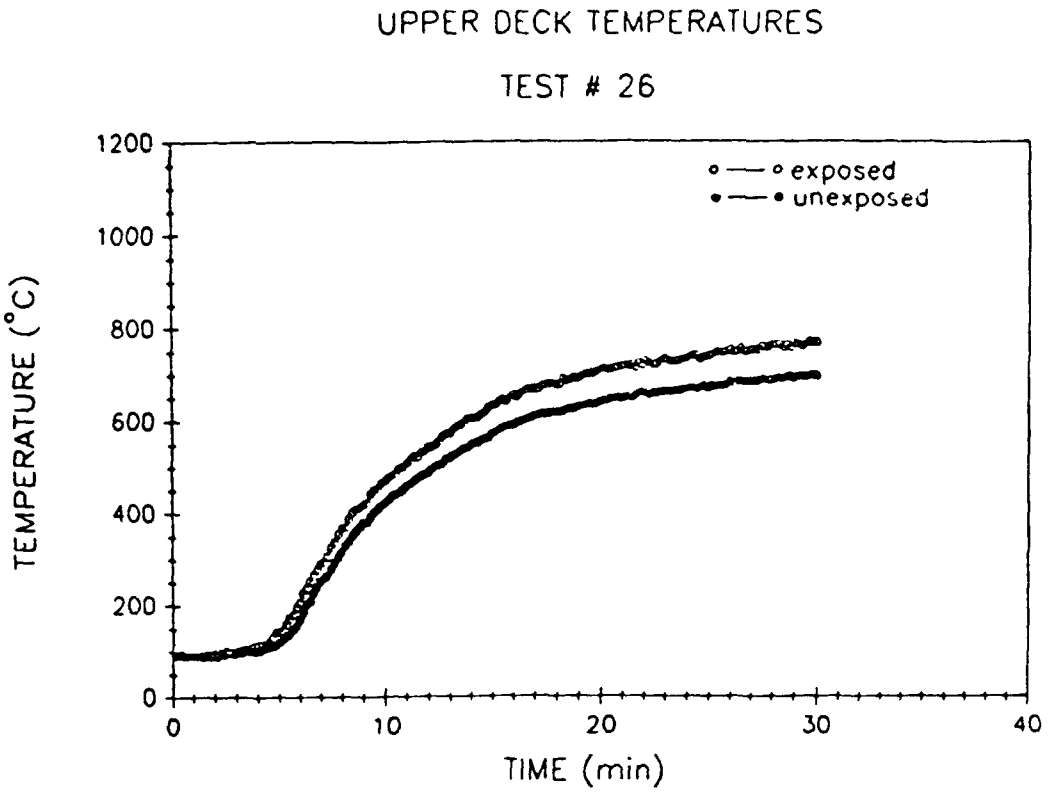

Fig. A70 – Upper deck surface temperatures

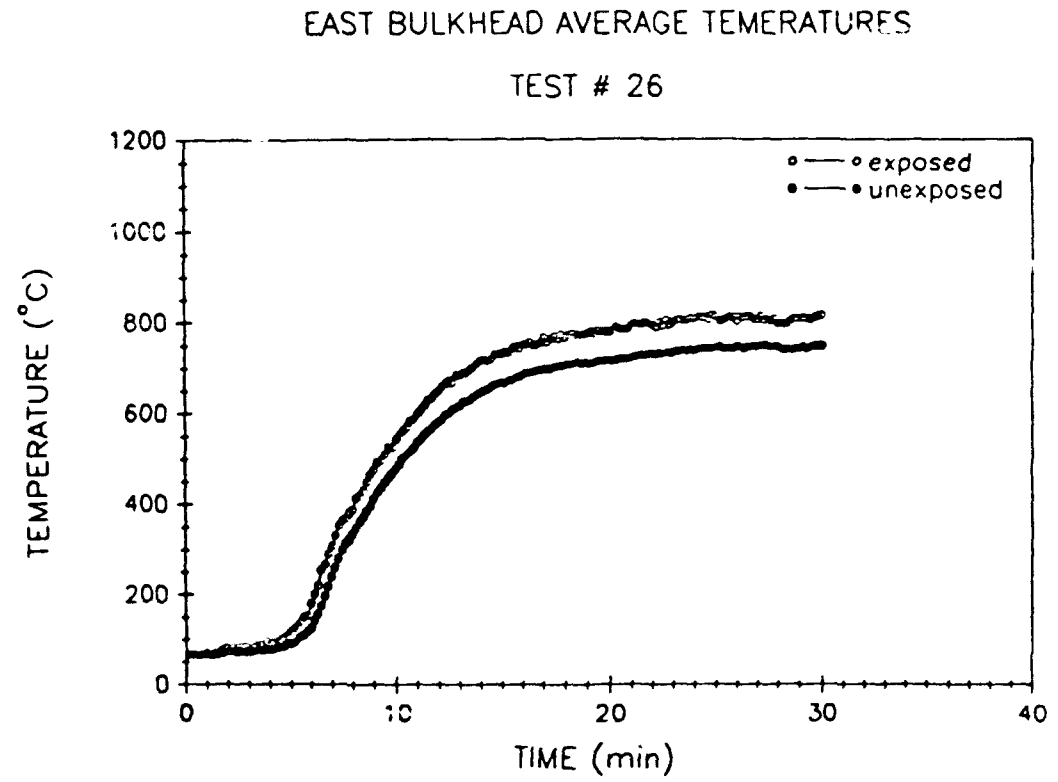

Fig. A71 – East bulkhead average surface temperatures

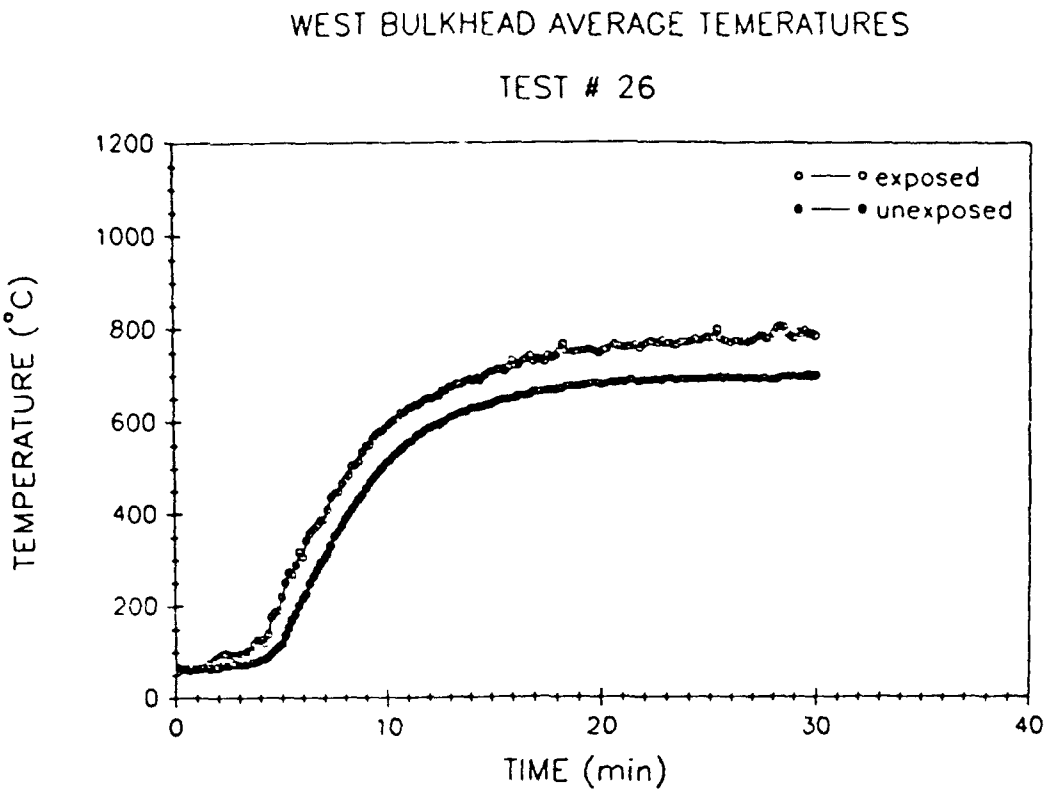

Fig. A72 – West bulkhead average surface temperatures

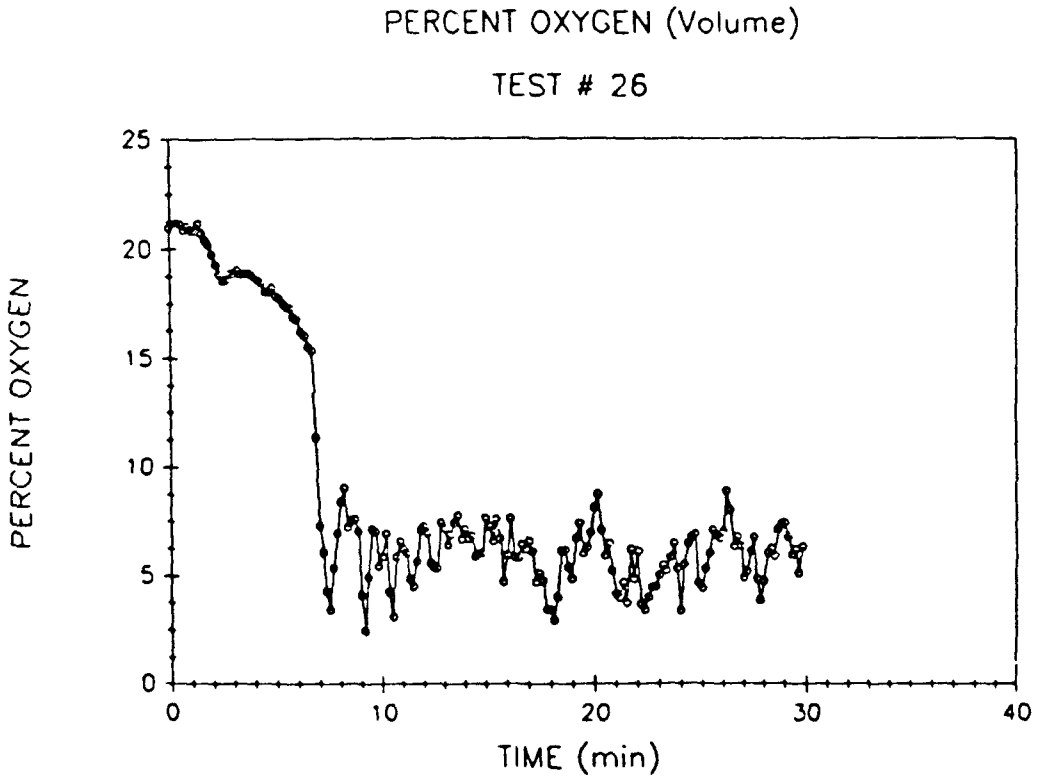

Fig. A73 – Percent oxygen (volume)

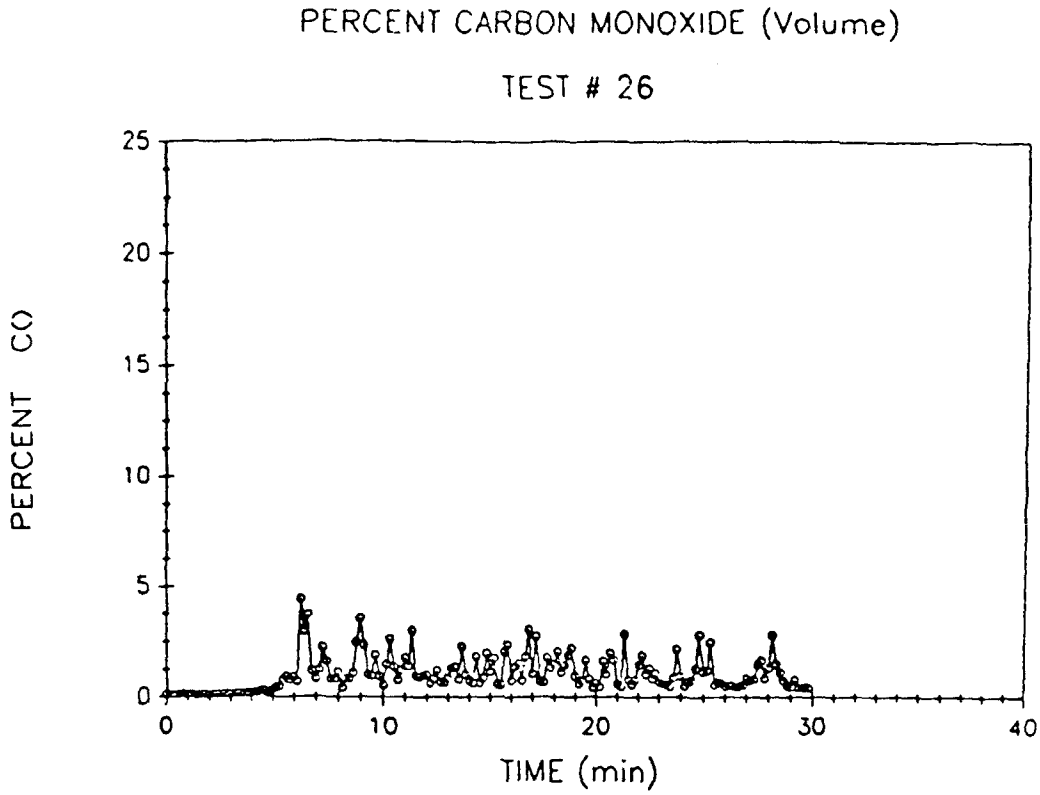

Fig. A74 – Percent carbon monoxide (volume)

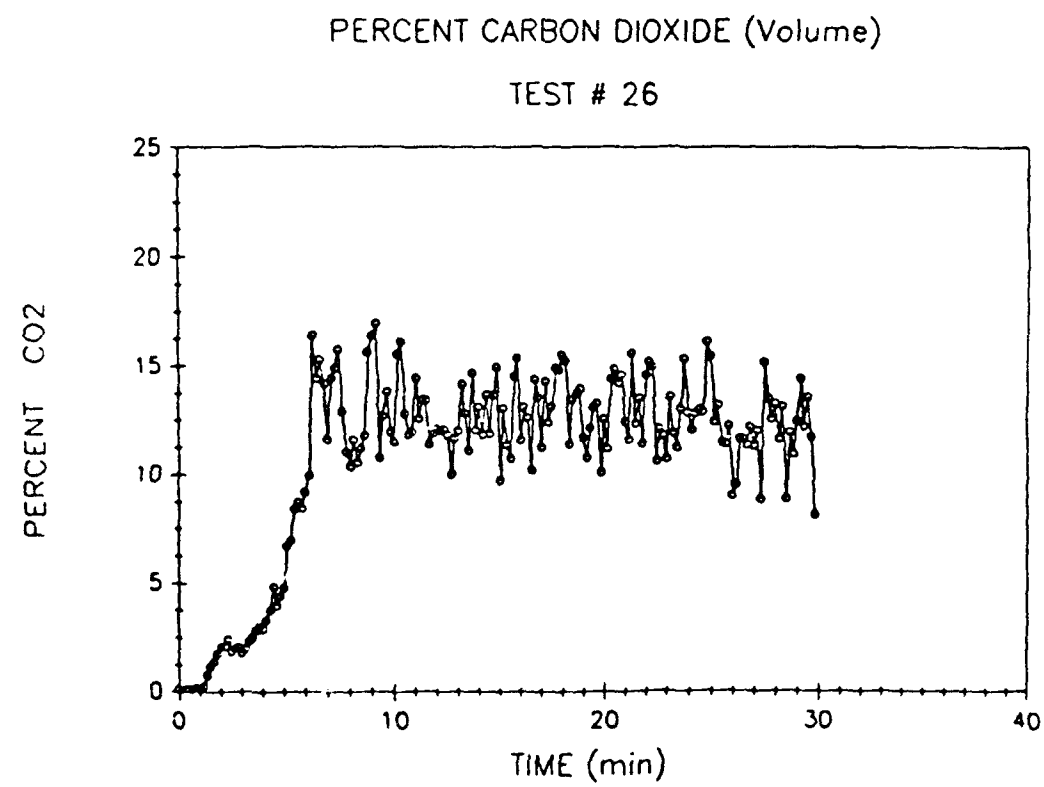

Fig. A75 – Percent carbon dioxide (volume)

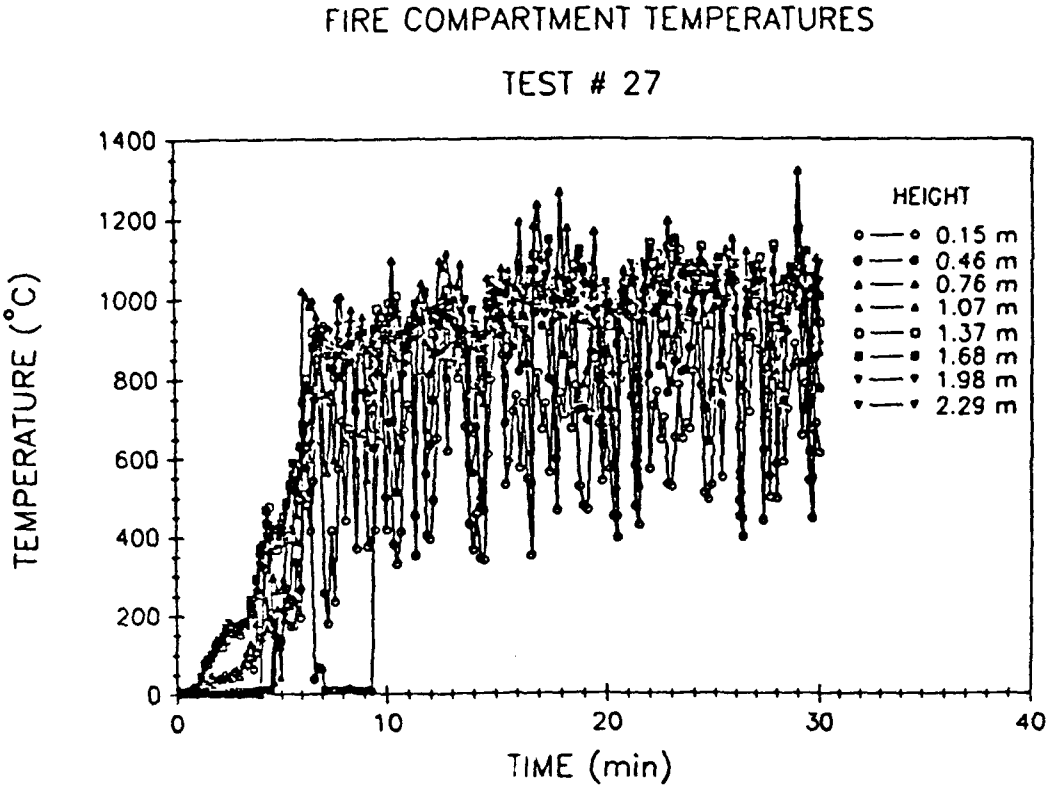

Fig. A76 – Fire comparment air temperatures

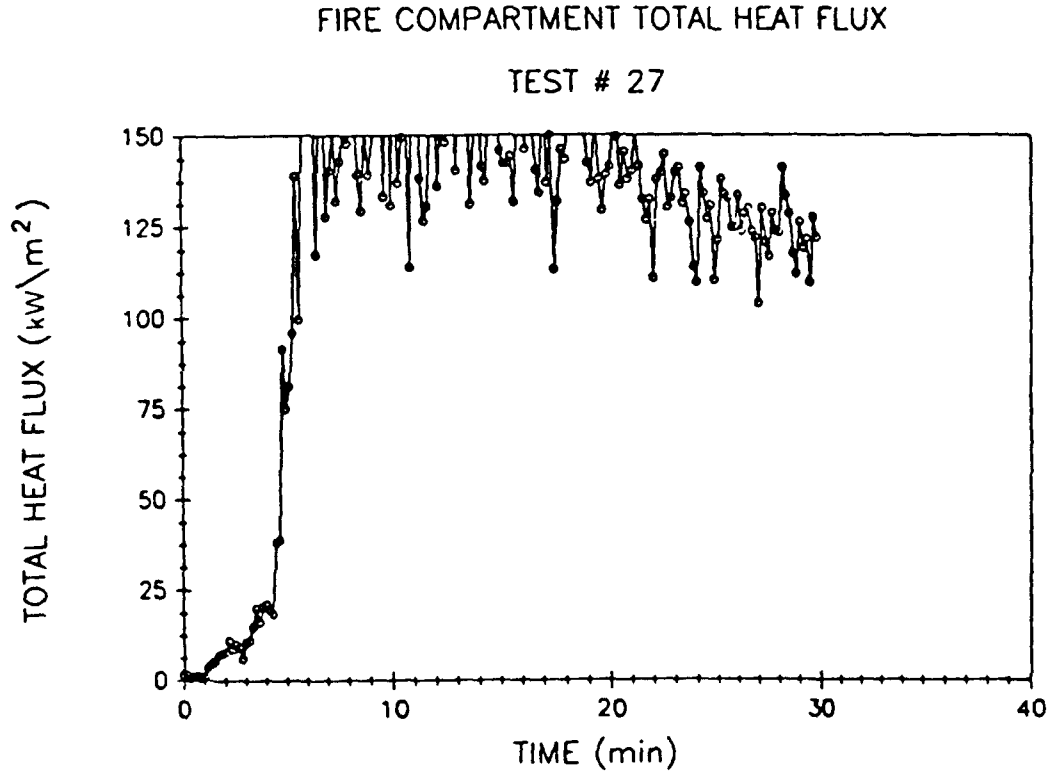

Fig. A77 – Fire compartment total heat flux

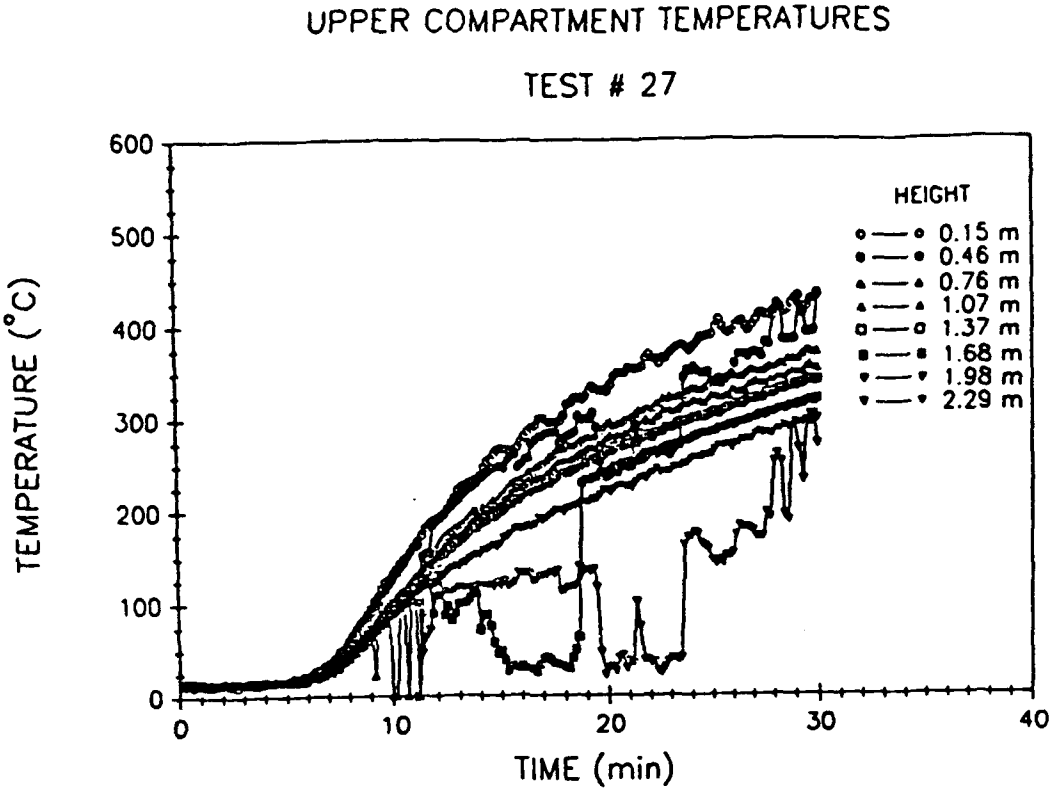

Fig. A78 – Upper compartment air temperatures

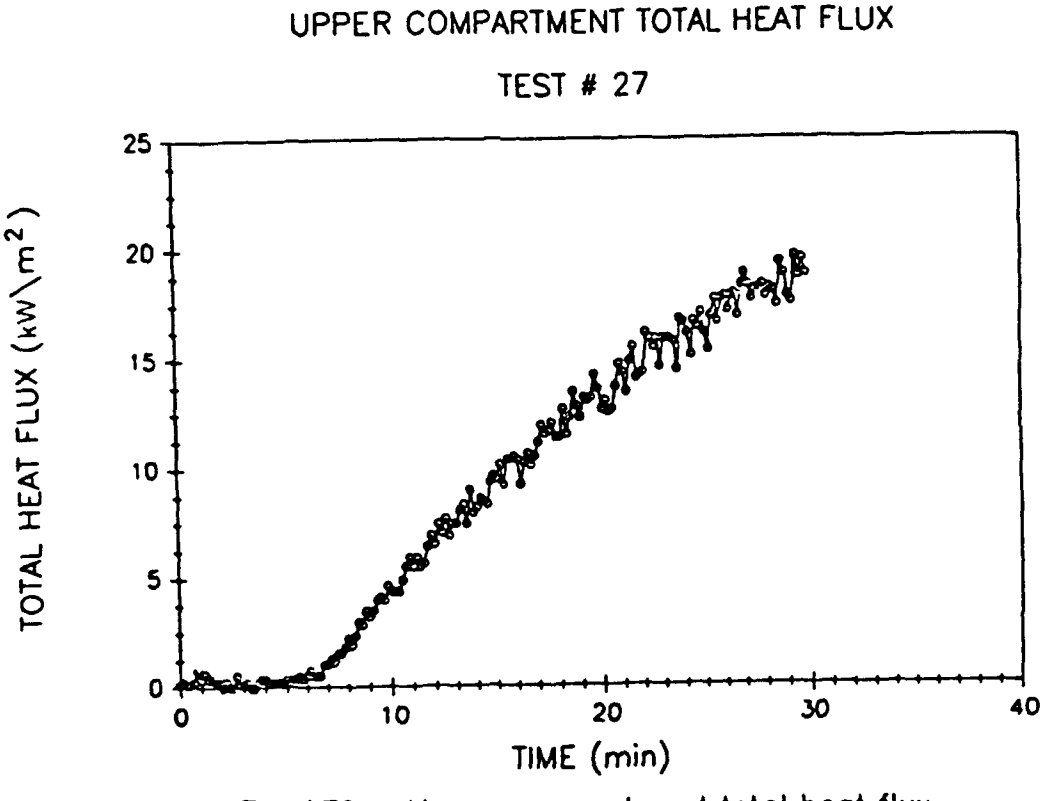

Fig. A79 – Upper compartment total heat flux

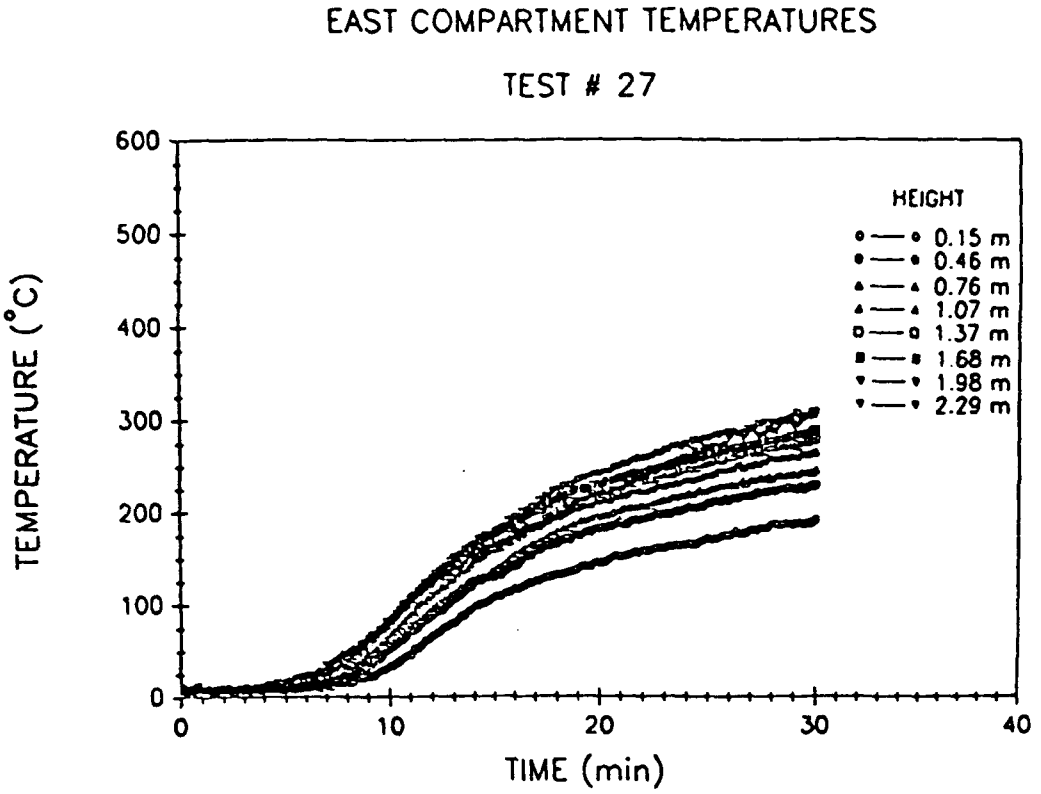

Fig. A80 – East compartment air temperatures

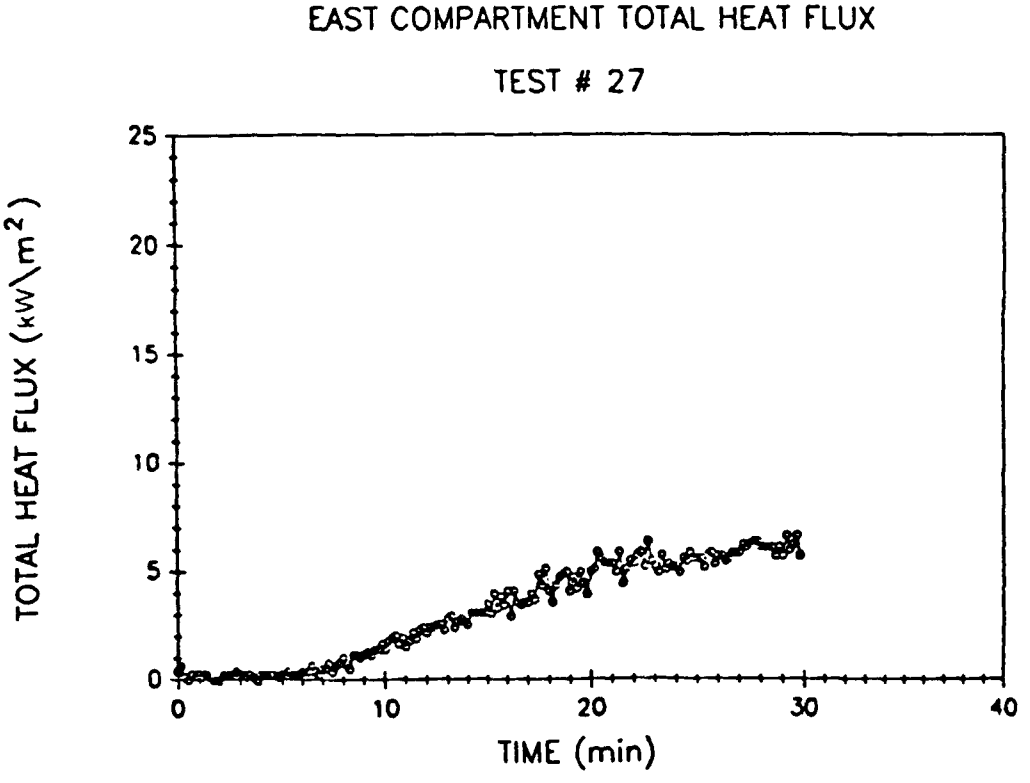

Fig. A81 – East compartment total heat flux

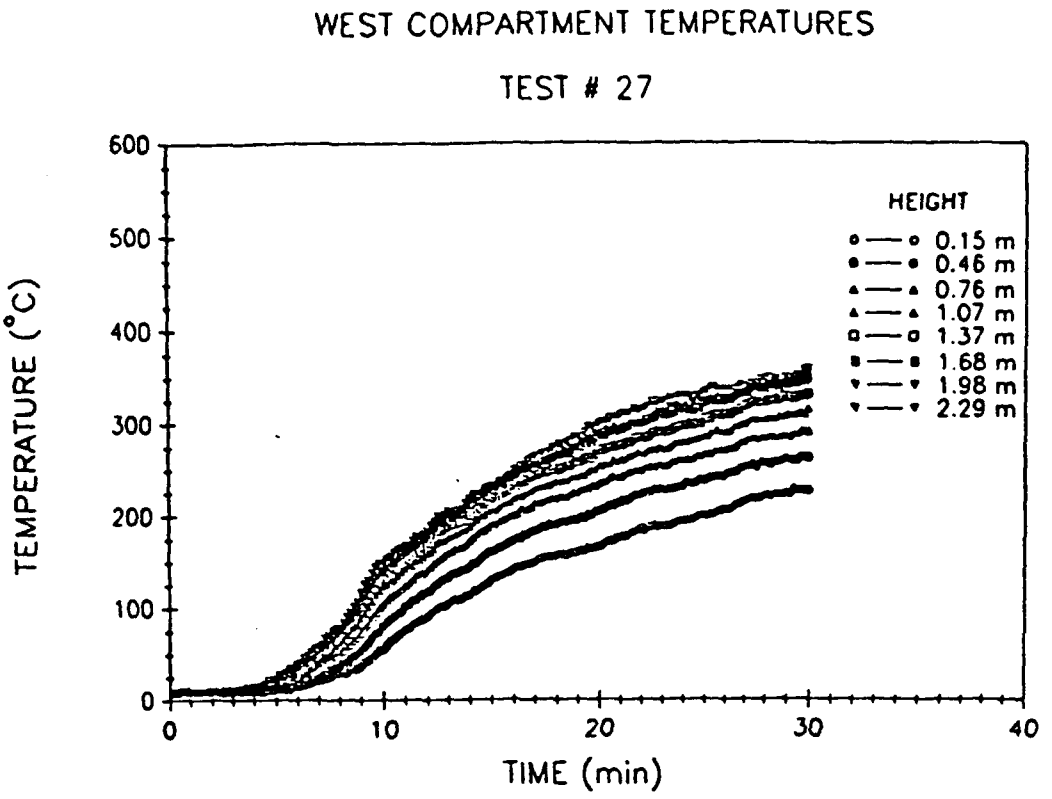

Fig. A82 – West compartment air temperatures

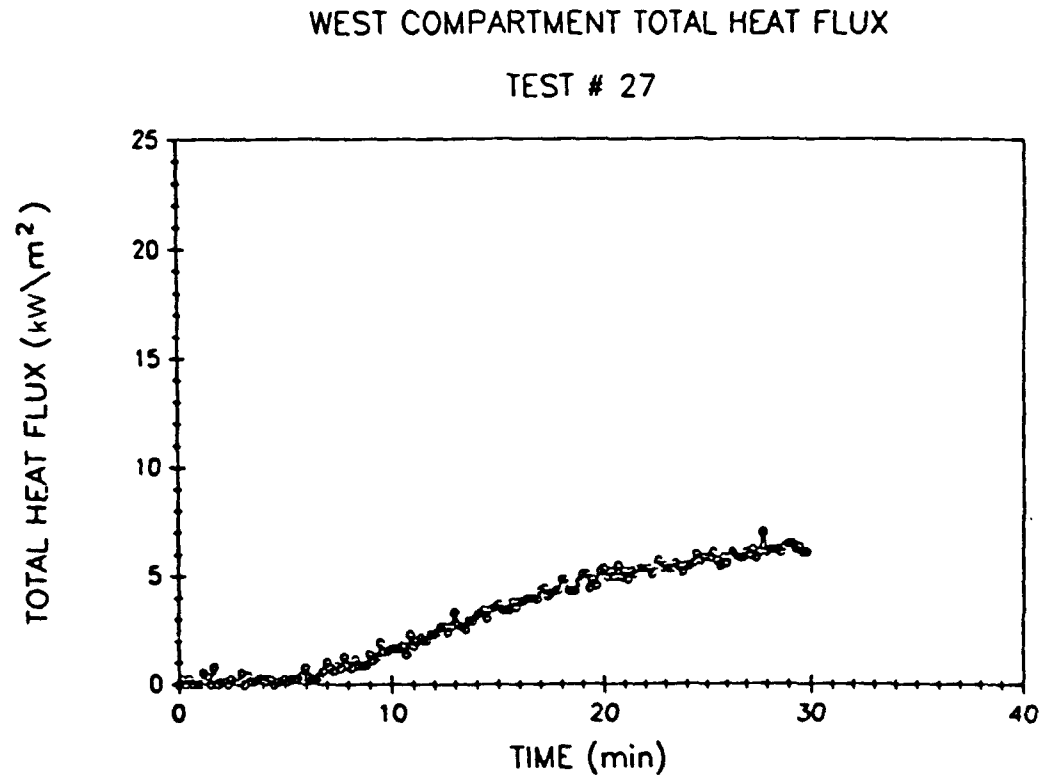

Fig. A83 – West compartment total heat flux

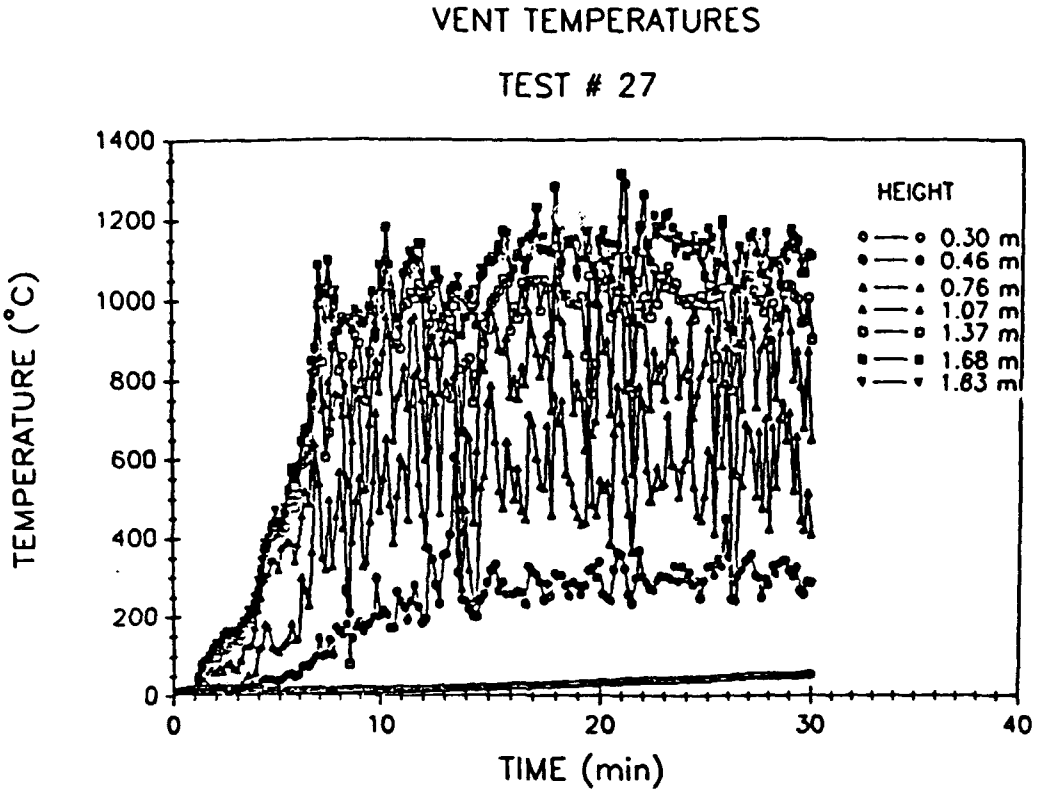

Fig. A84 – Vent air temperatures

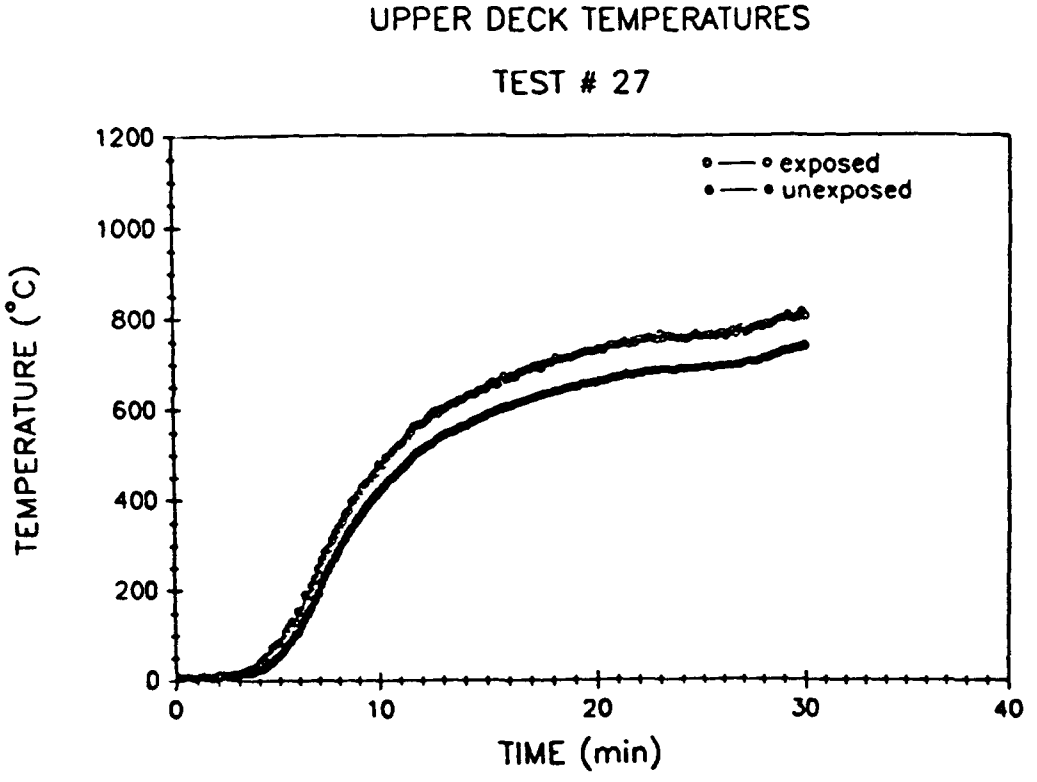

Fig. A85 – Upper deck surface temperatures

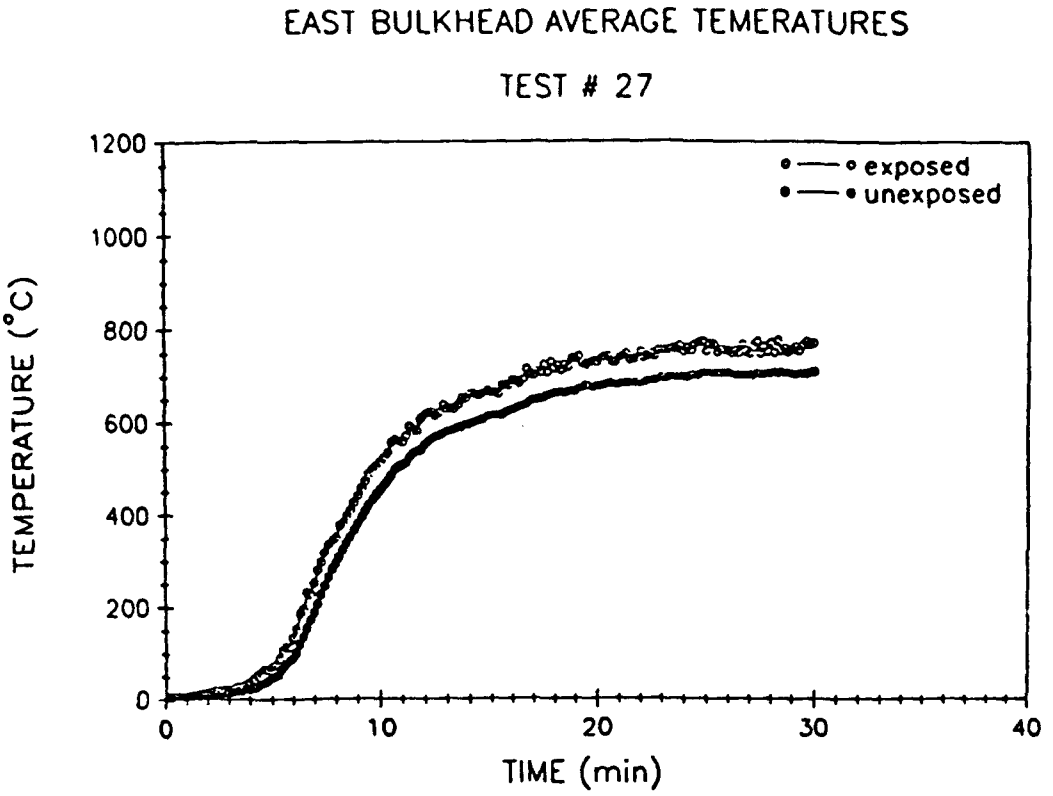

Fig. A86 – East bulkhead average surface temperatures

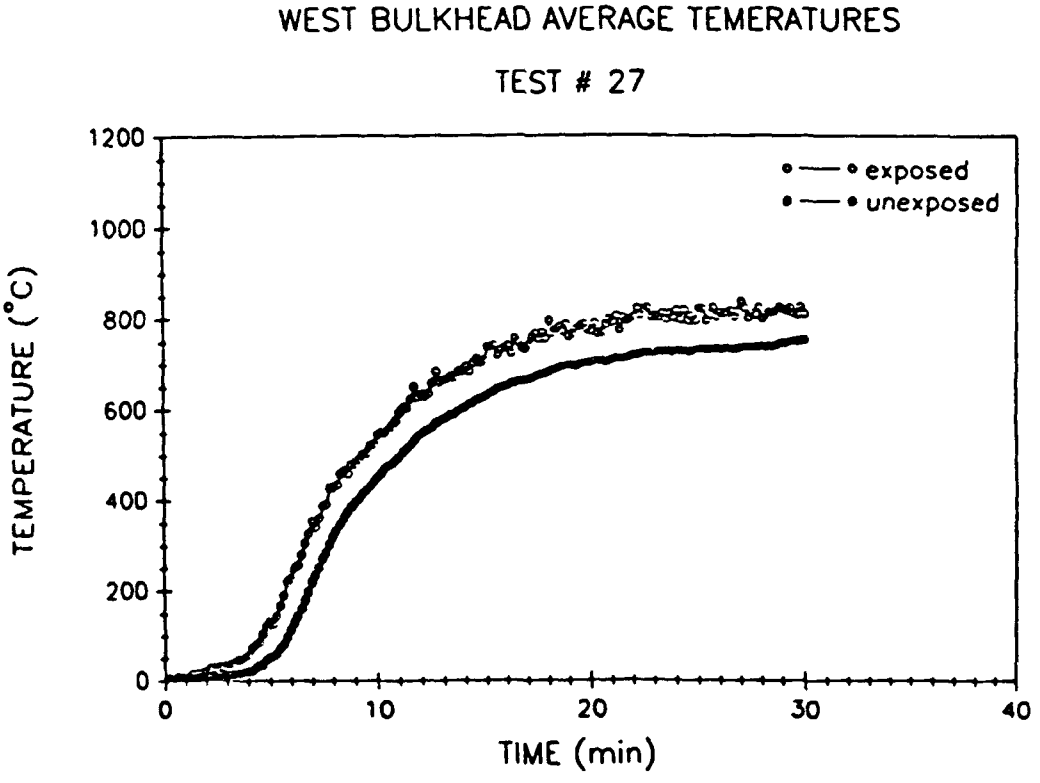

Fig. A87 – West bulkhead average surface temperatures

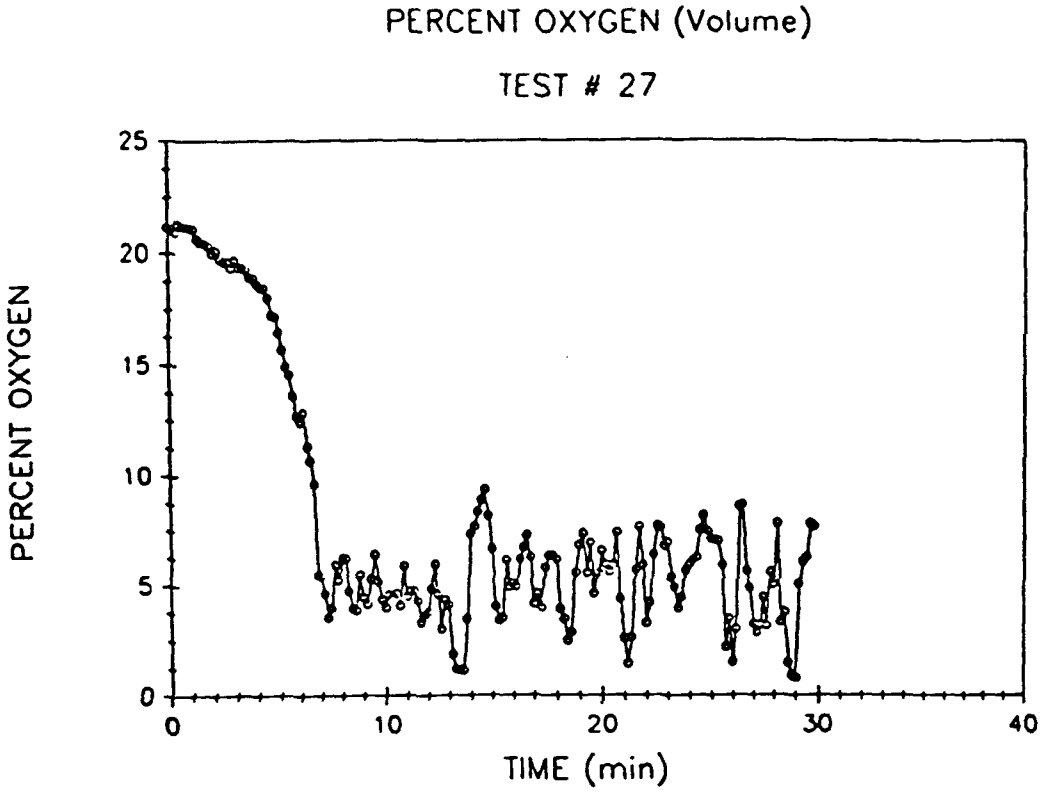

Fig. A88 – Percent oxygen (volume)

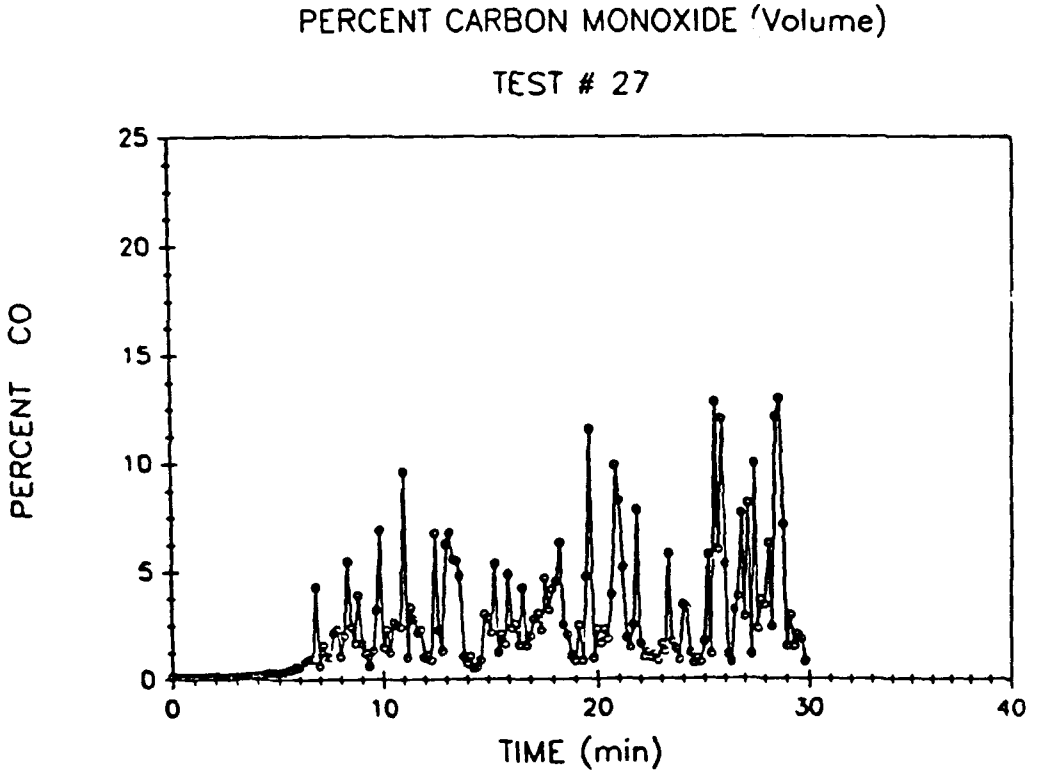

Fig. A89 – Percent carbon monoxide (volume)

PERCENT CARBON DIOXIDE (Volume)

TEST # 27

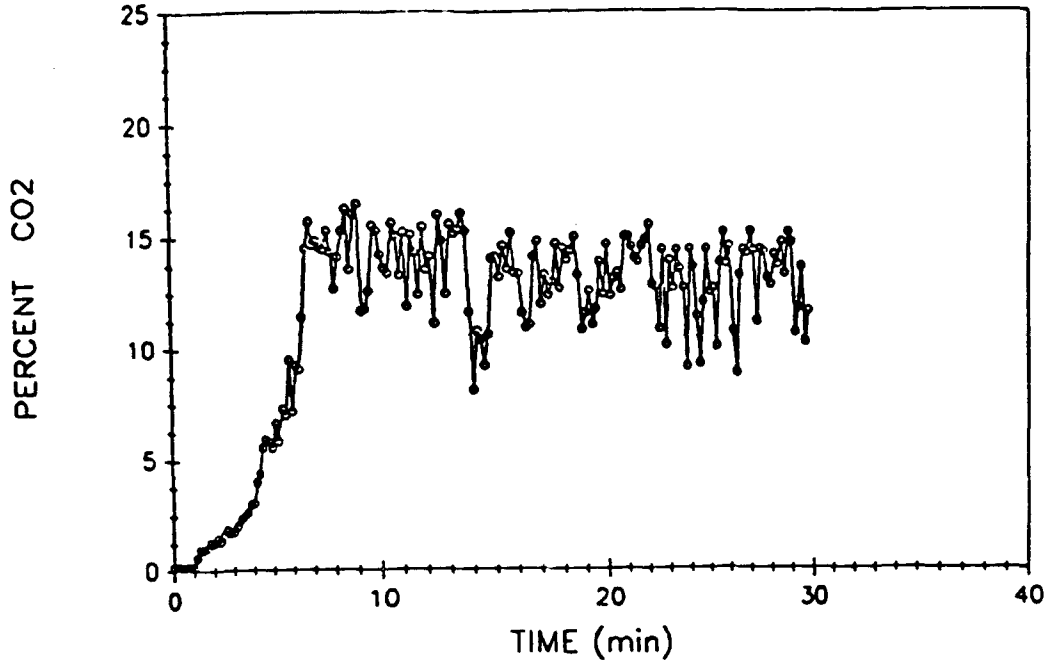

Fig. A90 – Percent carbon dioxide (volume)

FIRE COMPARTMENT TEMPERATURES

TEST # 28

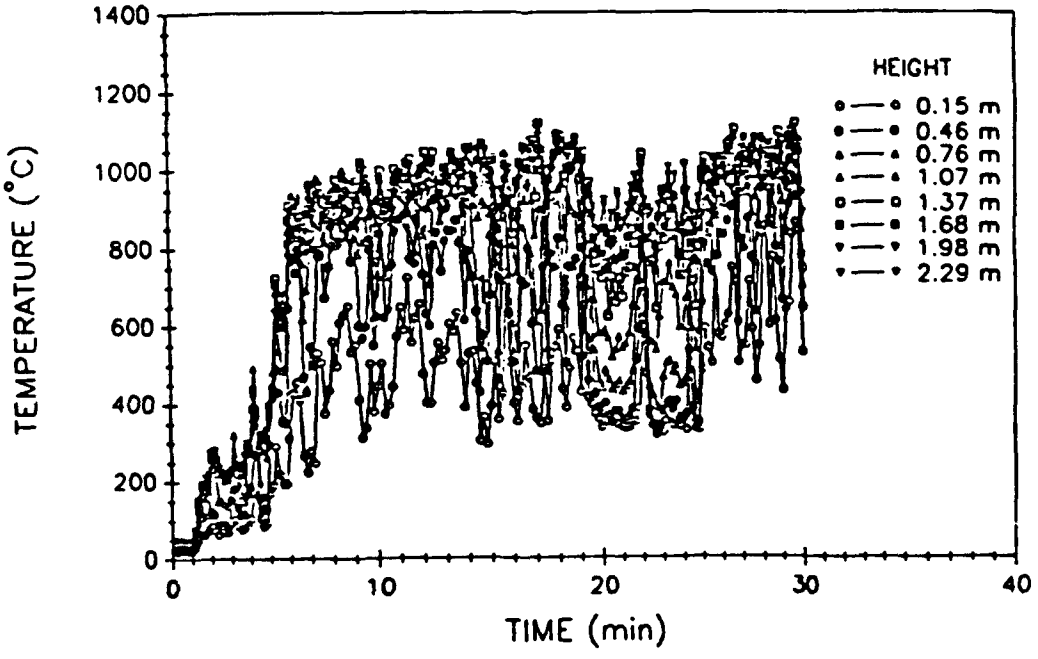

Fig. A91 – Fire comparment oir temperatures

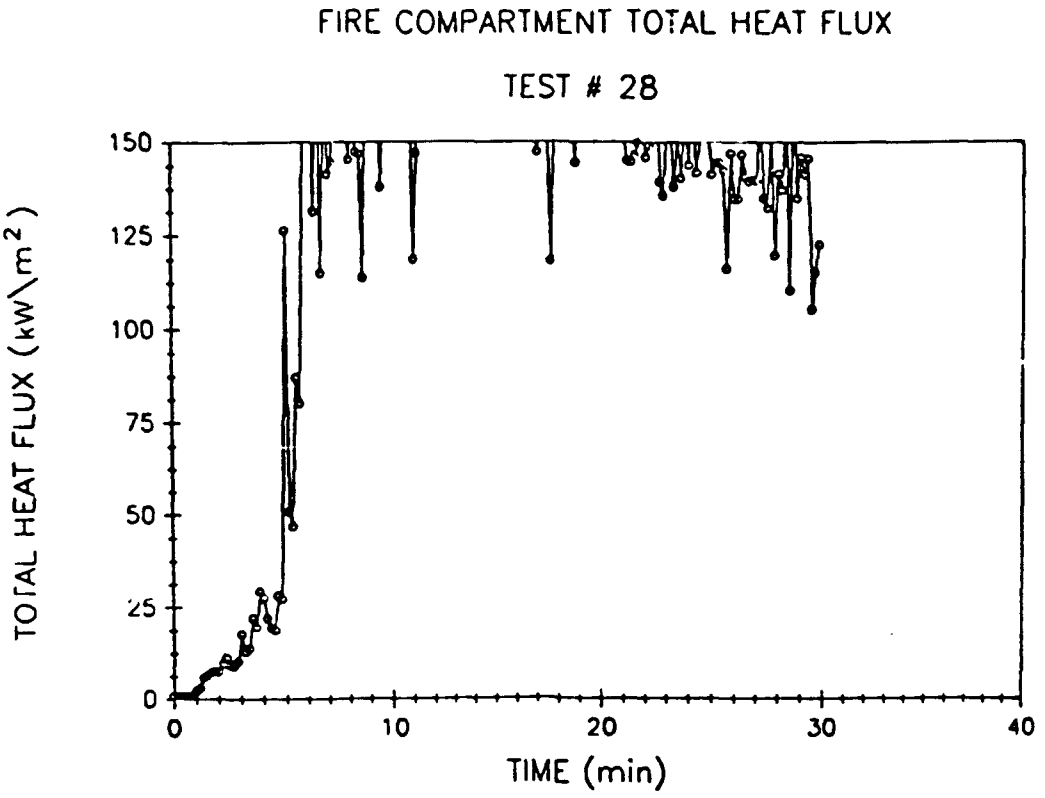

Fig. A92 – Fire compartment total heat flux

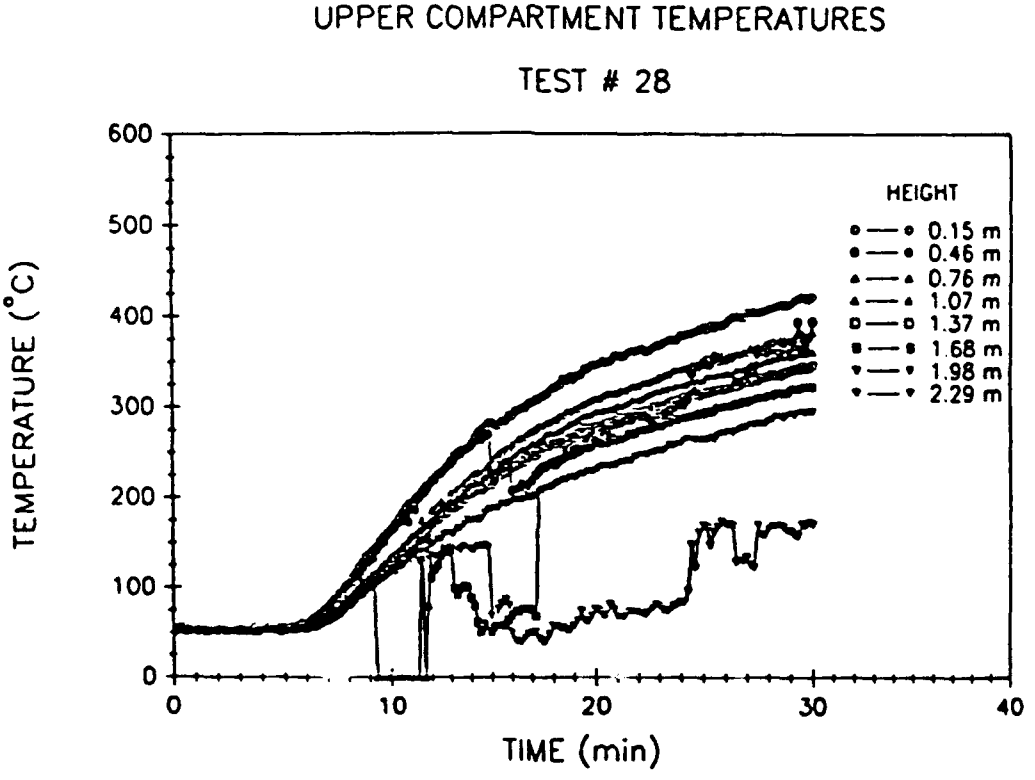

Fig. A93 – Upper compartment air temperatures

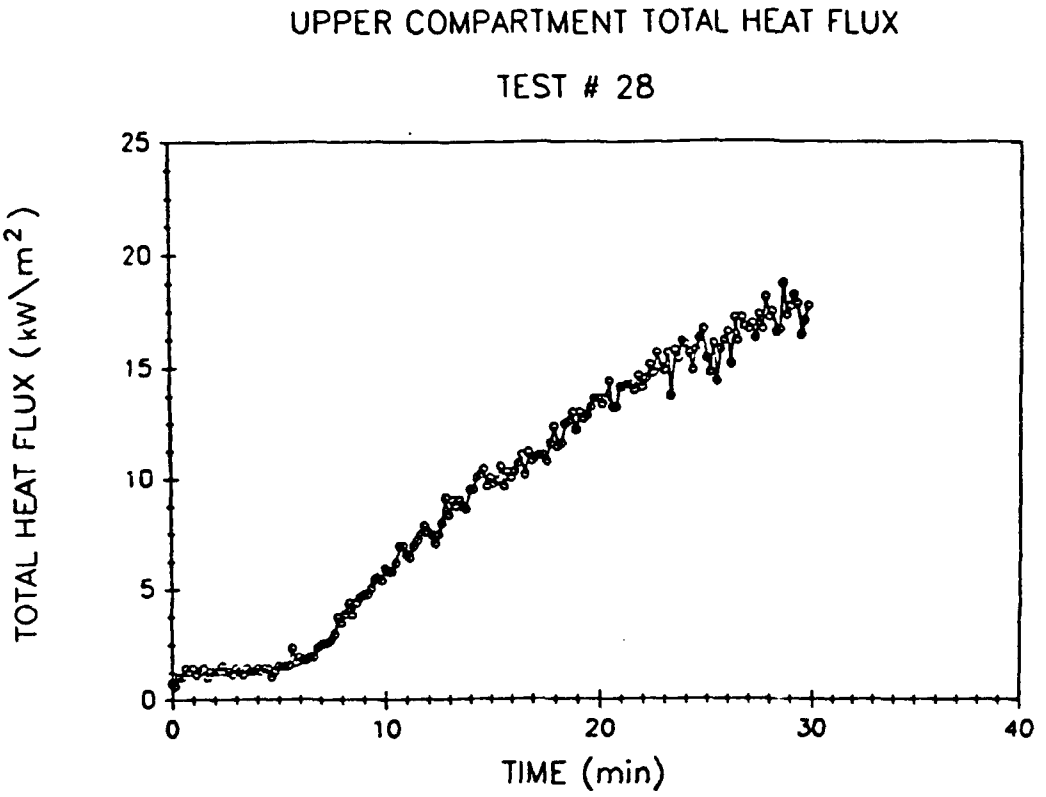

Fig. A94 – Upper compartment total heat flux

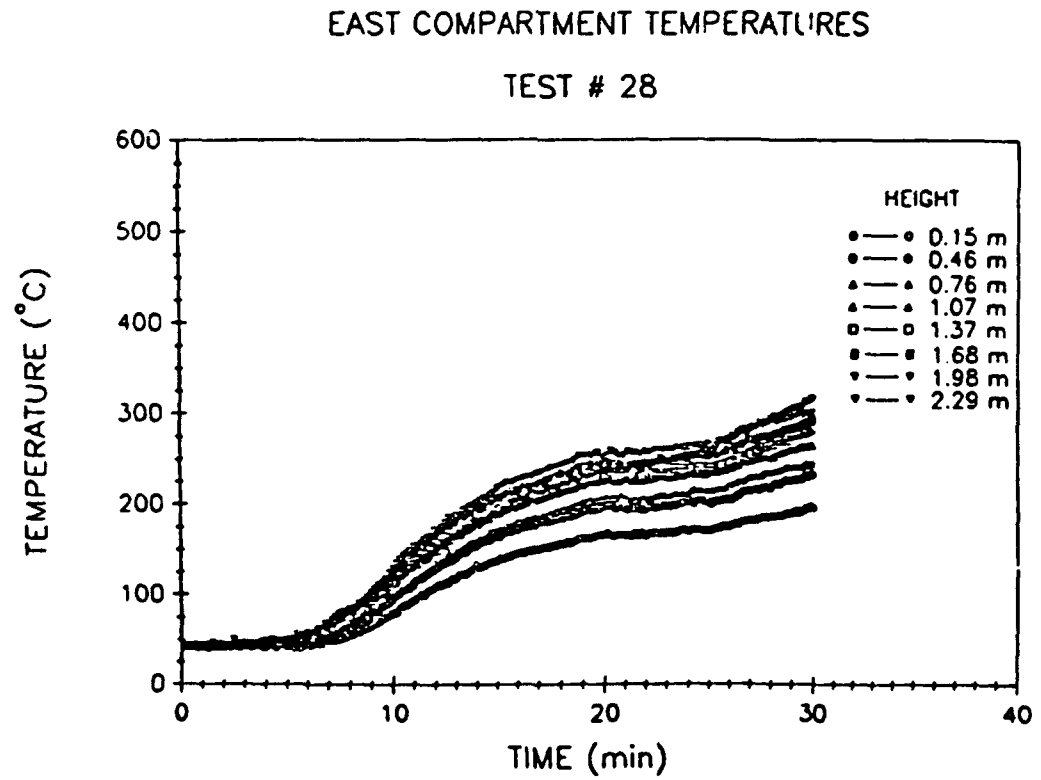

Fig. A95 – East compartment air temperatures

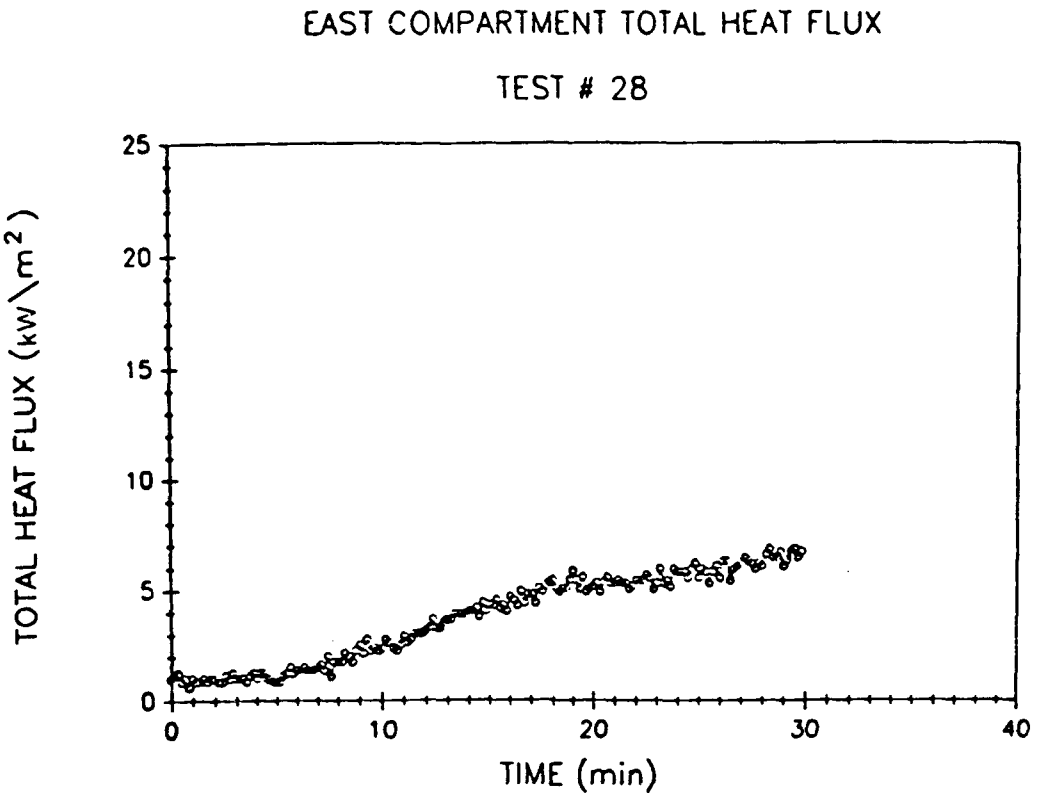

Fig. A96 – East compartment total heat flux

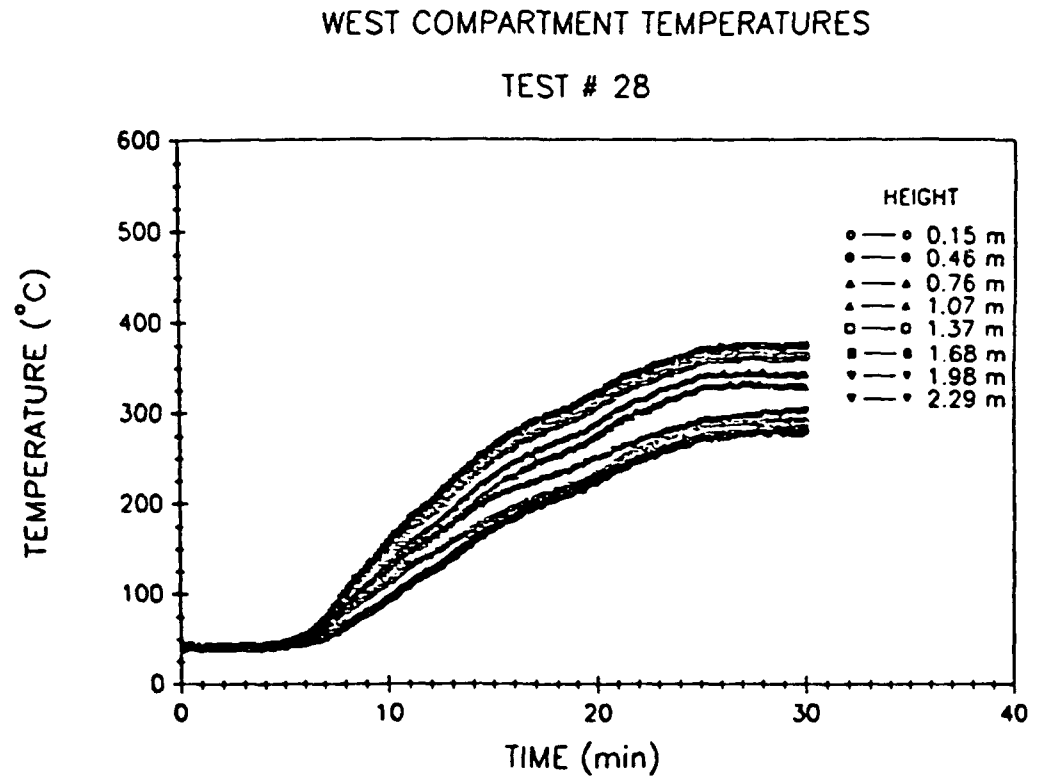

Fig. A97 – West compartment air temperatures

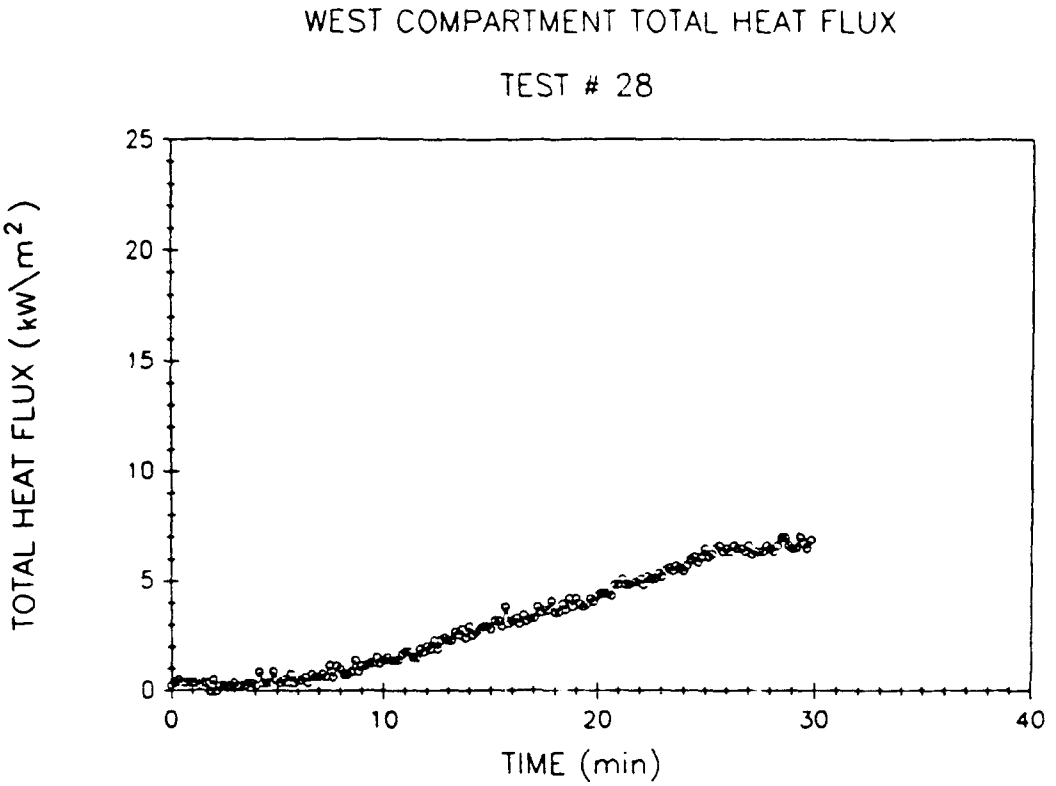

Fig. A98 – West compartment total heat flux

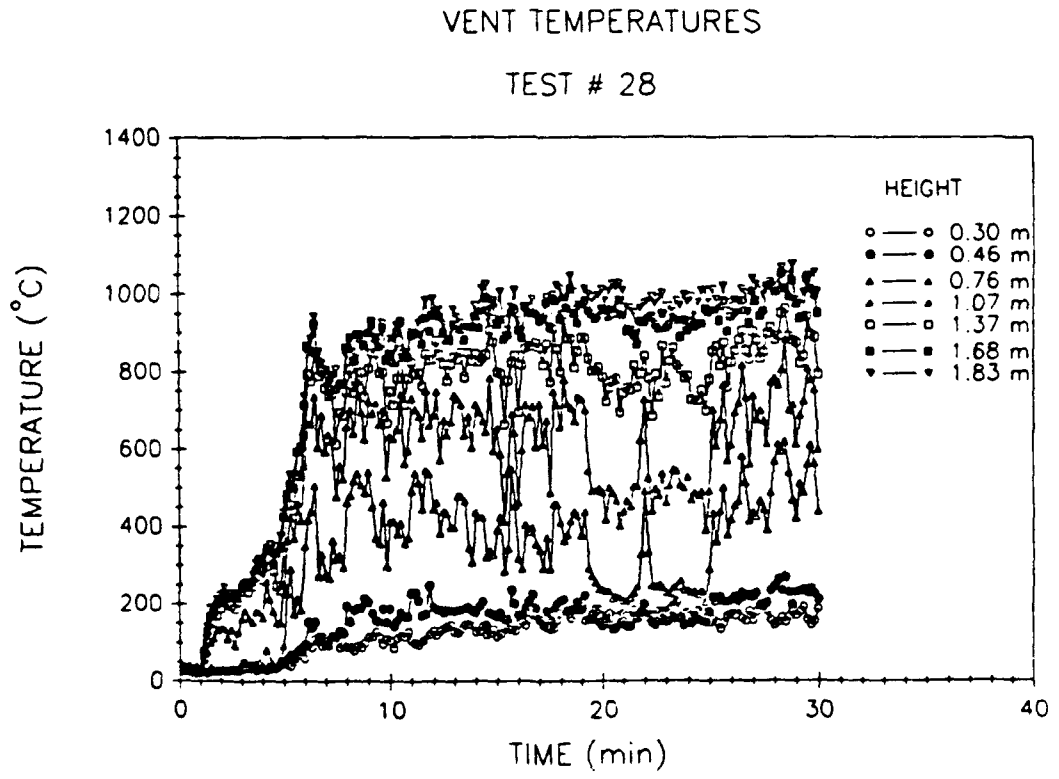

Fig. A99 – Vent air temperatures

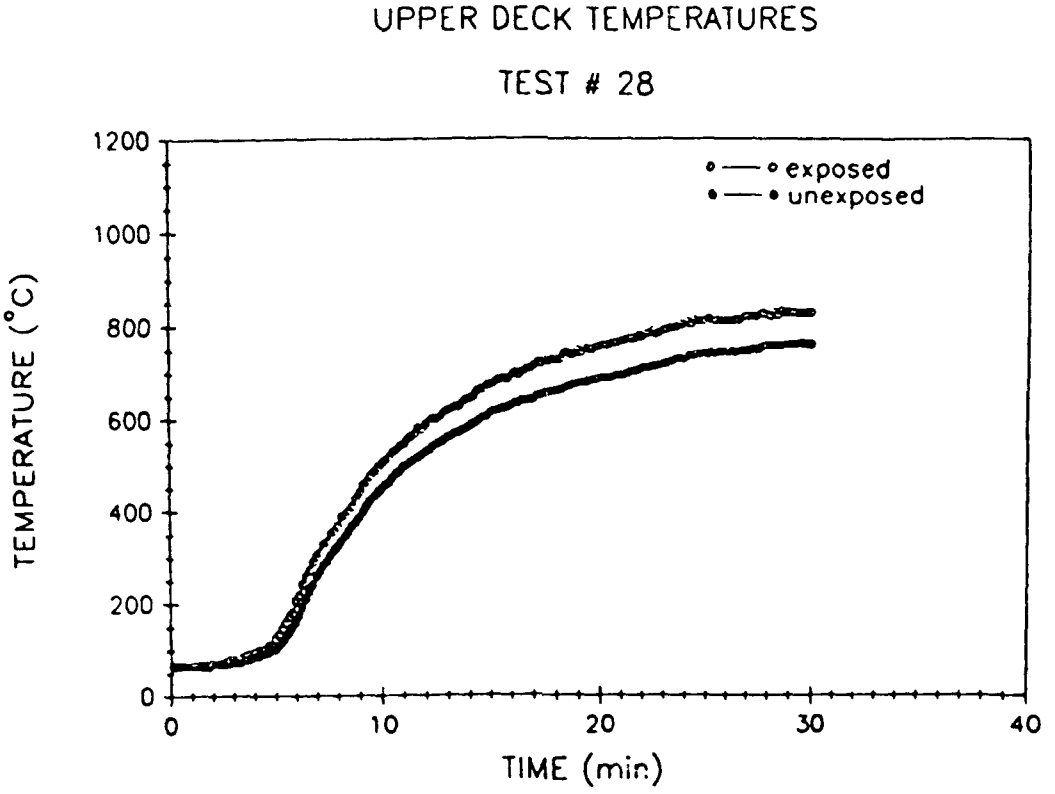

Fig. A100 – Upper deck surface temperatures

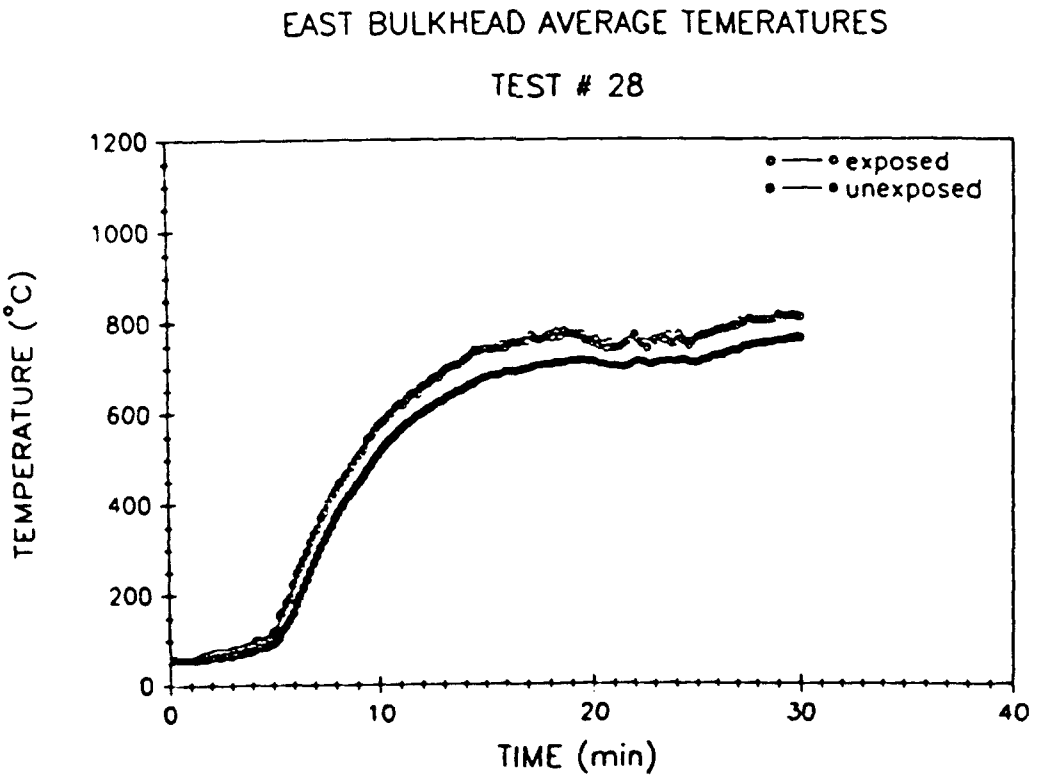

Fig. A101 – East bulkhead average surface temperatures

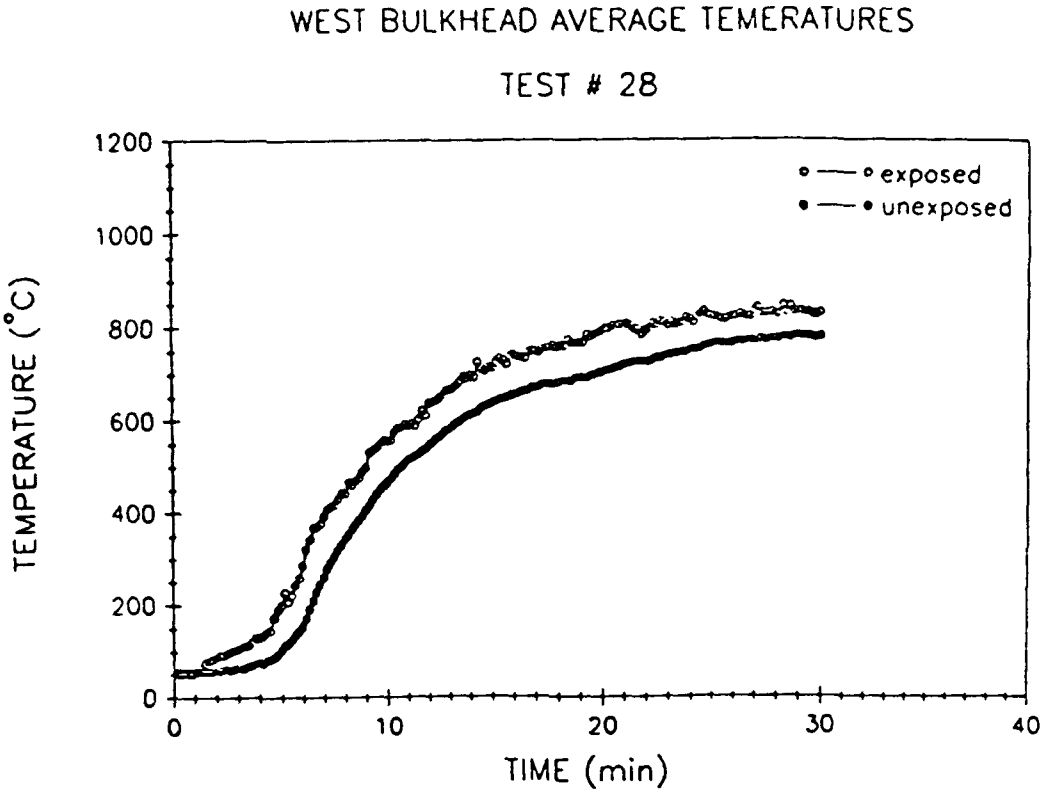

Fig. A102 – West bulkhead average surface temperatures

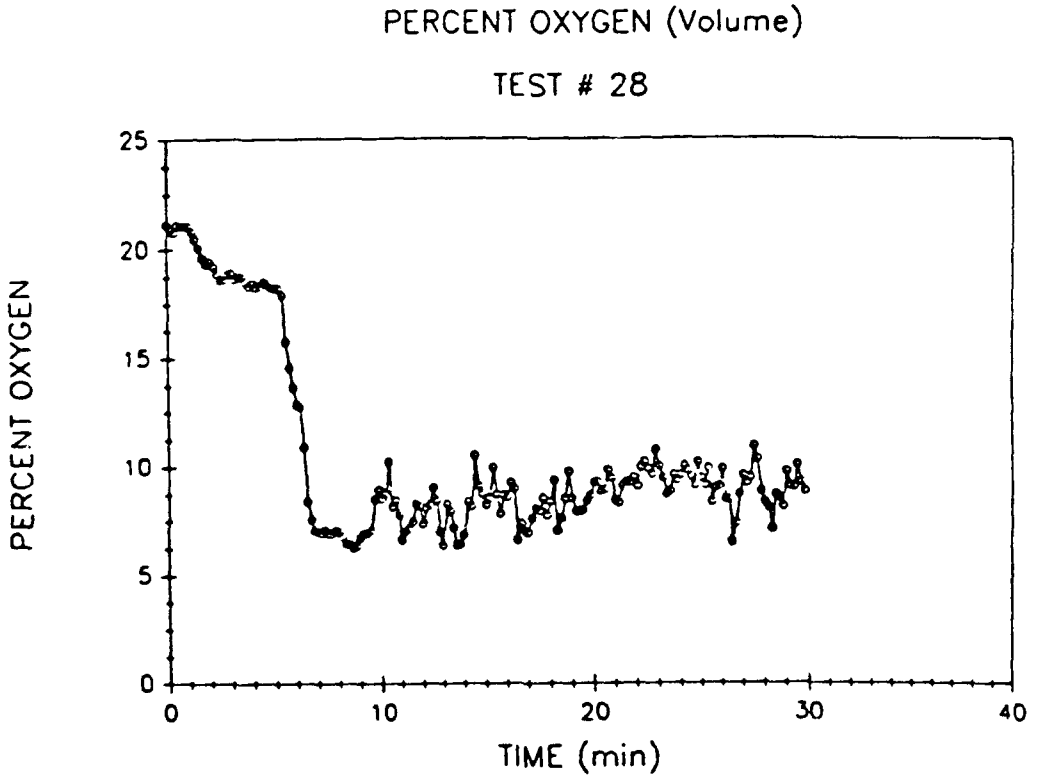

Fig. A103 – Percent oxygen (volume)

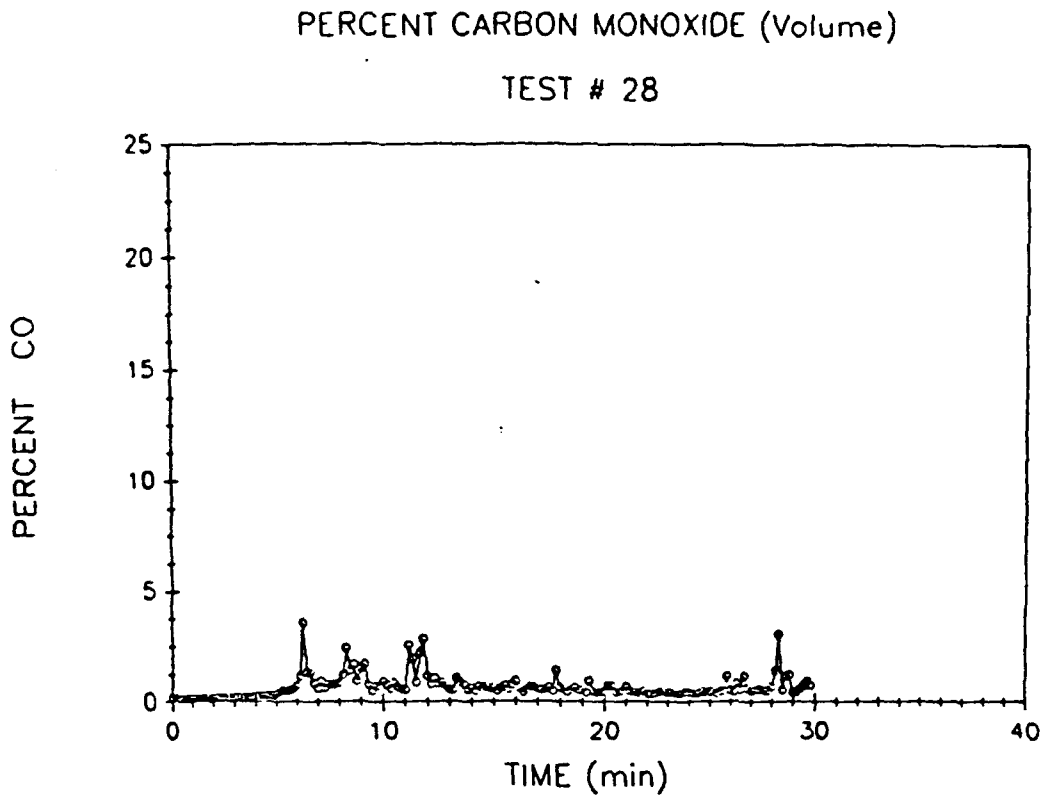

Fig. A104 – Percent carbon monoxide (volume)

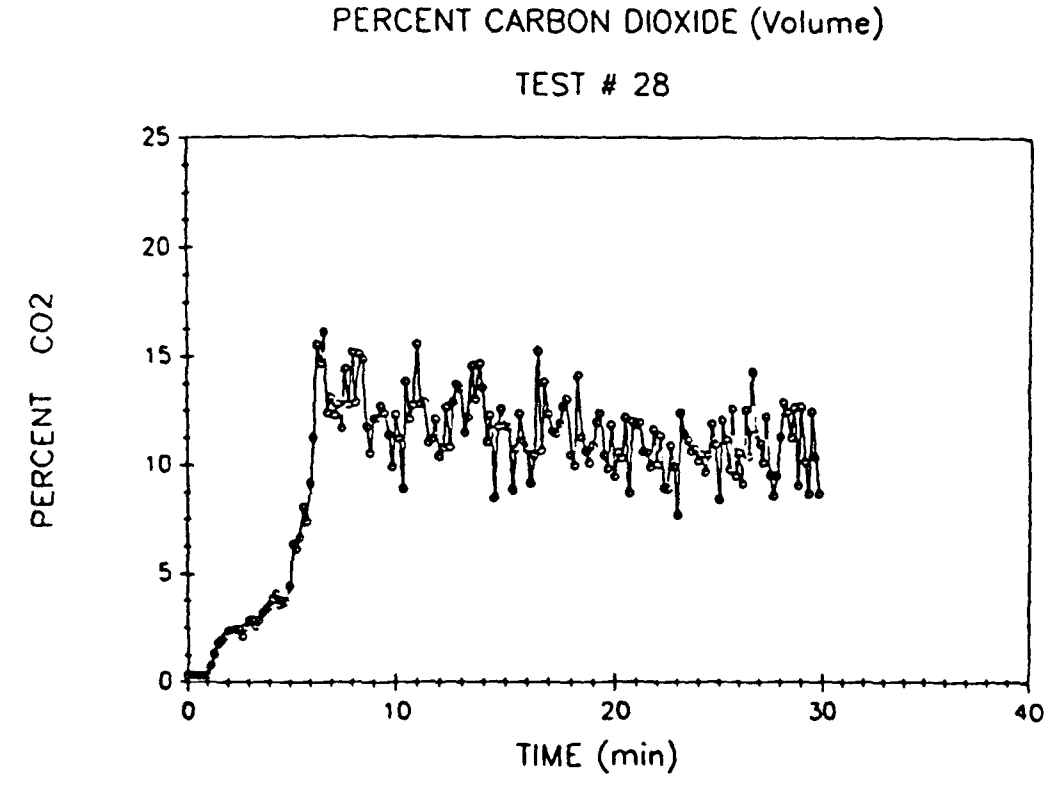

Fig. A105 – Percent carbon dioxide (volume)

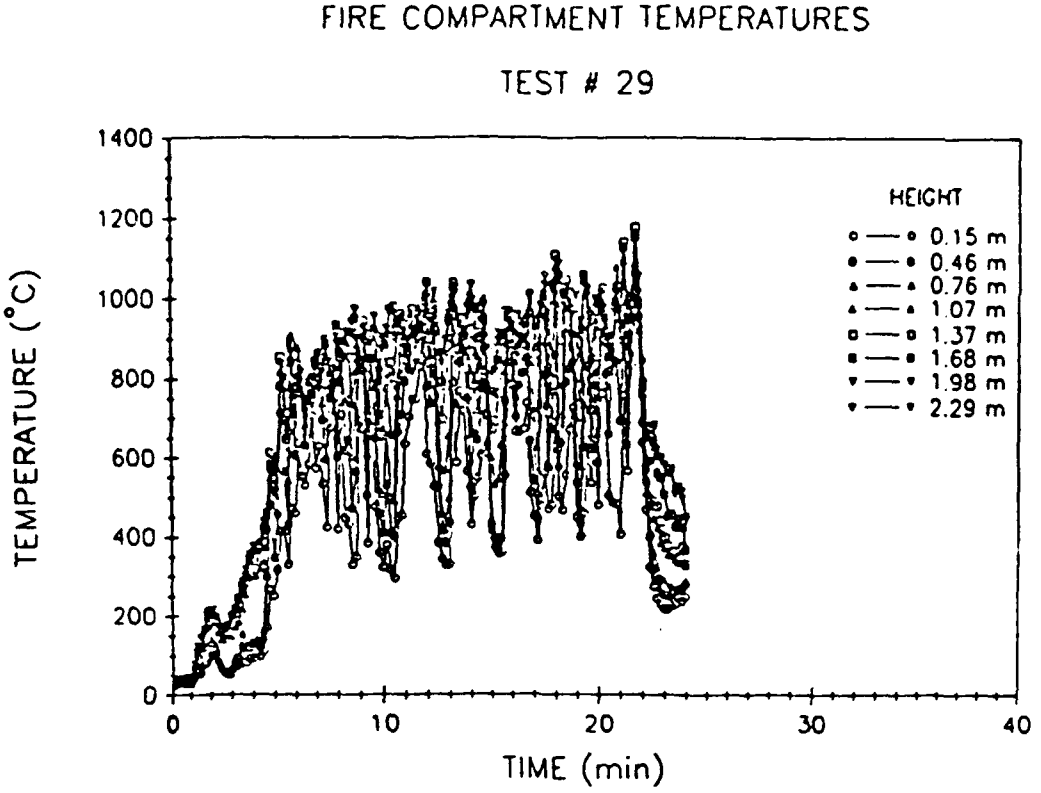

Fig. A106 – Fire comparment air temperatures

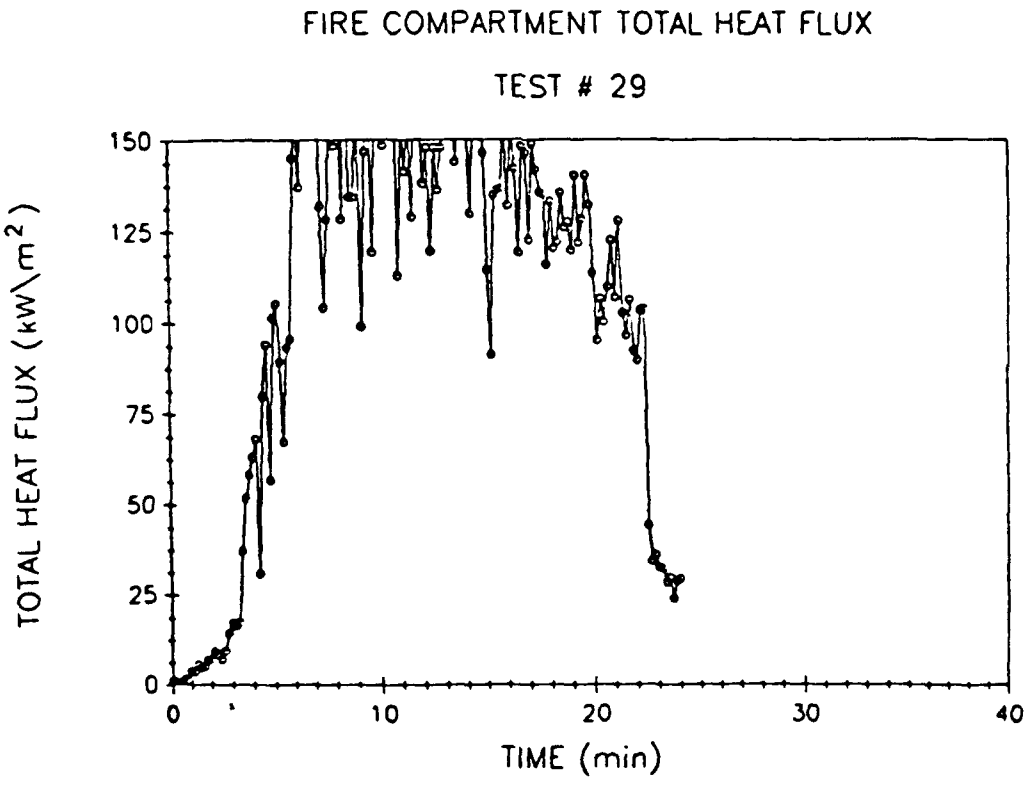

Fig. A107 – Fire compartment total heat flux

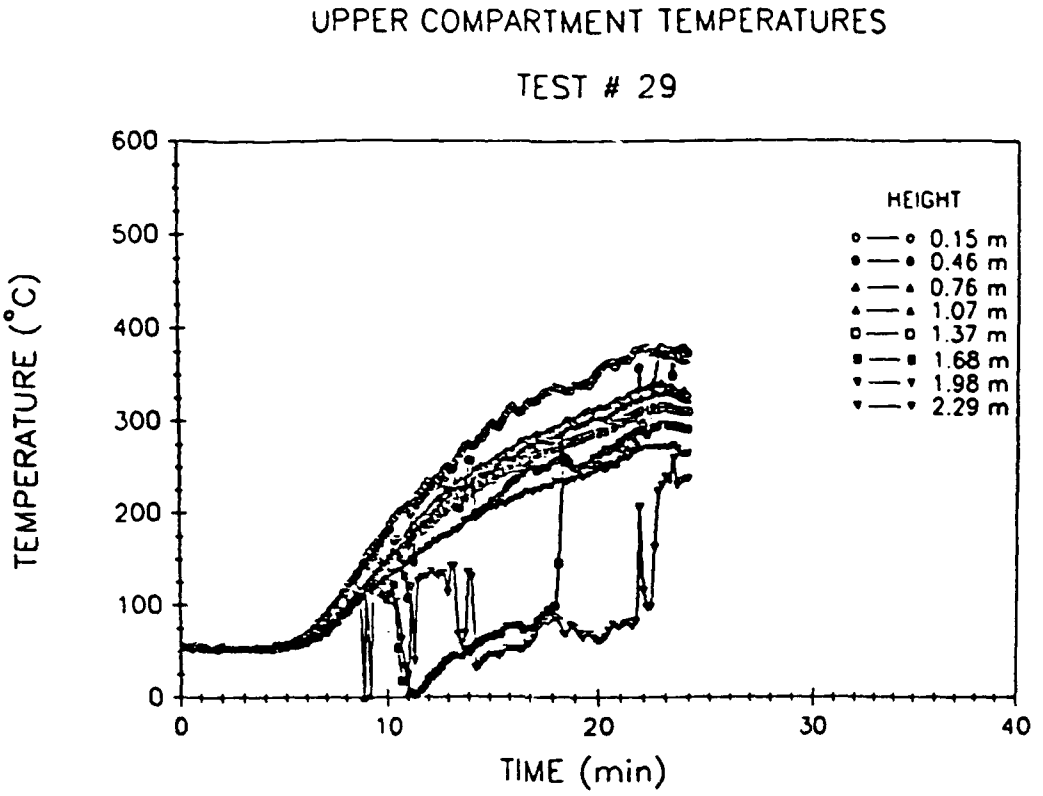

Fig. A108 – Upper compartment air temperatures

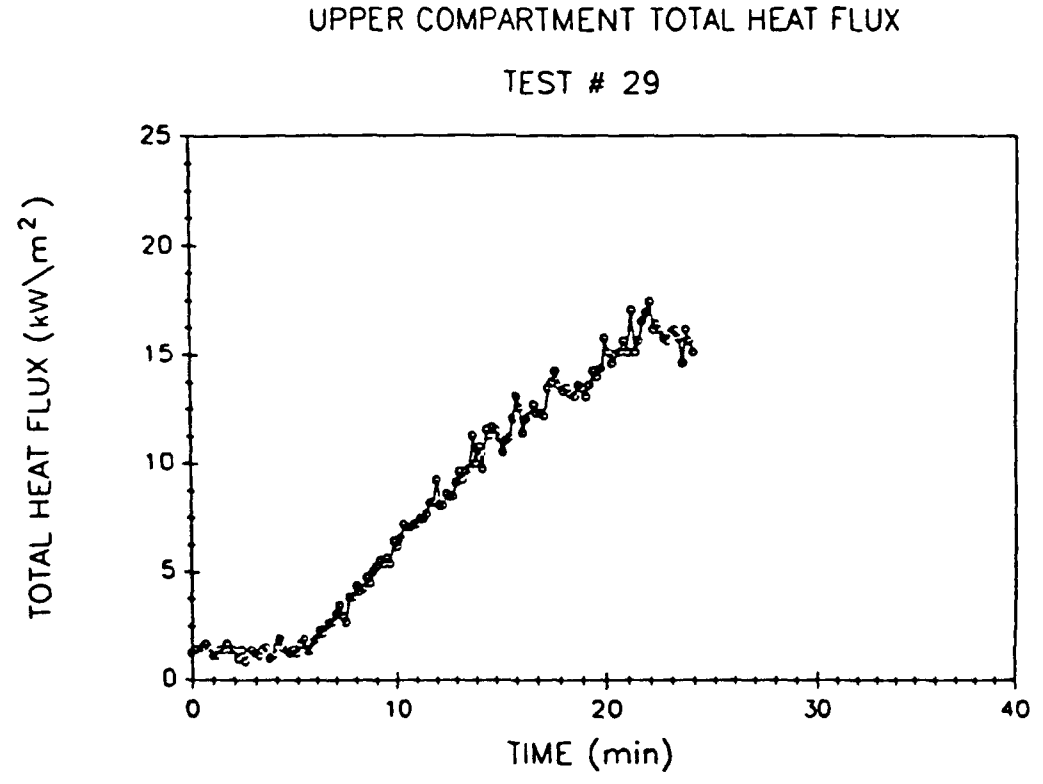

Fig. A109 – Upper compartment total heat flux

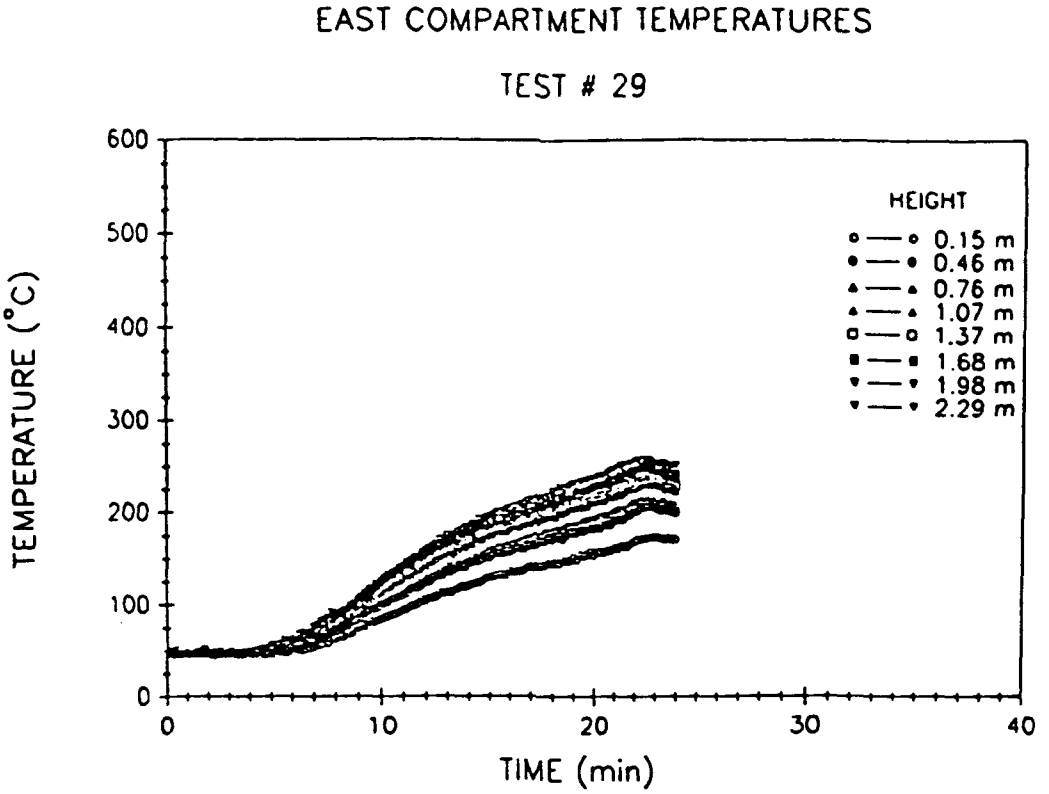

Fig. A110 – East compartment air temperatures

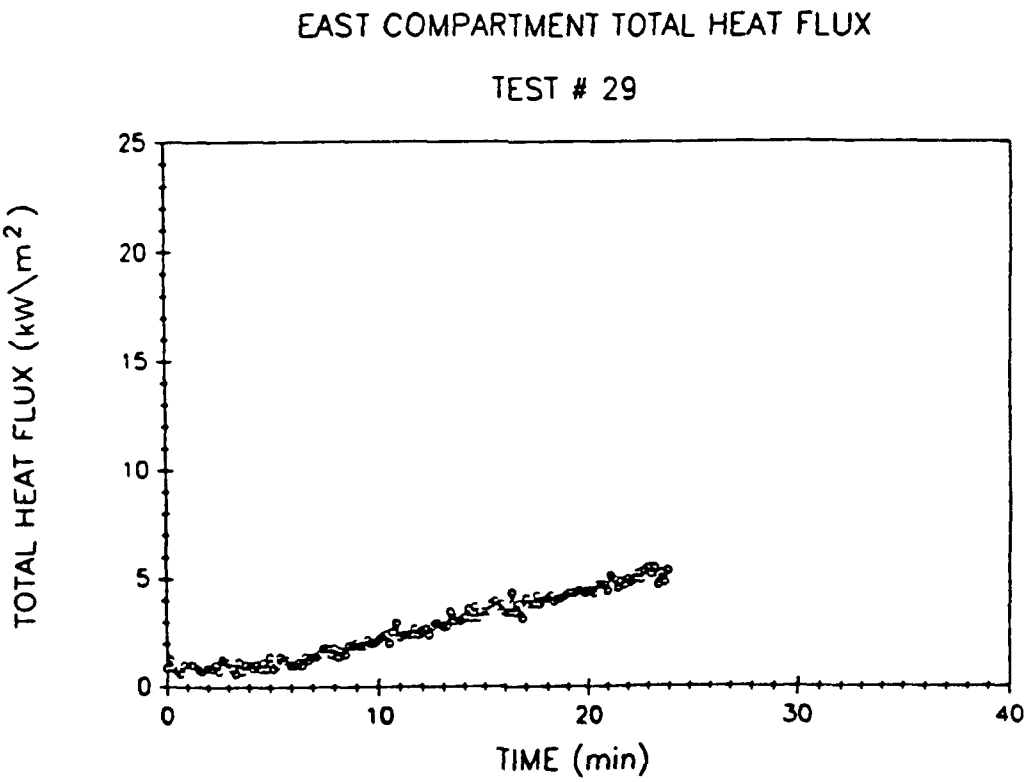

Fig. A111 – East compartment total heat flux

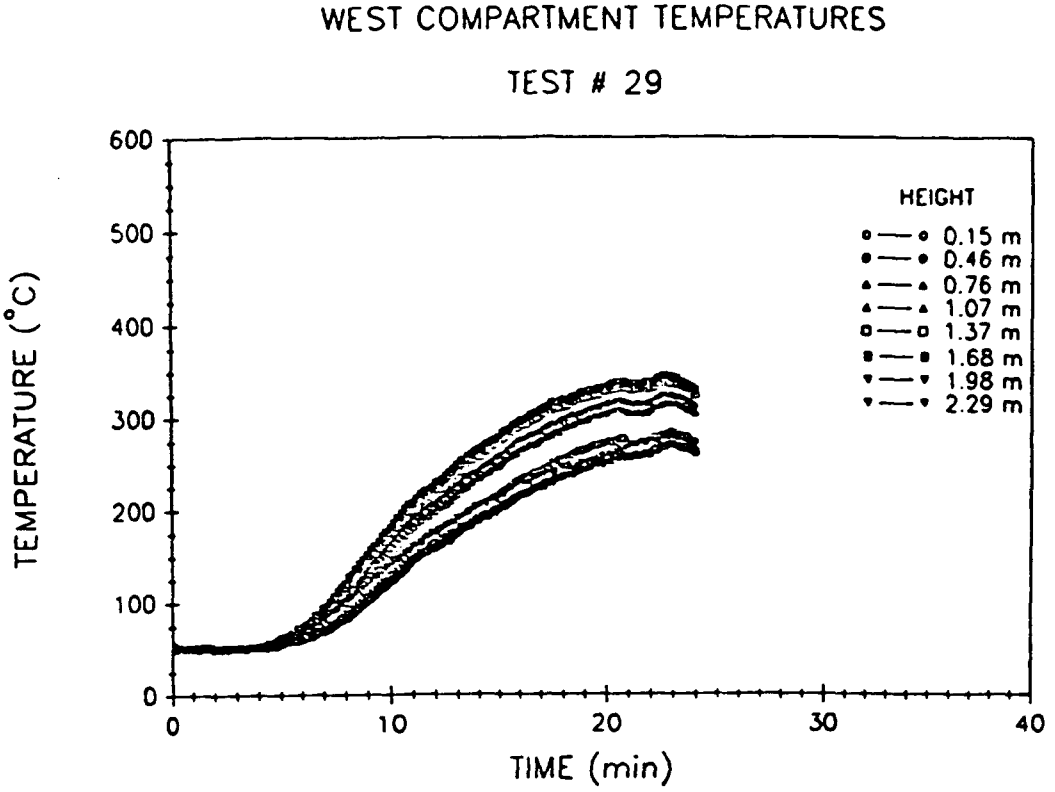

Fig. A112 – West compartment air temperatures

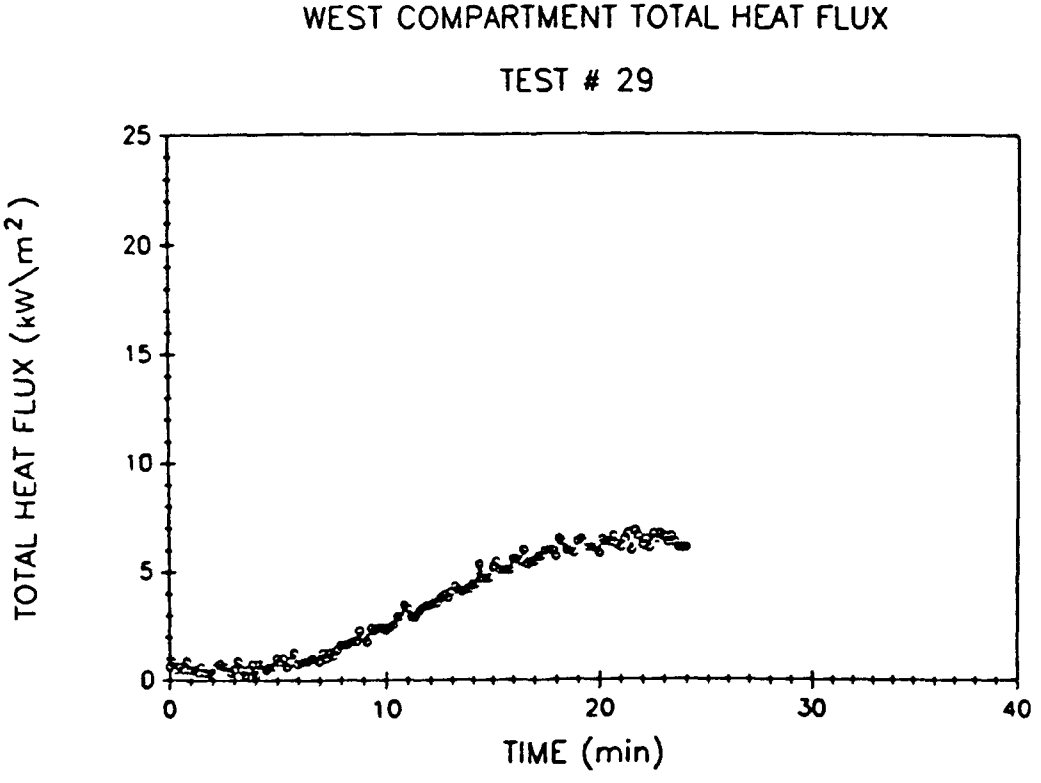

Fig. A113 – West compartment total heat flux

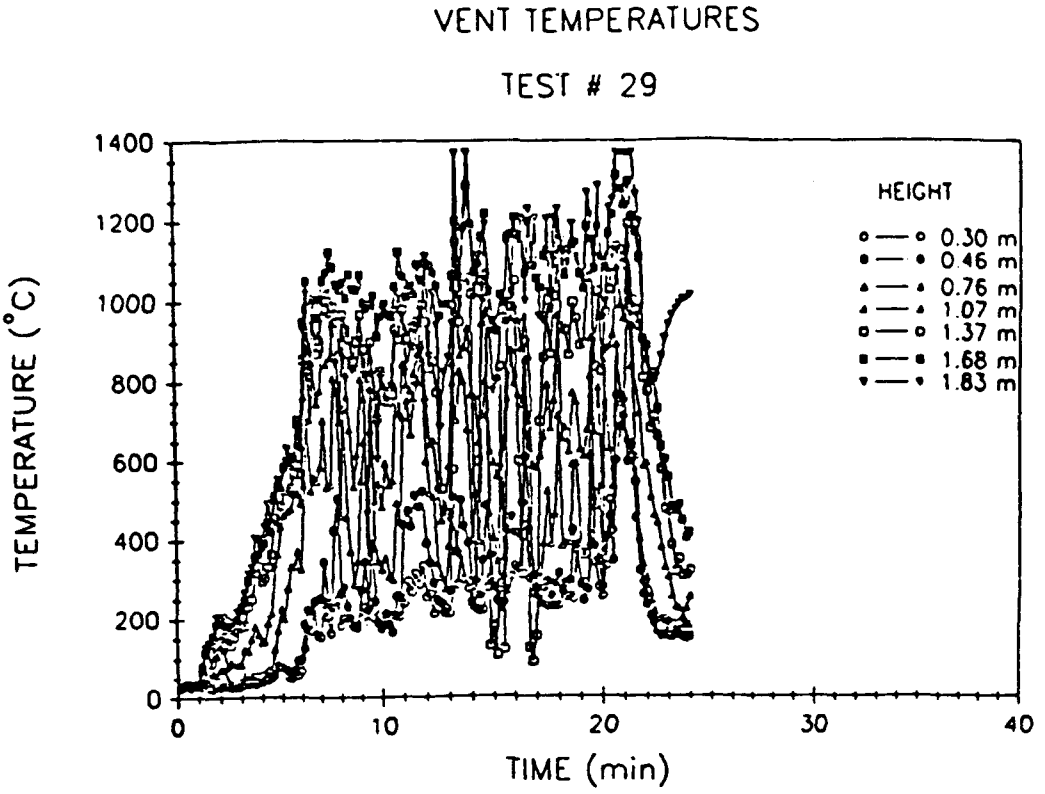

Fig. A114 – *Vent air temperatures*

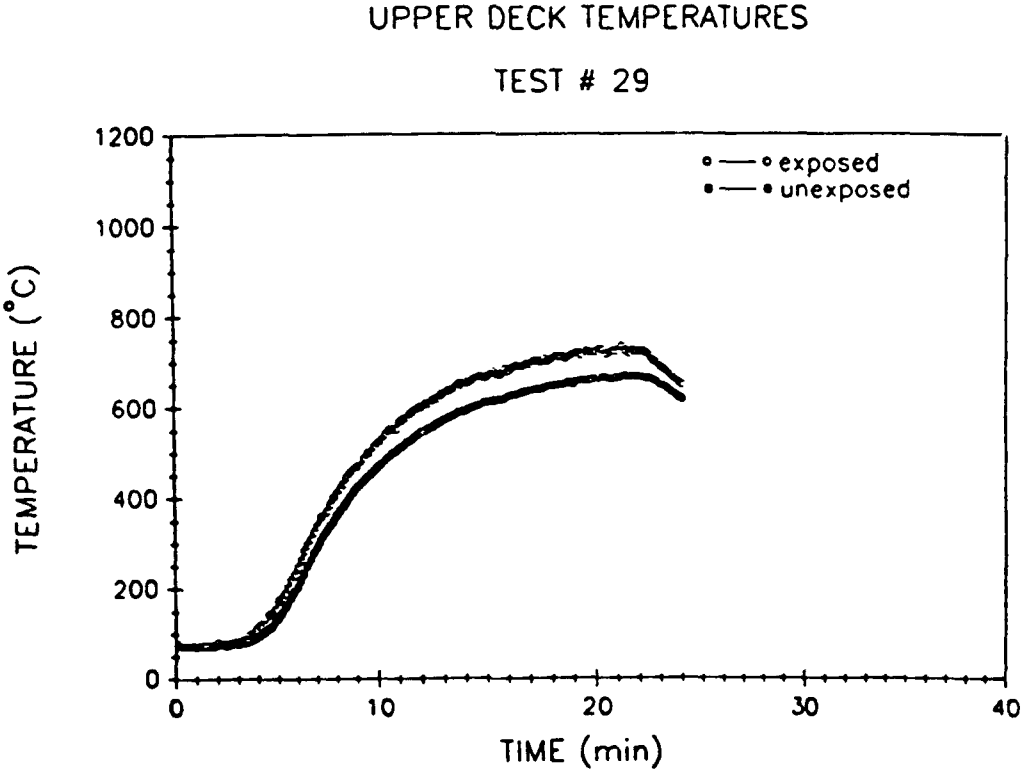

Fig. A115 – Upper deck surface temperatures

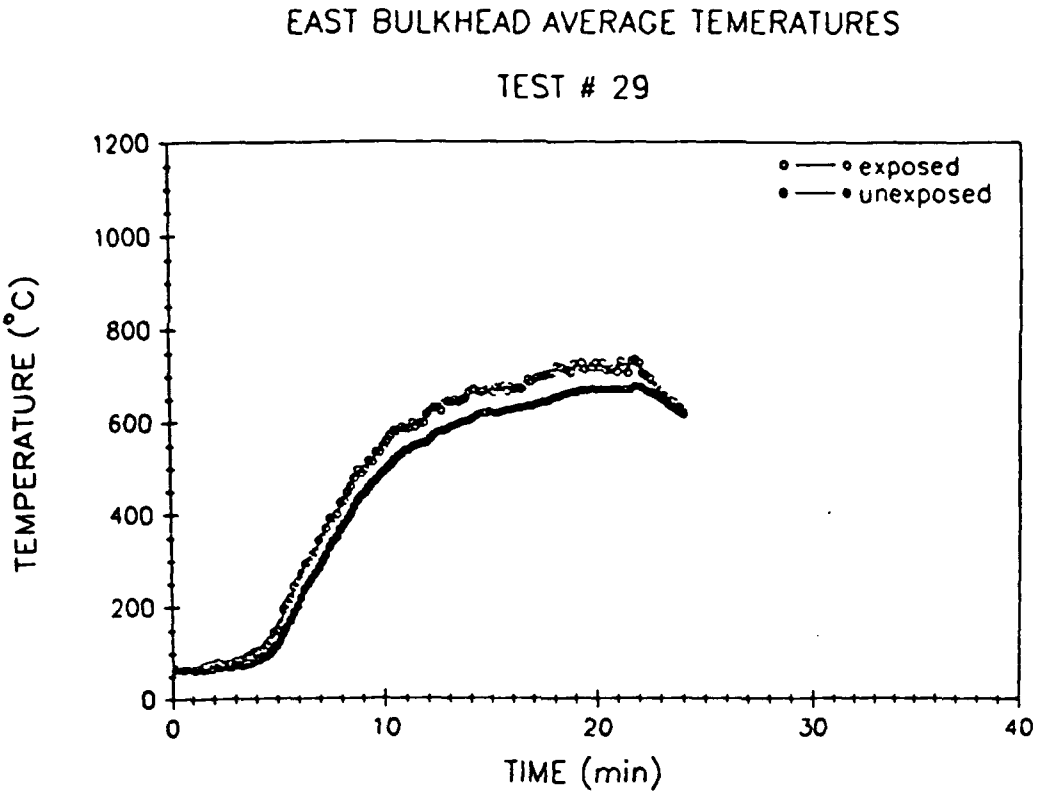

Fig. A116 – East bulkhead average surface temperatures

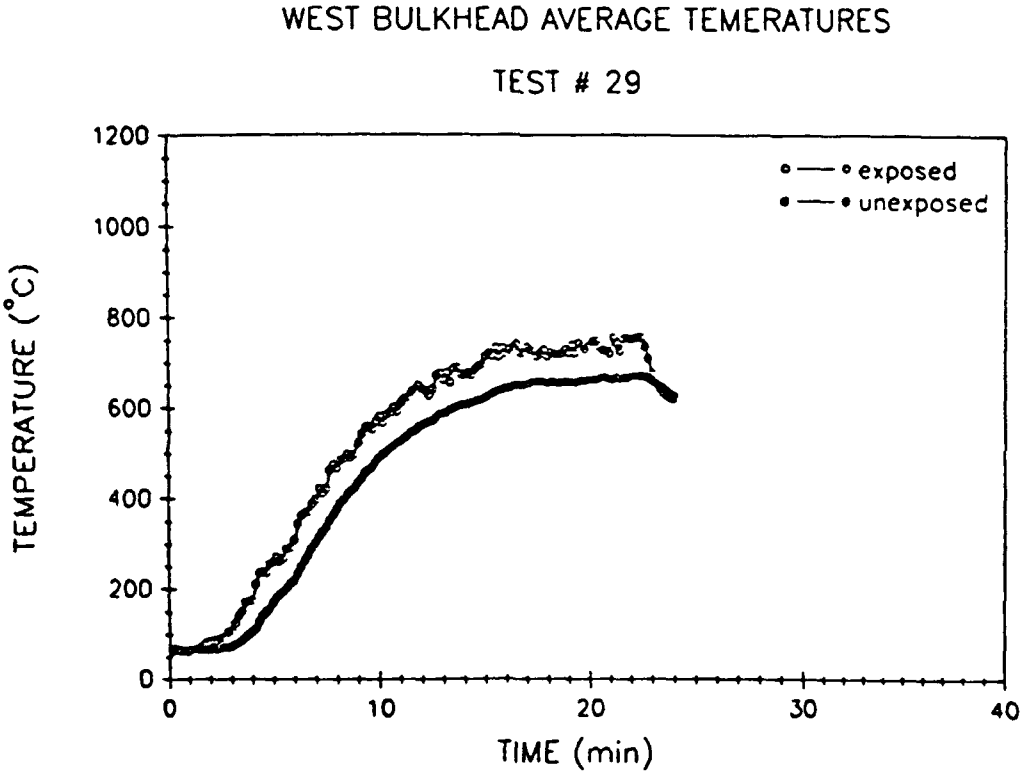

Fig. A117 – West bulkhead average surface temperatures

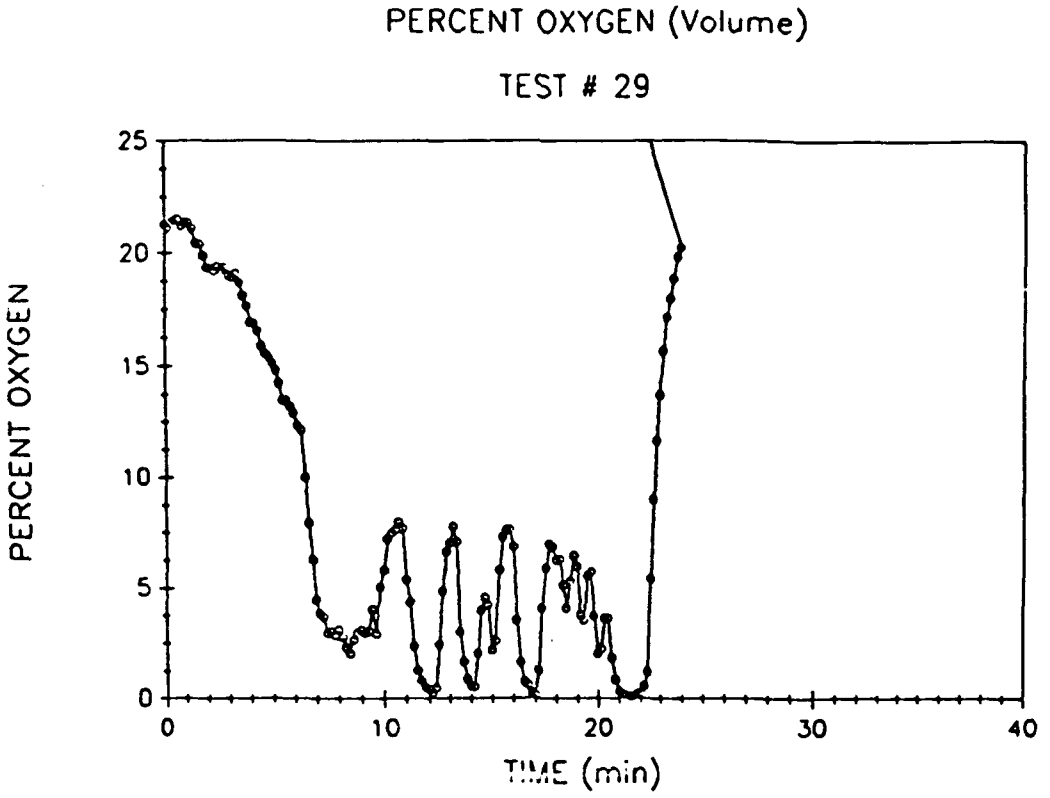

Fig. A118 – *Percent oxygen (volume)*

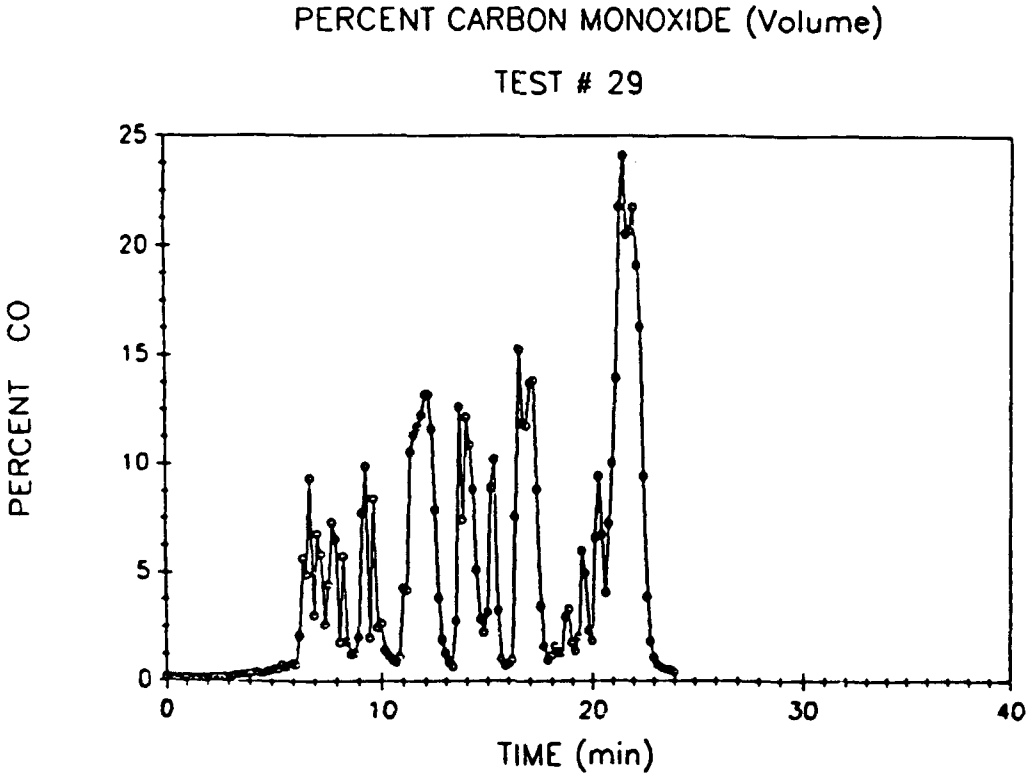

Fig. A119 – Percent carbon monoxide (volume)

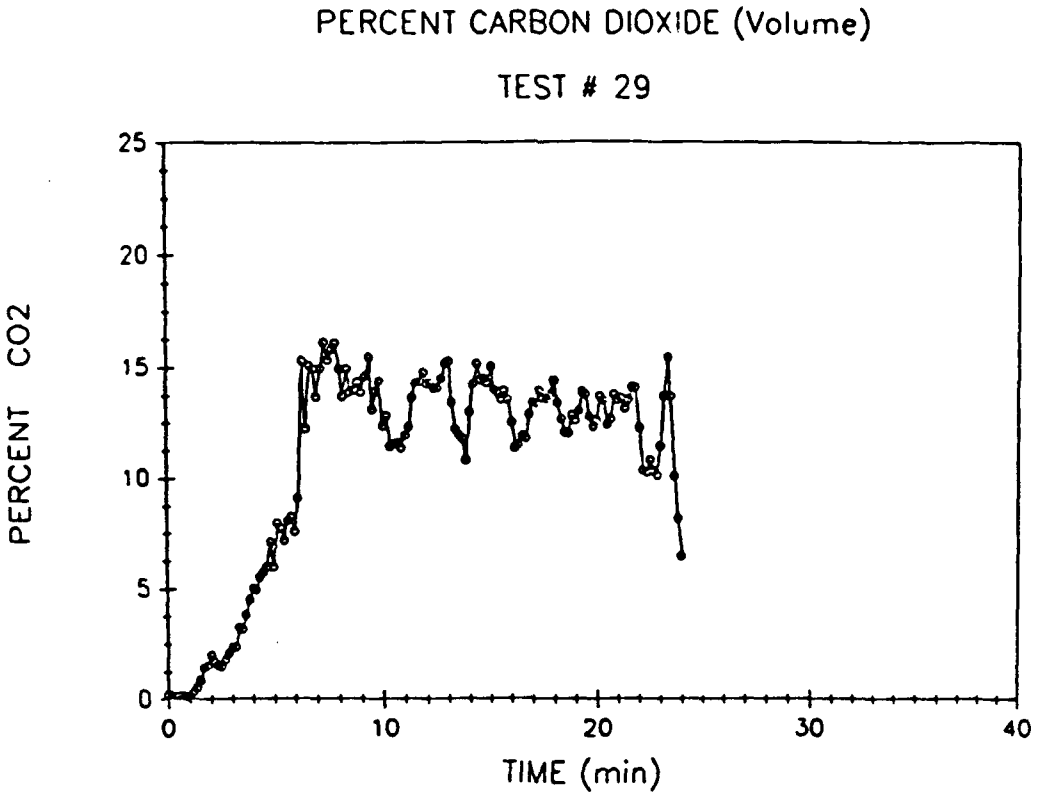

Fig. A120 – Percent carbon dioxide (volume)

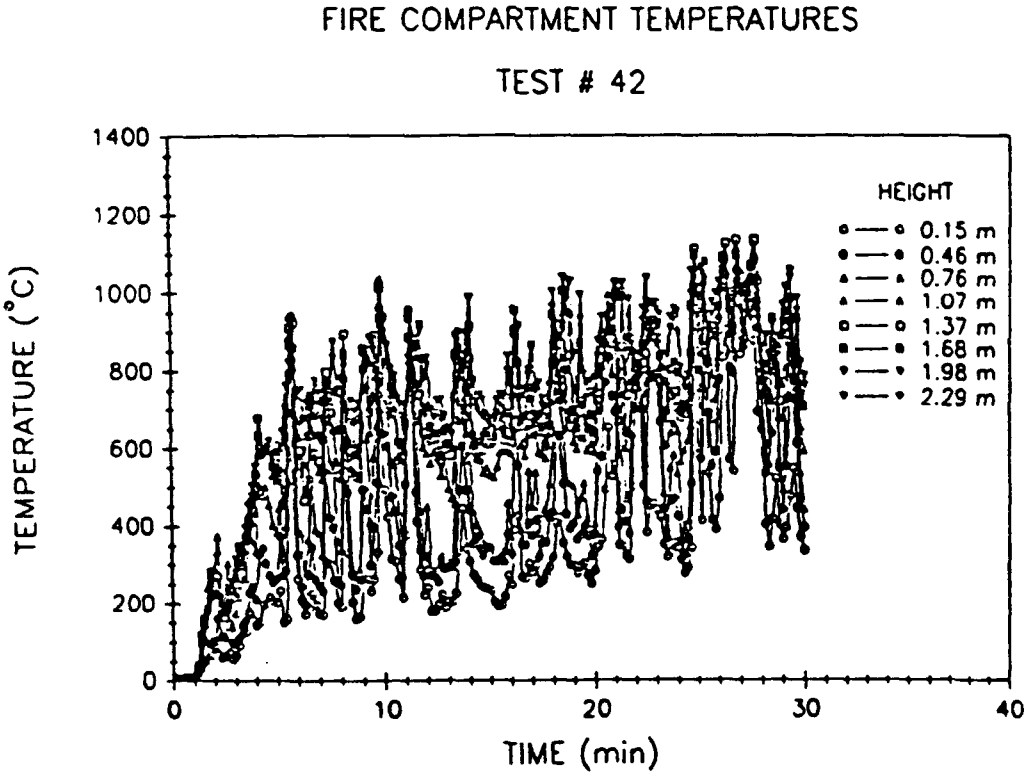

Fig. A121 – Fire comparment air temperatures

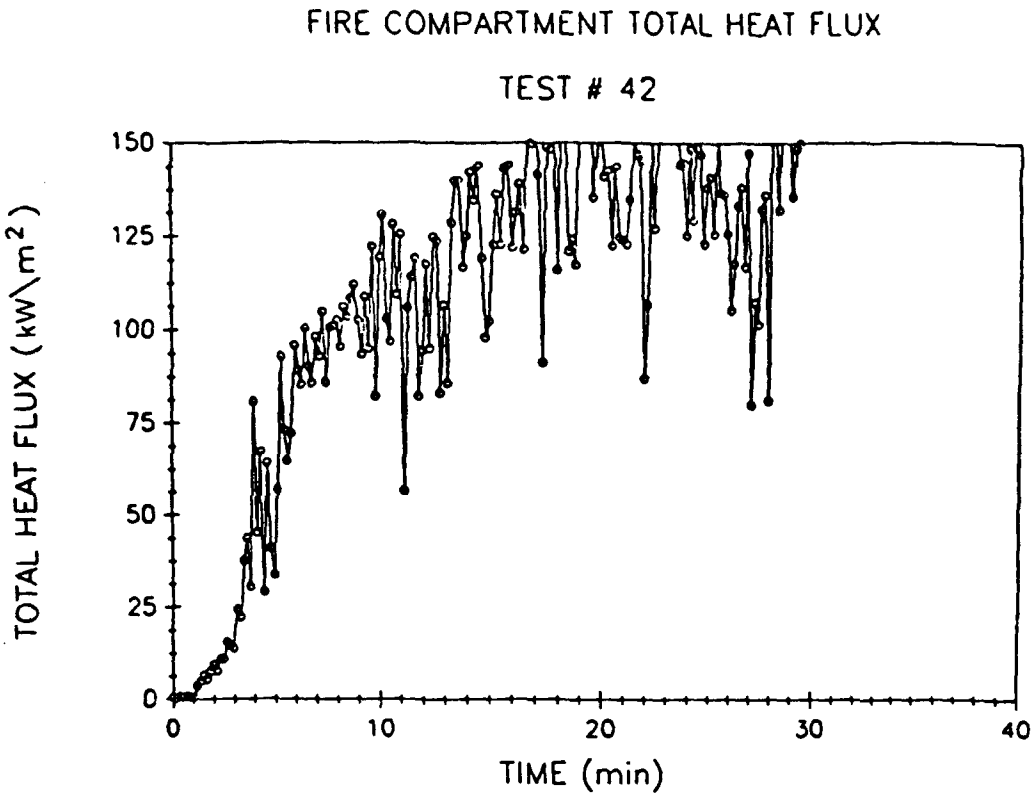

Fig. A122 – Fire comportment total heat flux

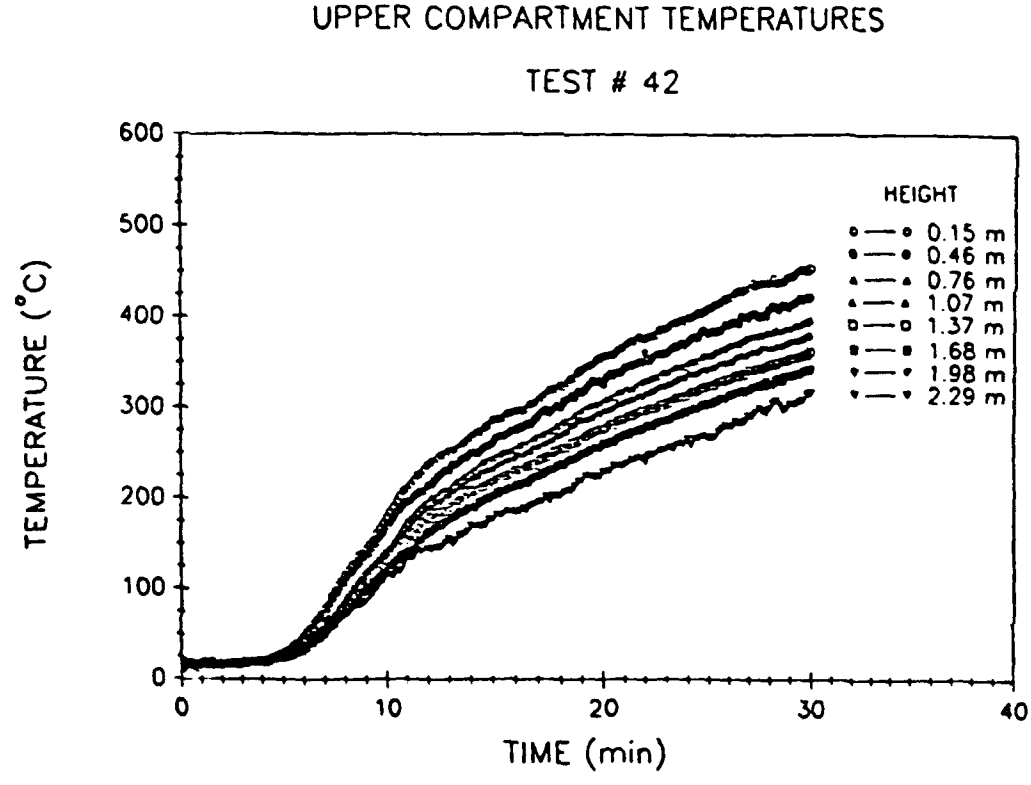

Fig. A123 – Upper compartment air temperatures

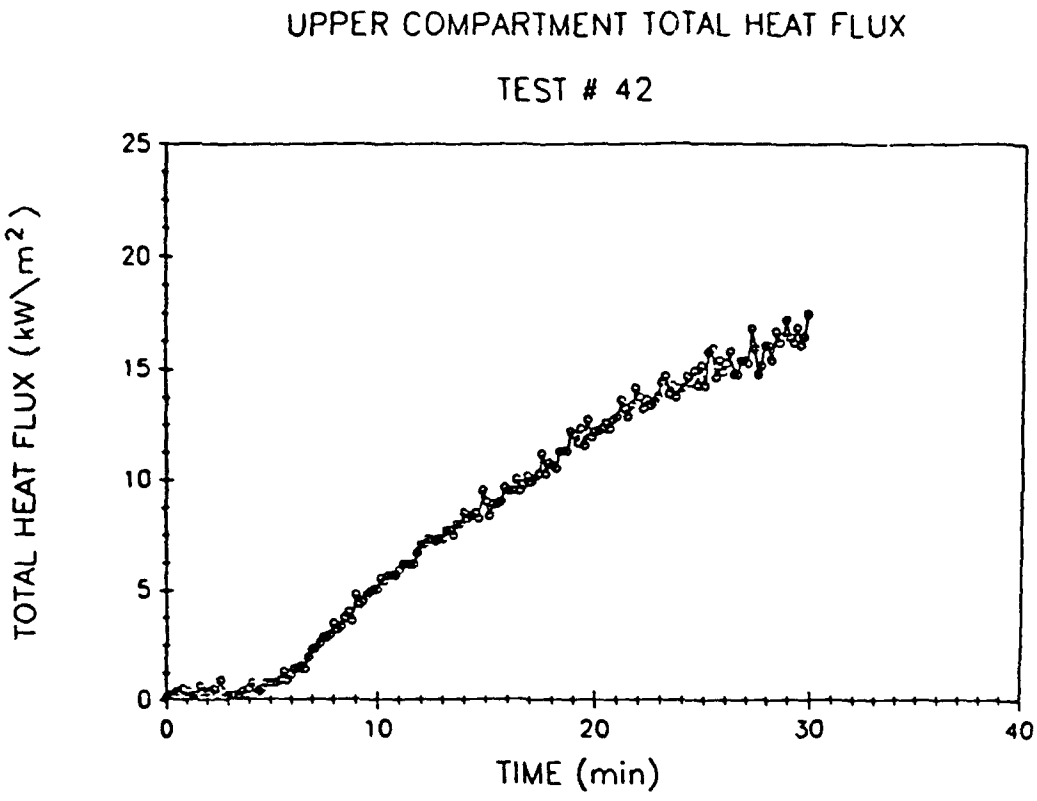

Fig. A124 – Upper compartment total heat flux

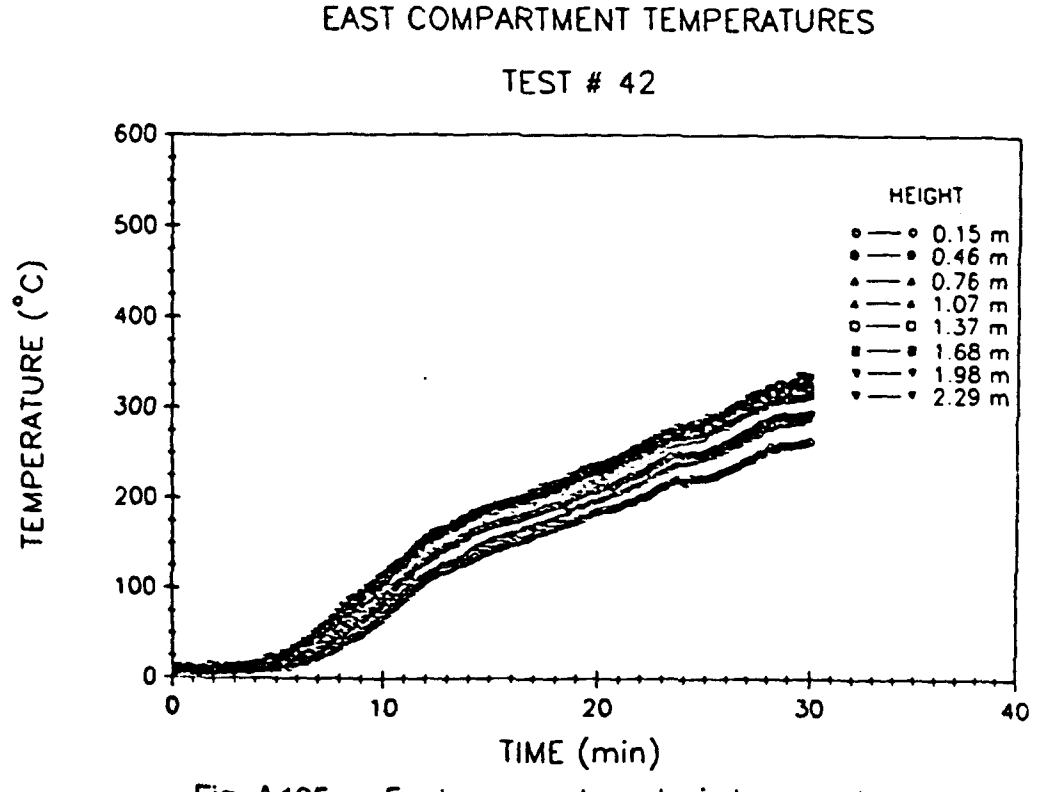

Fig. A125 – East compartment air temperatures

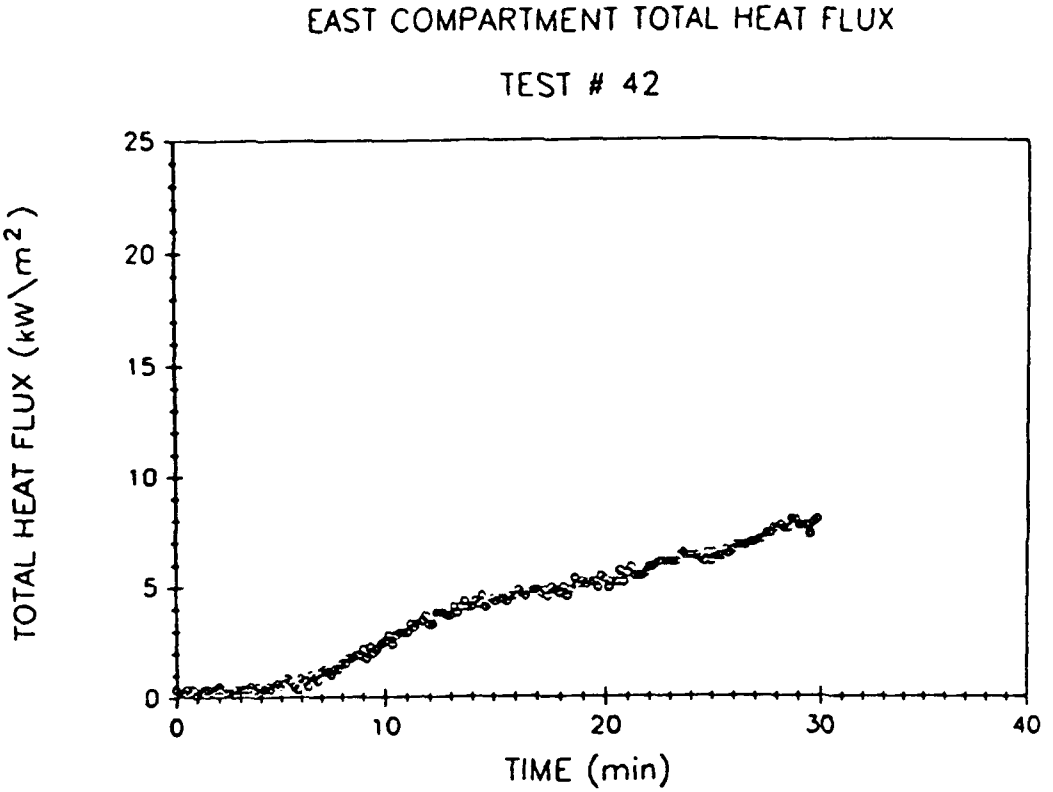

Fig. A126 – East compartment total heat flux

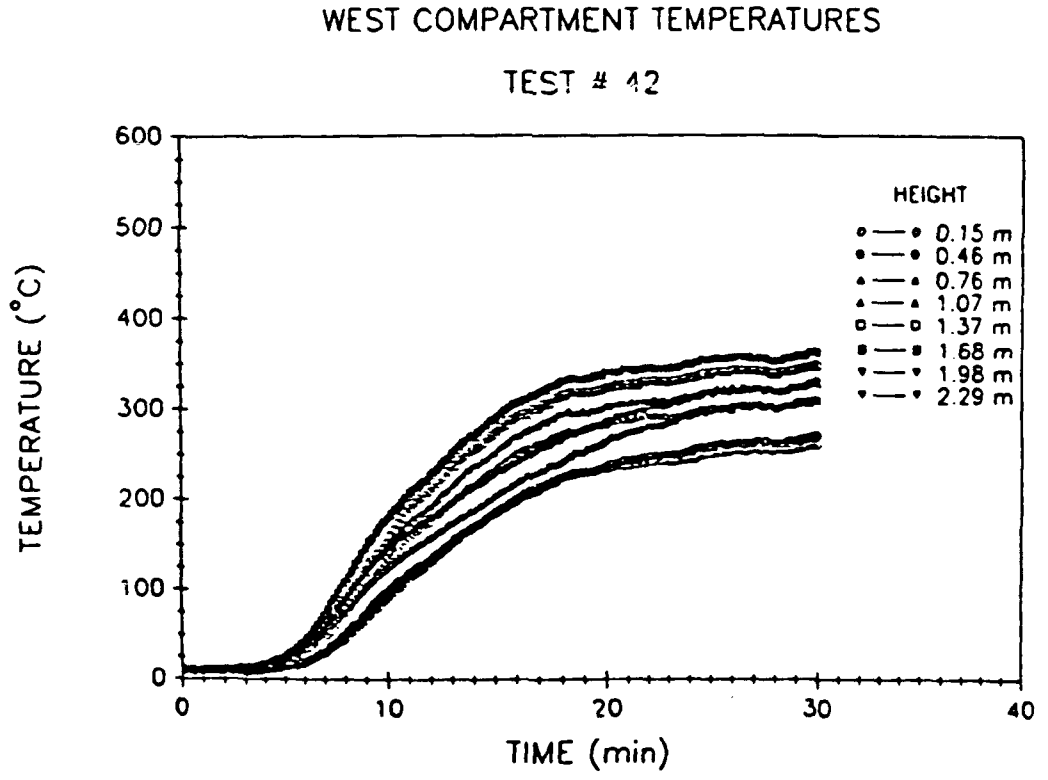

Fig. A127 – West compartment air temperatures

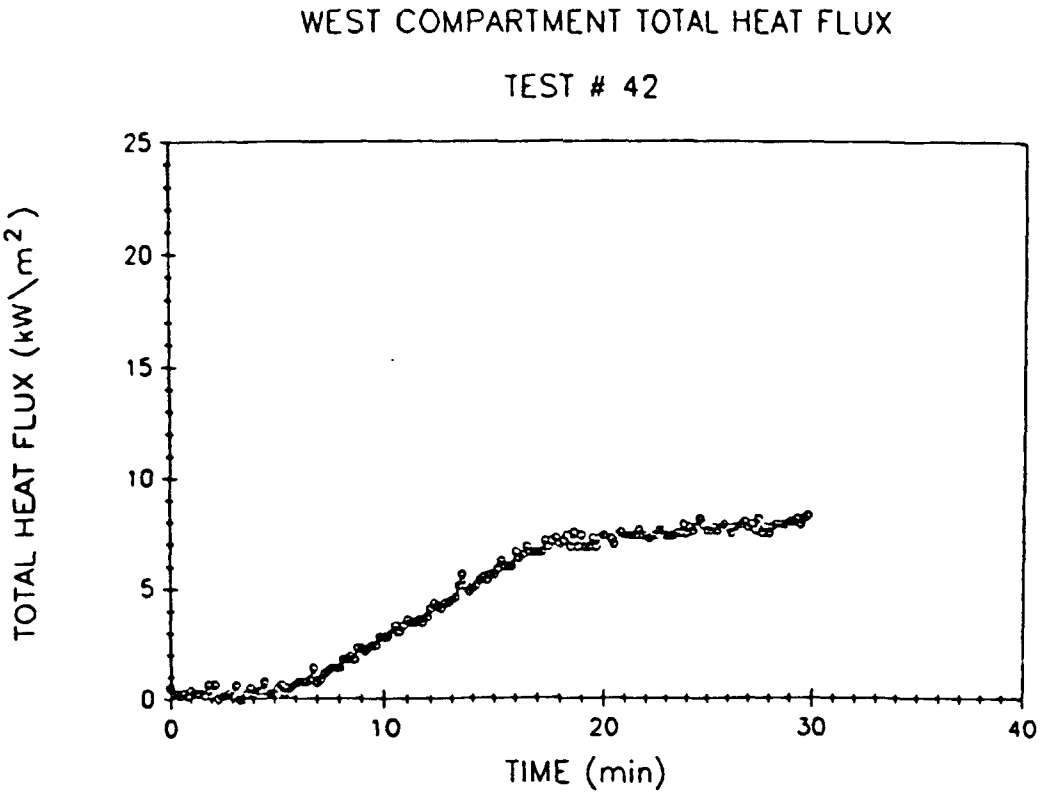

Fig. A128 – West compartment total heat flux

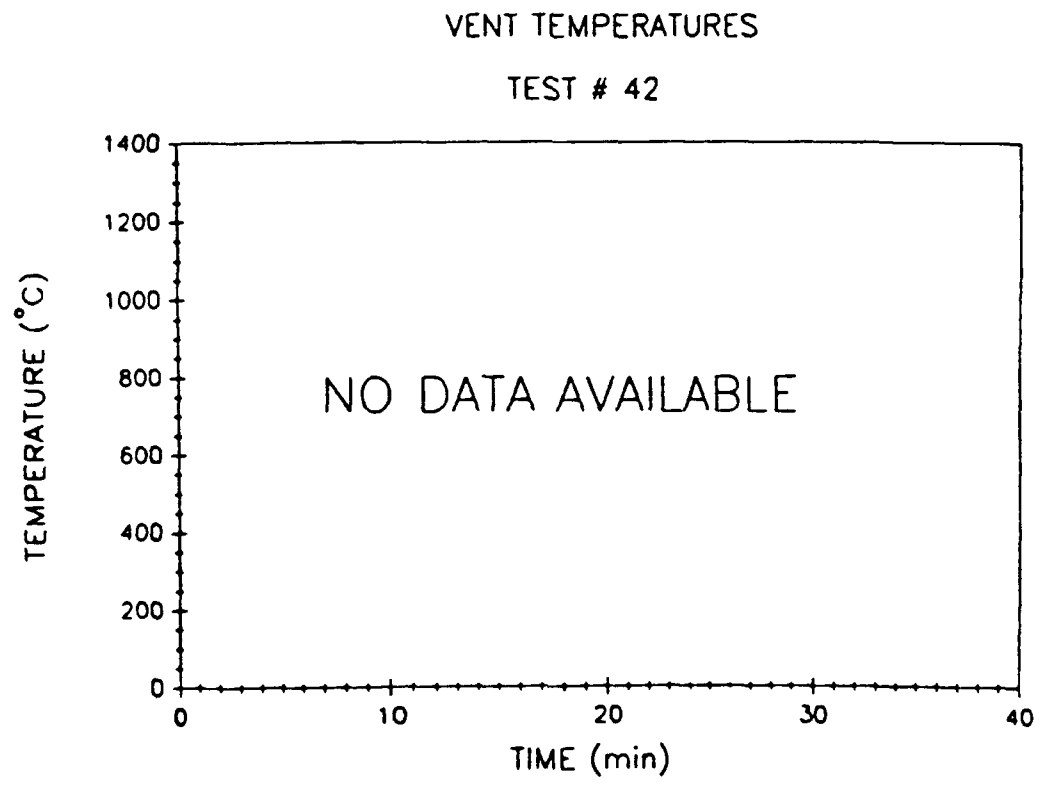

Fig. A129 – Vent air temperatures

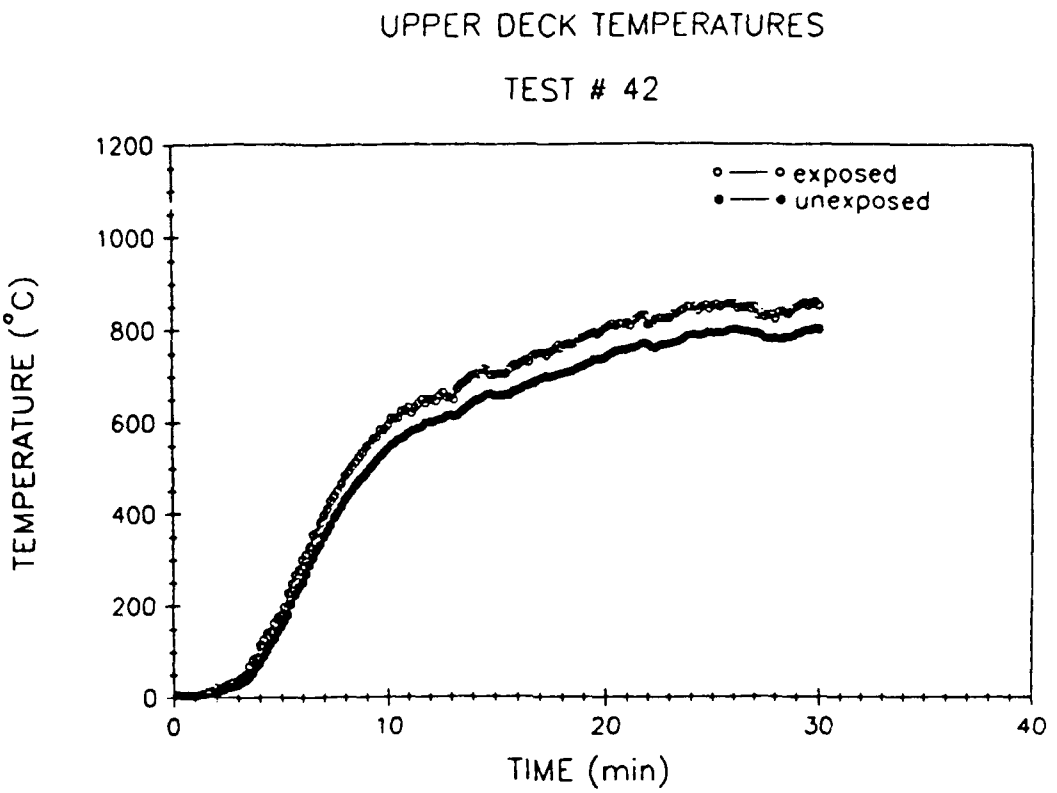

Fig. A130 – Upper deck surface temperatures

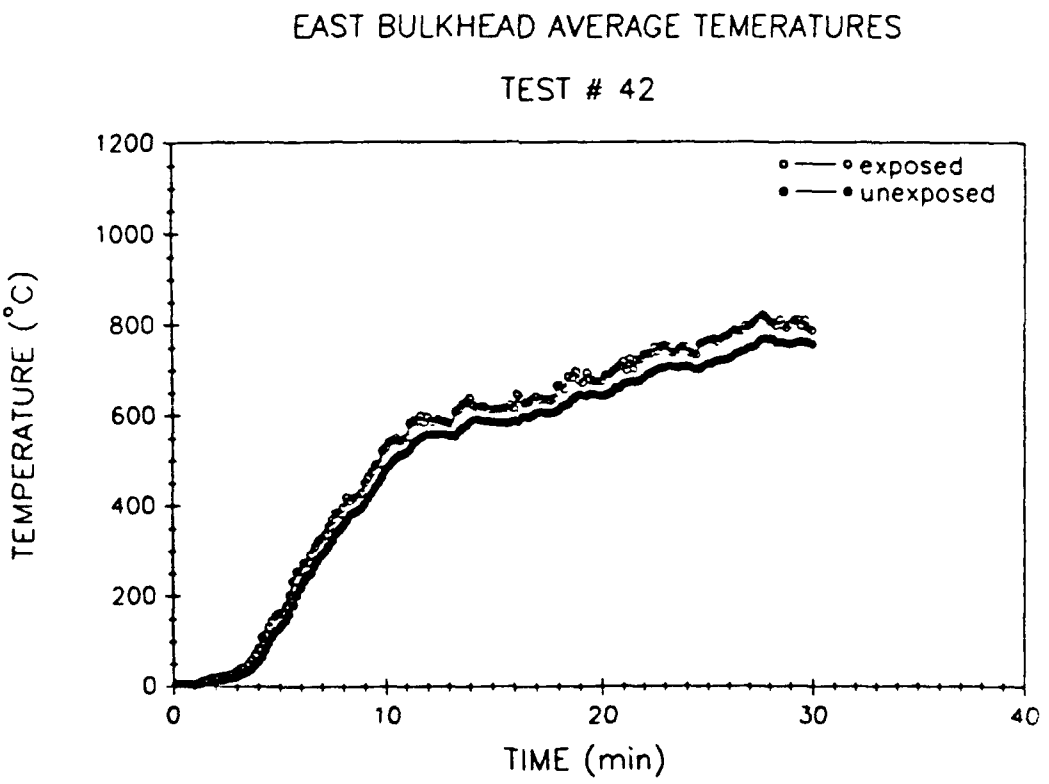

Fig. A131 – East bulkhead average surface temperatures

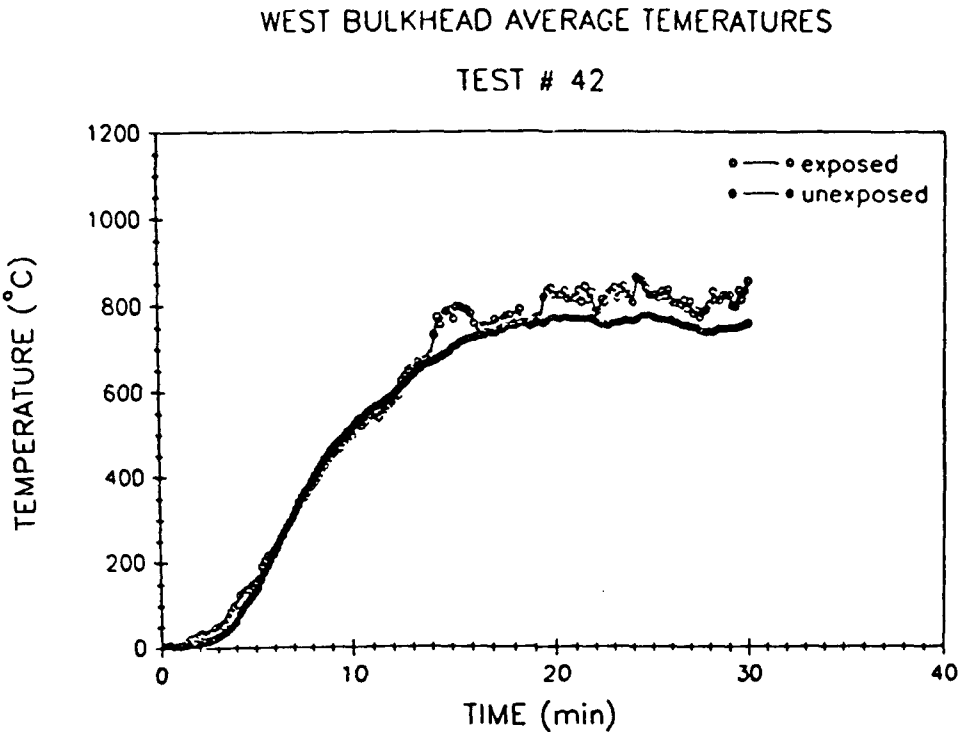

Fig. A132 – West bulkhead average surface temperatures

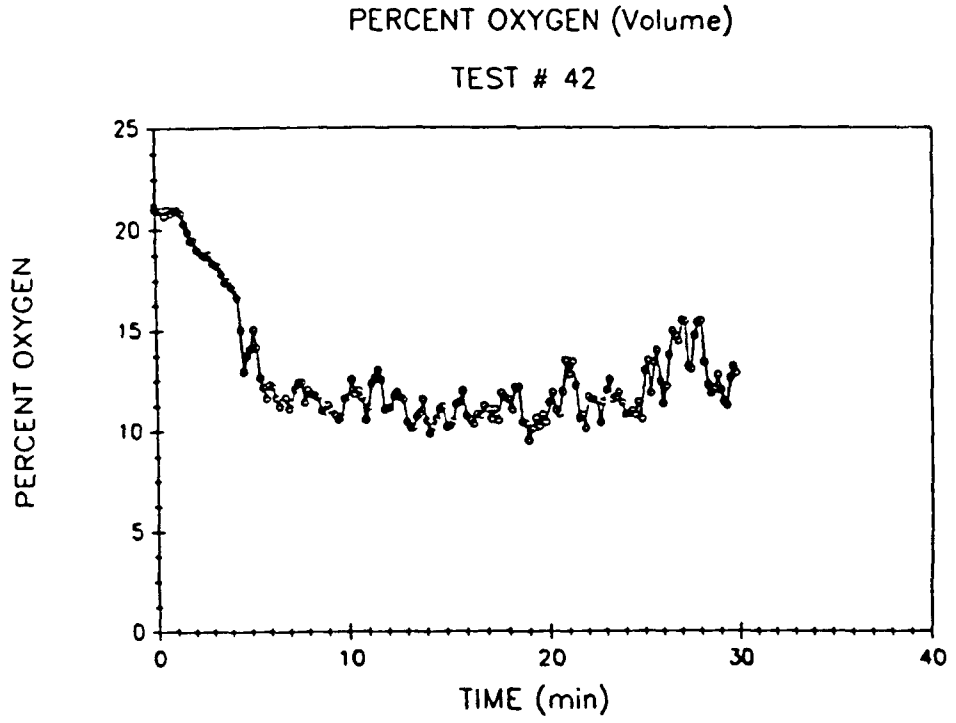

Fig. A133 – Percent oxygen (volume)

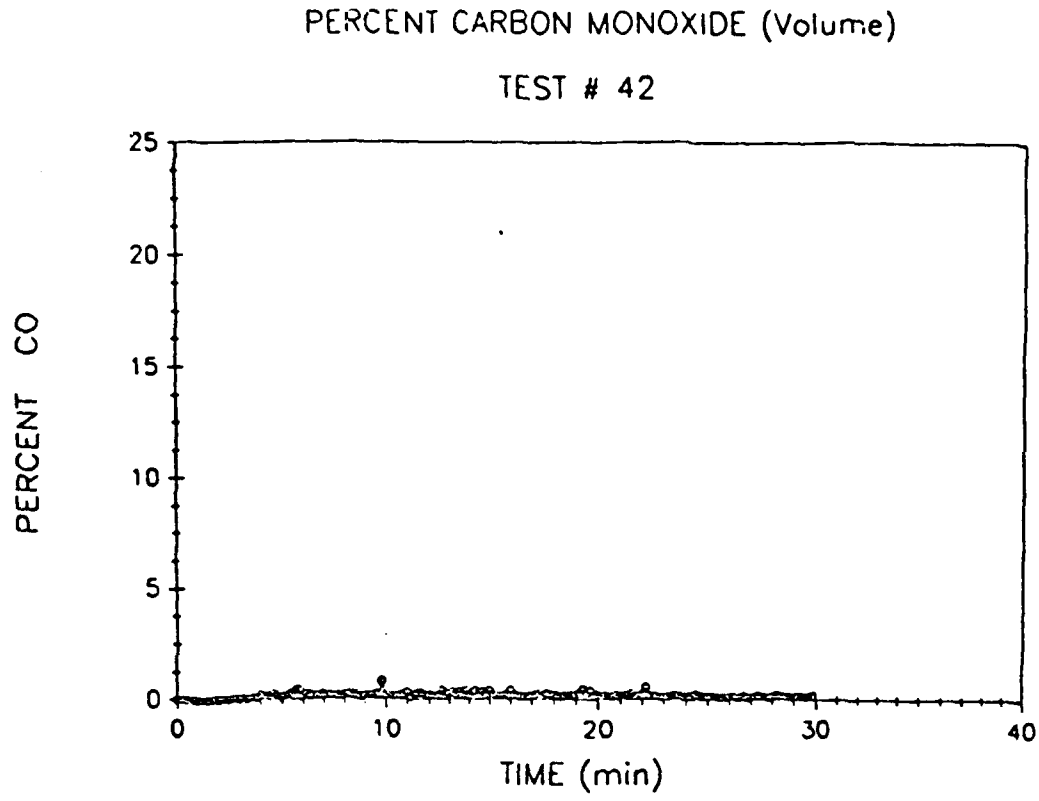

Fig. A134 – Percent carbon monoxide (volume)

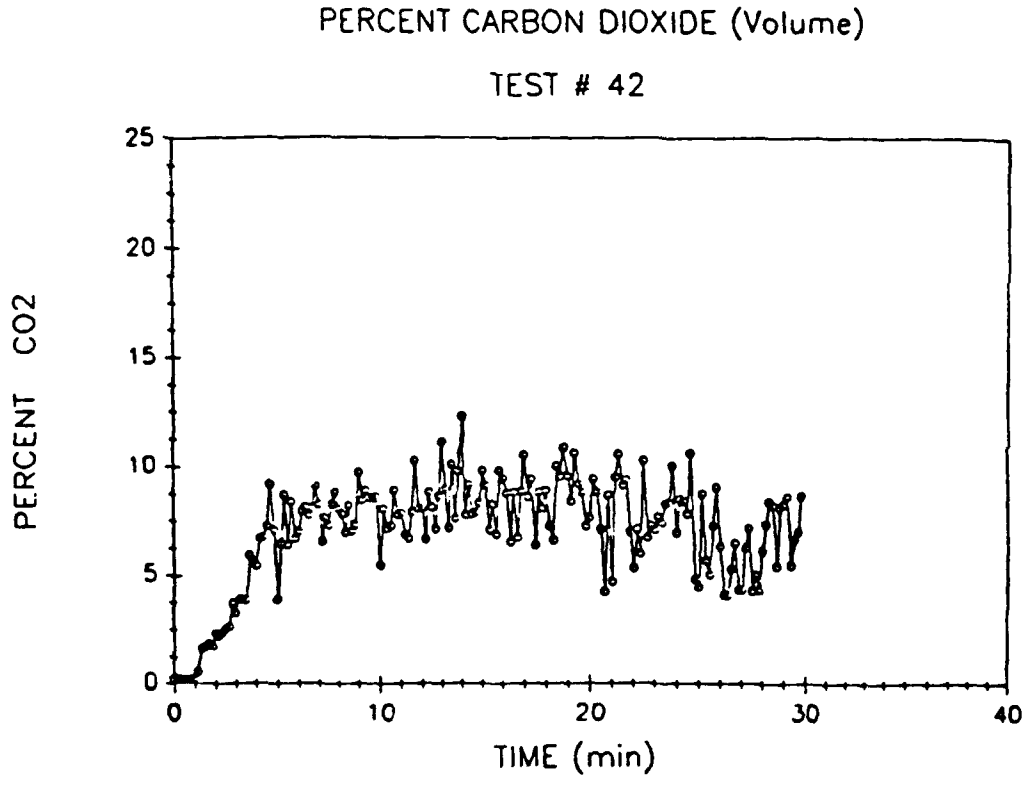

Fig. A135 – Percent carbon dioxide (volume)

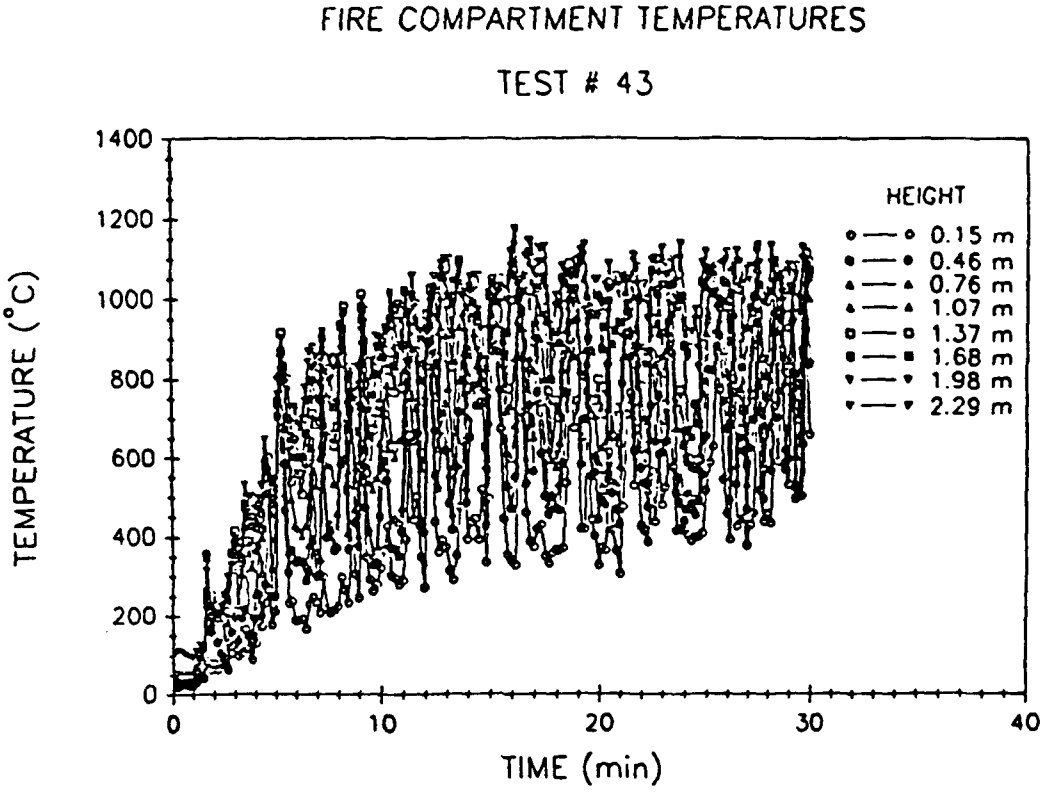

Fig. A136 – Fire comparment air temperatures

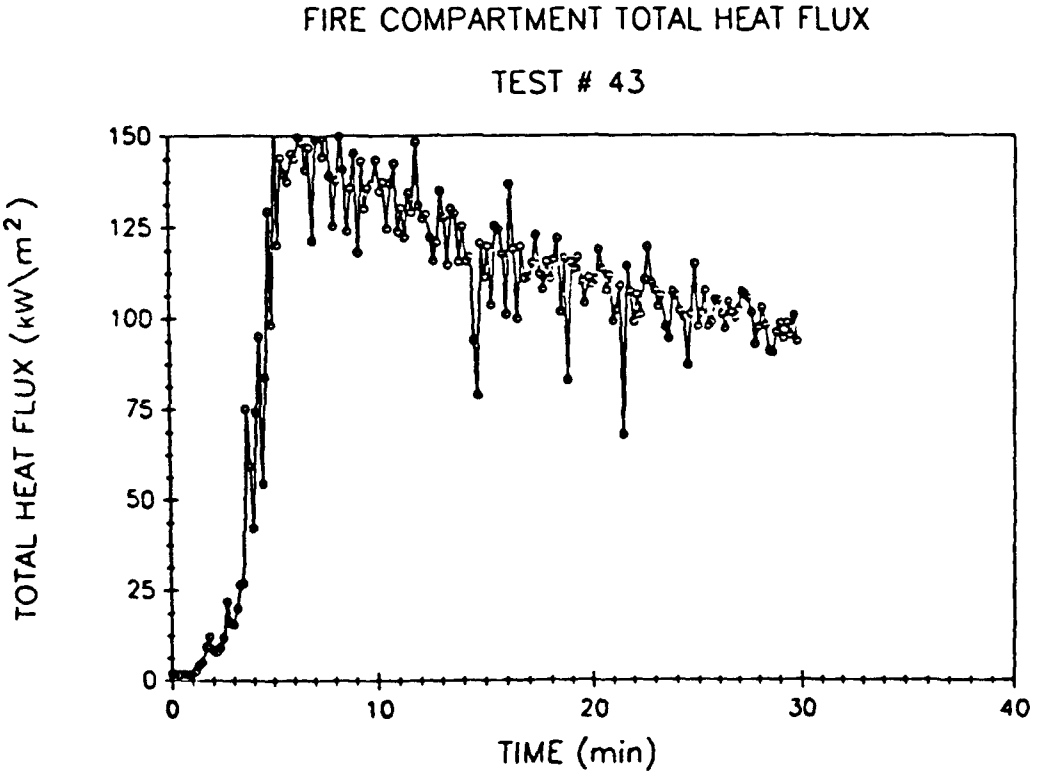

Fig. A137 – Fire compartment total heat flux

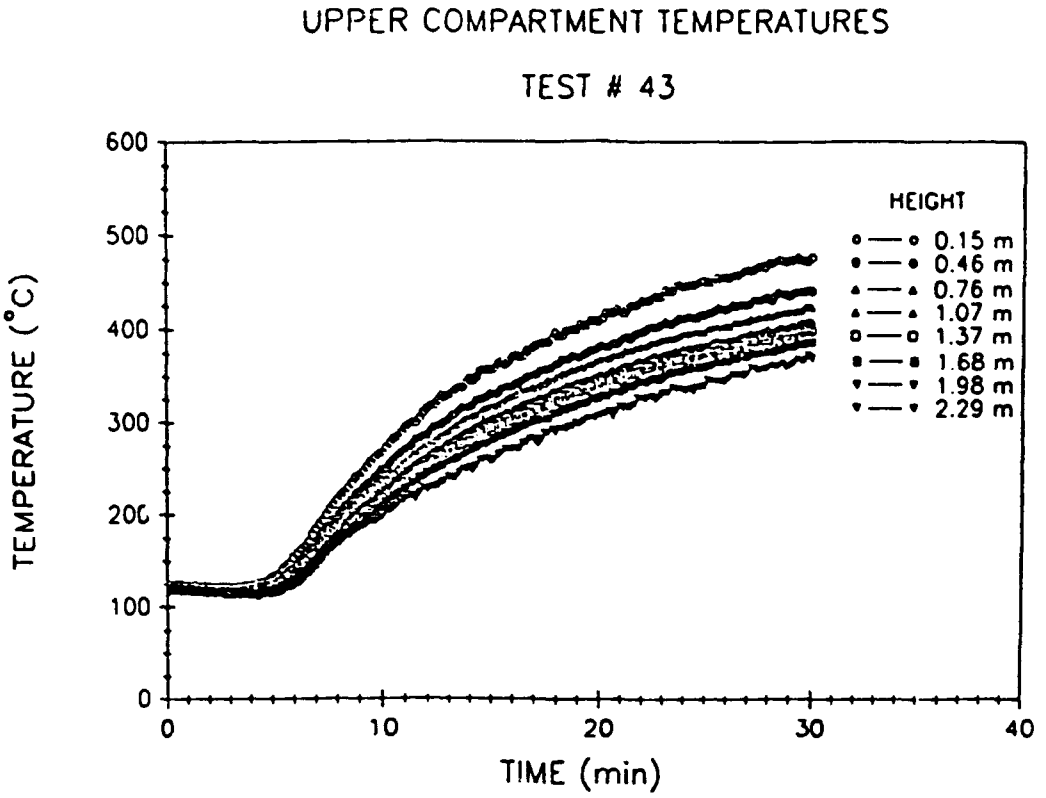

Fig. A138 – Upper compartment air temperatures

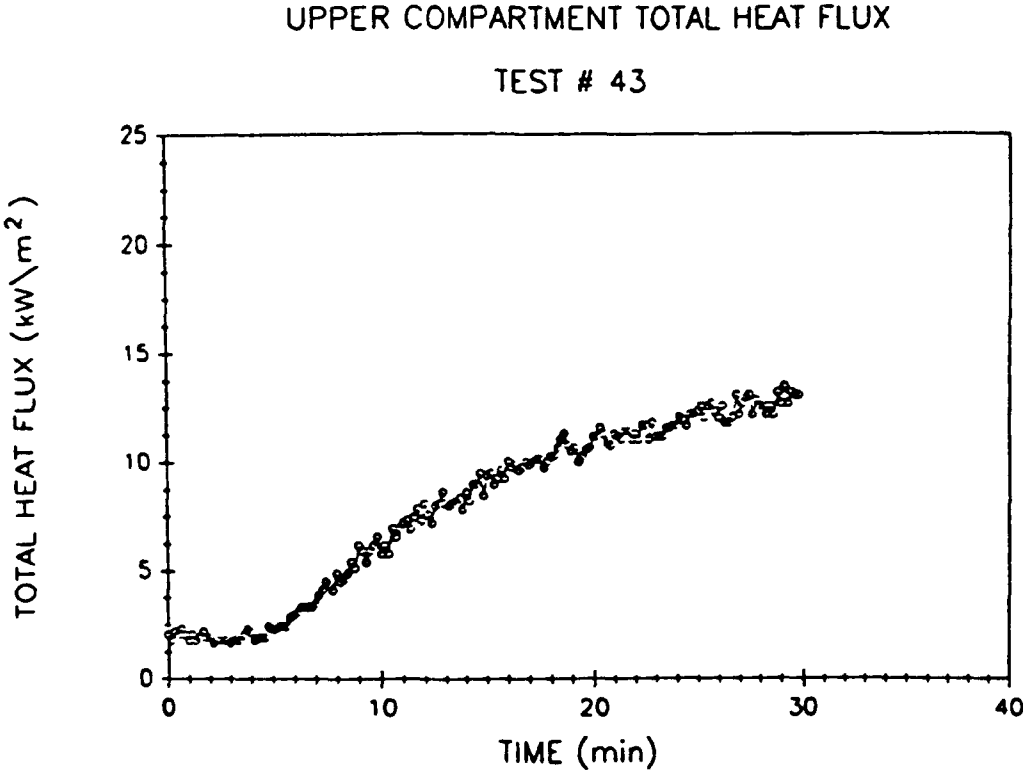

Fig. A139 – Upper compartment total heat flux

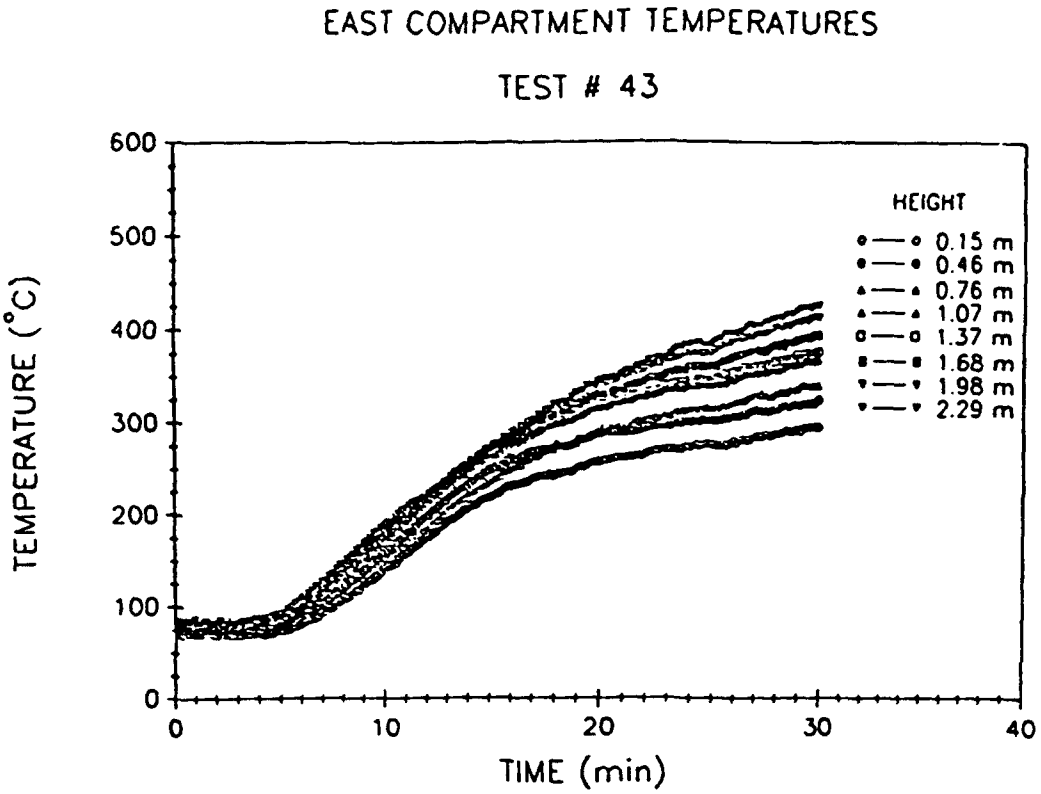

Fig. A140 – East compartment air temperatures

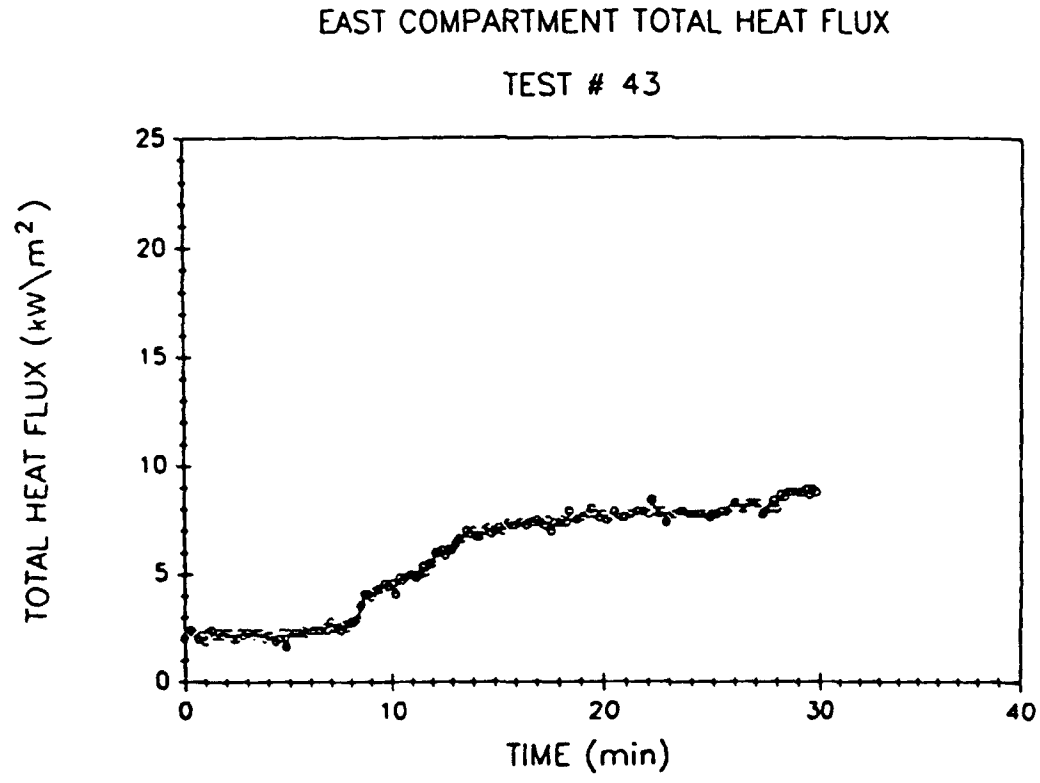

Fig. A141 – East compartment total heat flux

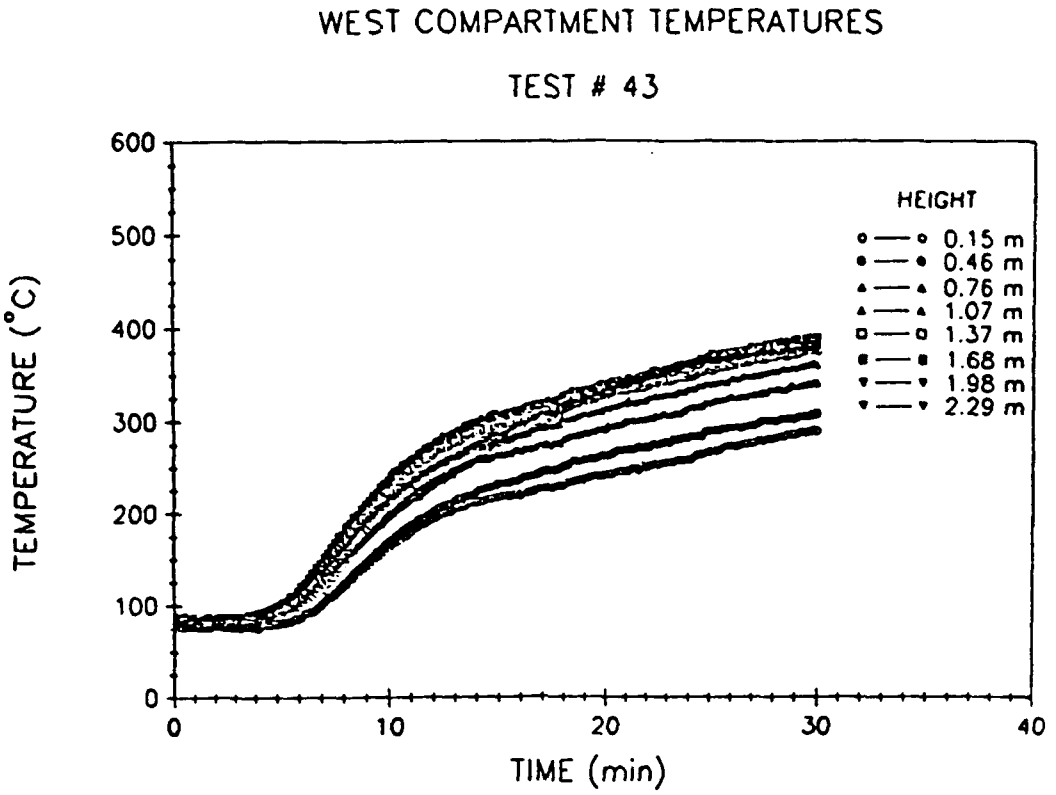

Fig. A142 – West compartment air temperatures

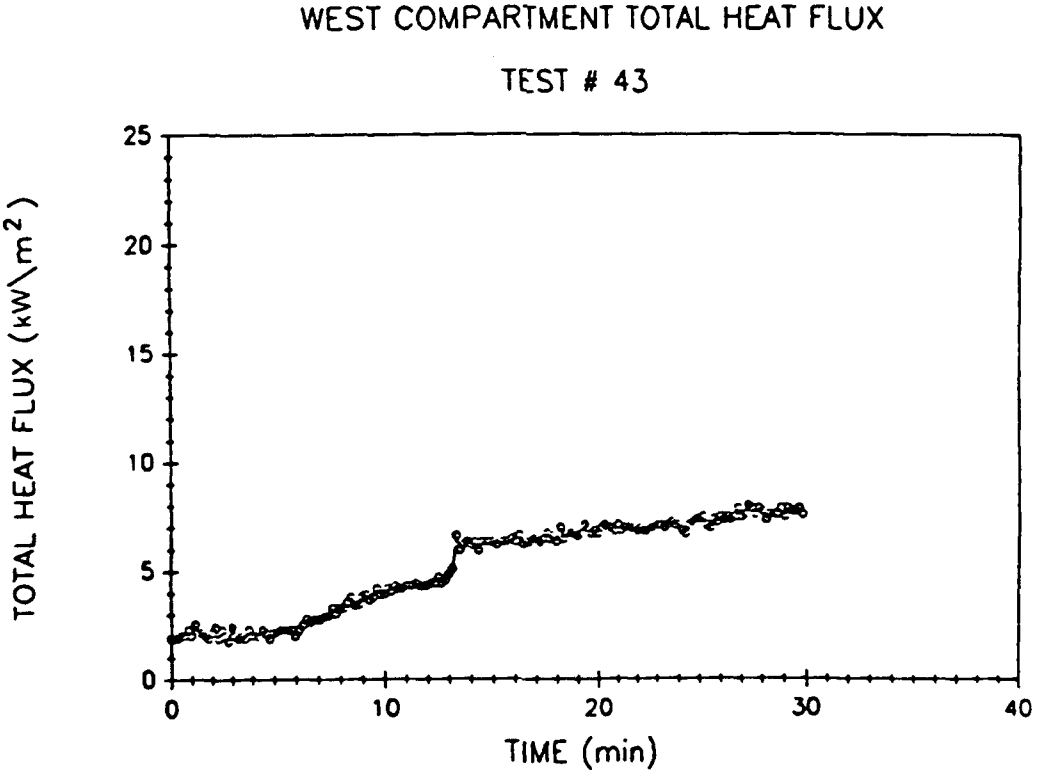

Fig. A143 – West compartment total heat flux

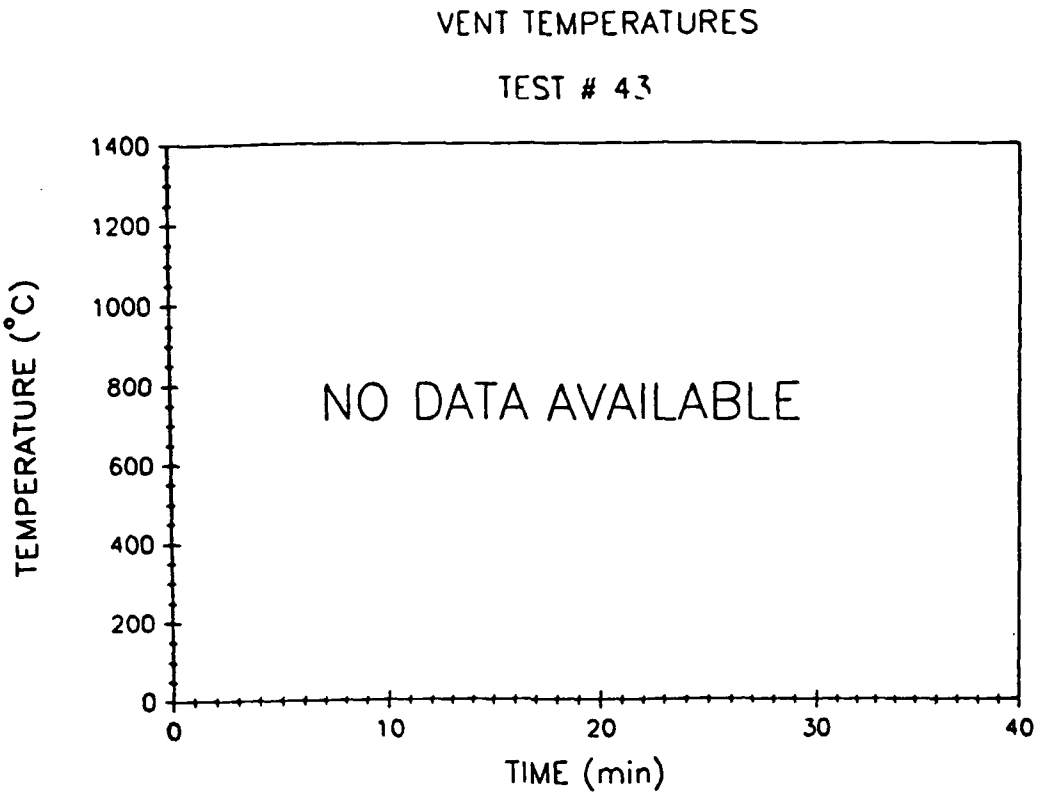

Fig. A144 – Vent air temperatures

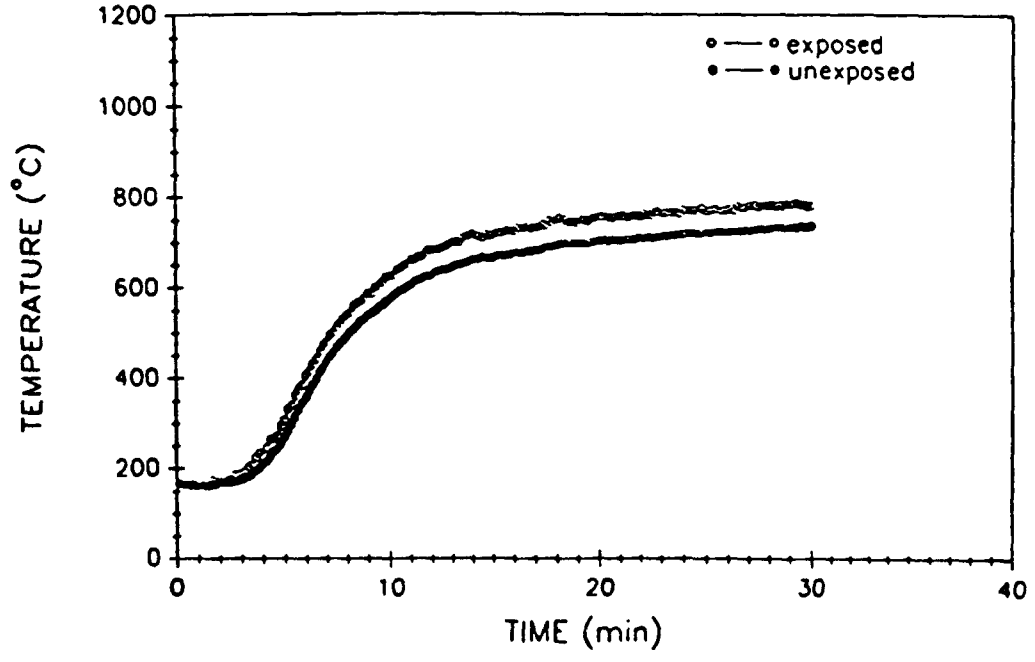

Fig. A145 – Upper deck surface temperatures

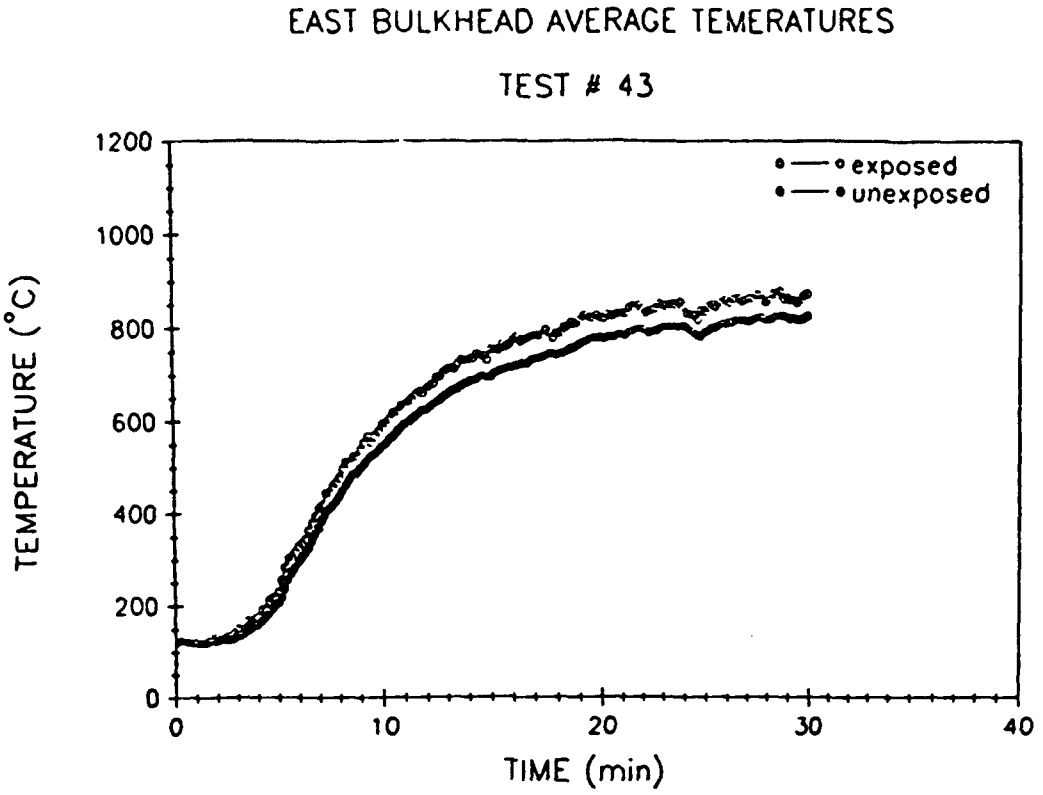

Fig. A146 – East bulkhead average surface temperatures

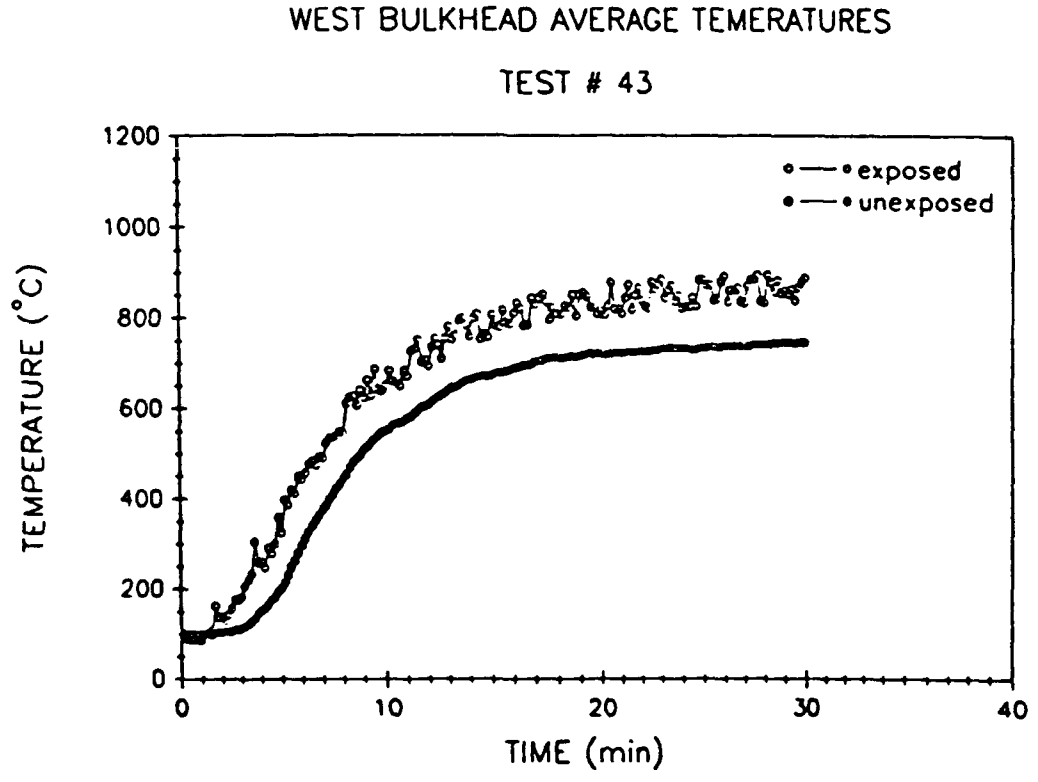

Fig. A147 – West bulkhead average surface temperatures

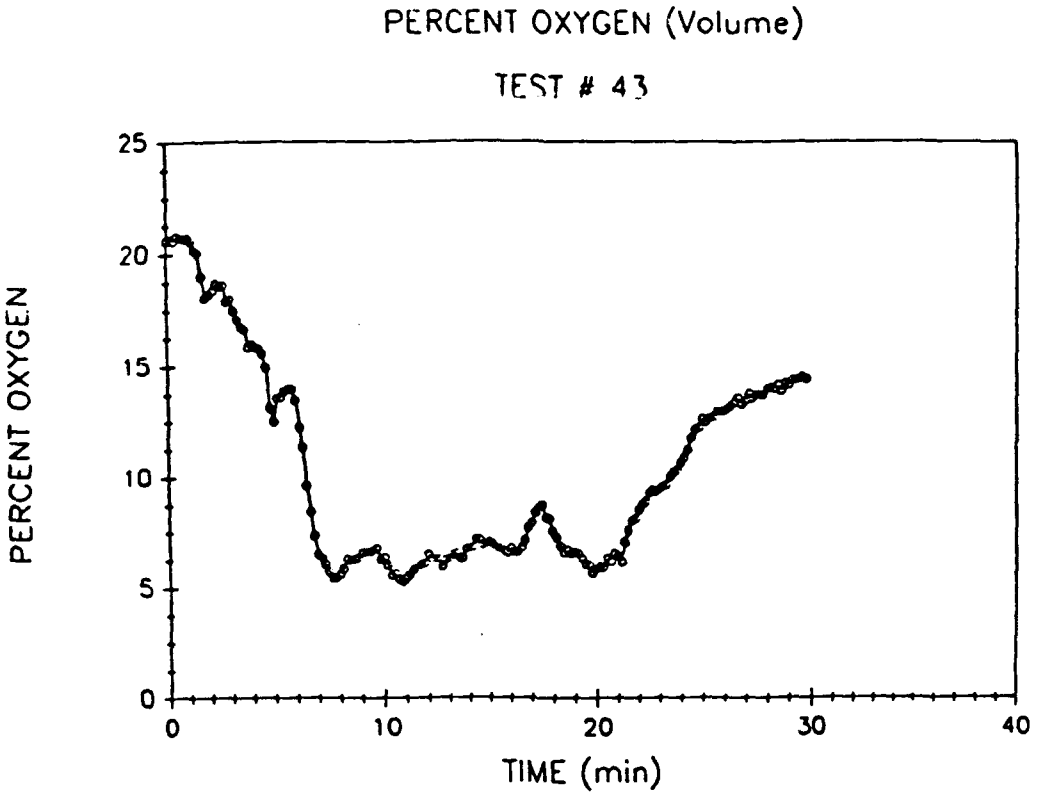

Fig. A148 – Percent oxygen (volume)

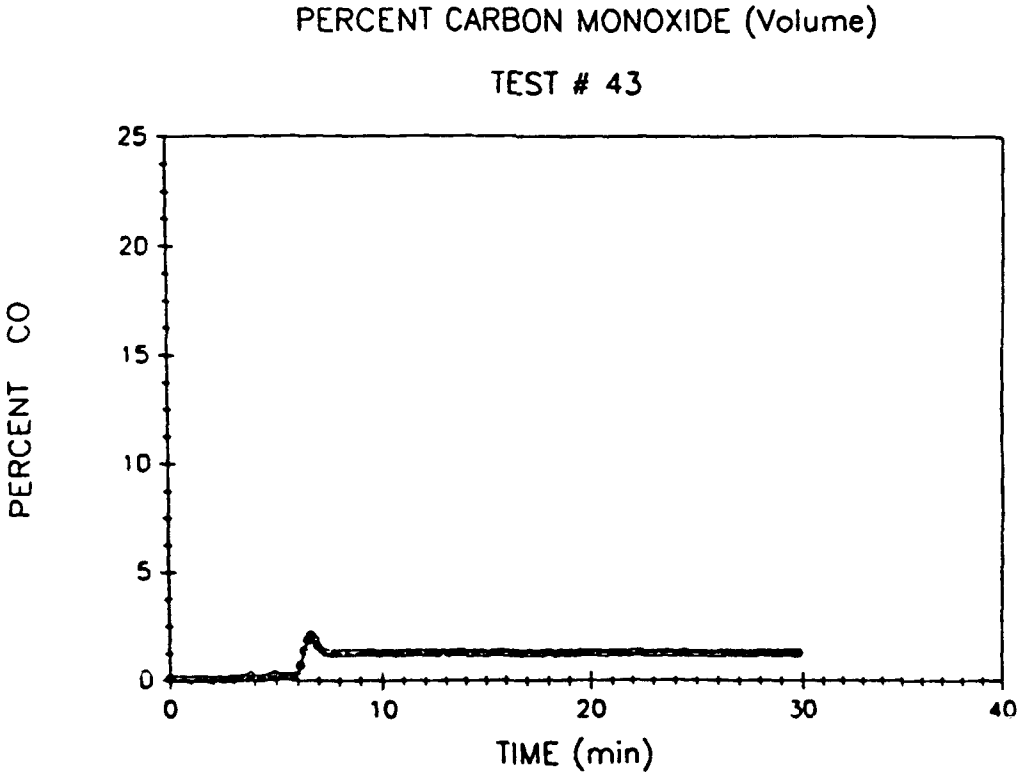

Fig. A149 – Percent carbon monoxide (volume)

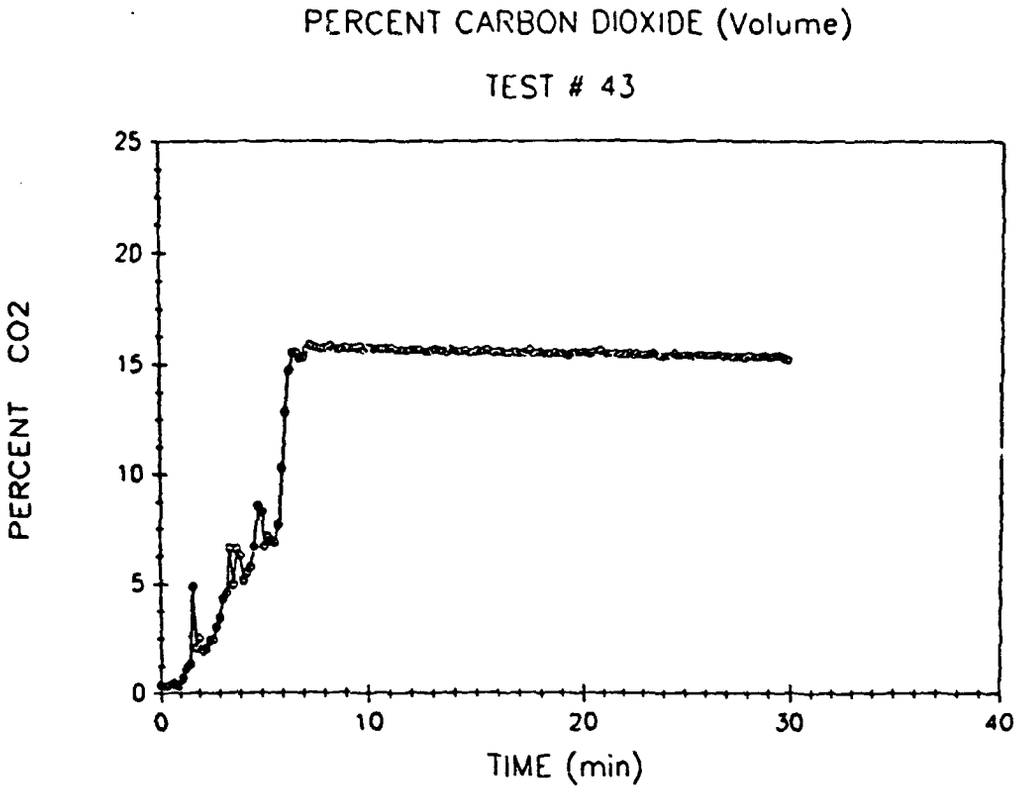

Fig. A150 – Percent corbon dioxide (volume)

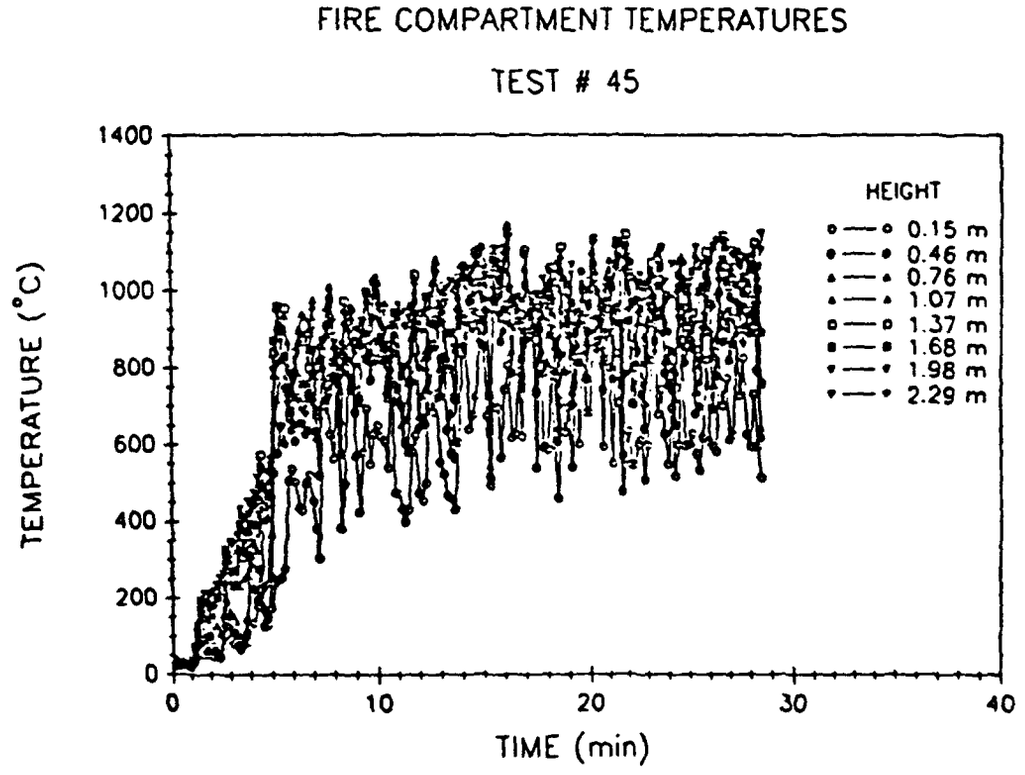

Fig. A151 – Fire comparment air temperatures

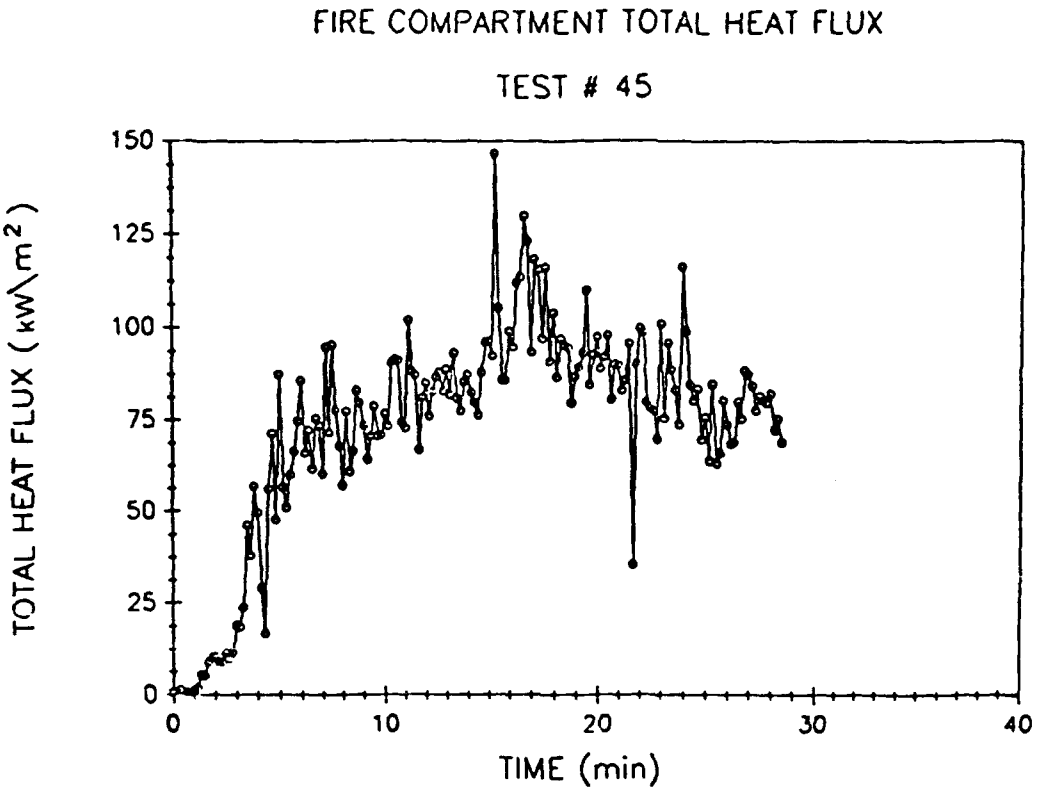

Fig. A152 – *Fire compartment total heat flux*

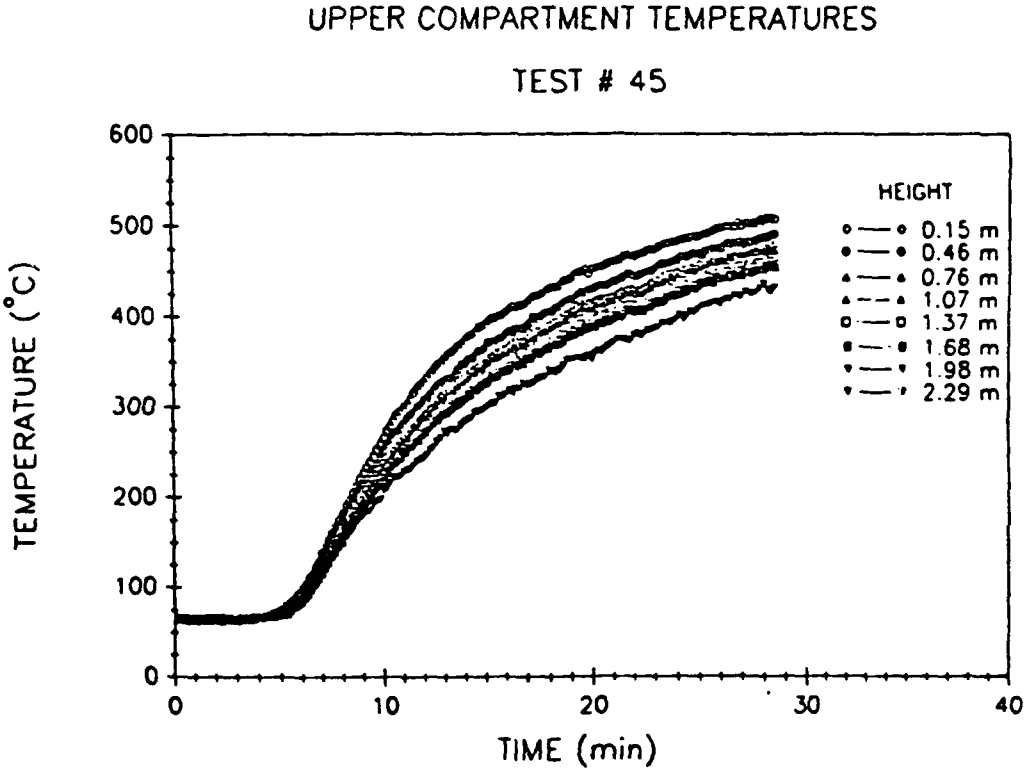

Fig. A153 – Upper compartment air temperatures

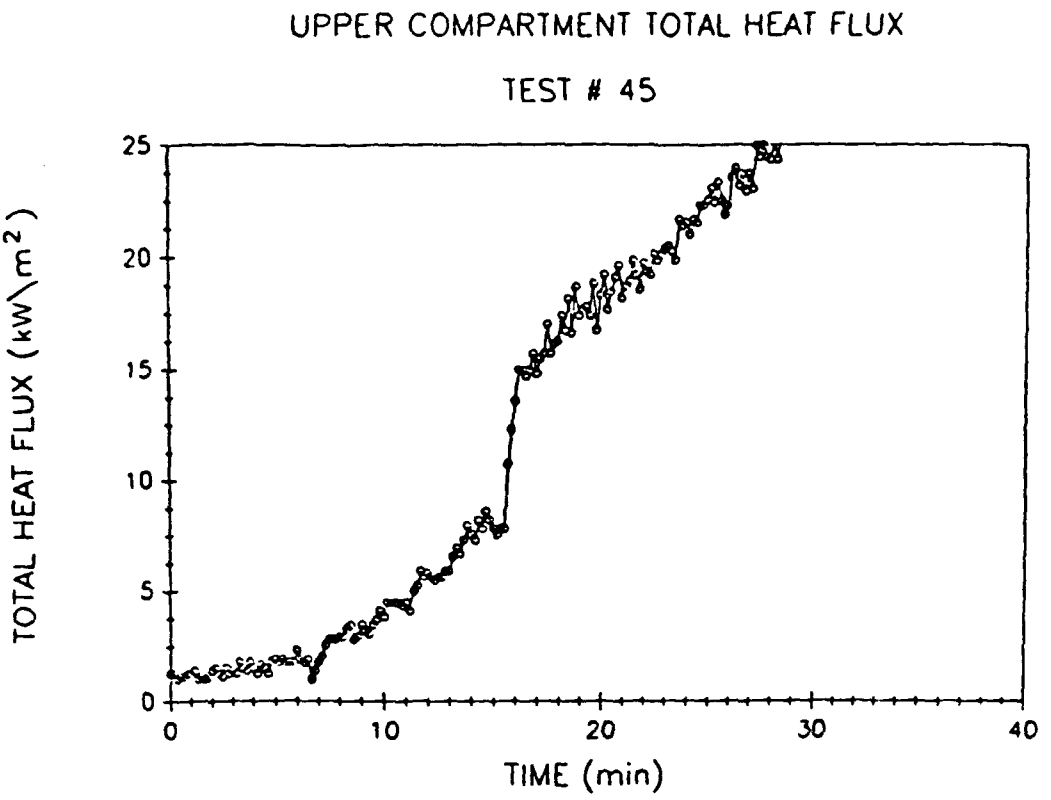

Fig. A154 – Upper compartment total heat flux

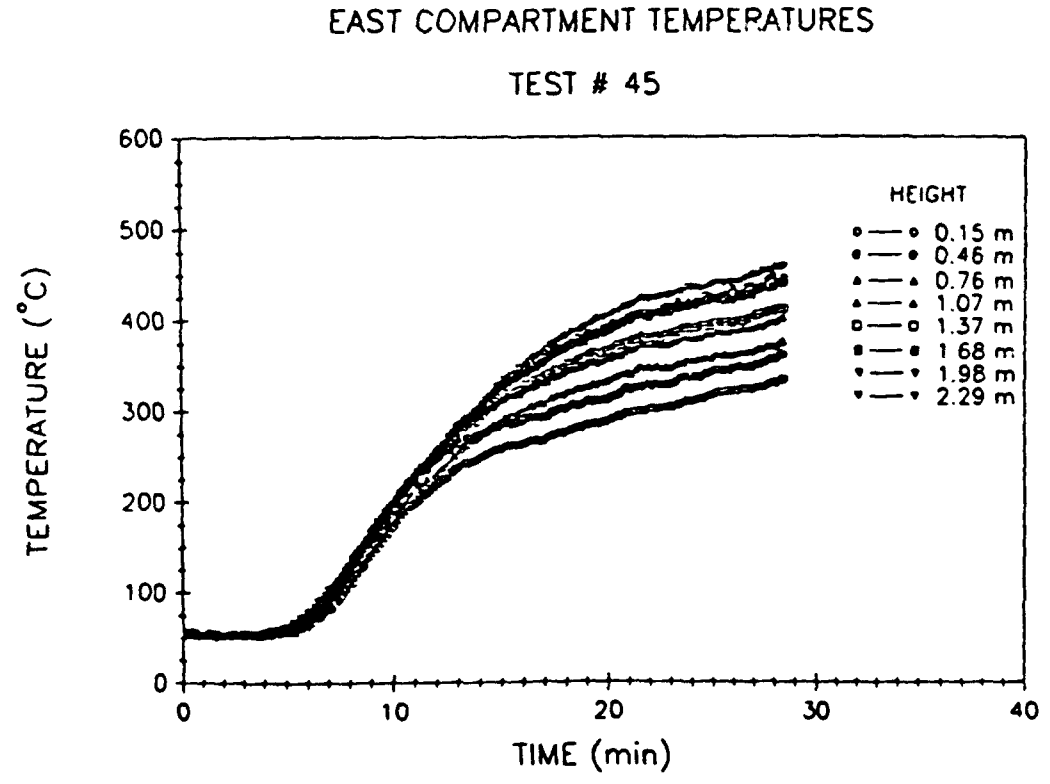

Fig. A155 – East compartment air temperatures

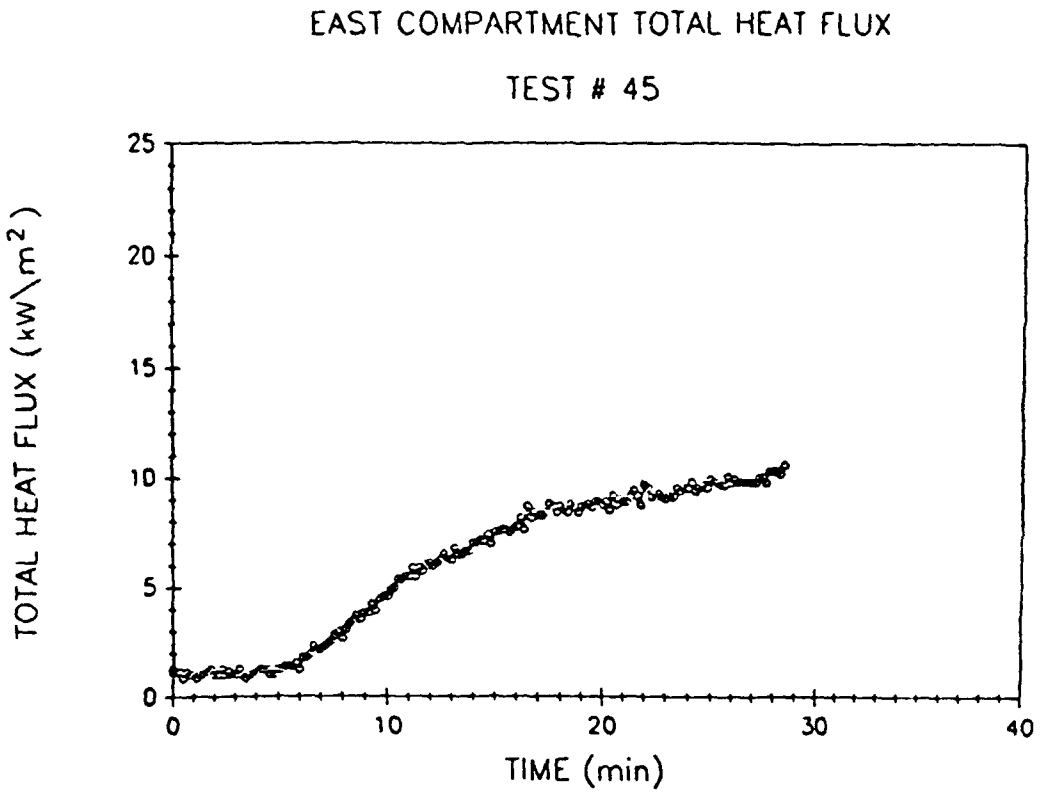

Fig. A156 – East compartment total heat flux

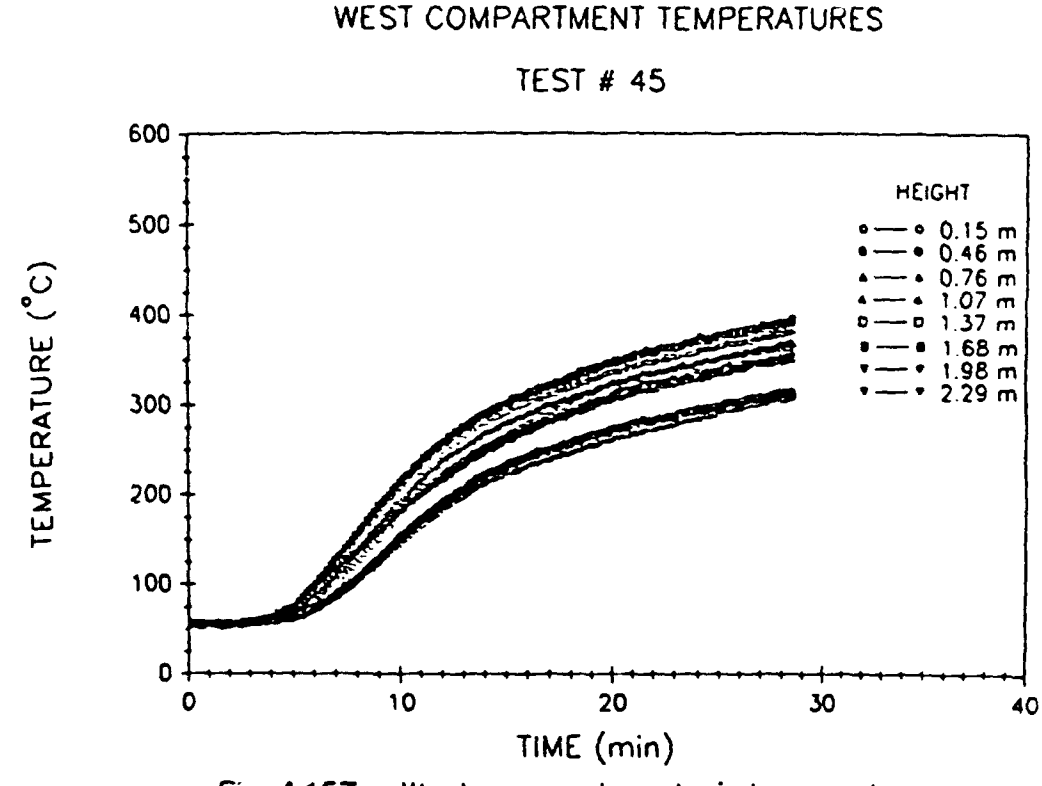

Fig. A157 – West compartment air temperatures

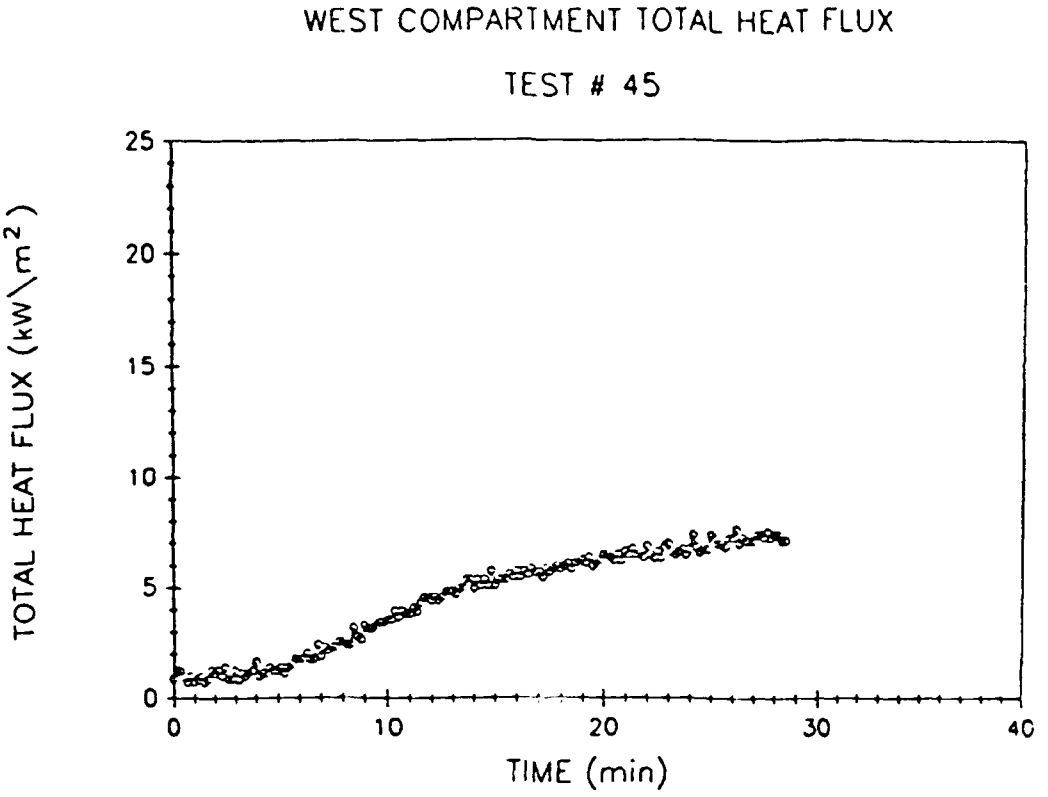

Fig. A158 – West comportment total heat flux

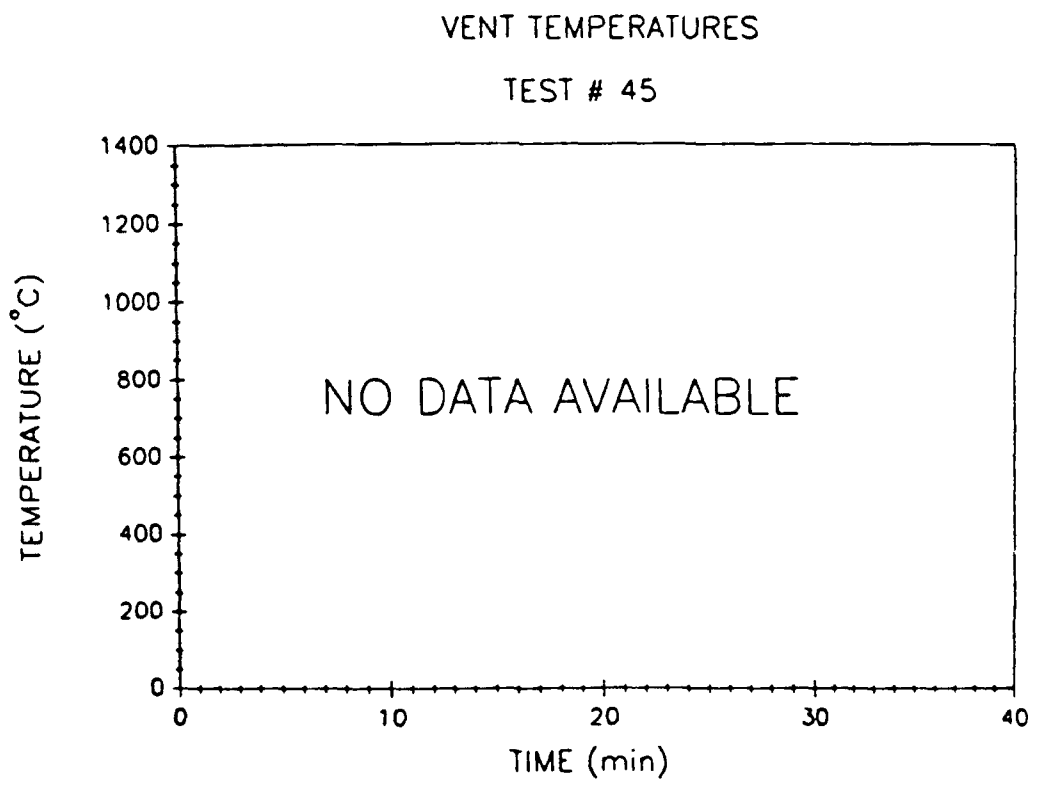

Fig. A159 – Vent air temperatures

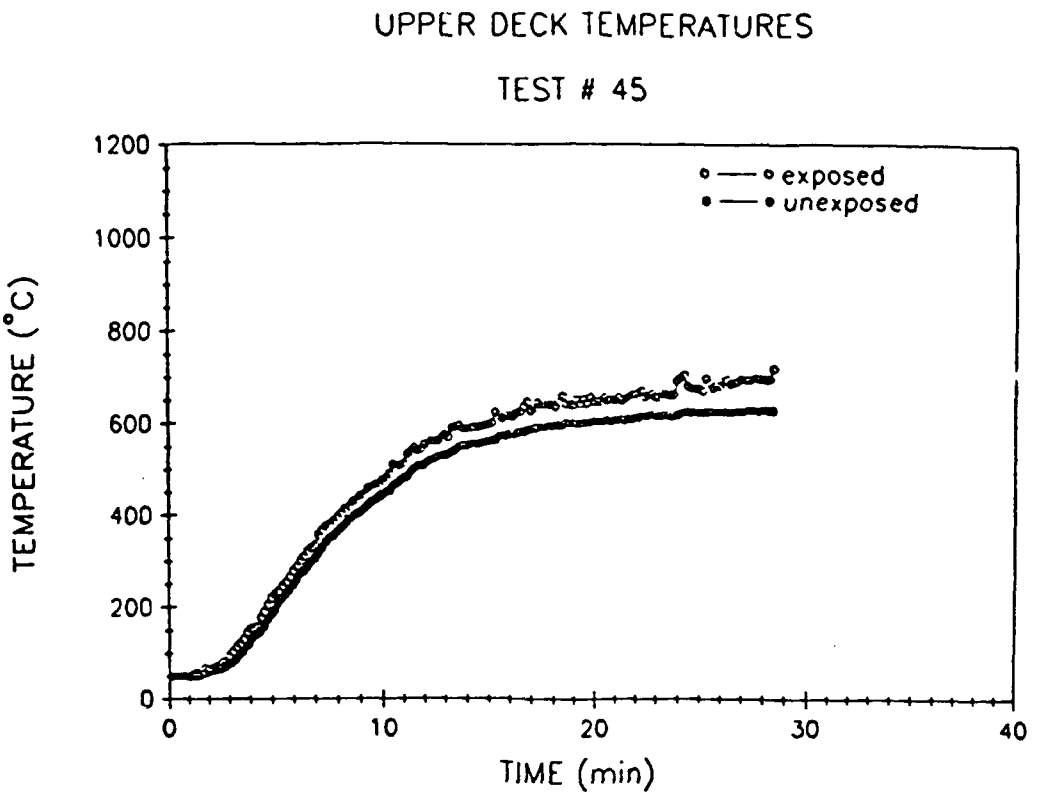

Fig. A160 – Upper deck surface temperatures

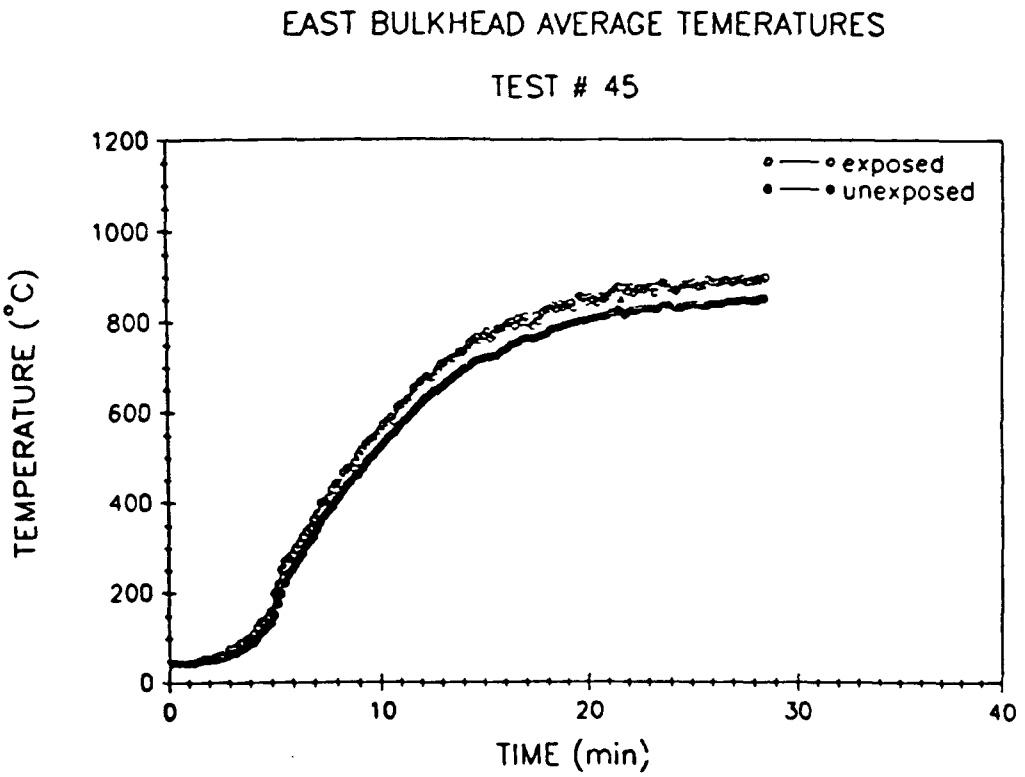

Fig. A161 – East bulkhead average surface temperatures

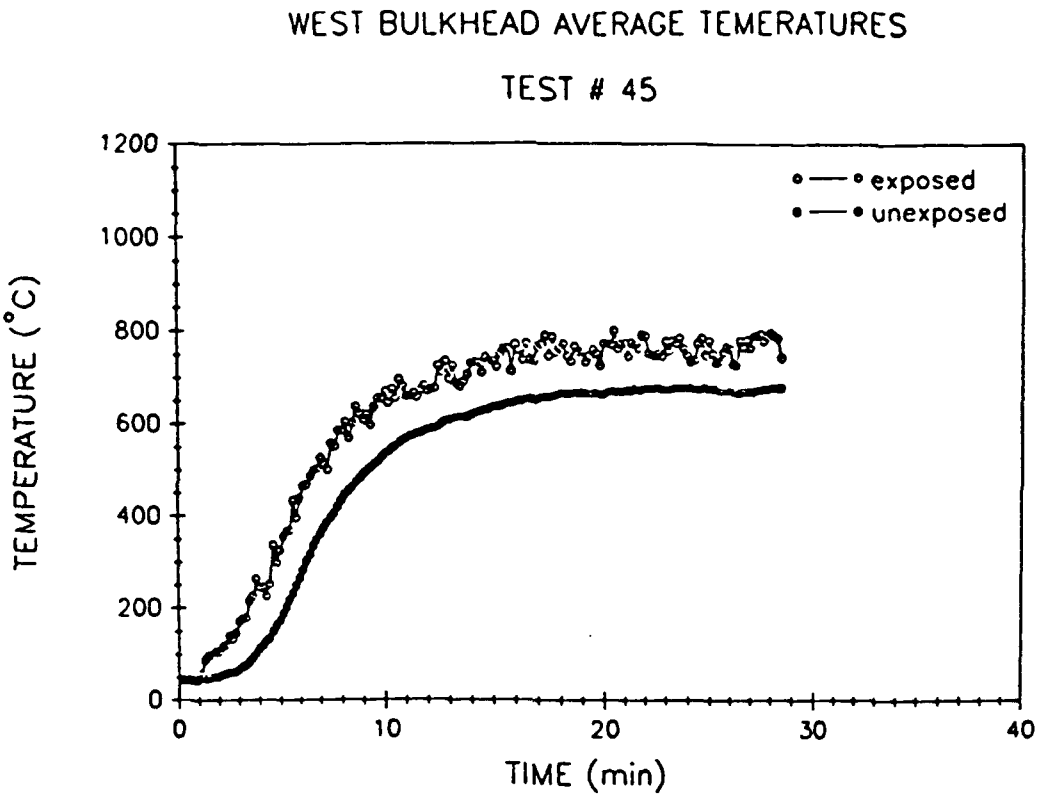

Fig. A162 – West bulkhead average surface temperatures

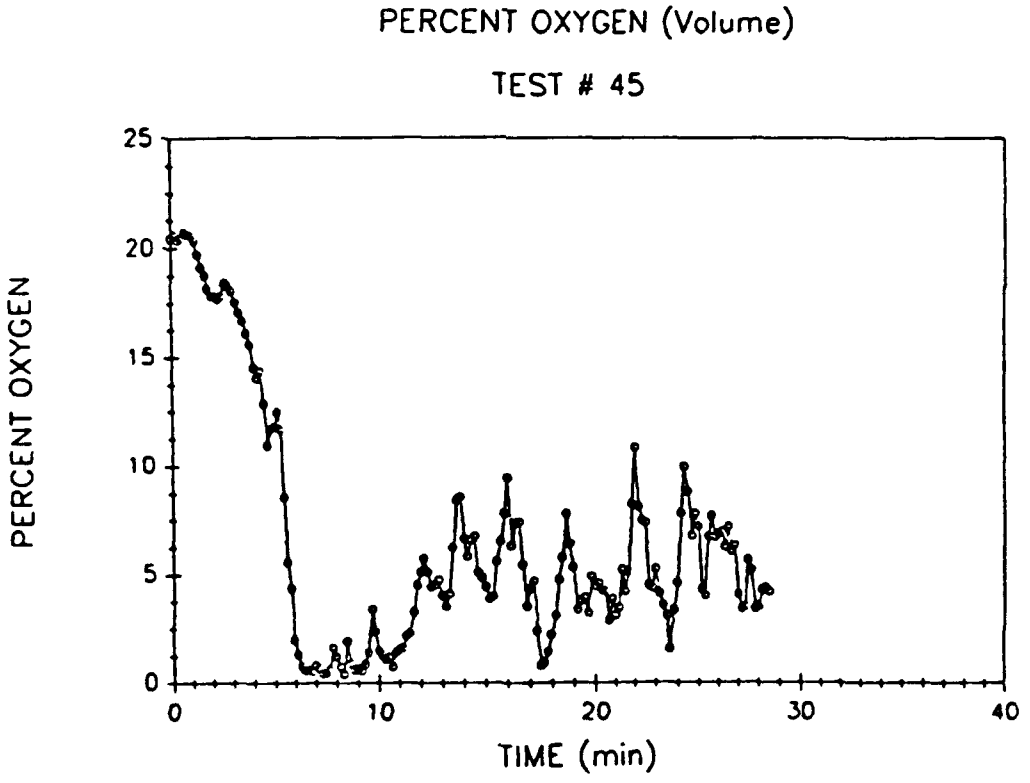

Fig. A163 – Percent oxygen (volume)

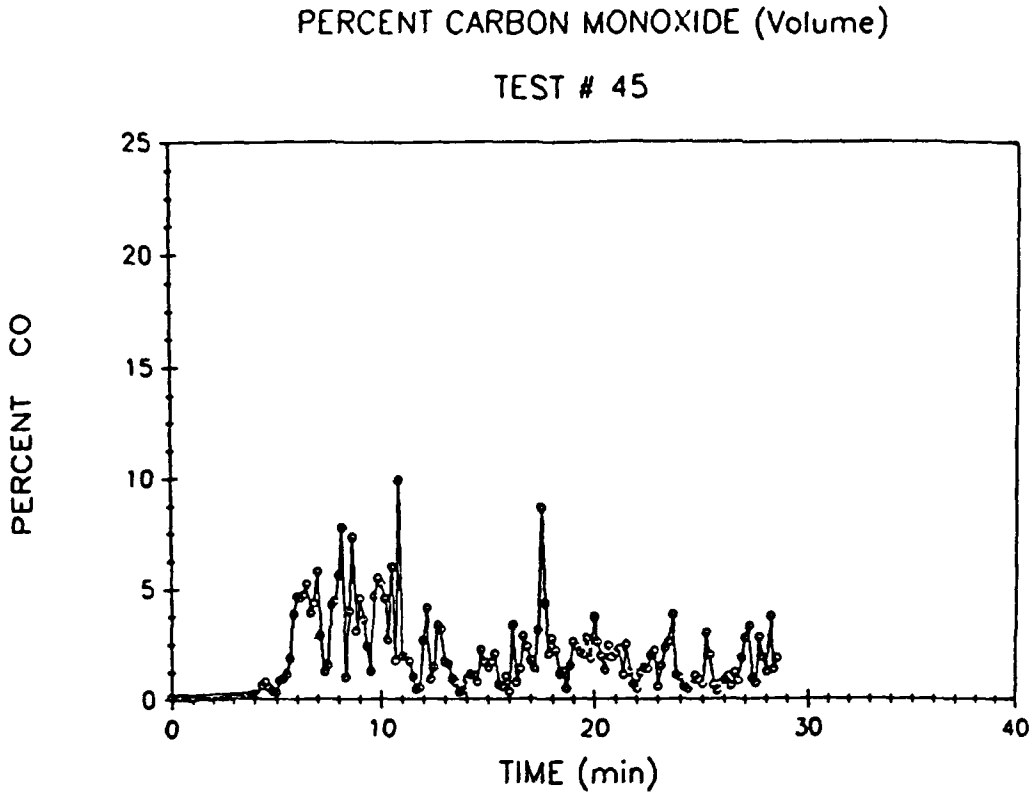

Fig. A164 – *Percent carbon monoxide* (volume)

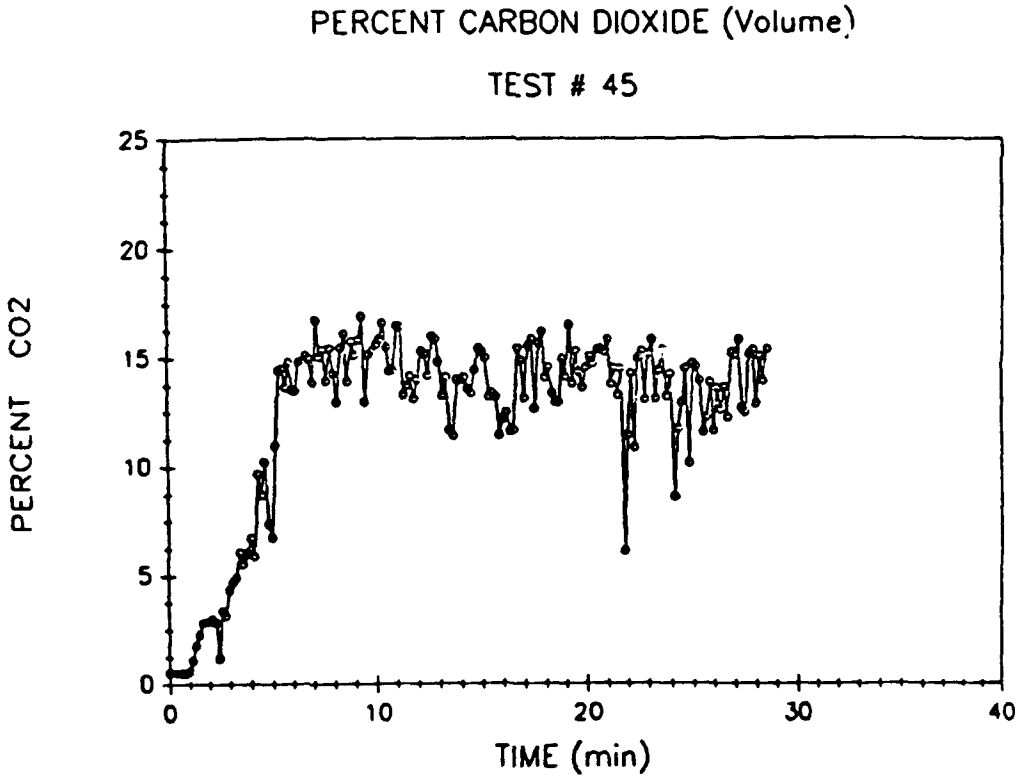

Fig. A165 – Percent carbon dioxide (volume)

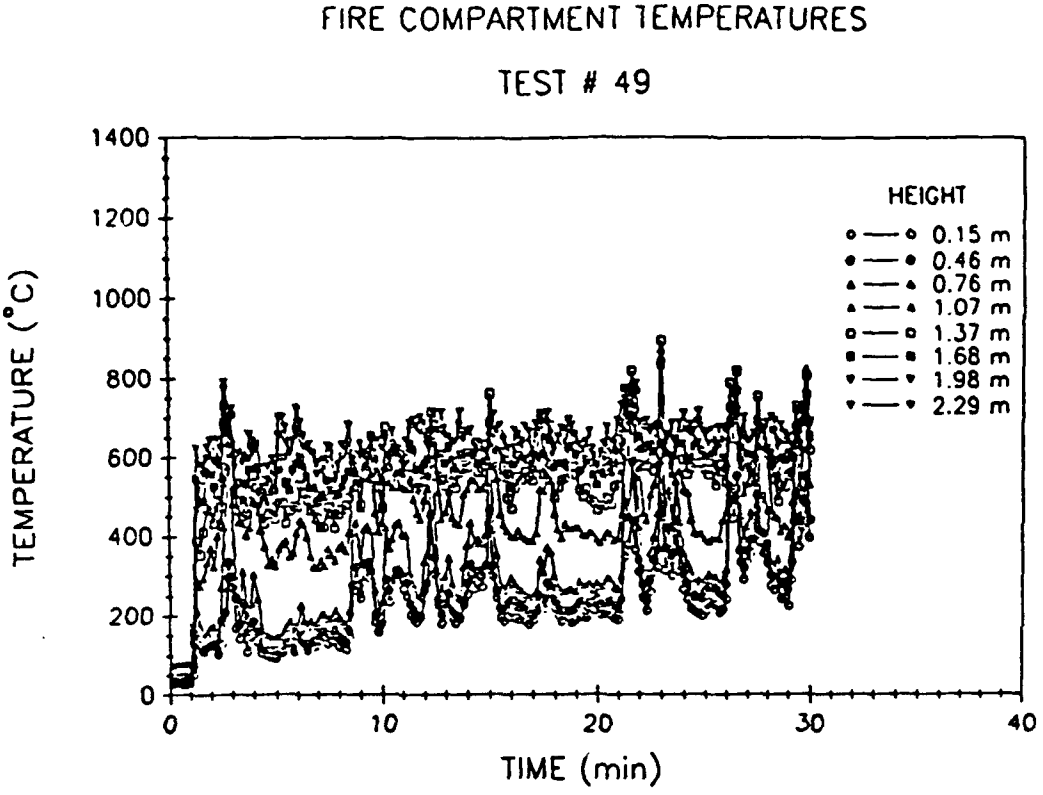

Fig. A166 – Fire comporment air temperatures

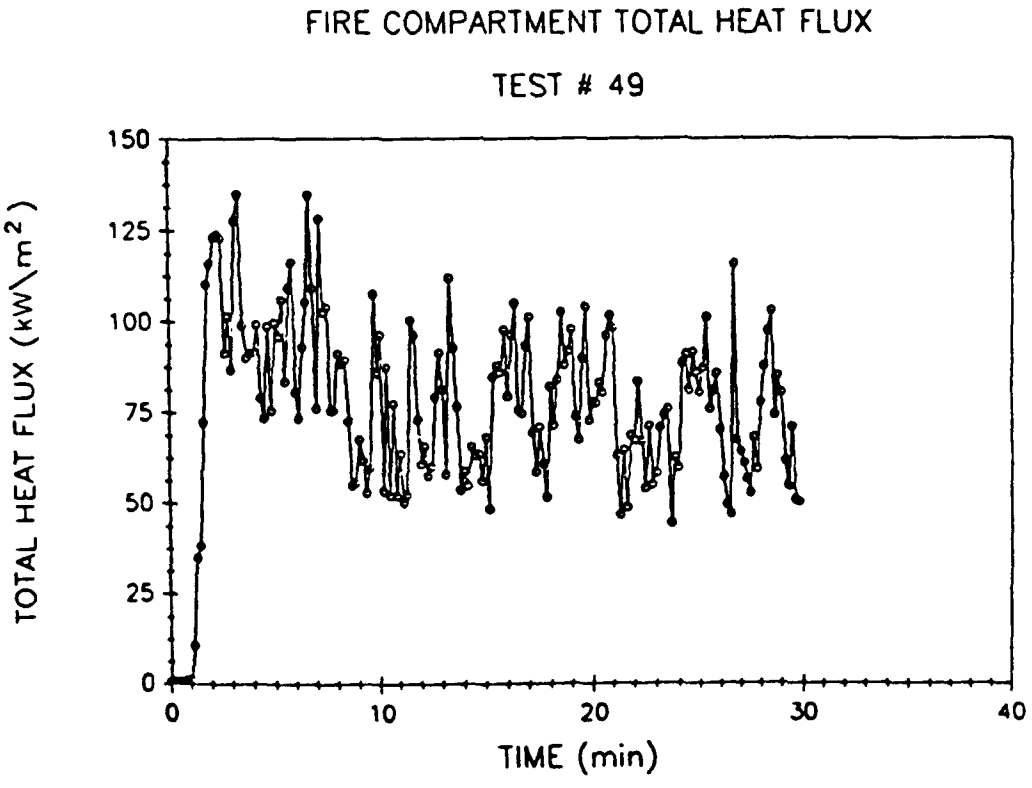

Fig. A167 – Fire compartment total heat flux

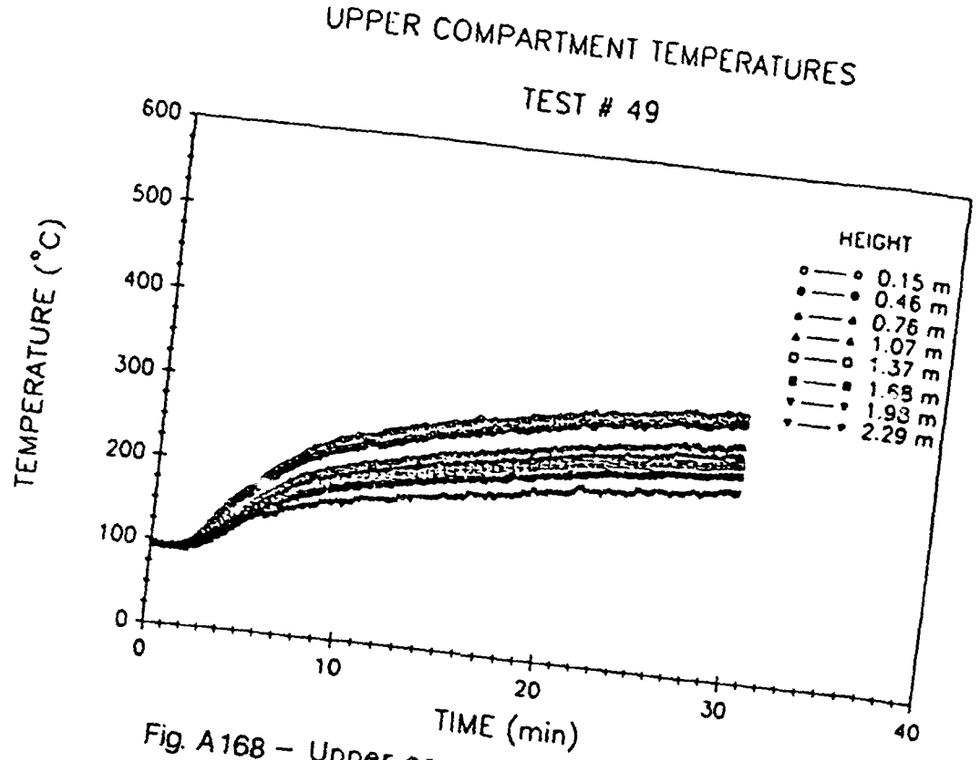

Fig. A168 – Upper compartment air temperatures

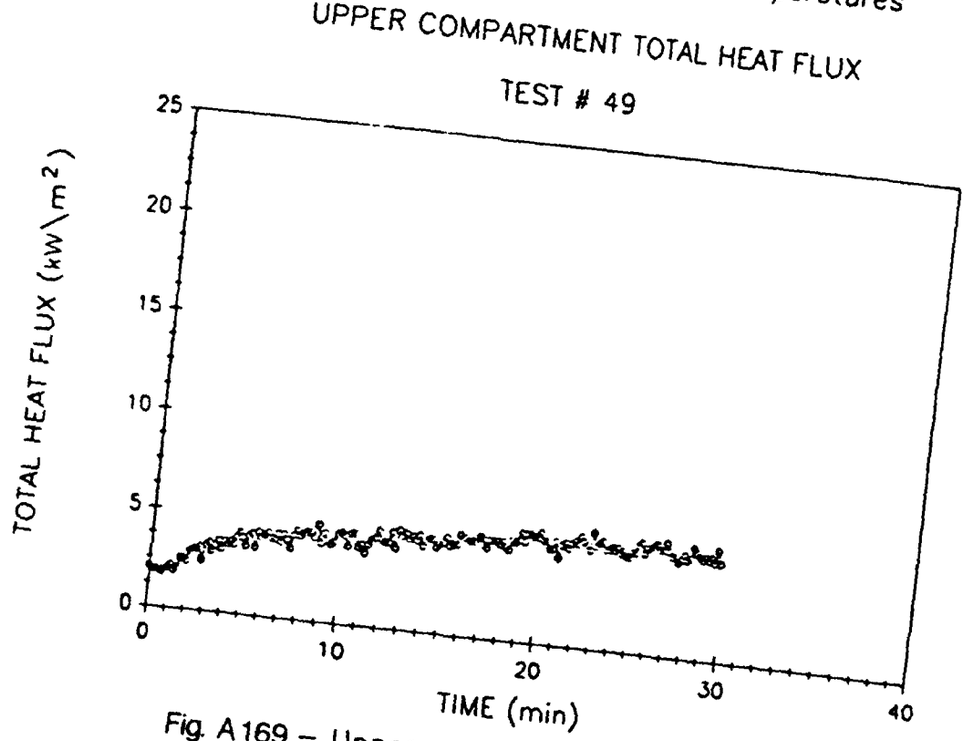

Fig. A169 – Upper compartment total heat flux

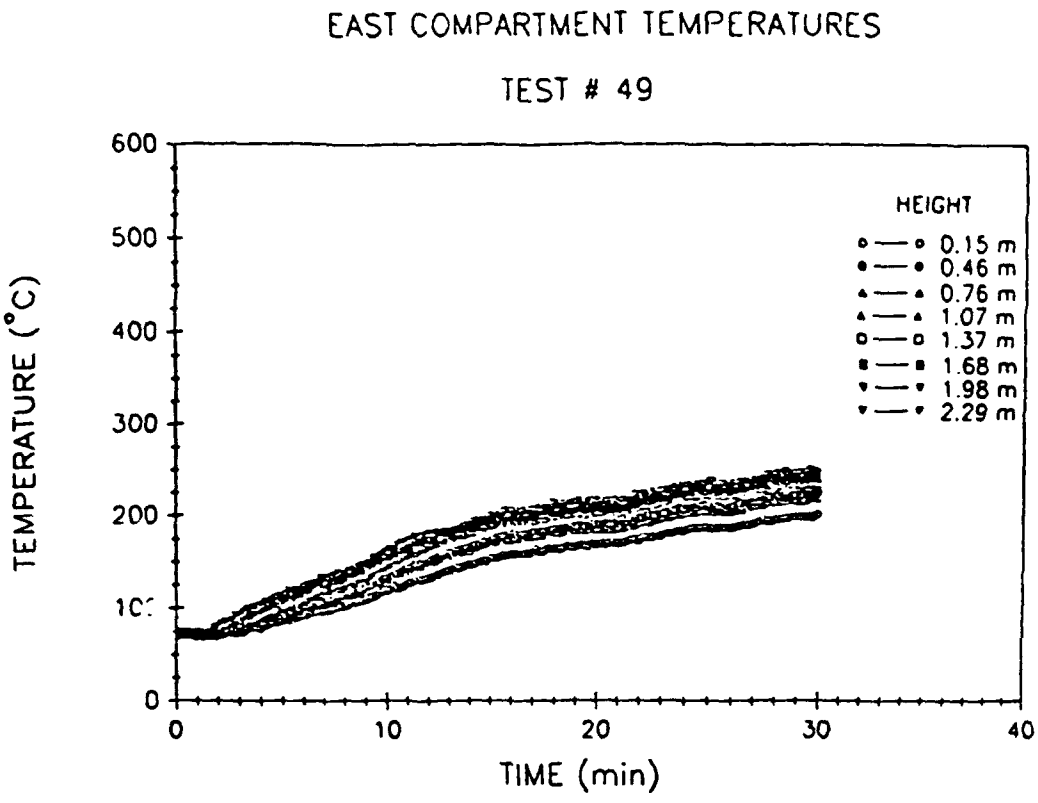

Fig. A170 – East compartment air temperatures

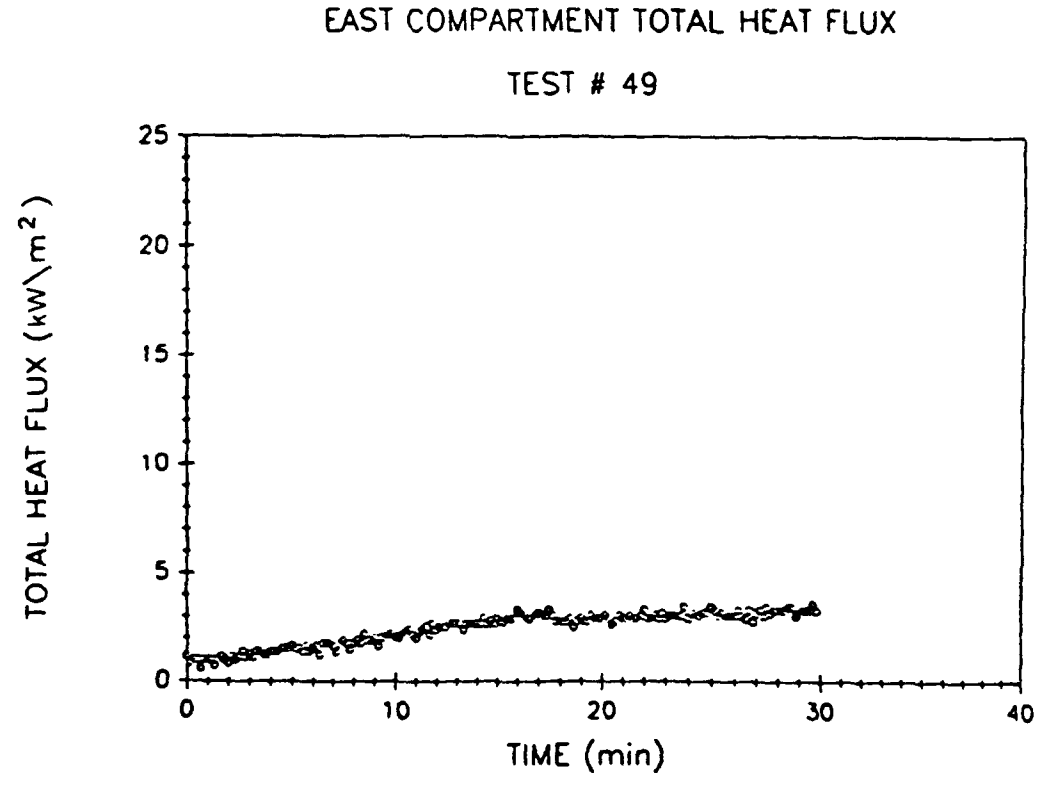

Fig. A171 – East compartment total heat flux

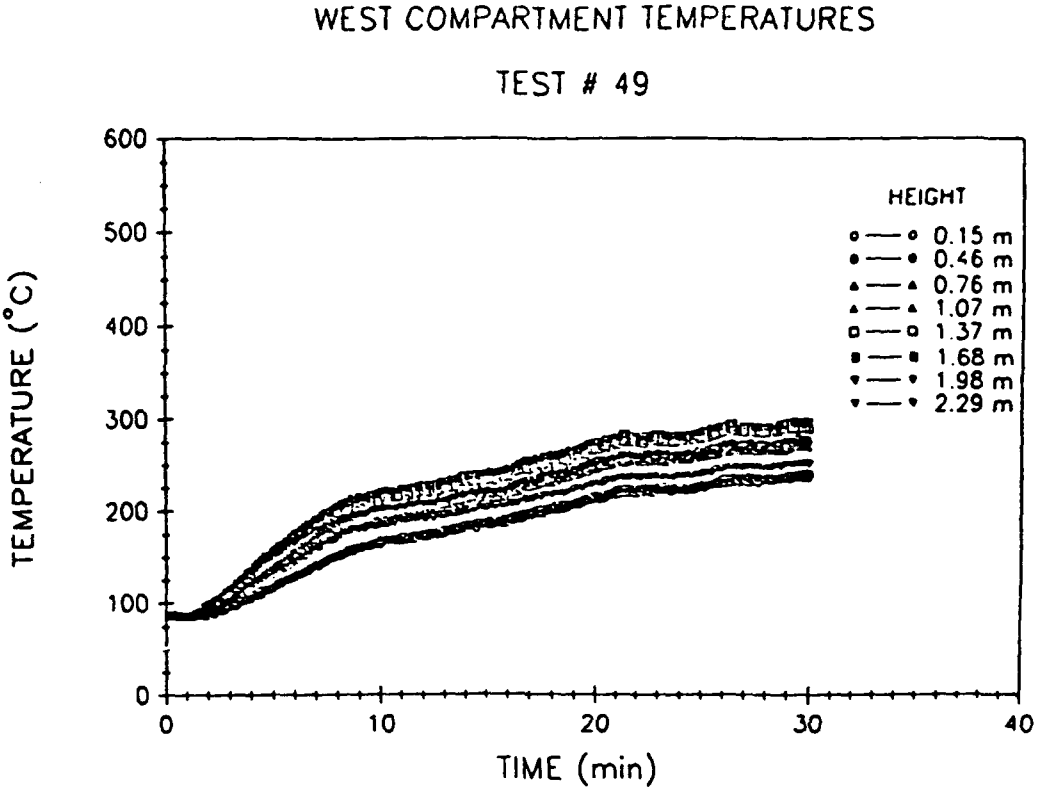

Fig. A172 – West compartment air temperatures

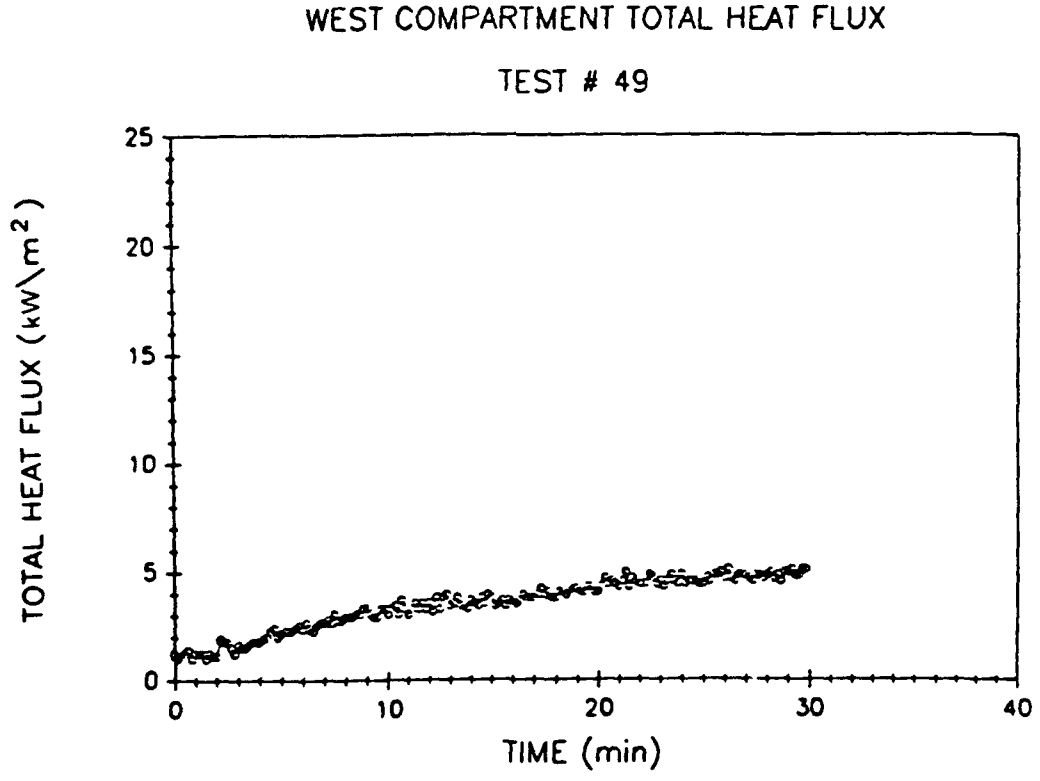

Fig. A173 – West compartment total heat flux

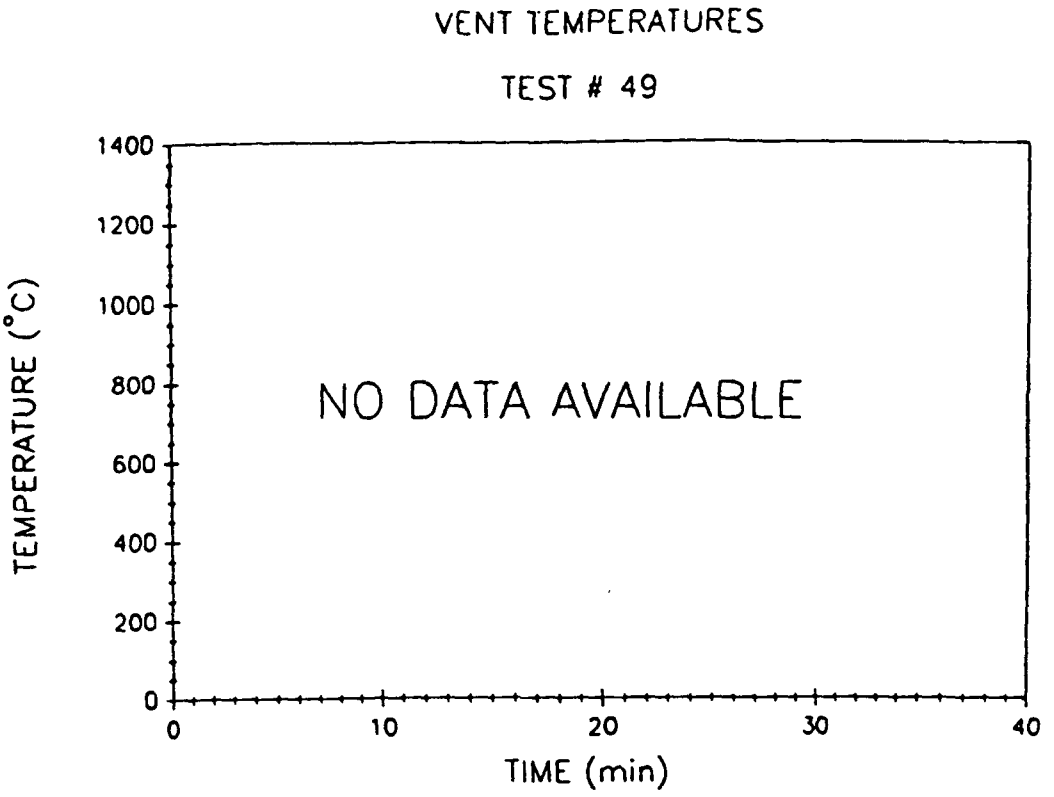

Fig. A174 – Vent air temperatures

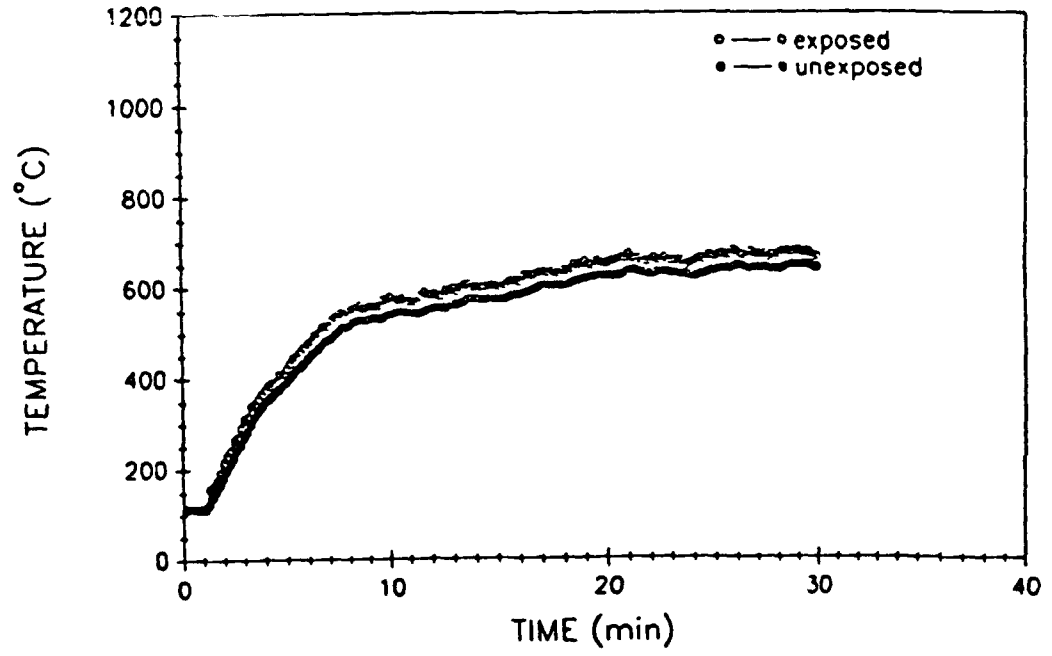

Fig. A175 – Upper deck surface temperatures

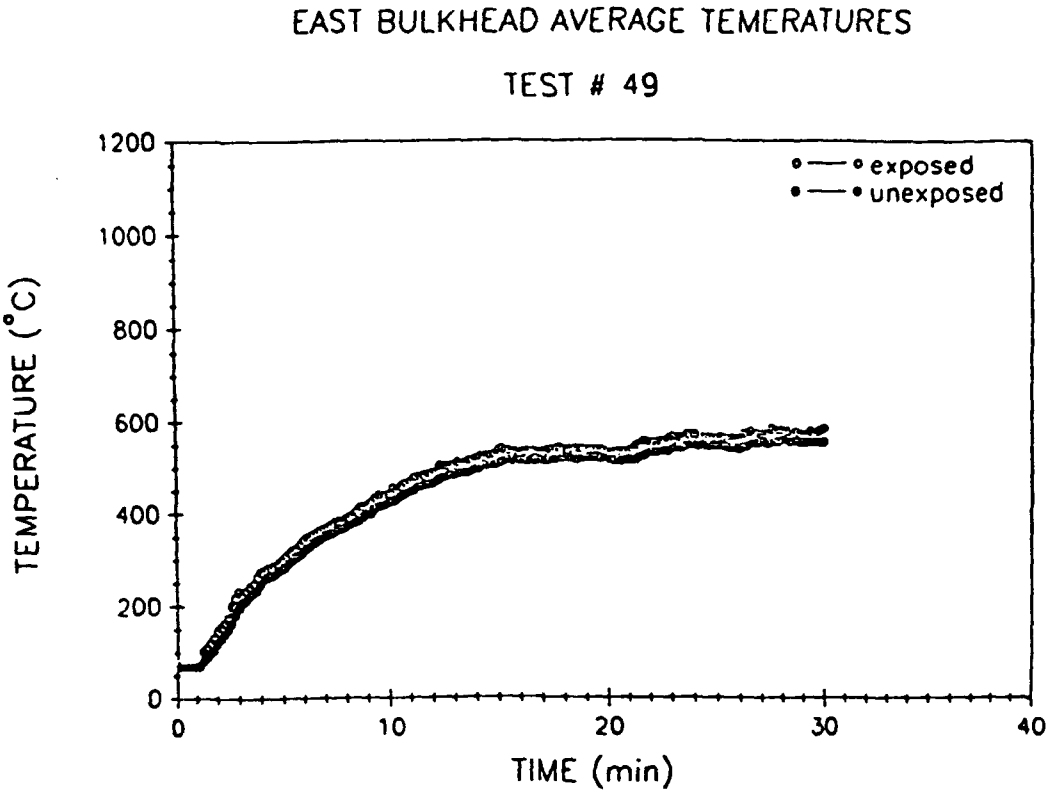

Fig. A176 – East bulkhead average surface temperatures

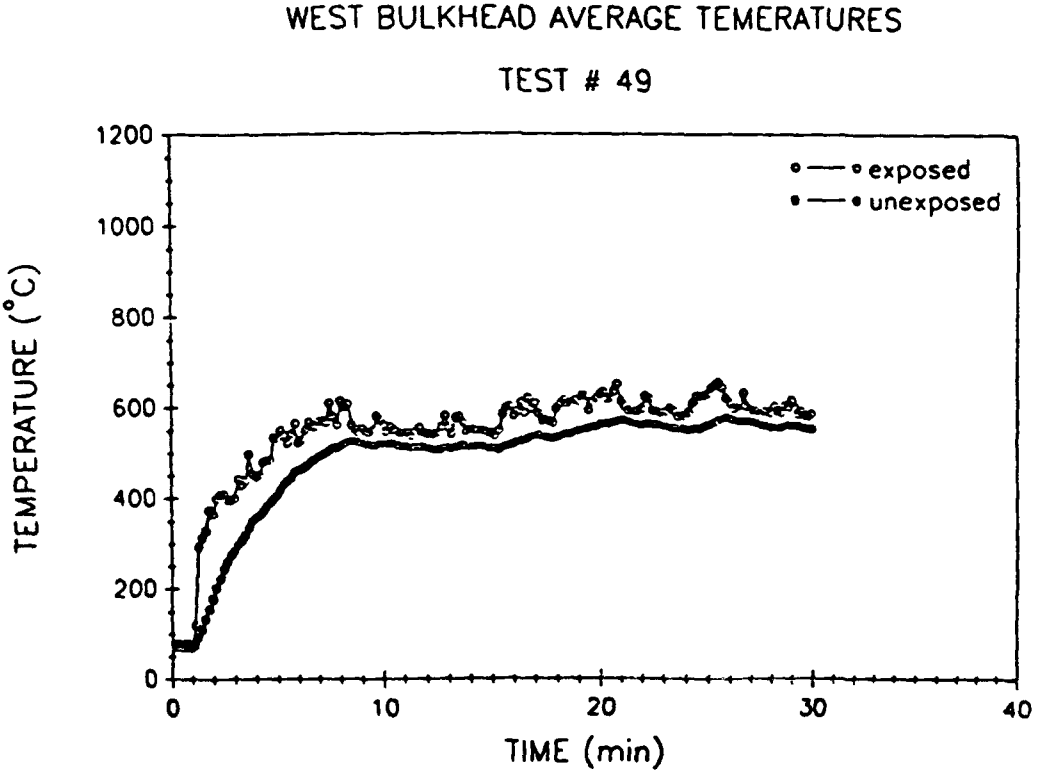

Fig. A177 – West bulkhead average surface temperatures

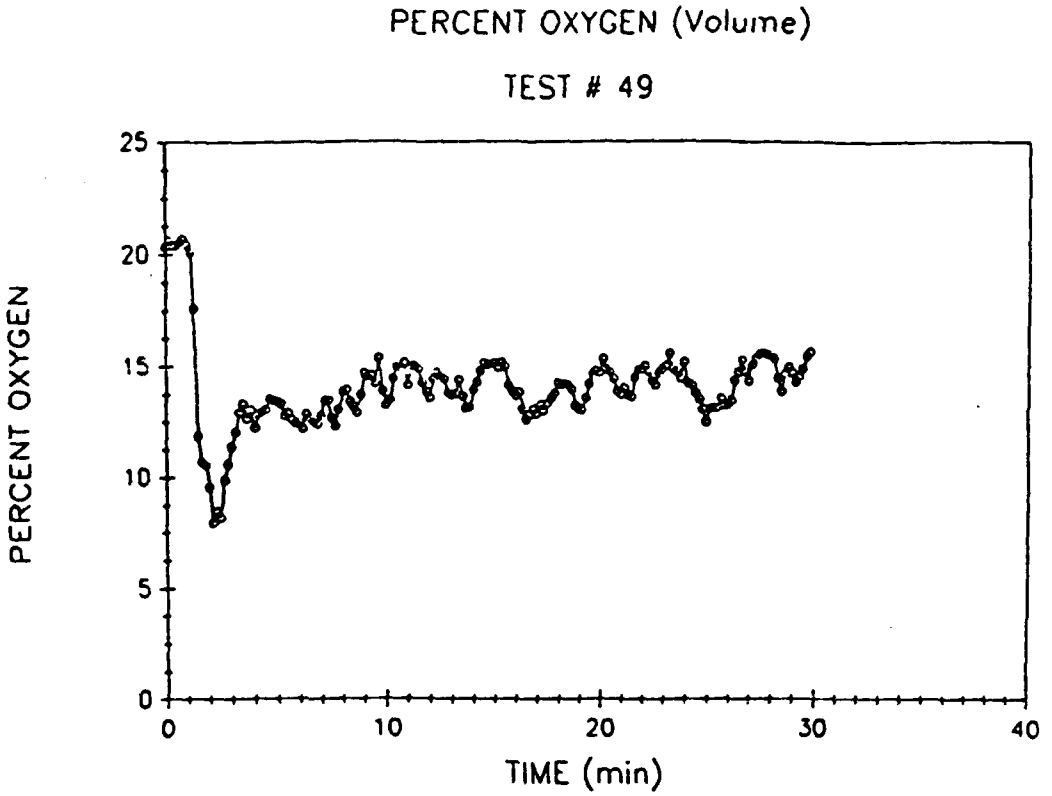

Fig. A178 – *Percent oxygen (volume)*

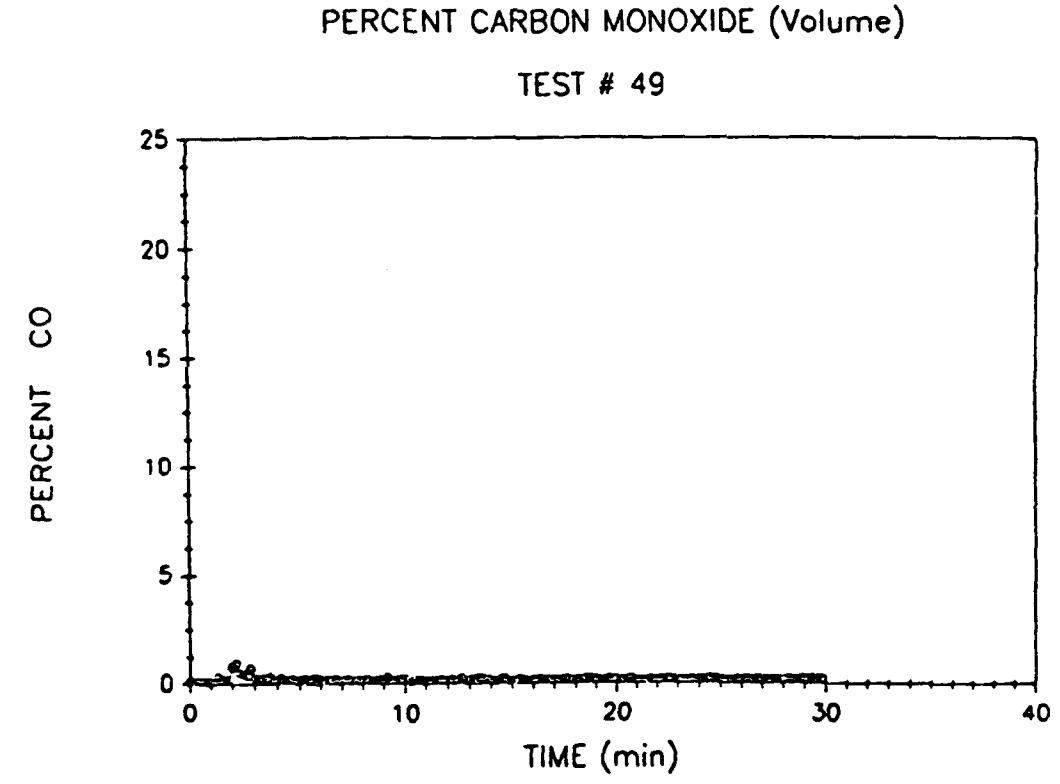

Fig. A179 – Percent carbon monoxide (volume)

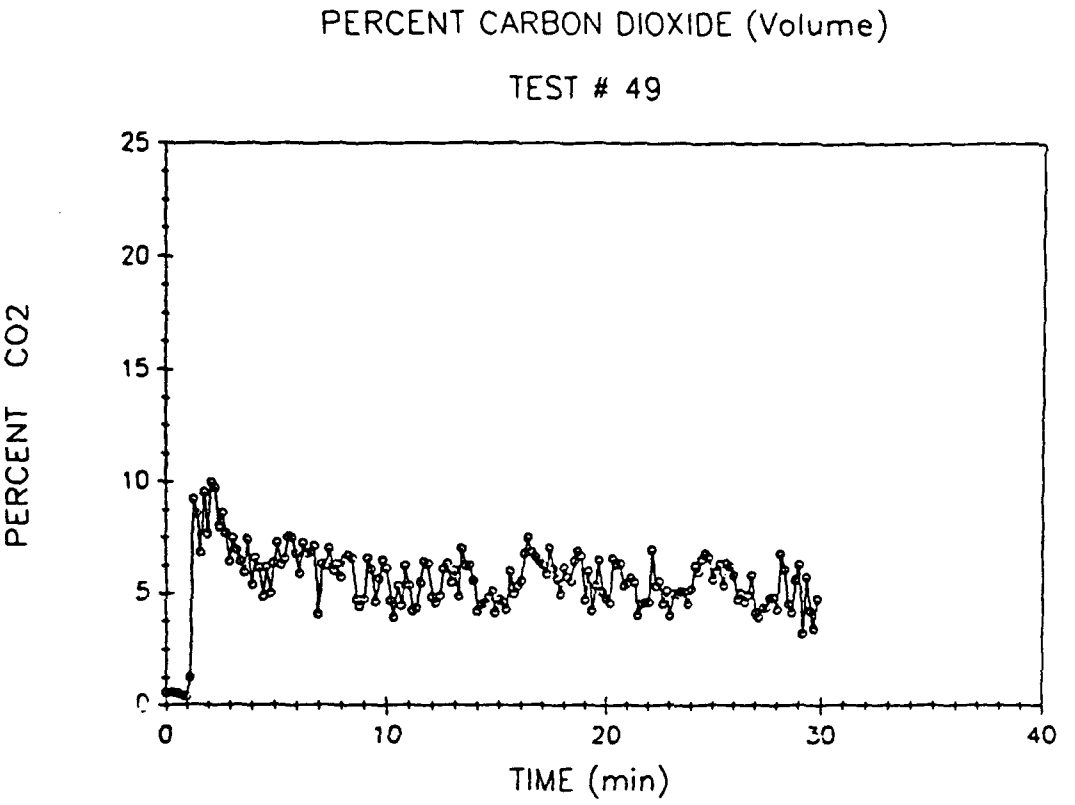

Fig. A180 – Percent carbon dioxide (volume)

Appendix B

Fire Compartment Modeling

Appendix B

Fire Compartment Modeling

This is a brief analysis of the compartment fire tests conducted under the Internal Ship Conflagration Control (ISCC) program initiated to address issues raised by the missile-induced fire on the USS STARK. This analysis focused on the conditions created in the fire compartment.

The tests conducted were designed to vary the ventilation to the compartment by varying the number of doors opened and to vary the supply of JP-5. The JP-5 was sprayed tangentially across the surface of a fuel pan. This design allowed for experiments to be conducted over a range of opening sizes and compartment stoichiometry. Simple examination of the data was sufficient to observe a characteristic increase in temperature with fuel supply rate as stoichiometric conditions were approached and a modest reduction in temperature with supply as the compartment conditions became fuel rich. Further, as the compartment ventilation increased, the compartment temperatures tended to increase overall as expected based on reduced heat losses to the walls for larger openings at constant stoichiometry. Because the trends were generally as one would expect (with some exceptions) it seemed worthwhile attempting some simple modeling of the compartment fire combustion.

The fires were modeled using the steady state energy equation for the compartment.

$$\dot{Q} = \dot{m} c_p \Delta T + h A_t \Delta T$$

where:

$$\dot{Q} = \min (\dot{Q}_f, \Delta H_{air} \dot{m})$$

where m is taken as the air inflow rate (and the total exhaust rate, i.e., fuel mass is ignored), h is the linearized heat loss coefficient, T is the compartment temperature rise, A_t is the total interior lining area, Q_f is the heat release rate if all fuel burns, and H_{air} is the heat of reaction of air. The mass flow into the compartment is modeled as:

$$\dot{m} = 0.5 A_v \sqrt{H_v} (1-D^2)^{3/2}$$

where A_v is the vent area, H_v is the vent height, and D is the location of the hot layer interface above the base of the vent divided by the vent height. D is bounded by 0 and 1. In these calculations the interface is assumed to be at the height of the pool. The D correction is included to reflect the effect of burner height on the compartment fire.

The above model was used in conjunction with the experimental data to deduce the linearized heat loss coefficient, h. The values of h found ranged from 0.03 to 0.15 kW/m^2K. There was no systematic trend of h with temperature. There was a small systematic increase in h with the vent area. Overall the model was unable to describe the experimental results. In particular, despite the constant compartment size no simple expression for h was able to reproduce the resulting compartment temperatures with even fair accuracy.

The oxygen concentration in the exhaust flow of many experiments was nonzero for conditions which according to the model the fire was ventilation limited. As a result the measured oxygen concentrations were plotted as a function of the estimated equivalence ratio in Figure 1 to help diagnose this discrepancy.

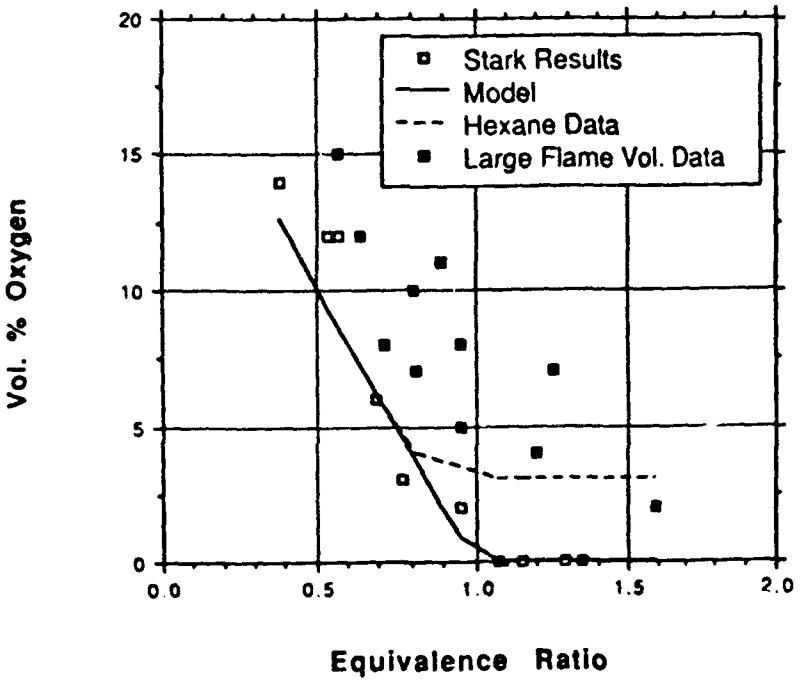

Figure 1. Measured oxygen concentration in the exhaust as a function of the estimated equivalence ratio.

The symbols in Figure 1 represent the Stark compartment fire test results. The solid line is the expected result based on the simple combustion model used here. The dashed line is a faired curve for results obtained for hexane in small scale hood

experiments by the author (Beyler (1983)). It can be seen that the oxygen concentrations were often much larger than expected. While some of the discrepancies can be the result of the estimation procedures for determining the equivalence ratio in the present model, such errors cannot explain the results fully. The higher oxygen concentrations suggest that the combustion reactions are not proceeding to completion in the compartment, presumably due to insufficient mixing.

This behavior has been observed in other experiments. In particular the author was able to show that erroneous CO measurements in compartment fires using an unquenched probe could be identified on the basis of the ratio of the flame volume to the compartment volume (Beyler (1986)). When this ratio is sufficiently high, reactions in the compartment were not completed prior to sampling. Extra CO was formed due to mixing of fuel and air in the uncooled probe. In that investigation the flame volume was estimated based on a volumetric heat release rate of 1200 kW/m^3 (observed by Rasbash and by Orloff & deRis (1982)). The critical ratio of the flame to the compartment volume was 0.165. The behavior of the measured CO yield with the flame to compartment volume ratio is shown in Figure 2.

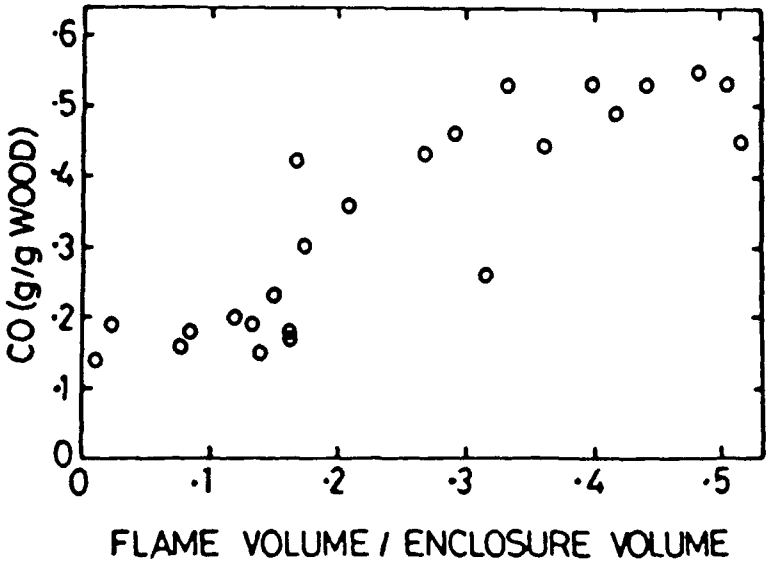

Figure 2. The CO yield measured as a function of the flame to compartment volume ratio (from Beyler (1986))

In Figure 1, the experiments in which the estimated flame to compartment volume ratio is greater than 0.2 are shown as solid symbols. This criterion is clearly able to distinguish between experiments which conform to the simple model and those which do not. This indicates that many of the experiments were conducted under conditions which did not allow the combustion reaction to proceed to completion in the compartment. In essence, those experiments with volume ratios greater than 0.2 are best

characterized as experiments in which the flame was deflected out the vent by the compartment, while experiments with volume ratios less than 0.2 are best characterized as well stirred compartments.

Clearly, models based on well-stirred compartment fire environments cannot reproduce the results of compartment fires in which the well-stirred assumption is not fulfilled. Despite this a plot of temperature as a function of $A_t/A_v\sqrt{H_v}$ shown as Figure 3 ("Thomas plot") does show a trend. The parameter, $A_t/A_v\sqrt{H_v}$, is a representation of the ratio of the energy flow through the wall to the energy convected through the opening, a parameter of clear importance in well-stirred compartment fires. Of course this type of plot does not include the effects of variable stoichiometry.

As Figure 3 shows, the vast majority of two and three door tests were not well-stirred compartment fires. With the exception of one data point, these nonwell-stirred fires had compartment temperatures of 900-1100°C (1652-2012°F). Measurements of maximum temperatures in an open fire are generally 1000°C (1832°F) (Beyler (1986)). This supports the interpretation that the flames in the two and three door tests were not well-stirred and are better characterized as bent open flames. This interpretation is further supported by the observation that the maximum temperatures observed in the CIB well insulated compartment fire test series (Thomas and Heselden (1972)) was approximately the same as in the present steel compartment tests. This indicates that the heat losses from the

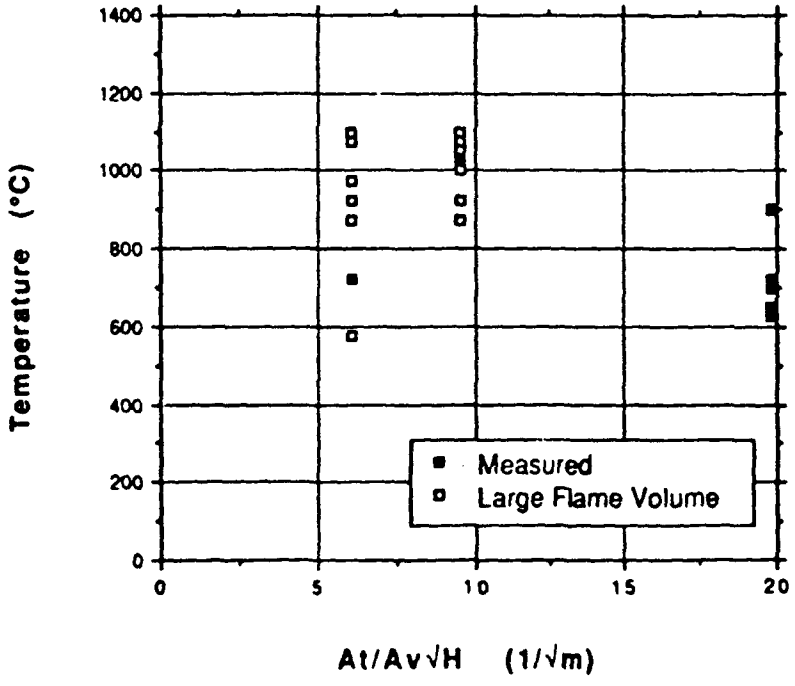

Figure 3. Correlation of compartment temperature with $A_t/A_v\sqrt{H_v}$ (Thomas plot).

compartment do not significant affect the compartment fire temperatures. This is, of course, not consistent with the well-stirred model. It may be that many of the low $A_t/A_v\sqrt{H_v}$ tests in the CIB test series were also not well-stirred and that the Thomas type plot correlates the data because the nonwell-stirred compartment fires occur at low $A_t/A_v\sqrt{H_v}$, i.e. large vent area well developed fire test conditions.

Harmathy (1971) has recognized that all energy is not always released in the fire compartment. He introduced a simple expression for the fraction of the energy released in the compartment, based on cellulosic fire data. According to his expression, all the energy from all the tests in this series should have occurred in the compartment. However, this expression based on cellulosic fuels is not expected to hold for JP-5 fires. Similarly, several Japanese models for combustion inefficiencies may also be applicable, but are not cast in terms which allow their application to this problem.

Having established which fires can be modeled as well-stirred, it was possible to reexamine the performance of the simple model used here. For those experiments where the compartment was well-stirred the value of h varied from 0.036-0.089 kW/m^2K. The results of predictions based on h = 0.045 kW/m^2K are shown in Figure 4. The prediction is respectable for equivalence ratios of less than one. However, the three data points which are fuel-rich are poorly predicted correspond to h values around 0.08 kW/m^2K. The drop off in temperature in these experiments is unexpectedly large. In general, the temperature drop off on the rich side of

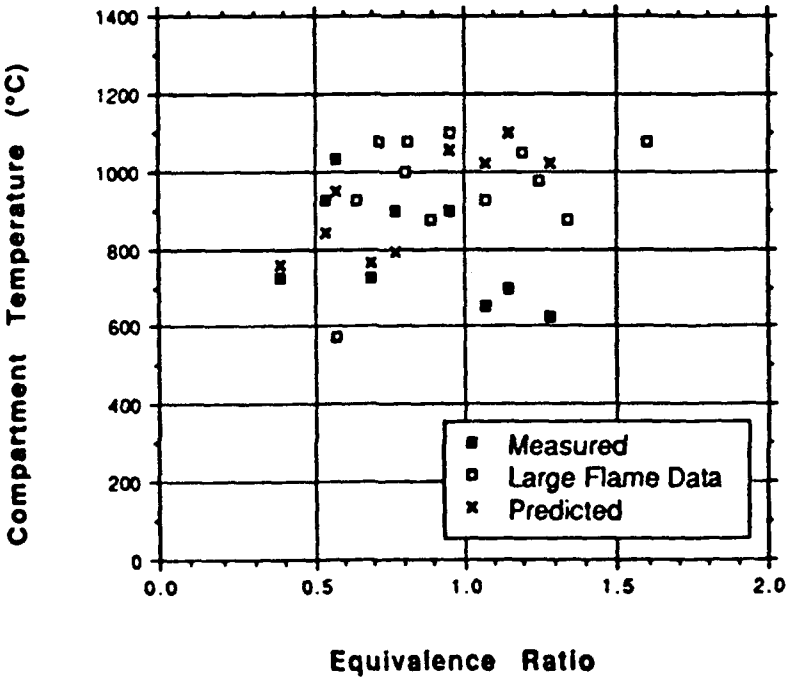

Figure 4. Compartment temperature as a function of equivalence ratio.

stoichiometric is quite small (see for instance Babrauskas(1981) or Beyler (1983)).

SUMMARY

This brief analysis has identified that the two and three door tests did not fulfill the assumption of a well-stirred compartment as is used in all post-flashover compartment fire models. The flame volume was sufficiently large that the mixing of fuel and air in the compartment cannot occur before the gases leave the compartment. In short the residence time was too short for combustion to proceed to use all of the limiting reagent, fuel or air. In these conditions, the flame is better characterized as an open flame bent by the presence of the ceiling and walls. The maximum temperatures observed were the same as for flames in the open. There is definite evidence that this phenomena can also occur for cellulosic fires and that some of the fires in the CIB test series were also not well-stirred compartment fires. For fires which are not well-stirred it is appropriate to use a compartment temperature of approximately 1000°C (1832°F), regardless of the heat losses through the compartment walls.

For the well stirred compartment fires, the simple model employed was not able to satisfactorily predict the results. In particular, the very low compartment temperatures observed for fuel rich fires were surprisingly low and appear to be unprecedented in the literature.

REFERENCES

1. Beyler, C.L., "Development and Burning of A Layer of Products of Incomplete Combustion Generated by a Buoyant Diffusion Flame," Ph.D. Thesis, Harvard University, 1983.

2. Beyler, C.L., "Major Species Production by Solid Fuels in a Two Layer Compartment Fire Environment," First International Symposium on Fire Safety Science, 1986, pp. 431-440.

3. Orloff, L., and deRis, J., "Froude Modeling of Fire," Nineteenth Symposium (International) on Combustion, The Combustion Institute, Pittsburgh, PA, 1982, p. 885.

4. Beyler, C.L., "Fire Plumes and Ceiling Jets," Fire Safety Journal, 11, 1986, pp. 53-75.

5. Thomas, P., Heselden, A., "Fully Developed Fires in a Single Compartment," Fire Research Note 923, Fire Research Station, Borehamwood, 1972.

6. Harmathy, T.Z., "Assessment of Fire Resistance Requirements," Fire Technology, 17, 1981, pp. 221-237.

7. Babrauskas, V., "A Closed-form Approximation for Post-flashover Compartment Fire Temperatures," Fire Safety Journal, 4, 1981, pp. 63-73.